Die Rolle von Ca^{2+}-aktivierten K^{+}-Kanälen für die Radioresistenz des Glioblastoms

Dissertation

der Mathematisch-Naturwissenschaftlichen Fakultät

der Eberhard Karls Universität Tübingen

zur Erlangung des Grades eines

Doktors der Naturwissenschaften

(Dr. rer. nat.)

vorgelegt von

Benjamin Stegen

aus Balingen

Tübingen

2015

Gedruckt mit Genehmigung der Mathematisch-Naturwissenschaftlichen Fakultät der Eberhard Karls Universität Tübingen.

Tag der mündlichen Qualifikation:	08.12.15
Dekan:	Prof. Dr. Wolfgang Rosenstiel
1. Berichterstatter:	Prof. Dr. Stephan Huber
2. Berichterstatter:	Prof. Dr. Peter Ruth

Inhaltsverzeichnis

Abkürzungsverzeichnis

AMD3100	CXCR4 Inhibitor, Plerixafor
AQP1	Aquaporin 1
BK	„Big conductance potassium channel“
Ca^{2+}	Kalziumion
CaMKII	„Ca^{2+}/Calmodulin-dependent protein kinase II“
$Cd11b^{+/-}$	Integrin alpha M, reguliert die Leukozytenadhäsion und -migration
$Cd133^{+/-}$	Prominin-1, Transmembranglykoprotein, $CD133^{+}$ Zellsubpopulationen Gelten als Krebsstammzellen
cdc2	„Cell division cycle protein 2 homolog“
Cl^{-}	Chloridion
ClC-3	„Chlorid channel 3“
CRAC	Ca^{2+} Release aktivierte Ca^{2+}-Kanäle
CXCL-12	CXC-Motiv-Chemokin 12, auch SDF-1
CXCR4	CXC-Motiv-Chemokinrezeptor 4, auch stromal cell-derived factor 1 receptor
DAG	Diacylglycerol
DNA	„Deoxyribonucleic acid“
EdU	5-Ethynyl-2’-Deoxyuridine
E_K	Kalium-Gleichgewichtspotential
ER	Endoplasmatisches Retikulum
fIR	Fraktionierte Bestrahlung
FURA-2	Fluoreszenzfarbstoffe, bildet Chelatkomplexe mit Ca^{2+}
g	Leitfähigkeit in pS
gBK	„Glioma big conductance potassium channel“
GBM	Glioblastoma multiforme
Gy	Gray, pro Masse absorbierte Energie
H_2O	Wasser
hbr5	„BK channel isoform human brain 5“
HIF-1α	„Hypoxia inducible factor-1 alpha“
hslo	„Human slowpoke gene“
$i[Ca^{2+}]_{free}$	Zytosolisch freie Ca^{2+}-Konzentration
IC_{50}	Mittlere inhibitorische Konzentration
ICA-17043	Senicapoc

IK	„Intermediate conductance potassium channel“
IP_3	Inositol-3-Phosphat
IR	„Ionizing radiation“
IUPHAR	„International Union of Basic and Clinical Pharmacology“
K^+	Kaliumion
KCl	Kaliumchlorid
kg	Kilogramm
ln	Natürlicher Logarithmus
mg	Milligramm
mM	Millimol
MMP-2/-9	Matrix-Metalloprotease 2/9
mRNA	Messenger RNA
MV	Megavolt
n	Anzahl
Na^+	Natriumion
NaCl	Natriumchlorid
nM	Nanomol
PF431396	Pyk2 Inhibitor
pH	*potentia hydrogenii*, Maßzahl für die Wasserstoffionenkonzentration
PI3K	Phosphoinositid-Kinase 3
PIP2	Phosphatidylinositoldiphosphat
PKA	Proteinkinase A
PKC	Proteinkinase C
PMCA	Plasmamembranständige Ca^{2+}-ATPase
pS	Pico Siemens, Leitfähigkeit
pS/pF	Pico Siemens/Pico Farad, kapazitativer Leitwert
Pyk2	Proteintyrosinkinase 2 beta
SDF-1	CXCL12, Stromal-derived cell-factor-1
SE	„Standard error“
SERCA	Ca^{2+}-ATPase des Sarkoplasmischen und Endoplasmatischen Retikulums
SF	„Survival fraction“
shRNA	„Small hairpin RNA“
SK4	„Small conductance potassium channel 4“

TEA	Tetraethylammonium
TRAM34	IK Kanal Inhibitor, 1-[(2-Chlorophenyl)diphenylmethyl]-1H-pyrazole
V_0	Tumorvolumen zu Beginn der Behandlung an Tag 0
V_t	Tumorvolumen
WHO	„World Health Organisation“
α-UE	Alpha-Untereinheit
γH2AX	Histon im Zellkern aller Eukaryoten
$\delta_{\ln(Vt/V0)}/\delta_t$	Maß für die exponentielle Wachstumskinetik
$\Delta\delta_{\ln(Vt/V0)}/\delta_t$	Maß für den durch die Behandlung induzierten Rückgang des Wachstums
µl	Mikroliter
µM	Mikromol

Zusammenfassung

Glioblastoma multiforme (Grad IV Astrozytome) sind die häufigsten und gleichzeitig malignesten primären Neoplasien im Gehirn. Glioblastomzellen können innerhalb des Gehirns weite Strecken zurücklegen, eine diffuse Infiltration des Gehirns ist die Folge. Eine komplette operative Entfernung und Erfassung der residuellen Tumorzellen durch das Zielvolumen während der adjuvanten Strahlentherapie ist daher oft nicht möglich.

Die Migration von Glioblastomzellen hängt sehr stark von hoch effizienten Zellvolumenänderungen ab, welche es der Zelle ermöglicht, sich durch die engen Zellzwischenräume hindurch zu zwängen. Diese Ab- und Zunahme des Zellvolumens schließt die Abgabe von KCl mit ein, welche von einem osmotisch bedingten Verlust an freiem Zellwasser gefolgt wird. Dieser Prozess wird bewerkstelligt durch Ca^{2+}-regulierte K^+- und Cl^--Kanäle in der Plasmamembran. Eine Bestrahlung (IR) dieser Zellen scheint die Migration von Glioblastomzellen sogar noch weiter zu stimulieren. Ein Schlüsselereignis in diesem Vorgang ist die Aktivierung von BK K^+-Kanälen in den bestrahlten Zellen (Reviews: Huber et al. 2013, 2014).

Der erste Teil dieser Doktorarbeit analysierte das Signaling „down"- und „upstream" der durch Bestrahlung induzierten BK K^+-Kanal-Aktivierung. Eine Bestrahlung induzierte die Bildung des CXCR4 Agonisten SDF-1 und veränderte das Ca^{2+}-Signaling, welches in einer Ca^{2+}-abhängigen Aktivierung von BK K^+-Kanälen resultierte. Wie bei einer Bestrahlung der Glioblastomzellen induzierte SDF-1 oder konditioniertes Medium von bestrahlten Zellen Ca^{2+}-Signale, die eine Hypermigration von unbehandelten Glioblastomzellen stimulierte. Der CXCR4 Antagonist AMD3100 und der BK-Kanal Inhibitor Paxilline unterbanden die Signale, die eine Hypermigration ermöglichen.

Die Ergebnisse deuten auf eine Stimulation der Hypermigration in bestrahlten Glioblastomzellen hin, ermöglicht durch ein Signaling via SDF-1, den CXCR4 Chemokinrezeptor, Ca^{2+}-aktivierte BK K^+-Kanäle und die Ca^{2+}-aktivierte CaMKII Serin/Threoninkinase. Letztere aktiviert ClC-3 Cl^--Kanäle, die zusammen mit BK K^+-Kanälen und Aquaporinen die Zellvolumenänderungen bewerkstelligen, welche für die Migration notwendig sind (Stegen et al. 2015; Butz und Stegen et al. 2015, eingereichtes Manuskript).

Neben BK-Kanälen überexprimieren Glioblastomzellen auch Ca^{2+}-aktivierte IK K^+-Kanäle. Der zweite Teil dieser Doktorarbeit untersuchte die Funktion dieser IK-Kanäle für die Radioresistenz der Glioblastomzellen.

Eine Bestrahlung von Glioblastomzellen erhöhte die Aktivität von TRAM34-sensitiven IK K^+-Kanälen, welche zu einem veränderten Ca^{2+}-Signaling und der Aktivierung von Ca^{2+}/Calmodulin-abhängigen Kinase II (CaMKII) Isoformen führten. Diese Aktivierung resultierte anschließend in einer Inaktivierung des cdc2 „mitosis promoting factor“ und einem vorübergehenden G_2/M Arrest. TRAM34 schwächte die IR-induzierte Aktivierung der CaMKII, eine cdc2 Dephosphorylierung und eine verringerte Akkumulierung der Zellen im G_2/M Arrest waren die Folge. Des Weiteren erhöhte TRAM34 die Anzahl der gamma-H2AX Foci 24 Stunden nach Bestrahlung, welche auf einen durch TRAM34 induzierten Anstieg von residuellen DNA Doppelstrangbrüchen hindeutet. TRAM34 radiosensitivierte T98G und U87MG Glioblastomzellen in Koloniebildungstests. Zudem zeigte das klonogene Überleben zweier mit Retroviren transfizierten T98G Glioblastomzellklone, welche sich in ihrer IK-Kanal Expression unterscheiden, sowohl eine durch IK-Kanäle vermittelte Radioresistenz als auch eine IK-Spezifität des TRAM34-Effektes. Es konnte ebenso gezeigt werden, dass eine zeitgleiche TRAM34-Behandlung und Bestrahlung zu einem verzögerten ektopen Tumorwachstum im hinteren rechten Oberschenkel von immunkompromittierten Nacktmäusen führte. Zusammenfassend zeigen die Daten eine Zellzyklus-regulatorische Funktion von IK K^+-Kanälen (Stegen et al. 2015).

Summary

Glioblastoma multiforme (astrocytoma grade IV) is the most frequent and at the same time most malignant primary neoplasia in the brain. Glioblastoma cells can migrate long distances within the brain resulting in diffuse infiltration. Complete surgical resection and capture of all residual tumour cells by the target volume of the adjuvant radiation therapy is often not possible.

Migration of glioblastoma cells strongly depends on highly efficient cell volume changes that enable the cells to squeeze between very narrow interstitial spaces. These cell volume changes reportedly comprise a cell volume decrease generated by loss of KCl followed by osmotically obliged cell water, which involves Ca^{2+}-regulated K^+ and Cl^- channels in the plasma membrane. Importantly, ionizing radiation (IR) has been demonstrated to further stimulate migration of glioblastoma cells. A key event in this process is the activation of BK K^+ channels in the irradiated cells (for review see: Huber et al. 2013, 2014).

The first part of the doctoral thesis analyzed the signaling down- and upstream of radiation-induced BK channel activation. As a result, radiation induced formation of the CXCR4 agonist SDF-1, modulated the Ca^{2+}-signaling leading to the consecutive Ca^{2+}-dependent activation of BK K^+ channels. Like radiation, SDF-1 or conditioned medium from irradiated cells induced Ca^{2+}-signals that stimulated hypermigration of untreated glioblastoma cells. The CXCR4 antagonist AMD3100 and the BK channel inhibitor paxilline blunted signaling events triggering hypermigration.

Together, these findings strongly suggest stimulation of hypermigration in irradiated glioblastoma cells via signaling through SDF-1, CXCR4 chemokine receptor, BK K^+ channels, and CaMKII serine/threonine kinase. The latter activates ClC-3 Cl^- channels, which in concert with BK K^+ and water channels accomplish cell volume changes required for migration (Stegen et al. 2015; Butz and Stegen et al. 2015, manuscript in preparation).

In addition to BK, glioblastoma cells overexpress Ca^{2+}-activated IK K^+ channels. The second part of the doctoral thesis tested IK channel function for the radioresistance of glioblastoma using cell lines and an ectopic glioblastoma mouse model.

Radiation increased the activity of TRAM34-sensitive IK channels leading to a modified Ca^{2+}-signaling and activation of Ca^{2+}/calmodulin-dependent kinase II (CaMKII) isoforms, which in turn resulted in inactivation of the cdc2 mitosis promoting

factor and a transient G_2/M arrest. TRAM34 blunted the IR-induced CaMKII activation resulting in cdc2 dephosphorylation and subsequent decreased accumulation in G_2/M arrest. Moreover, TRAM34 increased the number of residual gamma-H2AX foci 24 h after irradiation suggestive of a TRAM34-induced increase of residual DNA double strand breaks. TRAM34 radiosensitized T98G and U87MG glioblastoma cells as evident from colony formation assays. In addition, clonogenic survival of two retrovirally transfected T98G glioblastoma cell clones that differ in IK channel expression indicated both, IK-mediated radioresistance and IK-specificity of the TRAM34 effect. Finally, TRAM34 application concomitant to fractionated radiation delayed ectopic tumour growth in the upper right hind limb of immunocompromised nude mice. Together, the data confirm the cell cycle regulatory function of IK K^+ channels (Stegen et al. 2015).

EBERHARD KARLS
UNIVERSITÄT
TÜBINGEN

Mathematisch-Naturwissenschaftliche Fakultät

Erklärung nach § 5 Abs. 2 Nr. 7 der Promotionsordnung der Math.-Nat. Fakultät

-Anteil an gemeinschaftlichen Veröffentlichungen-

Name: **Benjamin Stegen**

Liste der Publikationen

1. **Stegen, B., L. Butz, L. Klumpp, D. Zips, K. Dittmann, P. Ruth and S. Huber (2015).**
„Ca^{2+}-activated IK K^+ Channel Blockade Radiosensitizes Glioblastoma Cells.“ Mol Cancer Res.

2. **Huber, S.M., L. Butz, B. Stegen, D. Klumpp, N. Braun, P. Ruth and F. Eckert (2013).**
„Ionizing radiation, ion transports, and radioresistance of cancer cells.“ Front Physiol 4:212.

3. **Huber, S.M., L. Butz, B. Stegen, L. Klumpp, D. Klumpp and F. Eckert (2014).**
„Role of ion channels in ionizing radiation-induced cell death.“ Biochim Biophys Acta.

4. **Butz L., B. Stegen, L. Klumpp, E. Haehl, K. Schilbach, R. Lukowski, M. Kühnle, G. Bernhardt, A. Buschauer, D. Zips, P. Ruth and S. Huber (2015).**
„BK K^+ channel blockade inhibits radiation-induced migration/brain infiltration of glioblastoma cells.” Oncotarget (submitted, shared first-authorship)

Nr.	Accepted for publication yes/no	Number of all authors	Position of the candidate in list of authors	Scientific ideas of candidate (%)	Data generation by candidate (%)	Analysis and interpretation by candidate (%)	Paper writing by candidate (%)
1.	Yes	7	1	50	70	70	60
2.	Yes	7	3	10	20	20	20
3.	Yes	7	3	10	20	20	20
4.	No	12	1 (2)	40	40	40	40

I certify that the above statement is correct.

_____

Date, Signature of the candidate

I/We certify that the above statement is correct.

_____

Date, Signature of the doctoral committee or at least of one of the supervisors

EBERHARD KARLS
UNIVERSITÄT
TÜBINGEN

Mathematisch-Naturwissenschaftliche Fakultät

Erklärung zum Eigenanteil der Dissertation

Die Arbeit wurde am Universitätsklinikum Tübingen, Abteilung Experimentelle Radioonkologie unter Betreuung von Prof. Dr. Stephan Huber und Prof. Dr. Peter Ruth durchgeführt. Sämtliche Versuche wurden nach Einarbeitung durch Prof. Dr. Stephan Huber, Heidrun Faltin und Ilka Müller von mir eigenständig, teils mit Unterstützung durch Heidrun Faltin und Ilka Müller durchgeführt. Die statistische Auswertung erfolgte eigenständig, nach Anleitung durch Prof. Dr. Stephan Huber.

Ich versichere, das Manuskript selbständig unter Mithilfe von Prof. Dr. Stephan Huber verfasst und keine weiteren als die von mir angegebenen Quellen verwendet zu haben.

Tübingen, den

[Benjamin Stegen]

1. Einleitung

„Diffuse glioma growth: a guerilla war“, „Glioblastoma multiforme: the terminator“ – so lauten die Titel zweier Publikationen, die damit vortrefflich die Eigenschaften des Glioblastoms und die damit verbundene Problematik beschreiben, wirkungsvolle therapeutische Ansatzpunkte gegen diese Tumorentität zu entwickeln (Holland 2000, Claes et al. 2007).
Trotz intensiven und umfassenden klinischen Studien konnten nur geringe Erfolge bei der Behandlung von Glioblastomen in den letzten Jahrzehnten erreicht werden. Ein Drittel aller Patienten lebt nicht länger als ein Jahr, und die durchschnittliche Lebenserwartung beträgt nur etwa 15 Monate nach Diagnose, auch wenn eine Operation, Radio- und Chemotherapie angewandt werden können (Catacuzzeno et al. 2012).
Es ist also verständlich, dass zahlreiche Forschergruppen sich darum bemühen, die biologischen Zusammenhänge eines Glioblastoms zu ergründen und anhand der gewonnen Ergebnisse neue Therapieansätze und Medikamente zu entwickeln.

1.1 Das Glioblastom

Der Begriff „Gliom“ ist ein Sammelbegriff für einige Hirntumorarten die glialen Ursprungs sind und repräsentiert den größten Anteil der primären Tumoren des Gehirns. Glioblastome sind die häufigsten und aggressivsten unter den primären Gehirntumoren (Catacuzzeno et al. 2012) und weisen eine Inzidenz von jährlich 3-5 Fällen / 100.000 Personen auf. Sie betreffen hauptsächlich Erwachsene zwischen 45 und 75 Jahren und kommen entweder als primäre Glioblastome vor (95%), die sich *de novo* bilden und keine Vorgängertumore besitzen, oder als sekundäre Glioblastome, welche sich aus weniger aggressiven primären Tumoren entwickelt haben (Molenaar 2011). Diese hochmaligne Tumorentität wird anhand der WHO-Einteilung als äußerst bösartiger Tumor klassifiziert (WHO-Grad IV). Zu den Gliomen zählen des Weiteren Astrozytome, Oligodendrogliome, Ependymome sowie Mischformen mit astrozytären und oligodendroglialen Anteilen (Louis et al. 2007).

Tumor	WHO-Grad
Tumoren des zentralen Nervensystems	
Astrozytäre Tumoren:	
Pilozytisches Astrozytom	WHO-Grad I
Diffuses Astrozytom	WHO-Grad II
Anaplastisches Astrozytom	WHO-Grad III
Glioblastom	WHO-Grad IV
Oligodendrogliale Tumoren:	
Oligodendrogliom	WHO-Grad II
Anaplastisches Oligodendrogliom	WHO-Grad III
Mischgliome:	
Oligoastrozytom	WHO-Grad II
Anaplastisches Oligoastrozytom	WHO-Grad III
Ependymale Tumoren:	
Ependymom	WHO-Grad II
Anaplastisches Ependymom	WHO-Grad III

Tabelle 1: WHO-Klassifikation der Gliome (Auszug) aus: Louis, Ohgaki et al. 2007.

Zu den klinischen Symptomen, die bei Glioblastomen auftreten, gehören unter anderem Kopfschmerzen, Krampfanfälle, fokale neurologische Defizite bis hin zu Gedächtnisverlust oder Persönlichkeitsveränderungen (Watkins and Sontheimer 2012). Ein Grund für das schlechte Ansprechen von Glioblastomen auf verschiedene therapeutische Maßnahmen ist der komplexe Charakter des Tumors selbst. Wie der Name – Glioblastoma multiforme – schon impliziert, handelt es sich um einen sehr heterogenen Tumor. Histologisch betrachtet finden sich Regionen aus nekrotischem Gewebe, soliden Tumorbereichen sowie zahlreichen Einblutungen. Auf mikroskopischer Ebene weisen Glioblastome mehrgestaltige Nuklei und Zellen auf, mehrkernige Tumorriesenzellen, Nekrosen sowie mikrovaskuläre Zellproliferation. Auch in der Genetik setzt sich diese Vielgestaltigkeit fort. Deletionen, Amplifikationen, Punktmutationen führen zur Aktivierung von Signalwegen, die sich Downstream von Tyrosinkinaserezeptoren befinden, sowie zur Unterbrechung von Signalwegen welche normalerweise für einen Zellzyklusarrest verantwortlich sind (Holland 2000).

1.2 „Go or Grow“

Zellmigration spielt eine zentrale Rolle in vielen physiologischen und pathophysiologischen Prozessen, wie der Embryogenese, Immunabwehr, Wundheilung oder der Bildung von Tumormetastasen. Neuralleistenzellen migrieren durch den Embryo um das Nervensystem zu bilden. Leukozyten jagen eindringende Bakterien. Die Migration von Epithelzellen stellt einen schnellen Reparaturmechanismus dar wenn Lücken in der Epithelschicht geschlossen werden müssen (Schwab 2001).
Die Fähigkeit von Glioblastomzellen in normales Gehirngewebe zu migrieren gilt im Gegensatz dazu jedoch als ein wesentlicher Faktor für die klinische Malignität. Auch nach erfolgter Tumorresektion und adjuvanter Chemo- und Radiotherapie führen diese invasiven Tumorzellen immer wieder zu Rezidiven und sind trotz fehlender Fernmetastasierung für die oft schlechte Prognose von Gliomen verantwortlich (Catacuzzeno et al. 2012).

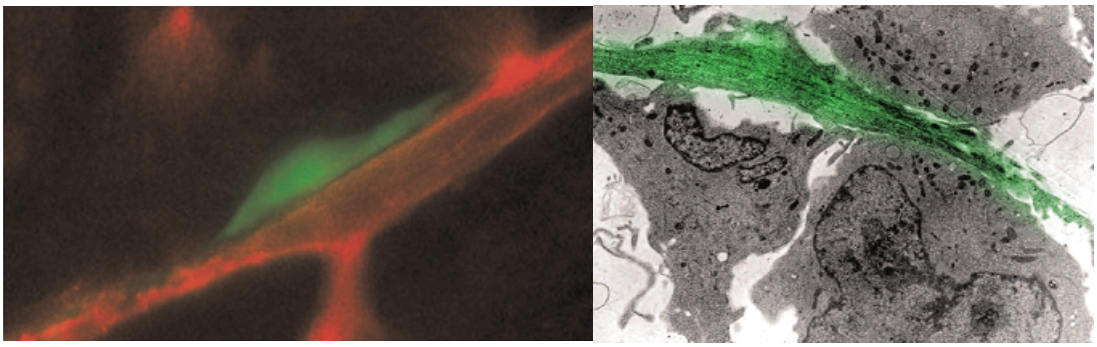

Abbildung 1: Glioblastomzellen migrieren entlang von Blutgefäßen und zwischen enge Zellzwischenräume des normalen Gehirnparenchyms, verändert nach: Sontheimer, 2008.

Das erneute Auftreten eines Glioblastoms nach einer Totalresektion kann nicht alleine auf einer Neubildung von Glioblastomzellen, hervorgerufen durch Mutationen, beruhen. Vielmehr scheinen Rezidive durch hoch motile Glioblastomzellen, welche bei einer Totalresektion nicht entfernt werden können, hervorgerufen zu werden. Der Wechsel von einem sessilen zu einem invasiven Phänotypen kann durch den sogenannten „Go or Grow“ Mechanismus erklärt werden, bei welchem es sich um das Phänomen der Migrations/Proliferations-Dichotomie handelt. Hoch motile

Glioblastomzellen tendieren demnach zu geringeren Proliferationsraten, wohingegen proliferierende Zellen weniger migrieren (Hatzikirou et al. 2012). Dem zu Grunde liegt das Konzept, dass genetische und zytoskelettale Maschinerien nicht zeitgleich für die Proliferation und Migration verwendet werden können, wodurch sich Migration und Zellteilung gegenseitig ausschließen (Giese et al. 1996).
Eine herausragende Rolle bei der Migration und Proliferation von Glioblastomzellen spielen verschiedene Ionenkanäle, die durch eine bessere technische Charakterisierbarkeit in den letzten Jahren verstärkt in den Fokus des wissenschaftlichen Interesses gerückt sind. Ihre Expression auf Glioblastomzellen variiert teilweise sehr stark von der auf normalen Gliazellen. Dies lässt eine funktionelle Bedeutung für das klinisch maligne Verhalten von Gliomen vermuten.

1.3 Ionenkanäle

Glioblastome sind durch eine hohe Anzahl und Vielfalt an genetischen Mutationen charakterisiert, welche die Hauptsignalwege, die das Zellüberleben, die Proliferation, die Differenzierung und Invasion regulieren, betreffen. Unter diesen fehlregulierten Signalwegen, die in Glioblastomzellen gefunden wurden, sind auch jene, die die Expression von Ionenkanälen regulieren. In den 555 Genen, die eine Rolle beim Transport von Ionen in Glioblastomen spielen, wurde in 90% der untersuchten Patientenproben eine Mutation entdeckt (Molenaar 2011).
Ionenkanäle spielen in verschiedenen zellulären Bereichen eine wichtige Rolle, wie etwa bei der Proliferation, Apoptose und Migration. In den meisten Fällen leisten sie ihren Beitrag, indem sie zwei wichtige zelluläre Parameter steuern, das Zellvolumen und die intrazelluläre freie Ca^{2+}-Konzentration (Catacuzzeno et al. 2012). Des Weiteren scheinen Ionenkanäle die Aktivität von Downstream-Effektormolekülen zu beeinflussen sowie die Epigenetik und Proteinexpression zu modifizieren. Ebenso leiten sie vermutlich Signale durch direkte molekulare Interaktionen in makromolekularen Komplexen oder sogar als Transkriptionsfaktoren weiter. Im Gegensatz zu Onkogenen sind Ionenkanäle aber nicht für die Initiation der neoplastischen Transformation von Zellen verantwortlich. Sie sind eher die Triebkraft

von onkogenen Prozessen, indem sie unter anderem die Ca^{2+}-Signatur, Membranspannung und Ionenkonzentrationen anpassen (Huber 2013).
Humane Gliomazellen exprimieren eine Vielzahl an Ionenkanälen. Diese beinhalten spannungsgesteuerte K^+-Kanäle (Chin et al. 1997), spannungsgesteuerte Na^+-Kanäle (Brismar and Collins 1989), Ca^{2+}-aktivierte K^+-Kanäle (Brismar and Collins 1989), spannungsabhängige (Ullrich et al. 1998) und volumenregulierte Cl^--Kanäle (Bakhramov et al. 1995).

1.3.1 Kaliumkanäle

K^+-Kanäle sind mitunter fundamentale Regulatoren für die Erregbarkeit einer Zelle. Sie kontrollieren die Frequenz und Form von Aktionspotentialen, die Sekretion von Hormonen und Neurotransmittern sowie das Potential der Zellmembran. Ihre Aktivität wird durch Spannung, Ca^{2+} und Neurotransmitter reguliert (Hille 1992). Der funktionsfähige K^+-Kanal entsteht durch die Zusammenlagerung mehrerer α-Untereinheiten, wobei vier dieser Untereinheiten sich zu einem Tetramer zusammen lagern und eine membranintegrierte Pore bilden. Weitere Proteine, so genannte akzessorische Proteine oder ß-Untereinheiten, können mit den α-Untereinheiten assoziiert sein (Jan and Jan 1997). Die große Vielfalt der bekannten K^+-Kanäle kommt zu Stande, da sich verschiedene Untereinheiten zu einem Heterotetramer mit neuen funktionellen Eigenschaften zusammen lagern können. Zusätzlich können die zytoplasmatischen ß-Untereinheiten die K^+-Kanaleigenschaften maßgeblich verändern (Christie et al. 1990). Die unterschiedlichen Untereinheiten entstehen durch alternatives Splicing und durch posttranslationale Modifikationen wie der Phosphorylierung, Lipidierung und Myristoylierung (Toro et al. 2014).
Von der „International Union of Basic and Clinical Pharmacology“ (IUPHAR) wurde eine standardisierte Nomenklatur für K^+-Kanäle aufgestellt. Demnach lassen sie sich in Ca^{2+}-aktivierte, einwärts gleichgerichtete, 2 Poren- und spannungsaktivierte K^+-Kanäle unterteilen.
Bei den Ionenkanälen, die wohl den größten Anteil an der Tumorentwicklung übernehmen, handelt es sich um die Ca^{2+}-aktivierten K^+-Kanäle. Sie vereinen all die Eigenschaften, die dort eine Rolle spielen, wo Ca^{2+}-Einstrom, Membranpotential und

auswärts gerichtete Ionenströme zusammen eine Vielzahl an zellulären Prozessen steuern (Molenaar 2011).

1.3.1.1 Ca^{2+}-aktivierte Kalium-Kanäle

Ca^{2+}-aktivierte K^+-Kanäle werden in drei Hauptgruppen unterteilt, entsprechend ihrer Einzelkanal-Leitfähigkeit, in „large conductance“ K^+-Kanäle (150-300 pS; **BK_{Ca}**, Maxi K^+ oder $K_{Ca}1.1$), „intermediate conductance“ K^+-Kanäle (20-60 pS; **IK_{Ca}**, IK1 oder $K_{Ca}3.1$) und „small conductance“ K^+-Kanäle (2-20 pS; SK oder $K_{Ca}2.1$, $K_{Ca}2.2$, $K_{Ca}2.3$). Jede der Klassen besitzt spezifische biophysikalische und pharmakologische Eigenschaften, die es erlaubt, die einzelnen Klassen zu identifizieren. $K_{Ca}1.1$-Kanäle, codiert durch das *Kcnma1* Gen, werden in verschiedensten Geweben exprimiert. Sie werden durch zytoplasmatisch freies Ca^{2+} aber auch durch das Membranpotential reguliert. In Abwesenheit von Ca^{2+} können $K_{Ca}1.1$-Kanäle nur durch extreme, nicht physiologische Depolarisation aktiviert werden. Eine Erhöhung an zytoplasmatisch freiem Ca^{2+} verschiebt den Bereich der Spannung, der aktivierend wirkt, hin zu negativeren Potentialen. Paxilline, Iberiotoxin und geringe Konzentrationen an Tetraethylammonium (TEA) sind spezifische Inhibitoren des $K_{Ca}1.1$-Kanals. Die $K_{Ca}3.1$-Kanäle sind spannungsunabhängig, aber durch intrazelluläres freies Ca^{2+} gesteuert, das an Calmodulin am C-Terminus bindet und als Ca^{2+}-Sensor fungiert. Clotrimazol und TRAM34 sind potente Inhibitoren des $K_{Ca}3.1$-Kanals.
„Intermediate“ und „large conductance“ K^+-Kanäle scheinen in zahlreichen Zelllinien an der Zellproliferation (Basrai et al. 2002, Jager et al. 2004, Ouadid-Ahidouch et al. 2004), der regulierten Volumenabnahme (Khanna et al. 1999, Roman et al. 2002) und Zellmigration (Bordey et al. 2000, Kraft et al. 2003) beteiligt zu sein.

1.3.1.2 $K_{Ca}1.1$ (BK)

$K_{Ca}1.1$-Kanäle kommen in verschiedenen Geweben vor, sowohl in erregbaren als auch in nicht erregbaren Zellen (Ransom et al. 2002). Erregbare Zellen weisen eine starke Depolarisation und aufgrund der Aktivierung von Kalziumkanälen einen Anstieg von freiem intrazellulärem Ca^{2+} auf, was zu einer Aktivierung von $K_{Ca}1.1$-

Kanälen führt. Sie beeinflussen dadurch in glatter Muskulatur durch Hyperpolarisation den Basaltonus und die Kontraktion, in Neuronen steuern sie die Repolarisation nach einem Aktionspotential und die Freisetzung von Neurotransmittern (Golding et al. 1999). K_{Ca}1.1-Kanäle werden auch in vielen nicht erregbaren Zellen exprimiert, beispielsweise in Lymphozyten, retinalen Müllerzellen und humanen primären Hirntumoren (Brismar and Collins 1989, Ransom and Sontheimer 2001, Kraft et al. 2003, Toro et al. 2014). Im Gegensatz zu primären Hirntumoren wurden jedoch keine K_{Ca}1.1-Kaliumströme in Astrozyten beschrieben (Ransom and Sontheimer 2001). K_{Ca}1.1-Kanäle werden zum größten Teil in der Plasmamembran gefunden, können aber auch intrazellulär vorliegen wie etwa im Endoplasmatischen Retikulum, dem Nukleus und den Mitochondrien (Toro et al. 2014).

Eine Fehlfunktion des Kanals kann zu Epilepsie führen, zu motorischer Beeinträchtigung, Bluthochdruck, Fettleibigkeit, Inkontinenz und Asthma (Cui et al. 2009).

Aktiviert werden K_{Ca}1.1-Kanäle sowohl durch einen intrazellulären Ca^{2+}-Anstieg als auch spannungsabhängig, wobei eine Zunahme der Depolarisation der Zelle in einer erhöhten Offenwahrscheinlichkeit der Kanäle resultiert (Kraft et al. 2000). Es kommt hierbei zu einem Kaliumausstrom aus der Zelle. Eine Aktivierung kann auch durch andere Stimuli, sowohl extern als auch intern, hervorgerufen werden. Dies ist unter anderem durch einen Anstieg der intrazellulären freien Ca^{2+}-Konzentration durch Wachstumsfaktoren, eine Phosphorylierung von K_{Ca}1.1-Kanal Proteinen, einen hohen intrazellulären pH-Wert und durch Interaktion mit dem Zytoskelett gegeben (McManus 1991, Ransom and Sontheimer 2001). Schon eine sehr kleine Dichte solcher K_{Ca}1.1-Kanäle pro Zelle kann aufgrund seiner hohen Leitfähigkeit zu großen Strömen führen und somit das Membranpotential dominieren.

Die Ca^{2+}-Sensitivität des Kanals ist je nach Gewebe sehr unterschiedlich ausgeprägt. Bei Skelettmuskelzellen und Neuronen ist für die Aktivierung eine höhere Konzentration an freiem intrazellulärem Ca^{2+} nötig als beispielsweise in glatter Muskulatur (McManus et al. 1995, Tseng-Crank et al. 1996).

In Gliomen wurden K_{Ca}1.1-Kanäle erstmalig von Brismar et al. (1989) beschrieben. Ransom und Sontheimer (2000) wiesen zusätzlich eine deutlich stärkere Expression in Gliomen im Vergleich zu normaler Glia nach. Zudem korreliert auch die Höhe der Expression positiv mit dem jeweiligen Malignitätsgrad der untersuchten

Gliomsubtypen (Liu et al. 2002). Bei den K_{Ca}1.1-Kanälen in Gliomen handelt es sich um eine neue Splicevariante von *hslo*, dem Gen welches die α-UE von humanen K_{Ca}1.1-Kanälen codiert. Die primäre Sequenz des „gBK“ genannten Kanals ist zu 97% identisch mit dem ähnlichsten Homolog, hbr5. Jedoch beinhaltet gBK ein zusätzliches 34 Aminosäuren großes Exon im C-Terminus des K_{Ca}1.1-Kanals (Ransom et al. 2002). Die Ströme von gBK zeigen signifikant langsamere Aktivierungszeiten und eine deutlich erhöhte Ca^{2+}-Sensitivität im Vergleich zu hbr5 (Liu et al. 2002). Die hohe Sensitivität von gBK gegenüber Ca^{2+} legt nahe, dass diese, verglichen mit anderen K_{Ca}1.1-Kanal Isoformen, als Antwort auf kleinere Anstiege der intrazellulären freien Ca^{2+}-Konzentration bereits bei typischen Ruhemembranpotentialen (-50 bis -20 mV) aktiv werden (Manning und Sontheimer, unveröffentlichte Ergebnisse).
In Gliomen scheinen K_{Ca}1.1-Kanäle unter anderem eine Rolle bei der Migration (Bordey et al. 2000, Kraft et al. 2003, Steinle et al. 2011), der Proliferation (Basrai et al. 2002) und dem Zellüberleben (Weaver et al. 2004) zu spielen.

1.3.1.3 K_{Ca}3.1 (IK)

Der K_{Ca}3.1 Kanal, aufgrund seiner Leitfähigkeit auch als IK („intermediate conductance“) oder SK4 („small conductance 4“) bezeichnet, wurde erstmals 1958 in Erythrozyten beschrieben, wo er zur Regulation des Zellvolumens und des Membranpotenzials beiträgt. Aufgrund seines Entdeckers wird er auch Gardos-Kanal genannt (Fioretti et al. 2006). K_{Ca}3.1-Kanäle sind unter anderem in Lunge, Darm, Prostata, Lymphknoten, im angeborenen und erworbenen Immunsystem verbreitet, nicht aber im humanen Zentralnervensystem. Ähnlich wie die K_{Ca}1.1-Kanäle werden sie jedoch sehr stark in Glioblastomen und anderen Tumorentitäten exprimiert (Weaver et al. 2006, Ruggieri et al. 2012). In 32% der Glioma-Patienten ist K_{Ca}3.1 überexprimiert, und die Proteinexpression korreliert signifikant mit der schlechten Überlebensprognose der Patienten (Turner et al. 2014). Der spannungsunabhängige Kaliumkanal scheint, auch in Abwesenheit von Ca^{2+}, konstitutiv mit Calmodulin assoziiert zu sein, und eine Bindung von Ca^{2+} an dieses assoziierte Calmodulin induziert eine Konformationsänderung welche die Permeation von Kaliumionen ermöglicht (Pardo and Stuhmer 2014). Durch die hohe Ca^{2+}-Sensitivität werden K_{Ca}3.1-Kanäle bereits durch submikromolare Ca^{2+}-Level aktiviert. Diese werden

leicht durch eine Freigabe aus intrazellulären Speichern erreicht oder durch Influx durch Ca^{2+}-permeable Kanäle. Auch diverse Kinasen wie PKC, PKA und PI3K scheinen $K_{Ca}3.1$ zu regulieren, jedoch nicht durch direkte Phosphorylierung der α-UE (Balut et al. 2012). Mehrere Studien konnten zeigen, dass $K_{Ca}3.1$-Kanäle im Zellzyklus, der Zellvolumenkontrolle und der Apoptose eine Rolle spielen (Bortner et al. 1997, Begenisich et al. 2004, Lallet-Daher et al. 2009, Catacuzzeno et al. 2012, D'Alessandro et al. 2013). Neben der Beteiligung an den genannten Zellfunktionen könnten $K_{Ca}3.1$-Kanäle die Glioblastomzellmigration durch die Modulierung von Ca^{2+}-Signalen unterstützen. Mehrere Arbeiten haben gezeigt, dass die Aktivität von $K_{Ca}3.1$-Kanälen den Eintritt von Ca^{2+} in die Zelle erleichtert, indem sie ein „Gegen-Ion" bereitstellen, um einer massiven Depolarisation am Ca^{2+}-Eintrittsort entgegenzuwirken, und somit die Triebkraft für einen Ca^{2+}-Einstrom erhöhen.

1.4 Die Rolle von Ionenkanälen bei der Migration von Glioblastomzellen

Aufgrund der schlechten Vaskulatur werden solide wachsende Tumoren schlecht mit Nährstoffen versorgt sobald sie eine gewisse Größe erreichen. Die daraus resultierende Hypoxie, der Schwund an Nährstoffen und der niedrige pH-Wert in der Tumorumgebung übt einen gewissen Stress auf die Tumorzellen aus (Stock and Schwab 2009, Hatzikirou et al. 2012). Die gerichtete Migration und die Invasion in gesundes Gewebe stellt hierbei eine Möglichkeit dar dem Stress zu entfliehen. Diese setzt extrazelluläre hapto- und chemotaktische Signale, intrazelluläres Signaling, Zellvolumenänderungen und eine Dynamik hinsichtlich des Zytoskeletts sowie den Abbau der extrazellulären Matrix voraus. Für Ionenkanäle wurde gezeigt, dass sie an all diesen Prozessen beteiligt sind (Schwab et al. 2007). Damit übereinstimmend wurde ein Zusammenhang zwischen einer abweichenden Aktivität gewisser Ionenkanäle mit einem hoch invasiven und metastasierenden Phänotypen nachgewiesen.

Glioblastomzellen legen weite Strecken innerhalb des Gehirns zurück (Johnson et al. 2009) wodurch diffuse, nicht definierbare Tumorgrenzen entstehen. Dadurch ist eine komplette, operative Tumorresektion und eine Radiotherapie, welche alle

Tumorzellen mit einschließt, normalerweise nicht möglich, woraus meist ein Therapie-Misserfolg und damit eine schlechte Prognose resultiert (Niyazi et al. 2011). Glioblastomzellen dringen in das umliegende Gehirnparenchym ein indem sie sich entlang von Axonbündeln oder Blutgefäßen bewegen. Um entlang diesen Pfaden zu wandern müssen die Zellen sehr enge Zellzwischenräume überwinden, was eine effektive lokale Volumenab- und -zunahme voraussetzt. Glioblastomzellen sind tatsächlich in der Lage, all ihr ungebundenes freies Zellwasser zu verlieren (Watkins and Sontheimer 2011). Die elektrochemische Triebkraft für diese Zellvolumenabnahme wird durch ungewöhnlich hohe zytosolische Cl^--Konzentrationen (100 mM) bereitgestellt, welche durch den $Na^+/K^+/2Cl^-$ Cotransporter aufgebaut werden (Haas and Sontheimer 2010). Dies erlaubt Glioblastomzellen Cl^- als Osmolyten zu nutzen, K^+ stellt das Gegen-Ion dar. Das Ausschleusen von Cl^- und K^+ entlang ihres elektrochemischen Gradienten während der lokalen Volumenabnahme scheint durch ein Zusammenspiel von ClC-3 Cl^--Kanälen (Olsen et al. 2003, Cuddapah and Sontheimer 2010, Lui et al. 2010), Ca^{2+}-aktivierten $K_{Ca}1.1$ (Ransom and Sontheimer 2001, Ransom et al. 2002, Ransom et al. 2003, Sontheimer 2008) und $K_{Ca}3.1$-Kanälen (Sciaccaluga et al. 2010, Catacuzzeno et al. 2012, Ruggieri et al. 2012) sowie durch AQP1 (McCoy and Sontheimer 2007, McCoy et al. 2010) gegeben zu sein. AQP1 vermittelt hierbei den isoosmotischen Ausstrom von H_2O.

Die Inhibition von einem dieser Kanäle vermindert oder verhindert gar die Migration und Invasion von Glioblastomzellen (Ernest et al. 2005, McFerrin and Sontheimer 2006, Haas and Sontheimer 2010, Lui et al. 2010, Sciaccaluga et al. 2010). Ein weiteres Indiz dafür, dass diese Transporter eine gewichtige Rolle bei der neoplastischen Transformation, malignen Tumorprogression und Migration spielen, ist ihre Abwesenheit in normalen Gliazellen und ihre hohe Expression in Glioblastom-Geweben von Patienten (Ransom and Sontheimer 2001, Liu et al. 2002, Ransom et al. 2002, Weaver et al. 2006, Ruggieri et al. 2012). ClC-3-Kanäle sind zudem normalerweise nicht an der Zelloberfläche zu finden. Im Gegensatz dazu werden in Glioblastomen zahlreiche ClC-3-Kanäle zur Plasmamembran transportiert (Olsen et al. 2003).

Interessanterweise scheinen einzelne Bestrahlungsdosen, wie sie bei der fraktionierten Bestrahlung vieler Krebstherapien Anwendung finden, den „Go“

Phänotypen bzw. die Migration und Invasion von Tumorzellen noch zu erhöhen (Wild-Bode et al. 2001, Steinle et al. 2011).

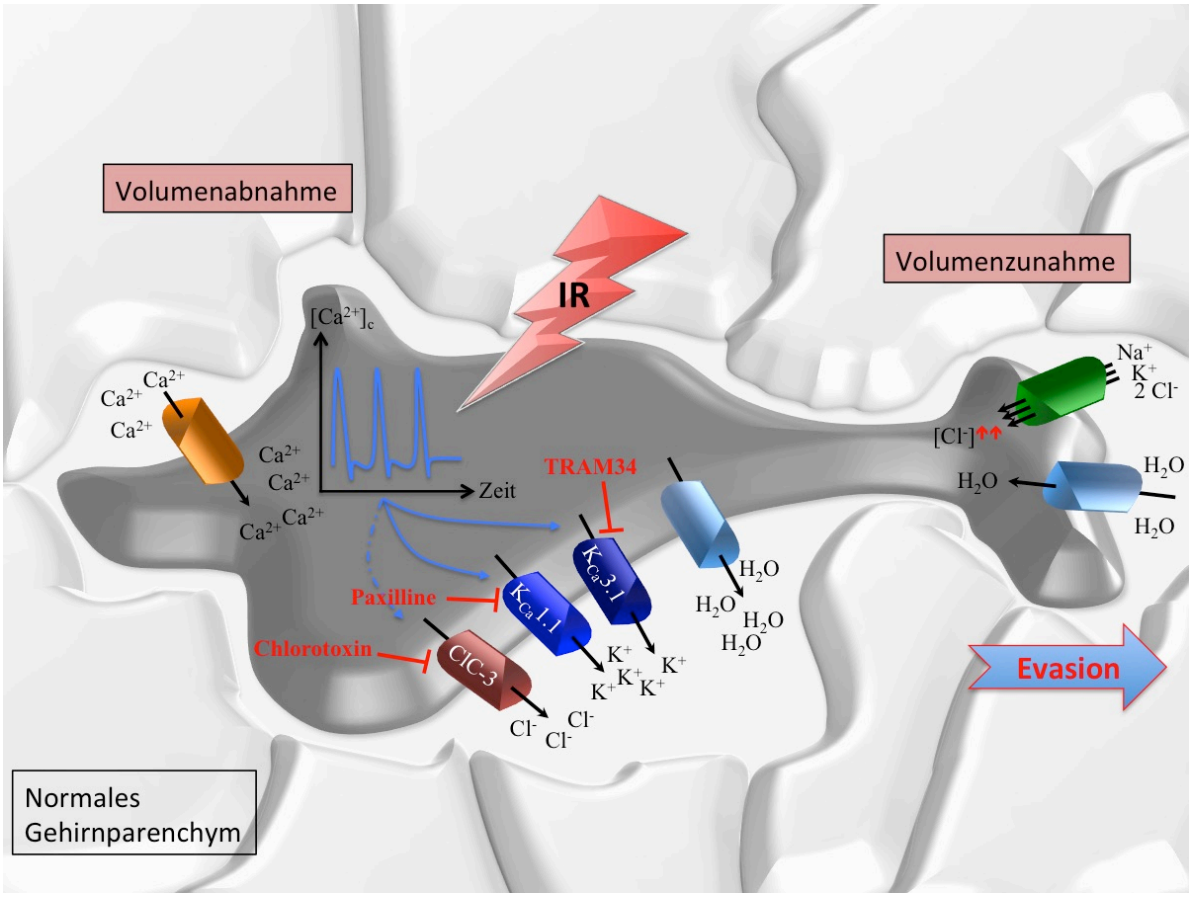

Abbildung 2: Lokale Zellvolumenabnahme einer Glioblastomzelle bei der Evasion in angrenzendes Gehirnparenchym. Die Aktivierung von $K_{Ca}1.1$-, $K_{Ca}3.1$- und ClC-3-Ionenkanälen durch intrazelluläres freies Ca^{2+} ermöglicht den osmotischen Austritt von zellungebundenem H_2O. Diese Kanalaktivität wird durch Bestrahlung (IR) noch gesteigert. Ermöglicht wird die Verwendung von Cl^- als Osmolyt durch den $Na^+/K^+/2Cl^-$ Cotransporter welcher Cl^- oberhalb des elektrochemischen Gleichgewichtes akkumuliert.

1.5 Die Rolle von Ionenkanälen bei der Zellzykluskontrolle und Radioresistenz

Die Radiotherapie vermindert das klonogene Überleben von Tumorzellen hauptsächlich indem der Zelle DNA Doppelstrangbrüche zugefügt werden. Die intrinsische Fähigkeit, diese DNA Schäden durch „non-homologous end joining“ oder homologe Rekombination zu reparieren legt fest, wie radioresistent die jeweilige

Tumorzelle ist. Bestrahlte Tumorzellen, welche nicht alle entstandenen Doppelstrangbrüche reparieren können, verlieren ihre Klonogenität. Dies bedeutet, dass sie keine neue Tumormasse aufbauen können. Ionenkanäle könnten hierbei direkt an der zellulären Stressreaktion als Antwort auf die Schädigung der DNA beteiligt sein, indem sie den Zellzyklus, Anpassungen des Metabolismus oder die Reparatur der DNA kontrollieren und somit zur intrinsischen Radioresistenz und dem Überleben der Tumorzellen beitragen (Huber et al. 2013).

Insbesondere K^+-Kanäle besitzen eine bedeutende Rolle bei der Kontrolle der Zellproliferation und der Differenzierung verschiedener Zellen. So zeigen K^+-Kanäle eine Zellzyklus abhängige Expression und Aktivität (Takahashi et al. 1993). Man nimmt unter anderem an, dass der fortschreitende Zellzyklus eine Hyperpolarisation des Membranpotentials und einen Einstrom an Ca^{2+}, speziell in der G_1 Phase und beim Übergang G_1/S, voraussetzt (Wonderlin and Strobl 1996). K^+-Kanäle könnten hierbei entscheidend sein um die Hyperpolarisation aufrecht zu erhalten und Ca^{2+}-Signale zu steuern, welche nahezu alle Zellprozesse regulieren (Lallet-Daher et al. 2009). So wurde unter anderem für Leukämie- und Glioblastomzellen gezeigt, dass eine Inhibition oder ein Knock Down von K^+-Kanälen zu einer Radiosensibilisierung führt (Palme et al. 2013, Stegen et al. 2015).

1.6 Ca^{2+}-Signaling

Ca^{2+} ist ein intrazellulärer „second messenger“ welcher eine Reihe zellulärer Prozesse, unter anderem die Proliferation, Sekretion, Differenzierung, Bewegung und die Transkription beeinflusst. Jedoch können erhöhte intrazelluläre Ca^{2+}-Level unter bestimmten Bedingungen zytotoxisch wirken. Daher haben viele Krebszellen die Expression oder Aktivität ihres Ca^{2+}-Signalosoms umgestaltet.

Viele Gene, die für Proteinkinasen codieren, werden als Ursache für die Entstehung von Krebs verantwortlich gemacht. Da Proteinkinasen oft am Anfang von Signalkaskaden stehen, mit anderen Signalwegen wechselwirken und die Aktivität und Abundanz von Transkriptionsfaktoren regulieren, hat eine aberrante Proteinkinase-Aktivität weit reichende Folgen. Dasselbe gilt für das Ca^{2+}-Signaling.

Dieses interagiert mit anderen biochemischen Signaltransduktionskaskaden um eine Reihe zellulärer Prozesse zu steuern.

Jede Zelle exprimiert Komponenten eines Ca^{2+}-Signaling-Komplexes, das intrazelluläre Ca^{2+}-Signale bestimmter Amplitude, Dauer und intrazellulärer Lokalisation ermöglicht. Diese verschiedenen Ca^{2+}-Signale kodieren verschiedene Informationen und ermöglichen die gleichzeitige Steuerung verschiedener Ca^{2+}-abhängiger zellulärer Prozesse (Roderick and Cook 2008).

Die Generierung eines Ca^{2+}-Transienten beruht auf der Abgabe von freiem Ca^{2+} aus intrazellulären Speichern via IP_3 oder Ryanodinrezeptoren, die auf der Membran des Endoplasmatischen und Sarkoplasmatischen Retikulums vorkommen sowie auf Ca^{2+}-permeablen Kanälen in der Plasmamembran. In nicht erregbaren Zellen führt eine Aktivierung der Phospholipase C zu einer Spaltung von PIP_2 in DAG und IP_3. IP_3 bindet anschließend seinen Rezeptor in der ER-Membran und bewirkt eine Freigabe an freiem Ca^{2+} (Shumilina et al. 2011).

Das meiste Ca^{2+}, welches das Zytoplasma betritt, wird schnell durch verschiedene zytosolische Puffer gebunden (z. B. Calretinin). Zytosolische Puffer beeinflussen die Amplitude und Dauer des Ca^{2+}-Signals. Diese treten normalerweise als kurze Spikes auf. Ist ein länger anhaltendes Signal notwendig, werden die Spikes wiederholt um Wellen mit unterschiedlicher Frequenz zu erzeugen, die zwischen 1-60 Sekunden bis zu 24 Stunden dauern (Berridge et al. 2000).

Physiologische Ca^{2+}-Signale hängen von der Aktivität von Signalterminatoren ab, welche freies Ca^{2+} zurück in die intrazellulären Kompartimente transportieren sowie über die Plasmamembran aus der Zelle ausschleusen. Die Beendigung des Signals wird durch eine Ca^{2+}-Extrusion durch Na^{+}/Ca^{2+}-Austauscher und durch eine Plasmamembranständige Ca^{2+}-ATPase (PMCA) bewerkstelligt. Um die leeren intrazellulären Ca^{2+}-Speicher wieder zu füllen induziert eine Aktivierung von IP_3-Rezeptoren im Endoplasmatischen Retikulum und der folgende Rückgang der Ca^{2+}-Level einen Ca^{2+}-Einstrom durch ORAI sowie durch kapazitative „Ca^{2+}-Release aktivierte Ca^{2+}-Kanäle“ (CRAC). Der Transport in die intrazellulären Speicher selbst wird dann durch Ca^{2+}-ATPasen gesteuert (SERCA) (Shumilina et al. 2011).

2. Zielsetzung

Patienten mit Glioblastoma multiforme, dem häufigsten Typ eines primären Gehirntumors und gleichzeitig einem der malignesten menschlichen Tumoren, überleben im Median weniger als 1.5 Jahre nach Diagnosestellung. Die hohe Malignität des Tumors resultiert aus der Eigenschaft der Glioblastomzellen das Gehirn zu infiltrieren sowie aus einer scheinbar hohen Therapieresistenz, insbesondere der Radioresistenz der Tumorzellen. Die Infiltration des Gehirns durch oft makroskopisch nicht sichtbare, aus der primären Läsion ausgewanderte und disseminiert proliferierende Glioblastomzellen erschweren die chirurgische Komplettresektion und das Erfassen aller residualen Tumorzellen im Zielvolumen der adjuvanten Radiotherapie. Die hohe Migrationsbereitschaft der Glioblastomzellen wird maßgeblich von ClC-3 Cl^--, IK K^+- und BK K^+-Kanälen reguliert. Eigene Daten sowie Daten aus anderen Laboren belegen, dass subletale Strahlungsdosen, wie sie routinemäßig in Anwendung bei der fraktionierten Strahlentherapie sind, die Migration und Invasion der Glioblastomzellen zusätzlich stimulieren können. Diese radiogene Hypermigration wird möglicherweise durch das SDF-1 (CXCL12)/CXCR4 Chemokin-Signaling ausgelöst und könnte zur Evasion von Glioblastomzellen aus dem Zielvolumen während der Radiotherapie führen.
Es wird ebenso angenommen, dass Ca^{2+}-aktivierte K^+-Kanäle wie BK und IK zentrale Funktionen in der Therapieresistenz von Glioblastomzellen einnehmen. In verschiedenen Zelllinien führt eine bestrahlungsinduzierte Aktivierung von sowohl Ca^{2+}-permeablen Kanälen als auch K^+-Kanälen zu einem Ca^{2+}-Signal, welches einen Zellzyklusarrest zur Folge hat.

Dieses Projekt soll daher *in vitro* als auch *in vivo* im ektopen und orthotopen Glioblastom-Mausmodell klären, inwiefern Ionenkanal-„Targeting“ die intrinsische und über Evasion erworbene Radioresistenz der Glioblastomzellen erniedrigt und als neuartiger Therapieansatz beim Glioblastom in Frage kommen könnte. Zudem soll erörtert werden, welche Ereignisse „up- und downstream“ der jeweiligen Ionenkanal-Aktivierung stattfinden und wie diese durch die in der Therapie angewandte Bestrahlung beeinflusst werden.

Ergebnisse I

3. Die Inhibition von Ca^{2+}-aktivierten IK K^+-Kanälen radiosensibilisiert Glioblastomzellen

Die radiobiologischen Mechanismen von Glioblastomen, die dem schlechten Ansprechen auf eine Strahlentherapie zu Grunde liegen, scheinen durch zahlreiche Faktoren bestimmt zu sein. Hierzu gehören die geringe zelluläre Strahlensensitivität, der hohe Anteil an Krebsstammzellen, eine erhöhte Repopulationsrate, ein protektives Tumormikromilieu, die Infiltration des Tumors mit Knochemarkstämmigen Zellen sowie der hoch invasive Phänotyp von Glioblastomzellen, welcher zu einem infiltrativen Tumorwachstum führt.

In humanen Astrozyten zeigen Ca^{2+}-aktivierte IK K^+-Kanäle eine sehr geringe bis keine Expression (Ishii et al. 1997), wohingegen sie während der neoplastischen Transformation und malignen Progression von Gliomen hochreguliert werden (Ruggieri et al. 2012). In Glioblastomzellen ist daher eine große Anzahl an IK K^+-Kanälen in der Plasmamembran nachweisbar (Fioretti et al. 2004, Fioretti et al. 2006, Fioretti et al. 2009, Abdullaev et al. 2010). Dies lässt auf eine spezifische Funktion bei der Entstehung von Glioblastomen schließen. Somit ist es auch nicht verwunderlich, dass IK K^+-Kanäle für die Glioblastomzellmigration unentbehrlich zu sein scheinen (Catacuzzeno et al. 2012). Dementsprechend korreliert die IK-Proteinexpression des Tumors signifikant mit der schlechten Überlebensprognose von Glioblastompatienten (Turner et al. 2014). IK K^+-Kanäle sind, ähnlich wie in Glioblastomen, auch in anderen Tumorentitäten wie Prostata- (Lallet-Daher et al. 2009), Brust- (Ouadid-Ahidouch et al. 2004) und Pankreaskrebs (Jager et al. 2004) sowie in Lymphomen (Wang et al. 2007) überexprimiert. Hier scheinen sie den Zellzyklus und das Tumorwachstum zu kontrollieren.

Zusätzlich zur Zellmigration und Proliferation könnten K^+-Kanäle zur Radioresistenz von Tumorzellen beitragen (Huber 2013, Huber et al. 2013, Huber et al. 2014). Für das Fungizid Clotrimazol, einen potenten IK-Kanal Inhibitor, wurde gezeigt, dass es das Glioblastomwachstum sowohl *in vitro* als auch *in vivo* vermindern (Khalid et al. 1999, Khalid et al. 2005) und den apoptotischen Zelltod von bestrahlten Glioblastomzellen *in vitro* begünstigen kann (Liu et al. 2010).

In diesem Teil der Arbeit sollte die Beteiligung des IK-Kanals an der Radioresistenz von Glioblastomzellen *in vitro* und *in vivo* mit den beiden Zelllinien T98G und U87MG dargestellt werden.

3.1 Expression von IK K^+-Kanälen

Um eine funktionelle Expression von IK K^+-Kanälen in den Glioblastomzelllinien T98G und U87MG nachzuweisen, wurden die Ströme über die Plasmamembran mittels der Patch-Clamp Methode im Whole-Cell-Modus mit einer physiologischen Bad- und Pipettenlösung aufgenommen. Die Messungen erfolgten vor und nach Ca^{2+}-Permeabilisierung der Plasmamembran mittels des Ca^{2+}-Ionophors Ionomycin (2,5 µM). Um die durch den Ca^{2+}-Einstrom stimulierte Stromfraktion zu ermitteln, wurden der BK K^+-Kanal Inhibitor Paxilline (5 µM) und IK K^+-Inhibitor TRAM34 (10 µM) nacheinander der ionomycinhaltigen Badlösung zugesetzt. Wie in Abb. 1A und B dargestellt (Stegen et al. 2015) inhibierte Paxilline etwa 80% des Auswärtsstromes in T98G Zellen. Die Gabe von TRAM34 inhibierte nahezu die gesamte restliche, Paxilline-insensitive Stromfraktion. Diese TRAM34-sensitive Fraktion ((Stegen et al. 2015); Abb. 1C) wies einen einwärts rektifizierenden Strom mit einer Stromdichte von etwa 100 pS/pF bei negativen Spannungen auf und besaß ein Umkehrpotential nahe dem K^+-Gleichgewichtpotential von E_K = -95 mV. Die Daten zeigen eine funktionelle Expression einer durch Ca^{2+}-aktivierten, einwärts gerichteten, K^+-selektiven und TRAM34-sensitiven Stromfraktion, welche charakteristisch für IK K^+-Kanäle ist. Ca^{2+}-permeabilisierte U87MG Zellen zeigen eine ähnlich hohe IK-Kanal Aktivität, jedoch mit kleineren Paxilline-sensitiven Strömen.

3.2 Ionisierende Strahlung bewirkt eine Änderung der IK K^+-Kanal Aktivität

Um zu prüfen, ob ionisierende Bestrahlung („ionizing radiation“, IR) eine Änderung der IK-Kanal Aktivität bewirkt, wurden T98G Zellen mit 2 Gy 6 MV Photonen mittels Linearbeschleuniger bestrahlt. Nach 2-6 Stunden wurden die Ströme im „Cell-Attached“-Modus mit einer KCl-Pipettenlösung gemessen ((Stegen et al. 2015); Abb.

2A). IR führte zu einem Anstieg der einwärts und auswärts gerichteten Anteile des makroskopischen Cell-Attached-Stromes ((Stegen et al. 2015); Abb. 2B, oben und Abb. 2C, links). Nach zusätzlicher Verwendung des IK-Kanal Inhibitors TRAM34 (10 µM) in der Pipettenlösung ((Stegen et al. 2015); Abb. 2B unten und 2C rechts) war ein durch IR stimulierter Einwärtsstrom nicht mehr zu erkennen ((Stegen et al. 2015); Abb. 2C und D). Dies deutet auf einen durch IR stimulierten IK-Strom hin.

3.3 Ionisierende Strahlung verändert das intrazelluläre Ca^{2+}-Signaling

Wie bereits durch Huber (2013) gezeigt, scheint IR das Ca^{2+}-Signaling zu verändern. Um die Eigenschaften des Ca^{2+}-Signaling „upstream“ der IK-Kanal Aktivierung zu untersuchen, wurde die zytosolisch freie Ca^{2+}-Konzentration ($i[Ca^{2+}]_{free}$) in Fura-2 Ca^{2+}-Imaging Experimenten in T98G Zellen unter Kontrollbedingungen und nach Bestrahlung (2 Gy, 3-5 Stunden nach IR) gemessen. Zusätzlich wurde die Oberflächenexpression des IK-Kanals in Kontroll- und bestrahlten T98G Zellen mittels Immunoblot bestimmt. Die Oberflächenexpression des IK-Kanals wurde durch IR nicht geändert (als Ladungskontrolle diente hier die α_1-Untereinheit der Na^+-Pumpe; (Stegen et al. 2015); Abb. 3A). Da IR einen Anstieg der intrazellulären Ca^{2+}-Konzentration zur Folge hatte ((Stegen et al. 2015); Abb. 3B-D), scheint die durch IR induzierte Zunahme der IK-Kanal Aktivität durch eine erhöhte Ca^{2+}-Konzentration ($i[Ca^{2+}]_{free}$) bedingt zu sein. IR (2Gy) induzierte einen signifikanten Anstieg des „steady-state“ $i[Ca^{2+}]_{free}$ ((Stegen et al. 2015); Abb. 3B und C). Nach Entfernen und erneuter Zugabe an extrazellulärem Ca^{2+} zeigten die bestrahlten Zellen einen stärkeren Abfall sowie einen größeren Wiederanstieg der intrazellulären Ca^{2+}-Konzentration verglichen mit den nicht bestrahlten Kontrollzellen ((Stegen et al. 2015); Abb. 3B und D). Dies deutet auf eine Verschiebung des Gleichgewichtes zwischen passiver Ca^{2+}-Aufnahme und aktiver Ca^{2+}-Extrusion über die Plasmamembran hin, welche somit für den beobachteten Anstieg der intrazellulären Ca^{2+}-Konzentration verantwortlich ist.

3.4 IK-Kanäle beeinflussen die Zellzykluskontrolle

Für K^+-Kanäle wurde gezeigt, dass sie eine Rolle bei der Zellzykluskontrolle von bestrahlten Tumorzellen spielen (Palme et al. 2013). Daher wurde hier der Einbau des Thymidin-Analogons EdU in bestrahlten (2 Gy) und unbestrahlten T98G Zellen 6 Stunden nach IR analysiert. Abb. 4A (Stegen et al. 2015) zeigt das eingebaute EdU (5-Ethynyl-2'-Deoxyuridine) in Abhängigkeit von der DNA-Menge, welche durch die zeitgleiche Färbung der Zellen mit Propidiumiodid als DNA-spezifischem Fluoreszenz-Farbstoff bestimmt wird. IR führte zu einem Anstieg der Zellpopulationen, welche sich in der G_1, S und G_2 Phase des Zellzyklus befinden, mit einer jeweils niedrigen EdU-spezifischen Fluoreszenz-Intensität ((Stegen et al. 2015); Abb. 4B, oben). Dies deutet auf einen durch IR induzierten Arrest in der G_1, S und G_2/M Phase in T98G Zellen hin. Genauer gesagt wird einerseits das Verhältnis zwischen den Zellen in der S Phase, welche EdU einbauen (S_{high}), und den Zellen in der G_1 Phase, welche kein EdU einbauen ($G_{1\ low}$), nach IR kleiner. Zum anderen wird das Verhältnis zwischen den $G_{2\ low}$ und den $G_{1\ low}$ Populationen ebenfalls kleiner ((Stegen et al. 2015); Abb. 4B, unten). Dies deutet auf eine Inhibierung des Übergangs von der G_1 in die S Phase und auf eine Inhibierung der Mitose in bestrahlten T98G Zellen hin.

Um die Aufgaben von IK-Kanälen während der Zellzykluskontrolle zu definieren, wurden die Auswirkungen von Bestrahlung (0, 2, 4, 6 Gy) in Kombination mit der Inhibierung von IK-Kanälen durch TRAM34 in T98G Zellen hinsichtlich der Zellzyklusverteilung untersucht. Dies erfolgte 24 und 48 Stunden nach Bestrahlung durch die Färbung der Zellen mit Propidiumiodid und anschließender Analyse mittels Durchflusszytometrie ((Stegen et al. 2015); Abb. 4C). 24 Stunden nach IR mit 2 und 4 Gy war die G_1 Population der Zellen, verglichen mit dem Kontrollwerten zum Zeitpunkt 0 Stunden, erniedrigt und die S und G_2 Population erhöht ((Stegen et al. 2015); Abb. 4D, links, weiße Kreise). Dies ist ein Hinweis darauf, dass der beobachtete G_1 Arrest, der in den EdU Experimenten beobachtet wurde, nur von kurzer Dauer war. Im Gegensatz dazu ist der prozentuale Anteil der Zellen in der S und G_2 Phase des Zellzyklus 24 Stunden nach IR mit 6 Gy verkleinert, verglichen mit den Zellen die mit 2 oder 4 Gy bestrahlt wurden. Dies deutet auf einen andauernden G_1 Arrest bei einem Teil der mit hoher Strahlendosis behandelten Zellen hin ((Stegen et al. 2015); Abb. 4D, links, weiße Kreise). 48 Stunden nach IR hingegen verringerte

sich der Anteil an Zellen, die sich in der G_1 Phase befanden, und erhöhte sich der Anteil der Zellen in der G_2 Phase, mehr oder minder linear mit der sich erhöhenden Strahlendosis ((Stegen et al. 2015); Abb. 4B,D, rechts, weiße Kreise). Der IK-Kanal Inhibitor TRAM34 (10µM) verzögerte oder verhinderte sogar den strahlungsinduzierten Rückgang der G_1 Zellpopulation und die Zunahme der Zellzahl in der G_2 Phase ((Stegen et al. 2015); Abb. 4D, schwarze Dreiecke). Zusammengenommen legen die Daten eine funktionelle Bedeutung von IK-Kanälen in der Zellzykluskontrolle nahe. Da TRAM34 nur einen geringen Einfluss auf die Zellzyklusverteilung unbestrahlter Zellen zeigt ((Stegen et al. 2015); Abb. 4D, 0Gy), scheinen IK-Kanäle den Zellzyklus nur in jenen Zellen zu regulieren, die genotoxischem Stress ausgesetzt sind.

3.5 TRAM34 verzögert die Reparatur von Doppelstrangbrüchen

Um die residualen DNA Doppelstrangbrüche in T98G Zellen 24 Stunden nach IR mit 0 bzw. 2 Gy zu ermitteln, wurden γH_2AX-Foci in fluoreszenzmikroskopischen Aufnahmen ausgezählt ((Stegen et al. 2015); Abb. 5A). TRAM34 (10µM) erhöhte die durchschnittliche Anzahl an residualen γH_2AX Foci 24 Stunden nach IR mit 2 Gy von etwa 4 (Kontrolle) auf etwa 6 (TRAM34) ((Stegen et al. 2015); Abb. 5B, rechts). Zudem scheint die Anzahl an Foci in Zellkernen mit geringer, mittlerer und hoher Foci-Dichte verglichen mit den jeweiligen Kontrollen ähnlich erhöht zu sein, wodurch ein durch TRAM34 induzierter „Shift“ nach rechts im Histogramm (Anzahl Foci/Anzahl Zellkerne) zu erkennen ist ((Stegen et al. 2015); Abb. 5C). Diese Verschiebung nach rechts könnte eine Verzögerung der Reparatur von DNA Doppelstrangbrüchen in mit TRAM34 behandelten Zellen als Ursache haben.

3.6 TRAM34 wirkt als Radiosensitizer in T98G und U87MG Glioblastomzellen

Nicht bestrahlte Zellen zeigen tendenziell eine erhöhte Foci-Bildung wenn sie für 24 Stunden mit TRAM34 behandelt wurden, wodurch ein genotoxischer Effekt von TRAM34 wahrscheinlich ist ((Stegen et al. 2015); Abb. 5B, links). Jedoch hatte

TRAM34 (10µM) keinen Einfluss auf die „plating efficiency“ (0.25 ± 0.001, n=36) in T98G Zellen verglichen mit Kontrollbedingungen (0.23 ± 0.001, n=36) in einem „delayed plating“ Koloniebildungstest. Ebenso hatte TRAM34 keinen Effekt auf die „plating efficiency“ von U87MG Zellen (0.56 ± 0.01 gegen 0.51 ± 0.01, n=36). Eine Blockade des IK-Kanals scheint demnach keinen Einfluss auf das klonogene Überleben von nicht bestrahlten Glioblastomzellen zu haben. Im Gegensatz dazu zeigen bestrahlte T98G und U87MG Zellen ((Stegen et al. 2015); Abb. 6A und B) einen signifikanten Rückgang des klonogenen Überlebens nach Behandlung mit TRAM34 mit einem Faktor von 1.4 und 1.3 (für T98G bzw. U87MG; Werte entsprechend einer „survival fraction, SF“ von 0.5). TRAM34 zeigt also ähnliche radiosensitivierende Effekte in 2 humanen Glioblastomzelllinien, die sich in ihrer Strahlenempfindlichkeit unterscheiden ((Stegen et al. 2015); „survival fractions“ bei 2 Gy (SF_{2Gy}) lagen bei SF_{2Gy} = 0.56 ± 0.01 bzw. SF_{2Gy} = 0.74 ± 0.02 (für T98G bzw. U87MG); Abb. 6A und B, weiße Balken).

3.7 IK Knock-down bestätigt Spezifität von TRAM34

Um die IK-Kanal Spezifität der beobachteten TRAM34 Effekte auf das klonogene Überleben zu bestätigen, wurde ein IK-Kanal Knock-down in T98G Zellen mittels lentiviraler Transduktion mit IK spezifischen bzw. Kontroll-shRNA enthaltenden Partikeln durchgeführt ((Stegen et al. 2015); Abb. 7A und B; Arbeiten durchgeführt von L. Klumpp). Der T98G Klon #3 mit einer geringen IK-Kanal Expression weist einen höheren prozentualen Anteil an Zellen auf, die sich in der G_1 Phase des Zellzyklus befinden, als der T98G Kontroll-Klon #2. Dies deutet auf unterschiedliche Verdopplungszeiten der beiden Klone hin. Innerhalb 24 Stunden führte eine Bestrahlung in beiden Klonen dosisabhängig zu einem Rückgang der Zellfraktion in der G_1 Phase ((Stegen et al. 2015); Abb. 7C, links) und zu einem Anstieg der Zellpopulation, die sich in der G_2 Phase des Zellzyklus befinden ((Stegen et al. 2015); Abb. 7C, rechts). Erstaunlicherweise hebt TRAM34 die durch Bestrahlung verursachten Veränderungen in der Zellzyklusverteilung im Kontroll-Klon #2 auf, hat aber keinerlei Auswirkungen auf den Klon #3 mit einer geringen IK-Kanal Expression. Beide T98G Klone waren radioresistenter als die parentale T98G Zelllinie ((Stegen et al. 2015); „delayed plating“ Koloniebildungstest, vergleiche Abb. 7D und 6A, weiße

Kreise). Klon #3 mit verminderter IK-Kanal Expression war jedoch signifikant radiosensitiver (SF_{2Gy} = 0.74 ± 0.03, n=12) als der Kontroll-Klon #2 (SF_{2Gy} = 0.83 ± 0.02, n=12; p = 0.02, Zweistichproben-t-Test, korrigiert nach Welch). TRAM34 radiosensitivierte lediglich den Kontroll-Klon #2 und hatte wiederum keinen Effekt auf den IK Knockdown-Klon #3 ((Stegen et al. 2015); Abb. 7D, blaue bzw. rote Dreieck-Symbole). Zusammengenommen zeigen diese Daten sowohl eine IK-Kanal vermittelte Radioresistenz in humanen Glioblastomzelllinien als auch eine Wirkspezifität des IK-Kanal Inhibitors TRAM34.

3.8 IK-Kanal Blockade erhöht Wirksamkeit einer fraktionierten Strahlentherapie in einem ektopen Mausmodell (Arbeiten wurden durchgeführt in Zusammenarbeit mit L. Butz)

Um zu überprüfen, ob eine IK-Kanal Blockade die Wirksamkeit einer fraktionierten Strahlentherapie in einem ektopen *in vivo* Glioblastom-Mausmodell erhöht, wurden immunkompromittierten Nacktmäusen humane U87MG Glioblastomzellen ins rechte Hinterbein injiziert. Hatten die ektopen Glioblastome ein Volumen von etwa 150 µl erreicht ((Stegen et al. 2015); Abb. 8A), wurden die Mäuse auf 4 Behandlungsarme aufgeteilt (Kontrolle, n = 5; TRAM34, n = 4; fraktionierte Bestrahlung (fIR), n = 9; TRAM34 / fIR, n = 6). Abb. 8B und C stellen das Tumorvolumen dar (V_t), normalisiert auf das entsprechende Tumorvolumen zu Beginn der Behandlung an Tag 0 (V_0), vor, während (blaue Pfeile) und nach Behandlung mit fIR (5 x 0 Gy oder 5 x 4 Gy) und TRAM34 Injektionen (5 x 0 mg oder 5 x 120 mg/kg Körpergewicht; 6 Stunden vor jeder IR Fraktion). Eine von 6 Mäusen, die mit fIR/TRAM34, und 2 von 9 Mäusen, die ausschließlich mit fIR allein behandelt wurden, zeigten einen kompletten Rückgang des Tumors. Abb. 8 zeigt die „time to progression“ (Zeitraum zwischen Behandlungsstart an Tag 0 und dem Zeitpunkt, an dem das behandelte Glioblastom das Anfangsvolumen V_0 überschritten hat) für alle 4 Behandlungsgruppen. Lediglich die fIR/TRAM34 Gruppe weißt eine signifikant längere „time to progression“ Zeitspanne auf als die Kontrollgruppe.

Das exponentielle Wachstum der ektopen Glioblastome kann durch das lineare Verhältnis zwischen dem mittleren (± SE) logarithmierten Tumorvolumen (ln (V_t / V_0)) und der Zeit dargestellt werden ((Stegen et al. 2015); Abb. 8E, F). Die Steigungen

dieser Verhältnisse ($\delta_{\ln(Vt/V0)}/\delta_t$) als Maß für die exponentielle Wachstumskinetik vor und während der Behandlung als auch der durch die Behandlung induzierte Rückgang der Steigung ($\Delta\delta_{\ln(Vt/V0)}/\delta_t$) sind für die einzelnen Tumore in Abb. 8 G-I gezeigt. Ausschließlich die fIR/TRAM34 Gruppe zeigte einen signifikanten durch die Behandlung induzierten Rückgang des exponentiellen Wachstums verglichen mit der Kontrollgruppe ((Stegen et al. 2015); Abb. 8I). Die *in vivo* Experimente zeigen zum einen, dass TRAM34 in pharmakologisch relevanten Dosen verabreicht werden kann und zum anderen, dass eine begleitende TRAM34-Chemotherapie die Wirksamkeit einer fraktionierten Strahlentherapie erhöhen könnte.

3.9 Patienten mit hoher IK mRNA Abundanz zeigen ein geringeres progressionsfreies Überleben

Um eine mögliche Beteiligung von IK-Kanälen bei der Resistenz von Glioblastomen während der Therapie in der Klinik zu erörtern, wurde der „Cancer Genome Atlas“ durchsucht unter Verwendung der provisorischen Glioblastoma Multiforme und „Low-Grade“ Glioblastom-Datenbanken. Eine hohe IK mRNA Abundanz ist demnach mit einem geringeren progressionsfreien Überleben in Patienten mit „Low-Grade“ Gliomen und Glioblastomen assoziiert ((Stegen et al. 2015); Abb. 9A und B).

Diskussion I

In diesem Teil der Arbeit wurde gezeigt, dass IR Einfluss auf das Ca^{2+}-Signaling nimmt und somit die Aktivierung von Ca^{2+}-aktivierten „intermediate conductance“ IK K^+-Kanälen in Glioblastomzellen steuert. Die durch IR stimulierten IK-Kanäle wiederum wirken bei der Stressantwort von Glioblastomzellen mit, indem sie möglicherweise den Zellzyklus anpassen. Diese durch IK-Kanäle vermittelte Stressantwort ist für das Überleben von bestrahlten Glioblastomzellen essenziell. Dies wird dadurch deutlich, dass eine pharmakologische Inhibierung der IK-Kanäle die Glioblastomzellen radiosensibilisiert.

Das durch Bestrahlung modifizierte Ca^{2+}-Signaling und/oder die K^+-Kanal Aktivität wurde bereits in verschiedenen Tumorentitäten nachgewiesen, wie beispielsweise in Leukämie-Zellen (Heise et al. 2010, Palme et al. 2013), Adenokarzinomen der Lunge (Huber et al. 2012) und Glioblastomen (Steinle et al. 2011). In Leukämiezellen führt eine bestrahlungsinduzierte, gleichzeitige Aktivierung von sowohl Ca^{2+}-permeablen Kanälen als auch K^+-Kanälen zu einem Ca^{2+}-Signal, welches einen Zellzyklusarrest durch eine CaMKII-vermittelte Inhibierung des „mitose-promoting factor“ cdc2 zur Folge hat. Eine Inhibierung des K^+-Kanals setzt den Zellzyklusarrest von bestrahlten Leukämiezellen außer Kraft und bewirkt damit eine Radiosensitivierung (Palme et al. 2013). In Adenokarzinomen der Lunge tragen K^+-Kanäle zu einer gesteigerten Glukoseaufnahme in bestrahlten Zellen bei. Eine erhöhte Glukosemenge ist möglicherweise notwendig, um der durch DNA-Schädigung entstandenen Energiekrise entgegen zu wirken und die Kohlenhydrate bereit zu stellen, die für die Histon-Acetylierung während der DNA-Kondensation notwendig sind (Dittmann et al. 2013).

In Glioblastomen ist eine IR-induzierte Aktivierung von BK K^+-Kanälen mit einer radiogenen Hypermigration der Tumorzellen verbunden (Huber 2013, Huber et al. 2013). Auch für IK-Kanäle wurde gezeigt, dass sie an der Serum- (Catacuzzeno et al. 2011), Bradykinin- (Cuddapah et al. 2013) und CXCL12- (SDF-1) abhängigen Glioblastomzellmigration mitwirken (Sciaccaluga et al. 2010). Übereinstimmend mit diesen *in vitro* Daten ist die Tatsache, dass der IK Inhibitor TRAM34 die Hirninfiltration von humanen *Xeno*graft-Glioblastomzellen in einem orthotopen Mausmodell inhibiert (D'Alessandro et al. 2013).

Eine hohe IK-Kanal Expression wurde auch mit einer Hochregulation von Stammzellmarkern in Verbindung gebracht (Ruggieri et al. 2012). Diese Glioblastomstammzellen zeigen einen hoch migrativen Phänotypen und scheinen hauptverantwortlich für die Hirninvasion zu sein (Liu et al. 2006, Nakada et al. 2013). Tatsächlich vermitteln IK-Kanäle die Migration von neuronalen Vorläuferzellen, so genannten Neuroblasten, hin zur Kopfvorderseite um sich zu Interneuronen im Riechkolben des adulten Maushirns zu entwickeln (Turner and Sontheimer 2014). Glioblastomstammzellen neigen auch dazu therapieresistenter zu sein als der Haupttumor, bestehend aus „differenzierten“ Glioblastomzellen (Huber 2013, Huber et al. 2013, Huber et al. 2014). Dieses Projekt zeigt, sowohl bei Glioblastomzelllinien *in vitro* als auch in einem ektopen *in vivo* Mausmodell, dass IK-Kanäle neben der Gehirninfiltration auch eine Rolle bei der Radioresistenz spielen könnten. Ein Nachweis für solch eine IK-Kanal Funktion in Glioblastomzellen wurde bereits *in vitro* nachgewiesen (Liu et al. 2010).

Die mögliche Doppelfunktion von IK-Kanälen bei der Hirninfiltration und Radioresistenz von Glioblastomen spiegelt sich auch in retrospektiven klinischen Daten wieder. Laut der REMBRANDT Patientendatenbank des „National Cancer Institute“ sind IK-Kanäle in 30% der Patienten um das 1.5 fache im Vergleich zu gesundem Hirngewebe hochreguliert. Noch wichtiger ist die Begebenheit, dass eine Überexpression von IK-Kanälen in Gliomen mit einer geringeren Lebenserwartung der Patienten korreliert (Turner et al. 2014). Eine Abfrage der „Cancer Genome Atlas“ Datenbank zeigt, dass eine höhere IK mRNA Abundanz in Gliomen mit einem kürzeren progressionsfreien Überleben von Glioblastom- und „Low-Grade“ Gliompatienten korreliert. Die Interpretation dieser Daten ist allerdings begrenzt, da eine Subgruppenanalyse der Patienten, die unter anderem die Tumorgröße, die Art der Strahlentherapie etc. einschließen würde, bei einer Abfrage des „Cancer Genome Atlas“ und der REMBRANDT Datenbank (Turner et al. 2014) nicht möglich war. Unter der Annahme, dass die Therapie der Patienten der Datenbanken eine Strahlentherapie mit beinhaltet, könnten die Zusammenhänge jedoch auf eine radioprotektive Wirkungsweise von IK-Kanälen in Gliomen hinweisen.

IK-Kanäle könnten daher einen neuen, hoch attraktiven Angriffspunkt für eine Anti-Gliomtherapie darstellen. Bereits für verschiedenste Krankheiten, wie etwa bei der Sichelzellanämie (Ataga et al. 2006, Ataga et al. 2008, Ataga and Stocker 2009), bei Alzheimer (Maezawa et al. 2012) und verschiedenen Entzündungskrankheiten (Lam

and Wulff 2011) wurde die Blockade von IK-Kanälen als Therapieansatz vorgeschlagen. Die TRAM34 Konzentration, die in diesem Projekt verwendet wurde (10 µM), liegt vermutlich weit über der Plasmakonzentration, die in klinischen Studien erreicht werden würde. Senicapoc (ICA-17043), ein weiterer IK Kanal Inhibitor, welcher wirksamer ist als TRAM34 ($IC_{50\text{-Senicapoc}}$ = 11 nM; $IC_{50\text{-TRAM34}}$ = 20 nM), kann oral verabreicht werden und wurde bereits in klinischen Studien als sicher befunden (Maezawa et al. 2012). Des Weiteren resultierte eine tägliche orale Gabe von 10 mg Senicapoc in einer durchschnittlichen Plasmakonzentration von 100 ng/ml (etwa 0.3 µM). Plasmaproben von Patienten, welche Senicapoc enthielten, inhibierten hierbei bis zu 70% der IK-Kanäle (Ataga et al. 2008). IK-Kanäle als Therapie-Target zu verwenden ist in einem klinischen Setting also wahrscheinlich realisierbar. Eine Verabreichung einer erhöhten Medikamentendosis bei geringeren Nebenwirkungen könnte bei Glioblastompatienten sogar durch eine intrakranielle Medikamentengabe erreicht werden.

IK-Kanäle scheinen sowohl einen migrativen und infiltrativen Phänotypen als auch die zelluläre Radioresistenz von Glioblastomen zu unterstützen. Sie tragen somit zu den Eigenheiten von Glioblastomen bei, die vermutlich für den Therapiemisserfolg und der damit verbundenen schlechten Prognose der Patienten verantwortlich sind. Somit wäre eine pharmakologische Blockade der IK-Kanäle in Kombination mit einer Operation und anschließender Strahlentherapie plausibel.

Ergebnisse II

4. Fraktionierte Bestrahlung stimuliert die Gehirninfiltration von Glioblastomzellen

Glioblastoma multiforme bestehen zum Teil aus Zellen die einen hoch migrativen Phänotypen aufweisen und weite Strecken innerhalb des Gehirns zurücklegen können (Johnson et al. 2009). Eine Verschlechterung des Tumormikromilieus wie etwa durch Hypoxie, Nährstoffmangel oder ein niedriger pH-Wert scheinen dafür verantwortlich zu sein, dass Tumorzellen von einem sessilen “Grow” zu einem invasiven “Go” Phänotypen wechseln. Durch Migration und Invasion in umliegendes Gewebe könnten Tumorzellen so der lokal entstandenen Belastung entkommen und auf diese Weise Tumorsatelliten in der Nähe des primären Tumorherdes bilden (Hatzikirou et al. 2012).

Eine Bestrahlung während der Strahlentherapie könnte den “Go” Phänotypen ebenfalls hervorrufen. Es wurde bereits gezeigt, dass subletale Bestrahlungsdosen die Migration, Invasion und die Streuung verschiedener Tumorentitäten *in vitro* als auch in Tumormodellen induzieren. Hierzu gehören das Plattenepithelkarzinom des Kopf-Hals-Bereiches (Pickhard et al. 2011), Adenokarzinom der Lunge (Jung et al. 2007, Zhou et al. 2011), Meningiom (Kargiotis et al. 2008), Medulloblastom (Asuthkar et al. 2011), und das Glioblastom (Wild-Bode et al. 2001, Wick et al. 2002, Tabatabai et al. 2006, Badiga et al. 2011, Canazza et al. 2011, Rieken et al. 2011, Steinle et al. 2011, Kil et al. 2012, Vanan et al. 2012, Wang et al. 2013, Shankar et al. 2014).

Da es in Glioblastomen deutliche Hinweise für solch eine radiogene Hypermigration gibt ist es naheliegend, dass eine durch die fraktionierte Strahlentherapie induzierte erhöhte Migrationsbereitschaft zu einem lokoregionalen Therapiemisserfolg durch ein Auswandern von Tumorzellen aus dem Bestrahlungszielvolumen führen kann. Die bisherigen *in vivo* Daten über eine radiogene Hypermigration von Glioblastomen wurden mit Hilfe von Zellen akquiriert, die vor der Transplantation bestrahlt wurden (Wild-Bode et al. 2001), nach einer Bestrahlung des gesamten Gehirns mit einer Einzeldosis von 8 Gy (Tabatabai et al. 2006), nach einer Teilbestrahlung des Gehirns mit einem großen Bestrahlungsfeld (1 cm^2) und Einzeldosen von 8 und 15 Gy (Wang et al. 2013) oder einer stereotaktischen Glioblastombestrahlung mit einer Einzeldosis

von 50 Gy (Shankar et al. 2014). Dieser Teil der Dissertation zeigt die radiogene Hypermigration von Glioblastomzellen in einem orthotopen *Xeno*graft-Mausmodel mit einem Setting, welches eher der klinischen Situation entspricht.

IR scheint ebenfalls die Expression des Chemokins SDF-1 ("stromal cell-derived factor 1", CXCL12) in verschiedenen Tumorentitäten zu induzieren, unter anderem in Glioblastomen (Tabatabai et al. 2006, Kioi et al. 2010, Kozin et al. 2010, Wang et al. 2013). Für Glioblastomzellen wurde gezeigt, dass sie den CXCR4 Chemokinrezeptor exprimieren und SDF-1 die Glioblastomzellmigration, durch ein über CXCR4 vermitteltes Ca^{2+}-Signal, stimuliert (Sciaccaluga et al. 2010). Dies deutet auf die Möglichkeit eines autokrinen SDF-1/CXCR4 Signalweges hin der zur radiogenen Hypermigration beiträgt.

Zudem wurde für BK K^+-Kanäle gezeigt, dass sie die Migration von Glioblastomzellen unterstützen, indem sie sowohl das Ca^{2+}-Signal, welches die Migration programmiert, als auch Zellvolumenänderungen, die die Migration motorisiert, steuern. Interessanterweise wird die Aktivität dieser Kanäle durch IR erhöht (Steinle et al. 2011).

Dieses Projekt hatte zum einen das Ziel, die radiogene Hypermigration von Glioblastomzellen in einem orthotopen Mausmodel zu quantifizieren, und zum anderen das Potential zu bestimmen, diese radiogene Hypermigration durch Targeting des BK-Kanals zu unterbinden. Andere Studien, die humane U87MG Glioblastomzellen für ihre orthotopen Mausmodelle verwendeten, zeigten abgekapselte Tumore mit geringem infiltrativen Wachstum (Woo et al. 2014). Da diese Zellen geeignet erschienen, eine quantitative Analyse der Zellzahl und Migrationsstrecke von Glioblastomzellen durchzuführen, wurden in diesem Projekt der stabil transfizierte U87MG-Katushka Klon verwendet. Dieser exprimiert das dunkelrote Fluoreszenzprotein Katushka welches es ermöglicht, Glioblastomzellen histologisch zu verfolgen.

4.1 Expression von BK K^+-Kanälen und klonogenes Überleben

Zunächst wurde für die U87MG-Katushka Zelllinie getestet, ob sie BK-Kanäle exprimieren, und ob der BK-Kanal Inhibitor Paxilline einen radiosensitivierenden Effekt besitzt. Letzteres war notwendig, da eine pharmakologische Blockade der BK-

verwandten Ca^{2+}-aktivierten IK-Kanäle T98G und U87MG Glioblastomzellen radiosensibilisiert (Stegen et al. 2015). Ähnliche radiosensitivierende Eigenschaften von Paxilline würden die Interpretation der *in vivo* Effekte auf die Tumorzellmigration und Gehirninfiltration erschweren.

Wie bereits für T98G und die parentale U87MG Zelllinie beschrieben (Steinle et al. 2011), exprimiert der U87MG-Katushka Klon BK-Kanäle. Dies konnte in Whole-Cell Patch-Clamp Experimenten mit K-Glukonat in der Pipettenlösung und NaCl in der Badlösung nachgewiesen werden. U87MG-Katushka Zellen zeigen große Auswärtsströme im Bereich von einigen Nano-Ampere ((Butz und Stegen et al. 2015, eingereichtes Manuskript); Abb. 1A, links). Diese Ströme waren auswärts rektifizierend und konnten durch den BK-Kanal Inhibitor Paxilline geblockt werden ((Butz und Stegen et al. 2015, eingereichtes Manuskript); Abb. 1A, rechts und 1B), was auf eine funktionelle Expression von BK-Kanälen schließen lässt. Ob eine Blockade der BK-Kanäle einen radiosensitivierenden Effekt zur Folge hat wurde in einem “delayed plating” Koloniebildungstest untersucht. Im Gegensatz zur Blockade von IK-Kanälen (Stegen et al. 2015) führt eine Inhibition von BK-Kanälen in den Zelllinien T98G und U87MG-Katushka durch Paxilline nicht zu einem reduzierten klonogenen Überleben nach Bestrahlung ((Butz und Stegen et al. 2015, eingereichtes Manuskript); Abb. 2C und D).

4.2 IR erhöht die Aktivität von BK K^+-Kanälen und die Migration

IR stimuliert *in vivo* die Expression des Chemokins SDF-1 an der Invasionsfront von Glioblastomen (Wang et al. 2013). Aus diesem Anlass wurde für die beiden Zelllinien T98G und U87MG-Katushka *in vitro* die radiogene BK-Kanal Aktivität, die Transfilter-Migration und die Rolle des SDF-1 Signaling hierbei untersucht, um IR-induzierte Signalereignisse „upstream“ einer BK-Kanal Aktivierung zu bestimmen. In “Cell-Attached” Patch-Clamp Messungen (KCl Pipetten- und NaCl Badlösung) von U87MG-Katushka Zellen ((Butz und Stegen et al. 2015, eingereichtes Manuskript); Abb. 2A) wurden hoch-leitende Ionenkanäle (unitary conductance, g ≈ 200 pS, ((Butz und Stegen et al. 2015, eingereichtes Manuskript); Abb. 2B)) mit zunehmender positiver Spannung aktiviert. In bestrahlten Zellen (2Gy, 2-4.5 h nach IR) wurde eine Aktivierung der Kanäle bereits unterhalb 0 mV beobachtet ((Butz und Stegen et al.

2015, eingereichtes Manuskript); Abb. 2A, rechts und Abb. 2C, schwarze Dreiecke). Im “Cell-Attached” Modus nimmt eine Spannungs-Klemme von 0 mV zwischen Pipetten- und Badlösung die Transmembranströme bei einem physiologischen Membranpotential auf. Daher deuten die Ströme, die in bestrahlten Zellen bei 0 mV gemessen wurden, auf eine Aktivität von “large conductance” Ionenkanälen bei physiologischem Membranpotential hin. In nicht bestrahlten Kontrollzellen hingegen konnte eine Aktivierung der Kanäle erst ab einer Spannungs-Klemme oberhalb +50 mV erreicht werden ((Butz und Stegen et al. 2015, eingereichtes Manuskript); Abb. 2C, weiße Kreise). Dementsprechend überstiegen die durchschnittlichen makroskopischen Cell-Attached Auswärtsströme der bestrahlten Zellen die von unbestrahlten Zellen um das Zweifache ((Butz und Stegen et al. 2015, eingereichtes Manuskript); Abb. 2D, schwarze Symbole und Abb. 2E, links). Paxilline (5 µM, (Butz und Stegen et al. 2015, eingereichtes Manuskript); Abb. 2D, rote Symbole und Abb. 2E, rechts) blockte etwa die Hälfte des Auswärtsstromes in bestrahlten Zellen, wohingegen es keinen Effekt auf die Kontrollzellen hatte. Die Paxilline-sensitive Stromfraktion von bestrahlten Zellen zeigt eine typische Auswärtsrektifizierung ((Butz und Stegen et al. 2015, eingereichtes Manuskript); Abb. 2F, schwarze Dreiecke). Die spannungsabhängige Offenwahrscheinlichkeit, der hohe Leitwert und die Paxilline-Sensitivität definieren den hoch-leitenden Kanal als BK K^+-Kanal. Am wichtigsten hierbei ist dass BK-Kanäle in bestrahlten Zellen bei einem physiologischen Membranpotential aktiv sind, wodurch eine funktionell wichtige Rolle in bestrahlten Glioblastomzellen vorhanden sein könnte.

Eine BK-Kanal Aktivierung in bestrahlten U87MG-Katushka Zellen wurde begleitet von einer schnelleren Chemotaxis in einem Transfilter-Migrationsassay mit einem FCS Gradienten, verglichen mit unbestrahlten Kontrollzellen ((Butz und Stegen et al. 2015, eingereichtes Manuskript); Abb. 2G und 2H, links). Der BK Kanal Inhibitor Paxilline (5 µM) unterband die radiogene Hypermigration, wohingegen er keinen Einfluss auf die basale Migration zeigte ((Butz und Stegen et al. 2015, eingereichtes Manuskript); Abb. 2H, rechts). Die radioinduzierte Hypermigration von U87MG-Katushka Zellen scheint also von einer radiogenen Erhöhung der BK Kanal Aktivität abhängig zu sein (Arbeiten wurden zusammen mit L. Butz durchgeführt).

Um die bereits zuvor publizierten Daten einer Paxilline-sensitiven radiogenen Hypermigration (Steinle et al. 2011) zu bestätigen, wurden bestrahlte T98G Zellen (0 oder 2 Gy, 2-4.5 h nach IR) im “Cell-Attached” Patch-Clamp Modus mit KCl Pipetten-

und NaCl Badlösung gemessen. Ähnlich den U87MG-Katushka Zellen zeigten bestrahlte T98G Glioblastomzellen eine spannungsabhängige Aktivierung von “large-conductance” (g ≈ 200 pS) Kanälen bei negativeren Spannungs-Klemmen als unbestrahlte T98G Kontrollzellen ((Butz und Stegen et al. 2015, eingereichtes Manuskript); Suppl. Abb. 1A-C). Die Kanäle waren in bestrahlten T98G Zellen bei physiologischen Membranpotentialen aktiv (d. h. bei 0 mV Spannungs-Klemme) und zeigten einen auswärts rektifizierenden, Paxilline-sensitiven, makroskopischen Cell-Attached Strom ((Butz und Stegen et al. 2015, eingereichtes Manuskript); Suppl. Abb. 1D-F). Dieser deutet auf eine radiogene BK-Kanal Aktivierung hin. Diese Aktivierung führte zu einer radiogenen Hypermigration ((Butz und Stegen et al. 2015, eingereichtes Manuskript); Suppl. Abb. 1G und 1H, links), welche abhängig war von BK-Kanälen, da ein Knockdown dieser Kanäle die Migrationsgeschwindigkeit von bestrahlten Zellen auf die Werte von nicht bestrahlten Kontrollzellen absenkte, wohingegen die basale Migration der Kontrollzellen nicht beeinflusst wurde ((Butz und Stegen et al. 2015, eingereichtes Manuskript); Suppl. Abb. 1H, rechts) (Arbeiten von L. Butz durchgeführt). Dies zeigt, dass die zuvor publizierte radiogene und Paxilline-sensitive Hypermigration von T98G Zellen (Steinle et al. 2011) durch eine radiogene BK-Kanal Aktivierung vermittelt wird.

4.3 Expression verschiedener Invasions-Marker nach IR

Um zu überprüfen, ob eine radiogene Hypermigration mit einem hyperinvasiven Phänotypen assoziiert sein könnte und um durch Bestrahlung ausgelöste Signalereignisse identifizieren zu können, wurden die Abundanzen einiger ausgewählter mRNAs nach fraktionierter Bestrahlung (5 x 2 Gy) und von U87MG-Katushka Kontrollzellen (5 x 0 Gy) verglichen (Arbeiten durchgeführt von L. Klumpp und L. Butz). Hierbei handelt es sich um die mRNAs des BK-Kanals, der Matrix-Metalloproteinasen MMP-2 und MMP-9, SDF-1 und dem SDF-1 Rezeptor CXCR4. Fraktionierte Bestrahlung hatte keinen Einfluss auf die Abundanz der BK-Kanal oder CXCR4 mRNAs, erhöhte jedoch signifikant die Abundanz der MMP-2, MMP-9 und SDF-1 mRNAs ((Butz und Stegen et al. 2015, eingereichtes Manuskript); Abb. 3A). Dies deutet auf einen durch Bestrahlung induzierten hyperinvasiven Phänotypen und ein verstärktes Chemokin-Signaling hin.

Der Transkriptionsfaktor HIF-1 α ("hypoxia-inducible factor-1 α) bewirkt eine erhöhte Expression von CXCR4 und SDF-1 (Greenfield et al. 2010). In U87MG-Katushka führt IR (1 x 2 Gy, 2 h nach IR) zu einer Stabilisierung des HIF-1 α Proteins ((Butz und Stegen et al. 2015, eingereichtes Manuskript); Abb. 3B, oberer Blot und Abb. 3C, links). In Übereinstimmung mit den mRNA Daten ist eine Stabilisierung von HIF-1 α nicht mit einer Erhöhung der Proteinabundanz des CXCR4 Chemokin-Rezeptors assoziiert ((Butz und Stegen et al. 2015, eingereichtes Manuskript); Abb. 3B, mittlerer Blot und Abb. 3C, rechts), jedoch mit einer signifikant erhöhten SDF-1 Immunofluoreszenz ((Butz und Stegen et al. 2015, eingereichtes Manuskript); Abb. 3D und 3E) (Arbeiten durchgeführt von L. Butz).

4.4 IR induziert SDF-1/CXCR4 Signaling

Für SDF-1 wurde bereits gezeigt, dass es eine Ca^{2+}-Freisetzung aus Ca^{2+}-Speichern via CXCR4, Phospholipase C und der Bildung von Inositol-1,4,5-Phosphat induzieren kann (Peng et al. 2004). Interessanterweise scheinen BK-Kanäle mit diesen Inositol-1,4,5-Triphosphat Rezeptoren in Lipid Rafts verknüpft zu sein (Weaver et al. 2007). Um den Einfluss des SDF-1 Signaling bei der radiogenen BK-Kanal-Aktivierung und der Hypermigration abschätzen zu können, wurde der Effekt von konditioniertem Medium (von bestrahlten U87MG-Katushka (2 h nach IR) und Kontrollzellen) auf das Ca^{2+}-Signaling untersucht, in Abhängigkeit einer Blockade des CXCR4 Chemokinrezeptors mit AMD3100 (1µM). Konditioniertes Medium von bestrahlten Zellen hatte einen signifikant schnelleren Anstieg des zytosolisch freien Ca^{2+} ($_{free}[Ca^{2+}]_i$) zur Folge als das unbestrahlter Kontrollzellen ((Butz und Stegen et al. 2015, eingereichtes Manuskript); Abb. 3F und 3G, weiße Balken). Wurde AMD3100 zusammen mit dem konditionierten Medium zugeführt, konnte der durch IR induzierte Effekt auf $_{free}[Ca^{2+}]_i$ komplett unterbunden werden ((Butz und Stegen et al. 2015, eingereichtes Manuskript); Abb. 3G, schwarze Balken). Dies bedeutet, dass IR eine Anreicherung an Faktoren im Medium bewirkt welche das CXCR4 Signaling stimulieren. Gleichermaßen inhibierte AMD3100 (1µM) die BK-Kanal Aktivierung durch IR (AMD3100-Gabe während IR und 2-4.5 h nach IR, (Butz und Stegen et al. 2015, eingereichtes Manuskript); Abb. 3H und 3I). Diese Daten zeigen demnach eine

Beteiligung des SDF-1/CXCR4 Signaling bei der radiogenen BK-Kanal Aktivierung in U87MG-Katushka Zellen.

Auch T98G Zellen exprimieren CXCR4 sowie SDF-1 mRNA und Protein. IR (2 Gy, 2 h nach IR) induzierte einen Anstieg der SDF-1 Proteinabundanz in T98G Zellen, sichtbar in Immunfluoreszenzbildern ((Butz und Stegen et al. 2015, eingereichtes Manuskript); Suppl. Abb. IIA-C) (Arbeiten durchgeführt von L. Butz). Konditioniertes Medium von bestrahlten T98G Zellen (2Gy, 2 h nach IR) zeigte in einem ELISA eine erhöhte SDF-1 Konzentration im Vergleich zu Kontrollzellen ((Butz und Stegen et al. 2015, eingereichtes Manuskript); Suppl. Abb. IID). Dementsprechend stimulierte konditioniertes Medium von bestrahlten T98G Zellen (2 Gy, 2 h nach IR) einen Anstieg an $_{free}[Ca^{2+}]_i$ in T98G Zellen, wohingegen konditioniertes Medium von Kontrollzellen dies nicht zur Folge hatte ((Butz und Stegen et al. 2015, eingereichtes Manuskript); Suppl. Abb. IIE und IIF, links). Der CXCR4 Antagonist AMD3100 (1 µM) verhinderte die Ca^{2+}-Signale in T98G Zellen die durch konditioniertes Medium von bestrahlten Zellen hervorgerufen wurden ((Butz und Stegen et al. 2015, eingereichtes Manuskript); Suppl. Abb. IIF, rechts). Diese Daten deuten daher auf ein radiogenes SDF-1 Signaling auch in T98G Zellen hin.

4.5 SDF-1 induziert Ca^{2+}-Signale

Um zu überprüfen, ob SDF-1 die radiogene BK-Kanal Aktivierung in U87MG-Katushka Zellen und die Hypermigration nachahmen kann, wurde $_{free}[Ca^{2+}]_i$ während der Gabe von SDF-1 gemessen ((Butz und Stegen et al. 2015, eingereichtes Manuskript); Abb. 4A und 4B). SDF-1 (50 nM) bewirkte einen lang andauernden Anstieg an $_{free}[Ca^{2+}]_i$. Zusätzlich stimulierte die Gabe von SDF-1 einen Paxilline-sensitiven Auswärtsstrom in “Cell-Attached” Messungen ((Butz und Stegen et al. 2015, eingereichtes Manuskript); Abb. 4C-F). Die durch SDF-1 hervorgerufene Stromfraktion ((Butz und Stegen et al. 2015, eingereichtes Manuskript); Abb. 4E) ähnelte stark den durch Bestrahlung induzierten Strömen bezüglich der Spannungsabhängigkeit und den absoluten Werten ((Butz und Stegen et al. 2015, eingereichtes Manuskript); vergleiche Abb. 4E mit Abb. 2D, schwarze Dreiecke). SDF-1 erhöhte ebenso die Transfilter-Migration von U87MG-Katushka Zellen ((Butz und Stegen et al. 2015, eingereichtes Manuskript); Abb. 4G und 4H, weiße Balken;

Arbeiten ausgeführt von E. Haehl und L. Butz). Der BK-Kanal Inhibitor Paxilline (5 µM) inhibierte die durch SDF-1 induzierte Steigerung der Transfilter-Migration ohne die basale Migration signifikant zu hemmen ((Butz und Stegen et al. 2015, eingereichtes Manuskript); Abb. 4H, schwarze Balken). Zusammengenommen stimuliert SDF-1, ähnlich der Bestrahlung, die Hypermigration die abhängig ist von einer BK-Kanal Aktivierung.

Auch in T98G Zellen induziert eine akute Gabe von SDF-1 (50 nM) einen lang andauernden Anstieg an $_{free}[Ca^{2+}]_i$ sowie eine Aktivierung eines makroskopischen Auswärtsstromes in "Cell-Attached" Messungen ((Butz und Stegen et al. 2015, eingereichtes Manuskript); Suppl. Abb. IIIC und IIID). Eine Analyse der Einzelkanäle ((Butz und Stegen et al. 2015, eingereichtes Manuskript); Suppl. Abb. IIIE) zeigt einen BK-ähnlichen "large conductance" Kanal (p ≈ 170 pS) der mit steigender Spannung aktiviert wird ((Butz und Stegen et al. 2015, eingereichtes Manuskript); Suppl. Abb. IIIF und IIIG). SDF-1 (50 nM) führte zu einer Verschiebung der aktivierenden Spannung hin zu negativeren Spannungen ((Butz und Stegen et al. 2015, eingereichtes Manuskript); Suppl. Abb. IIIG).

Diese *in vitro* Daten des U87MG-Katushka Klons zeigen eine radiogene BK K^+-Kanal abhängige Hypermigration, wie sie bereits zuvor für T98G und die parentalen U87MG Zellen beschrieben wurde (Steinle et al. 2011). Zudem deuten diese Daten darauf hin, dass ein radiogenes SDF-1 Signaling zumindest teilweise die radiogene Hypermigration „upstream" von BK hervorruft.

4.6 U87MG-Katushka in einem orthotopen Glioblastom-Mausmodel (Arbeiten wurden durchgeführt von L. Butz)

Für die Generierung von orthotopen Glioblastomen wurden U87MG-Katushka Zellen stereotaktisch in das rechte Striatum von NSG Mäusen eingebracht ((Butz und Stegen et al. 2015, eingereichtes Manuskript); Abb. 5A und 5B). Die Inokulation der Zellen resultierte in der Bildung eines soliden und weitestgehend eingekapselten Glioblastoms, welches exponentiell während der ersten 3 Wochen nach dem Setzen des Tumors wuchs ((Butz und Stegen et al. 2015, eingereichtes Manuskript); Abb. 5C und 5D). Die rechte, das Glioblastom tragende Hemisphäre der mit Isofluran

narkotisierten Mäuse wurde an den Tagen 8-12 fraktioniert bestrahlt (6 MV Photonen) mit einer täglichen Dosis von 2 Gy unter Verwendung von Mäusehalterungen, welche im Bestrahlungsfeld des Linearbeschleunigers befestigt wurden ((Butz und Stegen et al. 2015, eingereichtes Manuskript); Abb. 5D und 5E). Mauskörper und –kopf, die keine Strahlung abbekommen sollten, wurden durch Bleiblöcke abgeschirmt (Filmdosimetrie siehe (Butz und Stegen et al. 2015, eingereichtes Manuskript); Abb. 5F und 5G). Die fraktionierte Bestrahlung (5 x 2 Gy) wurde durch die Mäuse gut toleriert, erkennbar durch einen sehr schwachen Rückgang des Körpergewichtes ((Butz und Stegen et al. 2015, eingereichtes Manuskript); Abb. 5H, schwarze Symbole). Die Mäuse, die Paxilline erhielten, entwickelten eine vorrübergehende Ataxie und zeigten einen Gewichtsverlust von 10-15% verglichen mit der Kontrollgruppe, welcher sich nach Beendigung der Paxilline-Behandlung wieder normalisierte ((Butz und Stegen et al. 2015, eingereichtes Manuskript); Abb. 5H). An Tag 22 wurden die Mäuse der 4 Behandlungsgruppen sakrifiziert und die Gehirne für histologische Untersuchungen entnommen.

4.7 CXCR4, SDF-1 und BK K^+-Kanal Expression in orthotopen Glioblastomen

(Arbeiten wurden durchgeführt von L. Butz)

U87MG-Katushka Zellen exprimieren auch noch wenn sie im Mäusehirn wachsen den BK-Kanal ((Butz und Stegen et al. 2015, eingereichtes Manuskript); Abb. 5I-K). Zudem exprimieren sie ebenfalls SDF-1, wobei fraktionierte Bestrahlung (5 x 2 Gy) eine deutliche Hochregulation der SDF-1 Proteinexpression 9 Tage nach Beendigung der Radiotherapie zur Folge hatte ((Butz und Stegen et al. 2015, eingereichtes Manuskript); Abb. 6A und 6B). Genauer gesagt waren die das Gehirn infiltrierenden Glioblastomzellen an der Glioblastomfront und aus dem Tumor ausgewanderte Glioblastomzellen SDF-1 positiv, wohingegen nicht bestrahlte Glioblastome nur eine sehr schwache SDF-1 spezifische Färbung aufwiesen ((Butz und Stegen et al. 2015, eingereichtes Manuskript); Abb. 6A-E).

Neben SDF-1 exprimierten unbestrahlte und fraktioniert bestrahlte orthotope U87MG-Katushka Zellen den CXCR4 Chemokin-Rezeptor ((Butz und Stegen et al. 2015, eingereichtes Manuskript); Abb. 6D und 6E). Die CXCR4 Proteinabundanz war in den fraktioniert bestrahlten Tumoren geringfügig höher als in den nicht bestrahlten

Tumoren und sowohl in der Plasmamembran als auch im Zytoplasma lokalisiert ((Butz und Stegen et al. 2015, eingereichtes Manuskript); Abb. 6F und 6G).

4.8 BK K^+-Kanal abhängige radiogene Hypermigration von orthotopen U87MG-Katushka Zellen (Arbeiten wurden durchgeführt von L. Butz)

Um die Migrationsneigung von bestrahlten und unbestrahlten Tumoren zu bestimmen wurde die Zahl der ausgewanderten Glioblastomzellen und deren zurückgelegte Migrationsdistanz bestimmt. Der Rand der unbehandelten Tumoren war klar vom gesunden Gehirnparenchym abgegrenzt mit angrenzenden Glioblastomzellen an der Tumoroberfläche ((Butz und Stegen et al. 2015, eingereichtes Manuskript); Abb. 7A). Im Gegensatz dazu wiesen bestrahlte Tumore Bereiche auf in denen Glioblastomzellen in das angrenzende Gehirnparenchym einwanderten, wodurch der Tumorrand eine fransige Erscheinung erhielt ((Butz und Stegen et al. 2015, eingereichtes Manuskript); Abb. 7B). IR (5 x 2 Gy) stimulierte die Emigration von Glioblastomzellen aus dem Tumor, wohingegen Paxilline (8mg/kg Körpergewicht, 6 h vor und 6 h nach IR) diese radiogene Hypermigration, nicht jedoch die basale Migration, inhibierte ((Butz und Stegen et al. 2015, eingereichtes Manuskript); Abb. 7C-E). Weder IR noch Paxilline änderten hierbei das Volumen des Tumors ((Butz und Stegen et al. 2015, eingereichtes Manuskript); Abb. 7F), sodass ein Unterschied der Zahl der migrierenden Glioblastomzellen nicht auf eine Änderung des Tumorvolumens zurückzuführen ist.

Die *in vitro* Daten der radiogenen Hypermigration von Glioblastomzellen und die *in vivo* Daten des orthotopen Glioblastom-Mausmodels stimmen genau überein. Die Induktion dieser Migration hat möglicherweise ihren Beginn in der radiogenen Stabilisierung von HIF-1α. Die anschließende Hochregulation des HIF-1α Zielgens SDF-1 stimuliert einen Ca^{2+}-Transienten, welcher zu einer Aktivierung von BK K^+-Kanälen führt. Die Blockade dieser Kanäle führte sowohl *in vitro* als auch *in vivo* zu einer Inhibition der radiogenen Hypermigration. BK K^+-Kanäle scheinen demnach eine signifikante Rolle bei der radiogenen Hypermigration von Glioblastomzellen zu besitzen.

Diskussion II

Dieser Teil der Dissertation zeigt die Hypermigration von humanen Glioblastomzellen, stimuliert durch fraktionierte Bestrahlung, auf einem zellulären und quantitativen Level in einem orthotopen Mausmodel. Diese Hypermigration wird von einer durch Bestrahlung induzierten Hochregulation des Chemokins SDF-1 (stromal-derived cell-factor-1) begleitet. Genauer gesagt waren die aus dem primären Tumor emigrierenden, das Gehirnparenchym infiltrierenden Glioblastomzellen SDF-1 positiv. Dies deutet auf eine Beteiligung eines auto- und/oder parakrinen SDF-1 Signalweges bei der radiogenen Hypermigration *in vivo* hin.

Die Migration bzw. Hypermigration von Glioblastomzellen wird durch zelluläres Ca^{2+}-Signaling gesteuert, welches die „Calcium Calmodulin Kinase II“ (CaMKII) mit einschließt (Huber 2013). Radiogenes Ca^{2+}-Signaling und eine Aktivierung der CaMKII scheint nicht nur auf Glioblastome beschränkt zu sein, da dieser Signalweg auch bei Leukämie beschrieben wurde (Heise et al. 2010, Palme et al. 2013) sowie weiteren Tumorentitäten wie etwa bei Pankreaskrebs (Saur et al. 2005).

Genau wie IR führt eine Bindung von SDF-1 an den G-Protein gekoppelten Chemokinrezeptor CXCR4 zur Induktion des Ca^{2+}-Signalings und Invasion von Glioblastomzellen (Zagzag et al. 2006, Sciaccaluga et al. 2010). Bei SDF-1 handelt es sich um ein HIF-1α Zielgen. Unter Hypoxie ist daher eine starke SDF-1 Expression erkennbar. Eine Schädigung der Tumor-Vaskulatur und die daraus resultierende Hypoxie könnte demnach die SDF-1 Expression induzieren (Greenfield et al. 2010). Neben dieser durch Hypoxie induzierten SDF-1 Hochregulation könnte eine Bestrahlung die Expression von SDF-1 in Glioblastomen direkt stimulieren. Dies geht aus den *in vivo* Experimenten dieser Dissertation sowie aus einer Publikation hervor, welche SDF-1 Promotor Reporter-Assays verwendet hat (Tabatabai et al. 2006).

In vivo rekrutiert SDF-1, welches vom Glioblastom sezerniert wird, dem Knochenmark entstammende $CD11b^+$ Zellen hin zum Tumor und initiiert die Bildung neuer Blutgefäße, welche die Neovaskularisierung des Tumors fördern (Tabatabai et al. 2006, Kioi et al. 2010, Kozin et al. 2010, Tseng et al. 2011, Wang et al. 2013, Liu et al. 2014). Sowohl für das SDF-1 Signaling als auch für die Vaskularisierung wurde gezeigt, dass es hauptsächlich an der Invasionsfront von Glioblastomen stattfindet

(Zagzag et al. 2008). Ein Knock-down von SDF-1 in Glioblastomzellen reduziert sowohl die Vaskularisierung als auch die radiogene Hypermigration, sodass eine durch Bestrahlung induzierte Neubildung von Blutgefäßen die radiogene Hypermigration wahrscheinlich vereinfacht.

Des Weiteren wurde gezeigt, dass eine Bestrahlung zu einer Selektion von Krebsstammzellen führen kann oder sogar den Übergang von „differenzierten“ in stammzellähnliche Tumorzellen in Glioblastomen (Kim et al. 2011, Lagadec et al. 2012, Tamura et al. 2013) und anderen Tumorentitäten (Pajonk et al. 2010) induziert. Stammzellcharaktereigenschaften sind mit einer stark erhöhten CXCR4 Expression assoziiert (Liu et al. 2006) sowie mit einem hoch invasiven und migrativen Phänotypen (Ruggieri et al. 2012, Nakada et al. 2013). Es wäre daher plausibel, dass ein IR-induzierter Wandel von „differenzierten“ in stammzellähnliche Glioblastomzellen ebenfalls zur radiogenen Hypermigration beiträgt.

Es stellt sich dabei auch die Frage, ob die durch Bestrahlung hervorgerufene Hypermigration auch zu der hohen Radioresistenz von Glioblastomen beiträgt. Nach abgeschlossener Radio- und Chemotherapie liegen etwa 90% aller rezidivierenden Glioblastome innerhalb des Bestrahlungszielvolumens (Weber et al. 2009, Minniti et al. 2010). Dies würde zunächst bedeuten, dass aus dem Zielvolumen emigrierende Glioblastomzellen bei der Bildung von Rezidiven – wenn überhaupt – nur eine geringe Rolle spielen. Andererseits ist es wahrscheinlich, dass wiederkehrende Glioblastome vorzugsweise und viel schneller in das bestrahlte und nekrotische Zielvolumen expandieren als gesundes Gehirngewebe zu infiltrieren. Genaue Bildgebungsanalysen zeigten, dass ein signifikanter Anteil des Volumens rezidivierender Glioblastome im äußersten Bereich des Bestrahlungsvolumens liegt (Weber et al. 2009). Dies würde der gängigen Vorstellung entsprechen, dass zuvor aus dem Bestrahlungsvolumen ausgewanderte Glioblastomzellen dieses erneut besiedeln.

In einem *Xeno*graft Mausmodel zeigten stammzellähnliche, $CD133^+$ Glioblastomzell-Subpopulationen eine erhöhte Radioresistenz gegenüber $CD133^-$ Zellen, wohingegen kein Unterschied in der Radioresistenz *in vitro* zu beobachten war. Dies zeigt deutlich eine Beteiligung des Mikromilieus des Gehirns bei der Radioresistenz (Jamal et al. 2012). Genauer gesagt wurde gezeigt, dass Endothelzellen die Resistenz der Glioblastomtherapie fördern (Rao et al. 2012). Die wechselseitige Beziehung zwischen Glioblastom- und Endothelzellen hängt dabei stark von der MMP-2

Expression durch Glioblastomzellen (Maddirela et al. 2013) und dem SDF-1 Signaling der Endothelzellen ab (Rao et al. 2012). Erstaunlicherweise induziert IR die Hochregulation von MMP-2 in Glioblastomzellen, welche notwendig ist für die Invasion des Gehirnparenchyms (Wild-Bode et al. 2001, Badiga et al. 2011, Maddirela et al. 2013, Shankar et al. 2014). Dies deutet auf die Möglichkeit hin, dass eine radiogene Hypermigration das „Homing“ bzw. die Rückkehr von stammzellähnlichen Glioblastomzellen mit einer hohen CXCR4 Expression in perivaskulären Nischen unterstützt.

Die hier dargestellten Daten legen nahe, dass eine radiogene Hypermigration zur hohen Radioresistenz von Glioblastomzellen beiträgt, entweder durch die Evasion aus dem Bestrahlungszielvolumen oder durch Stimulation der Chemotaxis von Glioblastomzellen hin zu perivaskulären Nischen. Ein Targeting des BK-Kanals stellt daher eine effektive *in vivo* Strategie dar, um die radiogene Hypermigration zu unterbinden.

BK-Kanäle werden von Neuronen des zentralen Nervensystems (beispielsweise im Hippocampus) exprimiert, wo sie in prä- und postsynaptischen Membranen vorkommen (Sausbier et al. 2006). Bei dem in dieser Studie verwendeten BK-Kanal Inhibitor Paxilline handelt es sich um ein Neurotoxin, welches von dem Pilz *Penicillium paxilli* produziert wird. Dieser Pilz verursacht eine Vergiftung bei Schafen welche Ataxie und einen unkontrollierbaren Tremor hervorruft (Imlach et al. 2008). In den Mausversuchen rief Paxilline neben Ataxie keine Nebenwirkungen hervor und wurde von den Mäusen gut vertragen. Eine Anwendung von Paxilline bei der Therapie von Glioblastomen wäre daher möglich. Andere Medikamente, die eine Auswirkung auf BK-Kanäle besitzen, werden bereits verwendet. Klassische Neuroleptika wie Haloperidol oder Chlorpromazine inhibieren BK-Kanäle mit einer IC_{50} im niedrigen mikromolekularen Bereich. Haloperidol kann im menschlichen Gehirn im mikromolekularen Bereich, Chlorpromazine in noch größeren Konzentrationen akkumulieren (Huang and Ruskin 1964, Korpi et al. 1984, Lee et al. 1997). Die therapeutischen Konzentrationen der klassischen Neuroleptika können also wahrscheinlich die BK-Kanal Aktivität beeinflussen.

Eine fraktionierte Bestrahlung scheint die Hypermigration von Glioblastomzellen *in vivo* zu stimulieren. Dies könnte zur hohen Therapieresistenz von Glioblastomen beitragen. Die radiogene BK K^+-Kanal Aktivierung steuert die Hypermigration und

eine Inhibition dieser Kanäle unterbindet diese. Eine Blockade des BK-Kanals könnte daher in der Klinik Anwendung finden zulasten von extrapyramidalen Nebenwirkungen.

Schlussfolgerung

Ionenkanäle spielen eine zentrale Rolle bei verschiedenen zellulären Prozessen. Hierzu gehören die Proliferation, Differenzierung, Apoptose und Migration. Kaliumkanäle im Speziellen sind unter anderem wichtige Regulatoren für die Erregbarkeit einer Zelle und sind an der Zellproliferation, der regulierten Zellvolumenabnahme und Zellmigration beteiligt.

Bei der Entwicklung eines Tumors übernehmen K^+-Kanäle unter den Ionenkanälen wohl den größten Anteil. In Gliomen korreliert die Höhe der Expression zudem positiv mit dem jeweiligen Malignitätsgrad.

Ca^{2+}-aktivierte K^+-Kanäle wie BK und IK nehmen zentrale Funktionen in der Therapieresistenz von Glioblastomen ein. Eine Bestrahlung erhöhte die Aktivität von IK K^+-Kanälen, welche in einem vorübergehenden G_2/M Arrest resultierte. Der IK Inhibitor TRAM34 führte zu einer verringerten Akkumulierung der Glioblastomzellen im G_2/M Arrest und induzierte einen Anstieg von residuellen DNA Doppelstrangbrüchen. Ebenso zeigte die Behandlung mit TRAM34 einen radiosensitivierenden Effekt auf Glioblastomzellen und ein verzögertes Wachstum in einem ektopen Glioblastom-Mausmodel (Stegen et al. 2015).

Des Weiteren erhöht die Bestrahlung von Glioblastomzellen deren Migration durch die Bildung des CXCR4 Agonisten SDF-1. Das veränderte Ca^{2+}-Signaling führt zu einer Aktivierung von BK K^+- und ClC-3 Cl^--Kanälen, woraus eine Zellvolumenabnahme resultiert, die für eine radiogene Hypermigration notwendig ist. Der CXCR4 Antagonist AMD3100 sowie der BK K^+-Kanal Inhibitor Paxilline können diese radioinduzierte Migration verhindern (Butz und Stegen et al. 2015, eingereichtes Manuskript).

Diese und weitere Daten anderer Arbeitsgruppen legen nahe, dass eine Strahlentherapie, wie sie bei der Behandlung von Glioblastomen angewendet wird, in gewisser Hinsicht kontraproduktiv sein kann. Eine radioinduzierte Migration von Glioblastomzellen aus dem Bestrahlungszielvolumen wird teilweise für die Bildung

von Rezidiven verantwortlich gemacht. Durch die Strahlentherapie selbst könnte ein Zellzyklusarrest induziert und die hohe Radioresistenz hervorgerufen werden. Jedoch kann auf die Strahlentherapie selbst nicht verzichtet werden, da die Lebenserwartung von Glioblastompatienten durch diese signifikant verlängert werden kann. Ziel wäre es daher, verschiedene Inhibitoren, die den radioinduzierten Zellzyklusarrest sowie die radioinduzierte Hypermigration unterbinden, in Kombination mit einer adjuvanten Radio- und Chemotherapie zu verabreichen. Mögliche Kandidaten hierfür wären der IK-Kanal Inhibitor Senicapoc, der in Studien bereits als sicher eingestuft wurde, sowie der BK-Kanal Inhibitor Paxilline, der nur geringe Nebenwirkungen erwarten lässt. Der CXCR4-Inhibitor Plerixafor (AMD3100) ist ein weiterer Kandidat, der bereits als Arzneimittel zugelassen wurde.

Literaturverzeichnis

Abdullaev, I. F., A. Rudkouskaya, A. A. Mongin and Y. H. Kuo (2010). "Calcium-activated potassium channels BK and IK1 are functionally expressed in human gliomas but do not regulate cell proliferation." PLoS One 5(8): e12304.

Asuthkar, S., A. K. Nalla, C. S. Gondi, D. H. Dinh, M. Gujrati, S. Mohanam and J. S. Rao (2011). "Gadd45a sensitizes medulloblastoma cells to irradiation and suppresses MMP-9-mediated EMT." Neuro Oncol 13(10): 1059-1073.

Ataga, K. I., E. P. Orringer, L. Styles, E. P. Vichinsky, P. Swerdlow, G. A. Davis, P. A. Desimone and J. W. Stocker (2006). "Dose-escalation study of ICA-17043 in patients with sickle cell disease." Pharmacotherapy 26(11): 1557-1564.

Ataga, K. I., W. R. Smith, L. M. De Castro, P. Swerdlow, Y. Saunthararajah, O. Castro, E. Vichinsky, A. Kutlar, E. P. Orringer, G. C. Rigdon, J. W. Stocker and I. C. A. Investigators (2008). "Efficacy and safety of the Gardos channel blocker, senicapoc (ICA-17043), in patients with sickle cell anemia." Blood 111(8): 3991-3997.

Ataga, K. I. and J. Stocker (2009). "Senicapoc (ICA-17043): a potential therapy for the prevention and treatment of hemolysis-associated complications in sickle cell anemia." Expert Opin Investig Drugs 18(2): 231-239.

Badiga, A. V., C. Chetty, D. Kesanakurti, D. Are, M. Gujrati, J. D. Klopfenstein, D. H. Dinh and J. S. Rao (2011). "MMP-2 siRNA inhibits radiation-enhanced invasiveness in glioma cells." PLoS One 6(6): e20614.

Badiga, A. V., C. Chetty, D. Kesanakurti, D. Are, M. Gujrati, J. D. Klopfenstein, D. H. Dinh and J. S. Rao (2011). "MMP-2 siRNA inhibits radiation-enhanced invasiveness in glioma cells." PLoS One 6(6): e20614.

Bakhramov, A., C. Fenech and T. B. Bolton (1995). "Chloride current activated by hypotonicity in cultured human astrocytoma cells." Exp Physiol 80(3): 373-389.

Balut, C. M., K. L. Hamilton and D. C. Devor (2012). "Trafficking of intermediate (KCa3.1) and small (KCa2.x) conductance, Ca(2+)-activated K(+) channels: a novel target for medicinal chemistry efforts?" ChemMedChem 7(10): 1741-1755.

Basrai, D., R. Kraft, C. Bollensdorff, L. Liebmann, K. Benndorf and S. Patt (2002). "BK channel blockers inhibit potassium-induced proliferation of human astrocytoma cells." Neuroreport 13(4): 403-407.

Begenisich, T., T. Nakamoto, C. E. Ovitt, K. Nehrke, C. Brugnara, S. L. Alper and J. E. Melvin (2004). "Physiological roles of the intermediate conductance, Ca2+-activated potassium channel Kcnn4." J Biol Chem 279(46): 47681-47687.

Berridge, M. J., P. Lipp and M. D. Bootman (2000). "The versatility and universality of calcium signalling." Nat Rev Mol Cell Biol 1(1): 11-21.

Bordey, A., H. Sontheimer and J. Trouslard (2000). "Muscarinic activation of BK channels induces membrane oscillations in glioma cells and leads to inhibition of cell migration." J Membr Biol 176(1): 31-40.

Bortner, C. D., F. M. Hughes, Jr. and J. A. Cidlowski (1997). "A primary role for K+ and Na+ efflux in the activation of apoptosis." J Biol Chem 272(51): 32436-32442.

Brismar, T. and V. P. Collins (1989). "Potassium and sodium channels in human malignant glioma cells." Brain Res 480(1-2): 259-267.

Brismar, T. and V. P. Collins (1989). "Potassium and sodium channels in human malignant glioma cells." Brain Res 480(1-2): 259-267.

Brismar, T. and V. P. Collins (1989). "Potassium channels in human glioma cells." Pflugers Arch 414 Suppl 1: S137-138.

Canazza, A., C. Calatozzolo, L. Fumagalli, A. Bergantin, F. Ghielmetti, L. Fariselli, D. Croci, A. Salmaggi and E. Ciusani (2011). "Increased migration of a human glioma cell line after in vitro CyberKnife irradiation." Cancer Biol Ther 12(7): 629-633.

Catacuzzeno, L., F. Aiello, B. Fioretti, L. Sforna, E. Castigli, P. Ruggieri, A. M. Tata, A. Calogero and F. Franciolini (2011). "Serum-activated K and Cl currents underlay U87-MG glioblastoma cell migration." J Cell Physiol 226(7): 1926-1933.

Catacuzzeno, L., B. Fioretti and F. Franciolini (2012). "Expression and Role of the Intermediate-Conductance Calcium-Activated Potassium Channel KCa3.1 in Glioblastoma." J Signal Transduct 2012: 421564.

Chin, L. S., C. C. Park, K. M. Zitnay, M. Sinha, A. J. DiPatri, Jr., P. Perillan and J. M. Simard (1997). "4-Aminopyridine causes apoptosis and blocks an outward rectifier K+ channel in malignant astrocytoma cell lines." J Neurosci Res 48(2): 122-127.

Christie, M. J., R. A. North, P. B. Osborne, J. Douglass and J. P. Adelman (1990). "Heteropolymeric potassium channels expressed in Xenopus oocytes from cloned subunits." Neuron 4(3): 405-411.

Claes, A., A. J. Idema and P. Wesseling (2007). "Diffuse glioma growth: a guerilla war." Acta Neuropathol 114(5): 443-458.

Cuddapah, V. A. and H. Sontheimer (2010). "Molecular interaction and functional regulation of ClC-3 by Ca2+/calmodulin-dependent protein kinase II (CaMKII) in human malignant glioma." J Biol Chem 285(15): 11188-11196.

Cuddapah, V. A., K. L. Turner, S. Seifert and H. Sontheimer (2013). "Bradykinin-induced chemotaxis of human gliomas requires the activation of KCa3.1 and ClC-3." J Neurosci 33(4): 1427-1440.

Cui, J., H. Yang and U. S. Lee (2009). "Molecular mechanisms of BK channel activation." Cell Mol Life Sci 66(5): 852-875.

D'Alessandro, G., M. Catalano, M. Sciaccaluga, G. Chece, R. Cipriani, M. Rosito, A. Grimaldi, C. Lauro, G. Cantore, A. Santoro, B. Fioretti, F. Franciolini, H. Wulff and C. Limatola (2013). "KCa3.1 channels are involved in the infiltrative behavior of glioblastoma in vivo." Cell Death Dis 4: e773.

Dittmann, K., C. Mayer, H. P. Rodemann and S. M. Huber (2013). "EGFR cooperates with glucose transporter SGLT1 to enable chromatin remodeling in response to ionizing radiation." Radiother Oncol 107(2): 247-251.

Ernest, N. J., A. K. Weaver, L. B. Van Duyn and H. W. Sontheimer (2005). "Relative contribution of chloride channels and transporters to regulatory volume decrease in human glioma cells." Am J Physiol Cell Physiol 288(6): C1451-1460.

Fioretti, B., E. Castigli, I. Calzuola, A. A. Harper, F. Franciolini and L. Catacuzzeno (2004). "NPPB block of the intermediate-conductance Ca2+-activated K+ channel." Eur J Pharmacol 497(1): 1-6.

Fioretti, B., E. Castigli, M. R. Micheli, R. Bova, M. Sciaccaluga, A. Harper, F. Franciolini and L. Catacuzzeno (2006). "Expression and modulation of the intermediate- conductance Ca2+-activated K+ channel in glioblastoma GL-15 cells." Cell Physiol Biochem 18(1-3): 47-56.

Fioretti, B., L. Catacuzzeno, L. Sforna, F. Aiello, F. Pagani, D. Ragozzino, E. Castigli and F. Franciolini (2009). "Histamine hyperpolarizes human glioblastoma cells by activating the intermediate-conductance Ca2+-activated K+ channel." Am J Physiol Cell Physiol 297(1): C102-110.

Giese, A., M. A. Loo, N. Tran, D. Haskett, S. W. Coons and M. E. Berens (1996). "Dichotomy of astrocytoma migration and proliferation." Int J Cancer 67(2): 275-282.

Golding, N. L., H. Y. Jung, T. Mickus and N. Spruston (1999). "Dendritic calcium spike initiation and repolarization are controlled by distinct potassium channel subtypes in CA1 pyramidal neurons." J Neurosci 19(20): 8789-8798.

Greenfield, J. P., W. S. Cobb and D. Lyden (2010). "Resisting arrest: a switch from angiogenesis to vasculogenesis in recurrent malignant gliomas." J Clin Invest 120(3): 663-667.

Haas, B. R. and H. Sontheimer (2010). "Inhibition of the Sodium-Potassium-Chloride Cotransporter Isoform-1 reduces glioma invasion." Cancer Res 70(13): 5597-5606.

Hatzikirou, H., D. Basanta, M. Simon, K. Schaller and A. Deutsch (2012). "'Go or grow': the key to the emergence of invasion in tumour progression?" Math Med Biol 29(1): 49-65.

Heise, N., D. Palme, M. Misovic, S. Koka, J. Rudner, F. Lang, H. R. Salih, S. M. Huber and G. Henke (2010). "Non-selective cation channel-mediated Ca2+-entry and activation of Ca2+/calmodulin-dependent kinase II contribute to G2/M cell cycle arrest and survival of irradiated leukemia cells." Cell Physiol Biochem 26(4-5): 597-608.

Hille, B. (1992). "Pumping ions." Science 255(5045): 742.

Holland, E. C. (2000). "Glioblastoma multiforme: the terminator." Proc Natl Acad Sci U S A 97(12): 6242-6244.

Huang, C. L. and B. H. Ruskin (1964). "Determination of Serum Chlorpromazine Metabolites in Psychotic Patients." J Nerv Ment Dis 139: 381-386.

Huber, S. M. (2013). "Oncochannels." Cell Calcium 53(4): 241-255.

Huber, S. M., L. Butz, B. Stegen, D. Klumpp, N. Braun, P. Ruth and F. Eckert (2013). "Ionizing radiation, ion transports, and radioresistance of cancer cells." Front Physiol 4: 212.

Huber, S. M., L. Butz, B. Stegen, L. Klumpp, D. Klumpp and F. Eckert (2014). "Role of ion channels in ionizing radiation-induced cell death." Biochim Biophys Acta.

Huber, S. M., M. Misovic, C. Mayer, H. P. Rodemann and K. Dittmann (2012). "EGFR-mediated stimulation of sodium/glucose cotransport promotes survival of irradiated human A549 lung adenocarcinoma cells." Radiother Oncol 103(3): 373-379.

Imlach, W. L., S. C. Finch, J. Dunlop, A. L. Meredith, R. W. Aldrich and J. E. Dalziel (2008). "The molecular mechanism of "ryegrass staggers," a neurological disorder of K+ channels." J Pharmacol Exp Ther 327(3): 657-664.

Ishii, T. M., C. Silvia, B. Hirschberg, C. T. Bond, J. P. Adelman and J. Maylie (1997). "A human intermediate conductance calcium-activated potassium channel." Proc Natl Acad Sci U S A 94(21): 11651-11656.

Jager, H., T. Dreker, A. Buck, K. Giehl, T. Gress and S. Grissmer (2004). "Blockage of intermediate-conductance Ca2+-activated K+ channels inhibit human pancreatic cancer cell growth in vitro." Mol Pharmacol 65(3): 630-638.

Jamal, M., B. H. Rath, P. S. Tsang, K. Camphausen and P. J. Tofilon (2012). "The brain microenvironment preferentially enhances the radioresistance of CD133(+) glioblastoma stem-like cells." Neoplasia 14(2): 150-158.

Jan, L. Y. and Y. N. Jan (1997). "Voltage-gated and inwardly rectifying potassium channels." J Physiol 505 (Pt 2): 267-282.

Johnson, J., M. O. Nowicki, C. H. Lee, E. A. Chiocca, M. S. Viapiano, S. E. Lawler and J. J. Lannutti (2009). "Quantitative analysis of complex glioma cell migration on electrospun polycaprolactone using time-lapse microscopy." Tissue Eng Part C Methods 15(4): 531-540.

Jung, J. W., S. Y. Hwang, J. S. Hwang, E. S. Oh, S. Park and I. O. Han (2007). "Ionising radiation induces changes associated with epithelial-mesenchymal transdifferentiation and increased cell motility of A549 lung epithelial cells." Eur J Cancer 43(7): 1214-1224.

Kargiotis, O., C. Chetty, V. Gogineni, C. S. Gondi, S. M. Pulukuri, A. P. Kyritsis, M. Gujrati, J. D. Klopfenstein, D. H. Dinh and J. S. Rao (2008). "uPA/uPAR downregulation inhibits radiation-induced migration, invasion and angiogenesis in IOMM-Lee meningioma cells and decreases tumor growth in vivo." Int J Oncol 33(5): 937-947.

Khalid, M. H., S. Shibata and T. Hiura (1999). "Effects of clotrimazole on the growth, morphological characteristics, and cisplatin sensitivity of human glioblastoma cells in vitro." J Neurosurg 90(5): 918-927.

Khalid, M. H., Y. Tokunaga, A. J. Caputy and E. Walters (2005). "Inhibition of tumor growth and prolonged survival of rats with intracranial gliomas following administration of clotrimazole." J Neurosurg 103(1): 79-86.

Khanna, R., M. C. Chang, W. J. Joiner, L. K. Kaczmarek and L. C. Schlichter (1999). "hSK4/hIK1, a calmodulin-binding KCa channel in human T lymphocytes. Roles in proliferation and volume regulation." J Biol Chem 274(21): 14838-14849.

Kil, W. J., P. J. Tofilon and K. Camphausen (2012). "Post-radiation increase in VEGF enhances glioma cell motility in vitro." Radiat Oncol 7: 25.

Kim, M. J., R. K. Kim, C. H. Yoon, S. An, S. G. Hwang, Y. Suh, M. J. Park, H. Y. Chung, I. G. Kim and S. J. Lee (2011). "Importance of PKCdelta signaling in fractionated-radiation-induced expansion of glioma-initiating cells and resistance to cancer treatment." J Cell Sci 124(Pt 18): 3084-3094.

Kioi, M., H. Vogel, G. Schultz, R. M. Hoffman, G. R. Harsh and J. M. Brown (2010). "Inhibition of vasculogenesis, but not angiogenesis, prevents the recurrence of glioblastoma after irradiation in mice." J Clin Invest 120(3): 694-705.

Korpi, E. R., J. E. Kleinman, D. T. Costakos, M. Linnoila and R. J. Wyatt (1984). "Reduced haloperidol in the post-mortem brains of haloperidol-treated patients." Psychiatry Res 11(3): 259-269.

Kozin, S. V., W. S. Kamoun, Y. Huang, M. R. Dawson, R. K. Jain and D. G. Duda (2010). "Recruitment of myeloid but not endothelial precursor cells facilitates tumor regrowth after local irradiation." Cancer Res 70(14): 5679-5685.

Kraft, R., K. Benndorf and S. Patt (2000). "Large conductance Ca(2+)-activated K(+) channels in human meningioma cells." J Membr Biol 175(1): 25-33.

Kraft, R., P. Krause, S. Jung, D. Basrai, L. Liebmann, J. Bolz and S. Patt (2003). "BK channel openers inhibit migration of human glioma cells." Pflugers Arch 446(2): 248-255.

Lagadec, C., E. Vlashi, L. Della Donna, C. Dekmezian and F. Pajonk (2012). "Radiation-induced reprogramming of breast cancer cells." Stem Cells 30(5): 833-844.

Lallet-Daher, H., M. Roudbaraki, A. Bavencoffe, P. Mariot, F. Gackiere, G. Bidaux, R. Urbain, P. Gosset, P. Delcourt, L. Fleurisse, C. Slomianny, E. Dewailly, B. Mauroy, J. L. Bonnal, R. Skryma and N. Prevarskaya (2009). "Intermediate-conductance Ca2+-activated K+ channels (IKCa1) regulate human prostate cancer cell proliferation through a close control of calcium entry." Oncogene 28(15): 1792-1806.

Lam, J. and H. Wulff (2011). "The Lymphocyte Potassium Channels Kv1.3 and KCa3.1 as Targets for Immunosuppression." Drug Dev Res 72(7): 573-584.

Lee, K., F. McKenna, I. C. Rowe and M. L. Ashford (1997). "The effects of neuroleptic and tricyclic compounds on BKCa channel activity in rat isolated cortical neurones." Br J Pharmacol 121(8): 1810-1816.

Liu, G., X. Yuan, Z. Zeng, P. Tunici, H. Ng, I. R. Abdulkadir, L. Lu, D. Irvin, K. L. Black and J. S. Yu (2006). "Analysis of gene expression and chemoresistance of CD133+ cancer stem cells in glioblastoma." Mol Cancer 5: 67.

Liu, G., X. Yuan, Z. Zeng, P. Tunici, H. Ng, I. R. Abdulkadir, L. Lu, D. Irvin, K. L. Black and J. S. Yu (2006). "Analysis of gene expression and chemoresistance of CD133+ cancer stem cells in glioblastoma." Mol Cancer 5: 67.

Liu, H., Y. Li and K. P. Raisch (2010). "Clotrimazole induces a late G1 cell cycle arrest and sensitizes glioblastoma cells to radiation in vitro." Anticancer Drugs 21(9): 841-849.

Liu, S. C., R. Alomran, S. B. Chernikova, F. Lartey, J. Stafford, T. Jang, M. Merchant, D. Zboralski, S. Zollner, A. Kruschinski, S. Klussmann, L. Recht and J. M. Brown (2014). "Blockade of SDF-1 after irradiation inhibits tumor recurrences of autochthonous brain tumors in rats." Neuro Oncol 16(1): 21-28.

Liu, X., Y. Chang, P. H. Reinhart and H. Sontheimer (2002). "Cloning and characterization of glioma BK, a novel BK channel isoform highly expressed in human glioma cells." J Neurosci 22(5): 1840-1849.

Louis, D. N., H. Ohgaki, O. D. Wiestler, W. K. Cavenee, P. C. Burger, A. Jouvet, B. W. Scheithauer and P. Kleihues (2007). "The 2007 WHO classification of tumours of the central nervous system." Acta Neuropathol 114(2): 97-109.

Lui, V. C., S. S. Lung, J. K. Pu, K. N. Hung and G. K. Leung (2010). "Invasion of human glioma cells is regulated by multiple chloride channels including ClC-3." Anticancer Res 30(11): 4515-4524.

Maddirela, D. R., D. Kesanakurti, M. Gujrati and J. S. Rao (2013). "MMP-2 suppression abrogates irradiation-induced microtubule formation in endothelial cells by inhibiting alphavbeta3-mediated SDF-1/CXCR4 signaling." Int J Oncol 42(4): 1279-1288.

Maezawa, I., D. P. Jenkins, B. E. Jin and H. Wulff (2012). "Microglial KCa3.1 Channels as a Potential Therapeutic Target for Alzheimer's Disease." Int J Alzheimers Dis 2012: 868972.

McCoy, E. and H. Sontheimer (2007). "Expression and function of water channels (aquaporins) in migrating malignant astrocytes." Glia 55(10): 1034-1043.

McCoy, E. S., B. R. Haas and H. Sontheimer (2010). "Water permeability through aquaporin-4 is regulated by protein kinase C and becomes rate-limiting for glioma invasion." Neuroscience 168(4): 971-981.

McFerrin, M. B. and H. Sontheimer (2006). "A role for ion channels in glioma cell invasion." Neuron Glia Biol 2(1): 39-49.

McManus, O. B. (1991). "Calcium-activated potassium channels: regulation by calcium." J Bioenerg Biomembr 23(4): 537-560.

McManus, O. B., L. M. Helms, L. Pallanck, B. Ganetzky, R. Swanson and R. J. Leonard (1995). "Functional role of the beta subunit of high conductance calcium-activated potassium channels." Neuron 14(3): 645-650.

Minniti, G., D. Amelio, M. Amichetti, M. Salvati, R. Muni, A. Bozzao, G. Lanzetta, S. Scarpino, A. Arcella and R. M. Enrici (2010). "Patterns of failure and comparison of different target volume delineations in patients with glioblastoma treated with conformal radiotherapy plus concomitant and adjuvant temozolomide." Radiother Oncol 97(3): 377-381.

Molenaar, R. J. (2011). "Ion channels in glioblastoma." ISRN Neurol 2011: 590249.

Nakada, M., E. Nambu, N. Furuyama, Y. Yoshida, T. Takino, Y. Hayashi, H. Sato, Y. Sai, T. Tsuji, K. I. Miyamoto, A. Hirao and J. I. Hamada (2013). "Integrin alpha3 is overexpressed in glioma stem-like cells and promotes invasion." Br J Cancer 108(12): 2516-2524.

Nakada, M., E. Nambu, N. Furuyama, Y. Yoshida, T. Takino, Y. Hayashi, H. Sato, Y. Sai, T. Tsuji, K. I. Miyamoto, A. Hirao and J. I. Hamada (2013). "Integrin alpha3 is overexpressed in glioma stem-like cells and promotes invasion." Br J Cancer 108(12): 2516-2524.

Niyazi, M., A. Siefert, S. B. Schwarz, U. Ganswindt, F. W. Kreth, J. C. Tonn and C. Belka (2011). "Therapeutic options for recurrent malignant glioma." Radiother Oncol 98(1): 1-14.

Olsen, M. L., S. Schade, S. A. Lyons, M. D. Amaral and H. Sontheimer (2003). "Expression of voltage-gated chloride channels in human glioma cells." J Neurosci 23(13): 5572-5582.

Ouadid-Ahidouch, H., M. Roudbaraki, P. Delcourt, A. Ahidouch, N. Joury and N. Prevarskaya (2004). "Functional and molecular identification of intermediate-conductance Ca(2+)-activated K(+) channels in breast cancer cells: association with cell cycle progression." Am J Physiol Cell Physiol 287(1): C125-134.

Pajonk, F., E. Vlashi and W. H. McBride (2010). "Radiation resistance of cancer stem cells: the 4 R's of radiobiology revisited." Stem Cells 28(4): 639-648.

Palme, D., M. Misovic, E. Schmid, D. Klumpp, H. R. Salih, J. Rudner and S. M. Huber (2013). "Kv3.4 potassium channel-mediated electrosignaling controls cell cycle and survival of irradiated leukemia cells." Pflugers Arch 465(8): 1209-1221.

Pardo, L. A. and W. Stuhmer (2014). "The roles of K(+) channels in cancer." Nat Rev Cancer 14(1): 39-48.

Peng, H., Y. Huang, J. Rose, D. Erichsen, S. Herek, N. Fujii, H. Tamamura and J. Zheng (2004). "Stromal cell-derived factor 1-mediated CXCR4 signaling in rat and human cortical neural progenitor cells." J Neurosci Res 76(1): 35-50.

Pickhard, A. C., J. Margraf, A. Knopf, T. Stark, G. Piontek, C. Beck, A. L. Boulesteix, E. Q. Scherer, S. Pigorsch, J. Schlegel, W. Arnold and R. Reiter (2011). "Inhibition of radiation induced migration of human head and neck squamous cell carcinoma cells by blocking of EGF receptor pathways." BMC Cancer 11: 388.

Ransom, C. B., X. Liu and H. Sontheimer (2002). "BK channels in human glioma cells have enhanced calcium sensitivity." Glia 38(4): 281-291.

Ransom, C. B., X. Liu and H. Sontheimer (2003). "Current transients associated with BK channels in human glioma cells." J Membr Biol 193(3): 201-213.

Ransom, C. B. and H. Sontheimer (2001). "BK channels in human glioma cells." J Neurophysiol 85(2): 790-803.

Rao, S., R. Sengupta, E. J. Choe, B. M. Woerner, E. Jackson, T. Sun, J. Leonard, D. Piwnica-Worms and J. B. Rubin (2012). "CXCL12 mediates trophic interactions between endothelial and tumor cells in glioblastoma." PLoS One 7(3): e33005.

Rieken, S., D. Habermehl, A. Mohr, L. Wuerth, K. Lindel, K. Weber, J. Debus and S. E. Combs (2011). "Targeting alphanubeta3 and alphanubeta5 inhibits photon-induced hypermigration of malignant glioma cells." Radiat Oncol 6: 132.

Roderick, H. L. and S. J. Cook (2008). "Ca2+ signalling checkpoints in cancer: remodelling Ca2+ for cancer cell proliferation and survival." Nat Rev Cancer 8(5): 361-375.

Roman, R., A. P. Feranchak, M. Troetsch, J. C. Dunkelberg, G. Kilic, T. Schlenker, J. Schaack and J. G. Fitz (2002). "Molecular characterization of volume-sensitive SK(Ca) channels in human liver cell lines." Am J Physiol Gastrointest Liver Physiol 282(1): G116-122.

Ruggieri, P., G. Mangino, B. Fioretti, L. Catacuzzeno, R. Puca, D. Ponti, M. Miscusi, F. Franciolini, G. Ragona and A. Calogero (2012). "The inhibition of KCa3.1 channels activity reduces cell motility in glioblastoma derived cancer stem cells." PLoS One 7(10): e47825.

Saur, D., B. Seidler, G. Schneider, H. Algul, R. Beck, R. Senekowitsch-Schmidtke, M. Schwaiger and R. M. Schmid (2005). "CXCR4 expression increases liver and lung metastasis in a mouse model of pancreatic cancer." Gastroenterology 129(4): 1237-1250.

Sausbier, U., M. Sausbier, C. A. Sailer, C. Arntz, H. G. Knaus, W. Neuhuber and P. Ruth (2006). "Ca2+ -activated K+ channels of the BK-type in the mouse brain." Histochem Cell Biol 125(6): 725-741.

Schwab, A. (2001). "Function and spatial distribution of ion channels and transporters in cell migration." Am J Physiol Renal Physiol 280(5): F739-747.

Schwab, A., V. Nechyporuk-Zloy, A. Fabian and C. Stock (2007). "Cells move when ions and water flow." Pflugers Arch 453(4): 421-432.

Sciaccaluga, M., B. Fioretti, L. Catacuzzeno, F. Pagani, C. Bertollini, M. Rosito, M. Catalano, G. D'Alessandro, A. Santoro, G. Cantore, D. Ragozzino, E. Castigli, F. Franciolini and C. Limatola (2010). "CXCL12-induced glioblastoma cell migration requires intermediate conductance Ca2+-activated K+ channel activity." Am J Physiol Cell Physiol 299(1): C175-184.

Shankar, A., S. Kumar, A. S. Iskander, N. R. Varma, B. Janic, A. deCarvalho, T. Mikkelsen, J. A. Frank, M. M. Ali, R. A. Knight, S. Brown and A. S. Arbab (2014). "Subcurative radiation significantly increases cell proliferation, invasion, and migration of primary glioblastoma multiforme in vivo." Chin J Cancer 33(3): 148-158.

Shumilina, E., S. M. Huber and F. Lang (2011). "Ca2+ signaling in the regulation of dendritic cell functions." Am J Physiol Cell Physiol 300(6): C1205-1214.

Sontheimer, H. (2008). "An unexpected role for ion channels in brain tumor metastasis." Exp Biol Med (Maywood) 233(7): 779-791.

Stegen, B., L. Butz, L. Klumpp, D. Zips, K. Dittmann, P. Ruth and S. M. Huber (2015). "Ca2+-activated IK K+ Channel Blockade Radiosensitizes Glioblastoma Cells." Mol Cancer Res.

Stegen, B., L. Butz, L. Klumpp, D. Zips, K. Dittmann, P. Ruth and S. M. Huber (2015). "Ca2+-activated IK K+ Channel Blockade Radiosensitizes Glioblastoma Cells." Mol Cancer Res.

Steinle, M., D. Palme, M. Misovic, J. Rudner, K. Dittmann, R. Lukowski, P. Ruth and S. M. Huber (2011). "Ionizing radiation induces migration of glioblastoma cells by activating BK K(+) channels." Radiother Oncol 101(1): 122-126.
Steinle, M., D. Palme, M. Misovic, J. Rudner, K. Dittmann, R. Lukowski, P. Ruth and S. M. Huber (2011). "Ionizing radiation induces migration of glioblastoma cells by activating BK K(+) channels." Radiother Oncol 101(1): 122-126.
Stock, C. and A. Schwab (2009). "Protons make tumor cells move like clockwork." Pflugers Arch 458(5): 981-992.

Tabatabai, G., B. Frank, R. Mohle, M. Weller and W. Wick (2006). "Irradiation and hypoxia promote homing of haematopoietic progenitor cells towards gliomas by TGF-beta-dependent HIF-1alpha-mediated induction of CXCL12." Brain 129(Pt 9): 2426-2435.

Takahashi, A., H. Yamaguchi and H. Miyamoto (1993). "Change in K+ current of HeLa cells with progression of the cell cycle studied by patch-clamp technique." Am J Physiol 265(2 Pt 1): C328-336.

Tamura, K., M. Aoyagi, N. Ando, T. Ogishima, H. Wakimoto, M. Yamamoto and K. Ohno (2013). "Expansion of CD133-positive glioma cells in recurrent de novo glioblastomas after radiotherapy and chemotherapy." J Neurosurg 119(5): 1145-1155.

Toro, L., M. Li, Z. Zhang, H. Singh, Y. Wu and E. Stefani (2014). "MaxiK channel and cell signalling." Pflugers Arch 466(5): 875-886.

Tseng, D., D. A. Vasquez-Medrano and J. M. Brown (2011). "Targeting SDF-1/CXCR4 to inhibit tumour vasculature for treatment of glioblastomas." Br J Cancer 104(12): 1805-1809.

Tseng-Crank, J., N. Godinot, T. E. Johansen, P. K. Ahring, D. Strobaek, R. Mertz, C. D. Foster, S. P. Olesen and P. H. Reinhart (1996). "Cloning, expression, and distribution of a Ca(2+)-activated K+ channel beta-subunit from human brain." Proc Natl Acad Sci U S A 93(17): 9200-9205.

Turner, K. L., A. Honasoge, S. M. Robert, M. M. McFerrin and H. Sontheimer (2014). "A proinvasive role for the Ca(2+) -activated K(+) channel KCa3.1 in malignant glioma." Glia 62(6): 971-981.

Turner, K. L. and H. Sontheimer (2014). "KCa3.1 modulates neuroblast migration along the rostral migratory stream (RMS) in vivo." Cereb Cortex 24(9): 2388-2400.

Ullrich, N., A. Bordey, G. Y. Gillespie and H. Sontheimer (1998). "Expression of voltage-activated chloride currents in acute slices of human gliomas." Neuroscience 83(4): 1161-1173.

Vanan, I., Z. Dong, E. Tosti, G. Warshaw, M. Symons and R. Ruggieri (2012). "Role of a DNA damage checkpoint pathway in ionizing radiation-induced glioblastoma cell migration and invasion." Cell Mol Neurobiol 32(7): 1199-1208.

Wang, J., Y. Q. Xu, Y. Y. Liang, R. Gongora, D. G. Warnock and H. P. Ma (2007). "An intermediate-conductance Ca(2+)-activated K (+) channel mediates B lymphoma cell cycle progression induced by serum." Pflugers Arch 454(6): 945-956.

Wang, S. C., C. F. Yu, J. H. Hong, C. S. Tsai and C. S. Chiang (2013). "Radiation therapy-induced tumor invasiveness is associated with SDF-1-regulated macrophage mobilization and vasculogenesis." PLoS One 8(8): e69182.

Watkins, S. and H. Sontheimer (2011). "Hydrodynamic cellular volume changes enable glioma cell invasion." J Neurosci 31(47): 17250-17259.

Watkins, S. and H. Sontheimer (2012). "Unique biology of gliomas: challenges and opportunities." Trends Neurosci 35(9): 546-556.

Weaver, A. K., V. C. Bomben and H. Sontheimer (2006). "Expression and function of calcium-activated potassium channels in human glioma cells." Glia 54(3): 223-233.

Weaver, A. K., X. Liu and H. Sontheimer (2004). "Role for calcium-activated potassium channels (BK) in growth control of human malignant glioma cells." J Neurosci Res 78(2): 224-234.

Weaver, A. K., M. L. Olsen, M. B. McFerrin and H. Sontheimer (2007). "BK channels are linked to inositol 1,4,5-triphosphate receptors via lipid rafts: a novel mechanism for coupling [Ca(2+)](i) to ion channel activation." J Biol Chem 282(43): 31558-31568.

Weber, D. C., N. Casanova, T. Zilli, F. Buchegger, M. Rouzaud, P. Nouet, H. Vees, O. Ratib, G. Dipasquale and R. Miralbell (2009). "Recurrence pattern after [(18)F]fluoroethyltyrosine-positron emission tomography-guided radiotherapy for high-grade glioma: a prospective study." Radiother Oncol 93(3): 586-592.

Wick, W., A. Wick, J. B. Schulz, J. Dichgans, H. P. Rodemann and M. Weller (2002). "Prevention of irradiation-induced glioma cell invasion by temozolomide involves caspase 3 activity and cleavage of focal adhesion kinase." Cancer Res 62(6): 1915-1919.

Wild-Bode, C., M. Weller, A. Rimner, J. Dichgans and W. Wick (2001). "Sublethal irradiation promotes migration and invasiveness of glioma cells: implications for radiotherapy of human glioblastoma." Cancer Res 61(6): 2744-2750.

Wonderlin, W. F. and J. S. Strobl (1996). "Potassium channels, proliferation and G1 progression." J Membr Biol 154(2): 91-107.

Woo, S. R., Y. Ham, W. Kang, H. Yang, S. Kim, J. Jin, K. M. Joo and D. H. Nam (2014). "KML001, a telomere-targeting drug, sensitizes glioblastoma cells to temozolomide chemotherapy and radiotherapy through DNA damage and apoptosis." Biomed Res Int 2014: 747415.

Zagzag, D., M. Esencay, O. Mendez, H. Yee, I. Smirnova, Y. Huang, L. Chiriboga, E. Lukyanov, M. Liu and E. W. Newcomb (2008). "Hypoxia- and vascular endothelial growth factor-induced stromal cell-derived factor-1alpha/CXCR4 expression in glioblastomas: one plausible explanation of Scherer's structures." Am J Pathol 173(2): 545-560.

Zagzag, D., Y. Lukyanov, L. Lan, M. A. Ali, M. Esencay, O. Mendez, H. Yee, E. B. Voura and E. W. Newcomb (2006). "Hypoxia-inducible factor 1 and VEGF upregulate CXCR4 in glioblastoma: implications for angiogenesis and glioma cell invasion." Lab Invest 86(12): 1221-1232.

Zhou, Y. C., J. Y. Liu, J. Li, J. Zhang, Y. Q. Xu, H. W. Zhang, L. B. Qiu, G. R. Ding, X. M. Su, S. Mei and G. Z. Guo (2011). "Ionizing radiation promotes migration and invasion of cancer cells through transforming growth factor-beta-mediated epithelial-mesenchymal transition." Int J Radiat Oncol Biol Phys 81(5): 1530-1537.

Anhang - Publikationen

Liste der Publikationen

a) Akzeptierte Publikationen

1. **Stegen, B., L. Butz, L. Klumpp, D. Zips, K. Dittmann, P. Ruth and S. Huber (2015).**
   „Ca^{2+}-activated IK K^+ Channel Blockade Radiosensitizes Glioblastoma Cells.“ Mol Cancer Res.
2. **Huber, S.M., L. Butz, B. Stegen, D. Klumpp, N. Braun, P. Ruth and F. Eckert (2013).**
   „Ionizing radiation, ion transports, and radioresistance of cancer cells.“ Front Physiol 4:212.
3. **Huber, S.M., L. Butz, B. Stegen, L. Klumpp, D. Klumpp and F. Eckert (2014).**
   „Role of ion channels in ionizing radiation-induced cell death.“ Biochim Biophys Acta.

b) Eingereichte Manuskripte

1. **Butz, L., B. Stegen, L. Klumpp, E. Haehl, K. Schilbach, A. Buschauer, D. Zips, S. Huber and P. Ruth (2015).**
   „BK K^+channel blockade inhibits glioblastoma brain infiltration induced by fractionated radiation.” Mol Cancer Res. (submitted, shared first-authorship)

Danksagung

Ich danke meinem Doktorvater, Herr Prof. Dr. Stephan Huber sowie Herr Prof. Dr. Peter Ruth für das Überlassen des sehr interessanten Themas meiner Dissertation, die Möglichkeit der Teilnahme an verschiedenen Kongressen und Fortbildungen sowie die Unterstützung, Beratung und Hilfestellung zu jeder Zeit.

Bei Herr Prof. und Herr Prof. möchte ich mich ganz herzlich für die Abnahme meiner Promotionsprüfung bedanken.

Ein sehr großes Dankeschön gilt dem harten Kern meiner Arbeitsgruppe. Allen voran Heidi und Ilka, die mir so oft wie nur möglich bei Versuchen, Fragestellungen und sonstigen Angelegenheiten zur Seite standen und mir geholfen haben. Lena, Dominik, Ivan, Lukas und Erik danke ich für die tolle Zeit und die Unterstützung innerhalb und außerhalb des Labors. Eine Arbeitsatmosphäre und Freundschaft wie die unsere würde sich wohl jede Arbeitsgruppe wünschen.
Einen ganz besonderen Dank möchte ich hierbei nochmals an Stephan richten, der durch seine hilfreiche, unterstützende, lustige und freundliche Art mir von Anfang an die Freude an der Forschung nahe gebracht hat.

Weiterhin möchte ich der „erweiterten“ Arbeitsgruppe auf der 7. und 9. Ebene des pharmazeutischen Instituts danken. Ihr habt mir nicht nur eine schöne Zeit in Tübingen beschert, sondern seid zu wahren Freunden geworden.

Meinen Eltern, meinen Geschwistern sowie Elke und Chris danke ich sehr für die Unterstützung während meines Studiums und meiner Dissertation. Egal auf welche Art und Weise, ihr seid immer für mich da und dafür bin ich euch sehr dankbar.

Ein ganz spezieller Dank gilt meiner Freundin Stephanie, die mir während unseres Studiums als auch während der Promotion in allen Lebenslagen zur Seite stand. Auch in schwierigen Zeiten zeigst du mir gegenüber immer Geduld und Verständnis. Du bringst täglich Freude in mein Leben und dafür danke ich dir von Herzen.

Published OnlineFirst June 3, 2015; DOI: 10.1158/1541-7786.MCR-15-0075

Molecular Cancer Research

Ca^{2+}-Activated IK K^+ Channel Blockade Radiosensitizes Glioblastoma Cells

Benjamin Stegen[1], Lena Butz[1,2], Lukas Klumpp[1,3], Daniel Zips[1], Klaus Dittmann[4], Peter Ruth[2], and Stephan M. Huber[1]

Abstract

Ca^{2+}-activated K^+ channels, such as BK and IK channels, have been proposed to fulfill pivotal functions in neoplastic transformation, malignant progression, and brain infiltration of glioblastoma cells. Here, the ionizing radiation (IR) effect of IK K^+ channel targeting was tested in human glioblastoma cells. IK channels were inhibited pharmacologically by TRAM-34 or genetically by knockdown, cells were irradiated with 6 MV photons and IK channel activity, Ca^{2+} signaling, cell cycling, residual double-strand breaks, and clonogenic survival were determined. In addition, the radiosensitizing effect of TRAM-34 was analyzed *in vivo* in ectopic tumors. Moreover, The Cancer Genome Atlas (TCGA) was queried to expose the dependence of IK mRNA abundance on overall survival (OS) of patients with glioma. Results indicate that radiation increased the activity of IK channels, modified Ca^{2+} signaling, and induced a G_2–M cell-cycle arrest. TRAM-34 decreased the IR-induced accumulation in G_2–M arrest and increased the number of γH2AX foci post-IR, suggesting that TRAM-34 mediated an increase of residual DNA double-strand breaks. Mechanistically, IK knockdown abolished the TRAM-34 effects indicating the IK specificity of TRAM-34. Finally, TRAM-34 radiosensitized ectopic glioblastoma *in vivo* and high IK mRNA abundance associated with shorter patient OS in low-grade glioma and glioblastoma.

Implications: Together, these data support a cell-cycle regulatory function for IK K^+ channels, and combined therapy using IK channel targeting and radiation is a new strategy for anti-glioblastoma therapy. *Mol Cancer Res; 13(9); 1283–95. ©2015 AACR.*

Introduction

Glioblastoma multiforme (GBM) represents the most common primary brain tumor in adults. The therapeutic concept combines resection of the tumor followed by adjuvant radiation therapy combined with simultaneous temozolomide chemotherapy. Although the administration of the alkylating cytostatic agent significantly prolongs overall survival (OS), the prognosis of patients with glioblastoma remains very poor, with a median survival time of less than 2 years (1).

The underlying radiobiological mechanisms of the poor radiation response of glioblastoma appear to include multiple factors. Among those are low cellular radiation sensitivity, high proportion of cancer stem cells, enhanced repopulation, protective tumor microenvironment, infiltration of the tumor by immune cells, and highly migratory phenotype of the GBM cells giving rise to infiltrative tumor growth. In addition, glioblastoma cells have been proposed to evade therapy by persisting in potential subventricular neural stem cell niches outside of the radiation target volume (2).

Glioblastoma cells functionally express high numbers of Ca^{2+}-activated IK K^+ channels (other names are hIKCa1, hKCa4, hSK4, KCa3.1) in their plasma membrane (3–6). Notably, IK channels are low expressed or even absent in human astrocytes (7) but upregulated during neoplastic transformation and malignant progression of the glioma (8). This suggests a specific function of these channels in glioblastoma tumorigenesis. As a matter of fact, IK channels have been demonstrated to be indispensable for glioblastoma cell migration (for review, see ref. 9). Accordingly, IK protein expression in the tumor significantly correlates with poor survival of the patients with glioma (10). Similar to glioblastoma, IK channels are upregulated in a variety of further tumor entities such as prostate (11), breast (12), and pancreatic cancer (13) as well as lymphoma (14) where they have been proven to control cell cycling and tumor growth.

In addition to tumor cell migration and proliferation, K^+ channel activity may contribute to radioresistance of tumor cells (for review, see refs. 15–17). Remarkably, the fungicide clotrimazole has been shown to impair glioblastoma growth *in vitro* and *in vivo* (18, 19) and to promote apoptotic cell death of irradiated glioblastoma cells *in vitro* (20). Because clotrimazole is a potent IK channel inhibitor, we tested in the present study for a functional significance of IK channels in the radioresistance of glioblastoma cells *in vitro*. We could show by physiologic and cell biologic means that ionizing radiation activates IK channels in glioblastoma cells. Channel activation, in turn, contributes to the cellular stress response. Accordingly, inhibition or silencing of IK channels resulted in impaired cell-cycle arrest and DNA repair and decreased the clonogenic survival of irradiated glioblastoma cells. In addition, pharmacologic targeting of IK channels radiosensitized glioblastoma grown ectopically in mice during fractionated radiation therapy.

[1]Department of Radiation Oncology, University of Tübingen, Tübingen, Germany. [2]Department of Pharmacology, Toxicology and Clinical Pharmacy, Institute of Pharmacy, University of Tübingen, Tübingen, Germany. [3]Dr. Margarete Fischer-Bosch-Institute of Clinical Pharmacology, Stuttgart, Germany. [4]Division of Radiobiology and Molecular Environmental Research, Department of Radiation Oncology, University of Tübingen, Tübingen, Germany.

Corresponding Author: Stephan M. Huber, Department of Radiation Oncology, Laboratory of Experimental Radiation Oncology, University of Tübingen, Hoppe-Seyler-Str. 3, Tübingen 72076, Germany. Phone: 49-0-7071-29-82183; Fax: 0-7071-29-4944; E-mail: stephan.huber@uni-tuebingen.de

doi: 10.1158/1541-7786.MCR-15-0075

Published OnlineFirst June 3, 2015; DOI: 10.1158/1541-7786.MCR-15-0075

Furthermore, a Cancer Genome Atlas (TCGA) query suggests an association between glioma IK mRNA abundance and progression-free survival (PFS) of patients with glioma.

Materials and Methods

Cell culture

Human T98G and U87MG glioblastoma cells were from the ATCC and were grown in 10% FCS-supplemented RPMI-1640 medium as described (21). The human SVGA fetal astrocyte cell line has been kindly provided by Professor Walter J. Atwood, Brown University (Providence, RI), and was maintained in 10% FCS-supplemented DMEM. Exponential growing T98G and U87 MG cells were irradiated with 6 MV photons (IR, single dose of 0, 2, 4, and 6 Gy) by using a linear accelerator (LINAC SL25 Philips) at a dose rate of 4 Gy/min at room temperature. Following irradiation, cells were postincubated in RPMI-1640/10% FCS medium for 2 to 6 hours (immunoblot, patch-clamp, fura-2 Ca^{2+} imaging), 24 hours (γH2AX immunofluorescence), 24 and 48 hours (flow cytometry), and 2 weeks (colony formation; ref. 21). In some experiments, cells were preincubated (0.5 hours) and postincubated after IR with the IK K^+ channel inhibitor TRAM-34 (10 μmol/L) or vehicle alone (0.1% DMSO). Transfected T98G cells were grown in RPMI-1640/10% FCS selection medium containing puromycin (2 μg/mL).

Immunofluorescence

Subconfluent T98G glioblastoma cells and SVGA fetal astrocytes grown on object slides (Millicell EZ SLIDES; Millipore) were fixed with 4% paraformaldehyde in PBS for 1 hour and washed three times for 5 minutes with PBS. Cells were blocked for 1 hour with PBS containing 0.3% Triton X-100, 5% normal goat serum, and washed for 15 minutes with PBS. Incubation with rabbit anti-IK antibody (H-120, SantaCruz Biotechnology, Inc.; sc-32949, 1:50) and rabbit IgG isotype control antibody (1:250, Millipore), respectively, in antibody dilution buffer (PBS, 0.3% Triton X-100, 1% BSA) was performed for 1 hour at room temperature. Cells were washed three times for 5 minutes in PBS and incubated for 2 hours at room temperature in the dark with FITC-conjugated goat anti-rabbit IgG antibody (1:500, Novus Biologicals). Cells were washed three times with PBS, and object slides were mounted with cover slips using the DNA-specific fluorochrome DAPI-containing ECTASHIELD mounting medium with DAPI (Vectashield, Vector Laboratories, BIOZOL).

Patch-clamp recording

Semiconfluent cells were irradiated with 0 Gy (SVGA, T98G) or 2 Gy (T98G). Whole-cell and on-cell currents were evoked by 9 to 11 (whole-cell) or 41 (on-cell) voltage square pulses (700 ms each) from −50 or 0 mV holding potential to voltages between −100 and +100 mV delivered in 5 or 20 mV increments. The liquid junction potentials between the pipette and the bath solutions were estimated according to previously published data (22), and data were corrected for the estimated liquid junction potentials. Cells were superfused at 37°C temperature with NaCl solution (125 mmol/L NaCl, 32 mmol/L HEPES, 5 mmol/L KCl, 5 mmol/L D-glucose, 1 mmol/L $MgCl_2$, 1 mmol/L $CaCl_2$, titrated with NaOH to pH 7.4). In the whole-cell experiment shown in Fig. 1, ionomycin (2.5 μmol/L) and TRAM-34 (1 μmol/L) or ionomycin (2.5 μmol/L), paxilline (5 μmol/L), and TRAM-34 (1 μmol/L, all from Sigma-Aldrich) were sequentially added to the bath solution. For this recording, a K-D-gluconate pipette solution was used containing: 140 mmol/L K-D-gluconate, 5 mmol/L HEPES, 5 mmol/L $MgCl_2$, 1 mmol/L K_2-EGTA, 1 mmol/L K_2-ATP, titrated with KOH to pH 7.4. In the on-cell experiments (Fig. 2), the pipette solution contained 0 or 0.01 mmol/L TRAM-34 in DMSO, 130 mmol/L KCl, 32 mmol/L HEPES, 5 mmol/L D-glucose, 1 mmol/L $MgCl_2$, 1 mmol/L $CaCl_2$, titrated with KOH to pH 7.4. Whole-cell and macroscopic on-cell currents were analyzed by averaging the currents between 100 and 700 ms of each square pulse.

Western blotting

Surface proteins of irradiated (0 and 2 Gy) T98G cells were enriched by the use of a cell surface protein isolation kit (Pierce) according to the supplied protocol. Whole protein lysates were prepared from stably transfected T98G cells (see below). Proteins were lysed in a buffer containing 50 mmol/L HEPES, pH 7.5, 150 mmol/L NaCl, 1 mmol/L EDTA, 10 mmol/L sodium pyrophosphate, 10 mmol/L NaF, 2 mmol/L Na_3VO_4, 1 mmol/L phenylmethylsulfonylfluoride (PMSF), additionally containing 1% triton X-100, 5 μg/mL aprotinin, 5 μg/mL leupeptin, and 3 μg/mL pepstatin, and separated by SDS-PAGE under reducing conditions. Segregated proteins were electrotransferred onto polyvinylidene difluoride (PVDF) membranes (Roth). Blots were blocked in TBS buffer containing 0.05% Tween-20 and 5% non-fat dry milk for 1 hour at room temperature. The membrane was incubated overnight at 4°C with the following primary antibodies in TBS-Tween/5% milk against IK (H-120, sc-32949 SantaCruz, 1:500) or the α_1 subunit of the Na^+ pump (Cell Signaling #3010, New England Biolabs; 1:500). Equal gel loading was verified by an antibody against β-actin (mouse anti-β-actin antibody, clone AC-74, Sigma #A2228; 1:20,000). Antibody binding was detected with a horseradish peroxidase–linked goat anti-rabbit or horse anti-mouse IgG antibody (Cell Signaling #7074 and #7076, respectively; 1:2,000 dilution in TBS-Tween/5% milk) incubated for 1 hour at room temperature, and enhanced chemoluminescence (ECL Western blotting analysis system, GE Healthcare/Amersham-Biosciences) of indicated protein levels were quantified by densitometry using ImageJ software (ImageJ 1.40g, NIH, Bethesda, MD).

Fura-2 Ca^{2+} imaging

Fluorescence measurements were performed using an inverted phase-contrast microscope (Axiovert 100; Zeiss). Fluorescence was evoked by a filter wheel (Visitron Systems)-mediated alternative excitation at 340/26 or 387/11 nm (AHF, Analysentechnik). Excitation and emission lights were deflected by a dichroic mirror (409/LP nm beamsplitter, AHF) into the objective (Fluar x40/1.30 oil; Zeiss) and transmitted to the camera (Visitron Systems), respectively. Emitted fluorescence intensity was recorded at 587/35 nm (AHF). Excitation was controlled and data acquired by Metafluor computer software (Universal Imaging). The 340/380-nm fluorescence ratio was used as a measure of cytosolic free Ca^{2+} concentration ($i[Ca^{2+}]_{free}$). T98G cells were irradiated (0 or 2 Gy) and loaded with fura-2/AM (2 μmol/L for 30 minutes at 37°C; Molecular Probes) in RPMI-1640/10% FCS medium. $i[Ca^{2+}]_{free}$ was determined 2 to 3 hours post-IR at 37°C during superfusion with NaCl solution (125 mmol/L NaCl, 32 mmol/L HEPES, 5 mmol/L KCl, 5 mmol/L D-glucose, 1 mmol/L $MgCl_2$, 2 mmol/L $CaCl_2$, titrated with NaOH to pH 7.4), during extracellular Ca^{2+} removal in EGTA-buffered NaCl solution (125 mmol/L NaCl,

Published OnlineFirst June 3, 2015; DOI: 10.1158/1541-7786.MCR-15-0075

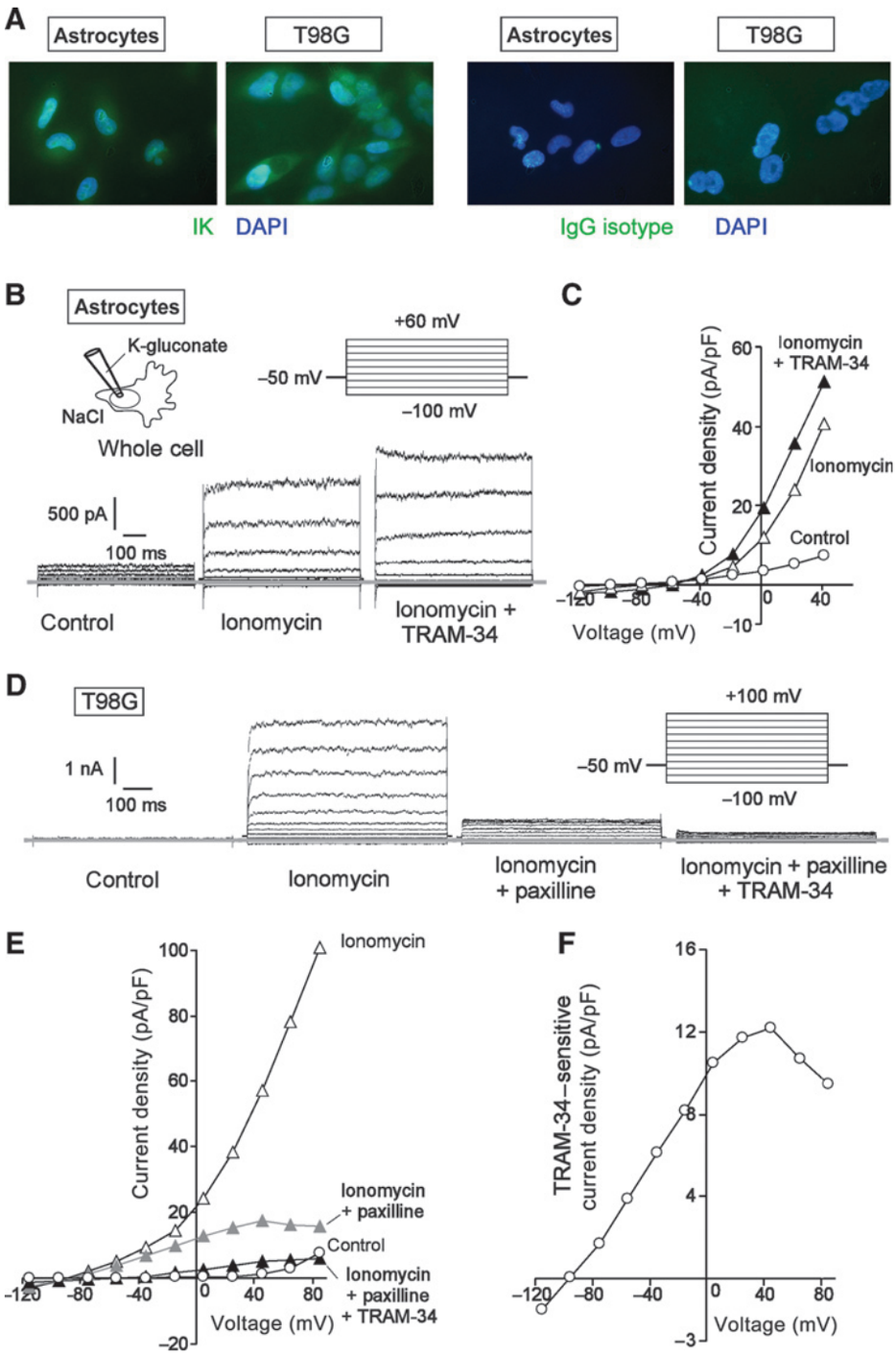

Figure 1.
T98G cells functionally express BK and IK K^+ channels. A, immunofluorescent micrographs of human astrocytes and T98G glioblastoma cells stained (green fluorescence) with an IK-specific antibody (left) or the IgG isotype control antibody (right). The nuclei were stained with the DNA-specific dye DAPI (blue). B, whole-cell current tracing of a human astrocyte recorded with K-gluconate pipette and NaCl bath solution before (first tracings) and after (second to third tracings) Ca^{2+} permeabilization of the plasma membrane with the Ca^{2+} ionophore ionomycin (2.5 μmol/L). Ca^{2+}-activated currents were recorded under control conditions (second tracings) or after bath application of the IK channel blocker TRAM-34 (1 μmol/L; third tracings; the inset in the middle shows the applied pulse protocol). C, dependence of the whole-cell current densities on voltage of the records shown in B. D, whole-cell current tracings of a T98G cell recorded as in B before (first tracings) and after (second to fourth tracings) Ca^{2+} permeabilization of the plasma membrane. Ca^{2+}-activated currents were recorded under control conditions (second tracings) or after bath application of the BK channel inhibitor paxilline (5 μmol/L, third tracings) and additional administration of the IK channel blocker TRAM-34 (1 μmol/L; fourth tracings; the inset on the right shows the applied pulse protocol). E, dependence of the whole-cell current densities on voltage of the records shown in D. F, TRAM-34–sensitive current density fraction as calculated by subtracting the current densities of E recorded with paxilline and TRAM-34 from those obtained with paxilline alone.

32 mmol/L HEPES, 5 mmol/L KCl, 5 mmol/L D-glucose, 1 mmol/L $MgCl_2$, 0.6 mmol/L EGTA, titrated with NaOH to pH 7.4), and during Ca^{2+} re-addition in $CaCl_2$-containing NaCl solution.

Flow cytometry

T98G cells were preincubated (0.25 hours), irradiated (0 or 2 Gy), and incubated for further 6 hours in RPMI-1640/10% FCS medium additionally containing the base analogue 5-ethynyl-2′-deoxyuridine (EdU; 5 μmol/L). EdU incorporation was analyzed by the use of a EdU flow cytometry kit (BCK-FC488, baseklick) after fixing the cells and co-staining the DNA with propidium iodide (PI; Sigma-Aldrich) according to the manufacturer's instructions. EdU-specific fluorescence and PI fluorescence were measured by flow cytometry (FACS Calibur, Becton Dickinson; 488 nm excitation wavelength) in fluorescence channel FL-1 (log scale, 515–545 nm emission wavelength) and FL-3 (linear scale, >670 nm emission wavelength), respectively. In additional experiments, T98G cells were preincubated (30 minutes),

Published OnlineFirst June 3, 2015; DOI: 10.1158/1541-7786.MCR-15-0075

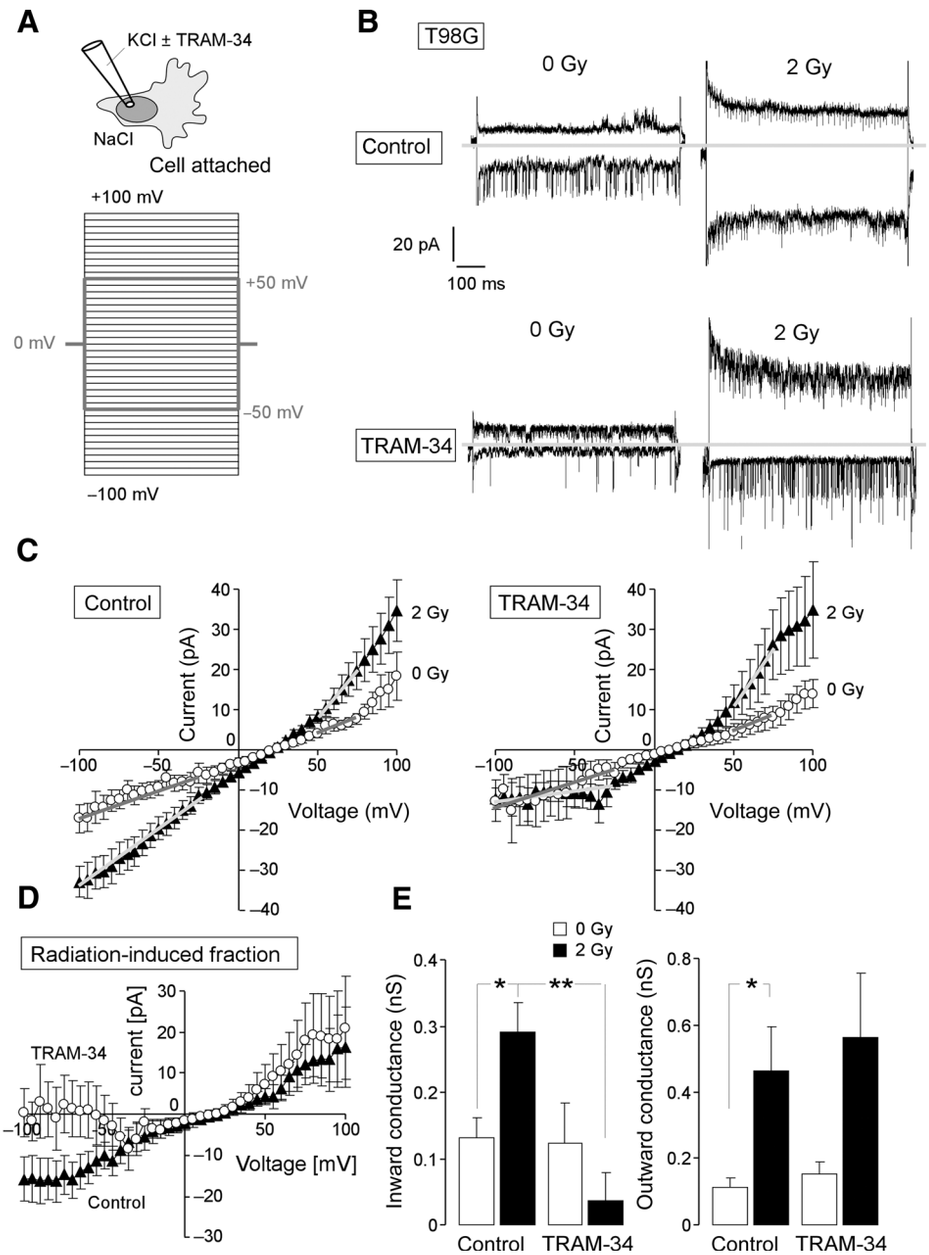

Figure 2.
IR increases the activity of IK K^+ channels. A, experimental setup: macroscopic on-cell currents were recorded from control and irradiated T98G cells with KCl pipette and NaCl bath solution applying the depicted pulse protocol. Currents obtained in the presence and absence of the IK channel inhibitor TRAM-34 (10 μmol/L) were compared between unpaired experiments. B, macroscopic on-cell current tracings recorded during voltage square pulses to −50 and +50 mV, respectively (as shown by the gray pulse protocol in A) from control (left) and irradiated (2 Gy) T98G cells with (lower traces) and without (upper traces) TRAM-34 in the pipette solutions. Note that the prominent single-channel current deflections are generated by BK K^+ channels, which are also activated by IR as reported (ref. 21; also evident from E, right). C, dependence of the mean macroscopic on-cell currents (±SE) on holding potential in control (open circles) and 2 Gy–irradiated T98G cells (2.5–5.5 hours after irradiation, closed triangles) recorded in the absence (left, $n = 26$–28) and presence (right, $n = 8$–9) of TRAM-34 in the pipette. D, mean (±SE) radiation-induced current fractions as calculated from the data in C for control (closed triangles) and TRAM-34-treated (open circles) T98G cells. E, mean (± SE) inward (left) and outward (right) conductance as calculated from the data in C by linear regression (voltage ranges are indicated by gray lines) for control (open bars) and irradiated (closed bars) T98G cells recorded in the absence (first and second bars) or presence of TRAM-34 (third and fourth bars; ** and * indicate $P \leq 0.01$ and $P \leq 0.05$, respectively, Kruskal–Wallis nonparametric ANOVA test).

irradiated (0, 2, 4, or 6 Gy), and incubated for further 24 or 48 hours in RPMI-1640/10% FCS medium additionally containing either TRAM-34 (10 μmol/L) or vehicle alone (0.1% DMSO). For cell-cycle analysis, cells were permeabilized and stained (30 minutes at room temperature) with PI solution (containing 0.1% Na citrate, 0.1% Triton X-100, 10 μg/mL PI in PBS), and the DNA amount was analyzed by flow cytometry in fluorescence channel FL-3 (linear scale). Data were analyzed with the FCS Express 3 software (De Novo Software).

γH2AX foci formation

T98G cells cultured on CultureSlides (Becton Dickinson) in RPMI-1640/10% FCS medium were irradiated (0 or 2 Gy) post-incubated for 24 hours in the presence of TRAM-34 (10 μmol/L) or vehicle alone (0.1% DMSO) and fixed with 70% ice-cold ethanol. For immunofluorescent analysis, cells were incubated with anti-γH_2AX antibody (Upstate, Millipore; clone JBW301; 1:500) at room temperature for 2 hours. Positive foci were visualized by incubation with a 1:500 dilution of Alexa488-labeled goat anti–mouse serum (Molecular Probes) for 30 minutes. CultureSlides were mounted in Vectashield/DAPI (Vector Laboratories) and evaluated by conventional fluorescence microscopy.

IK shRNA

IK was downregulated in T98G cells by stable transfection with IK-specific and—for control—nontargeting shRNA using MISSION pLKO.1 lentiviral transduction particles

Published OnlineFirst June 3, 2015; DOI: 10.1158/1541-7786.MCR-15-0075

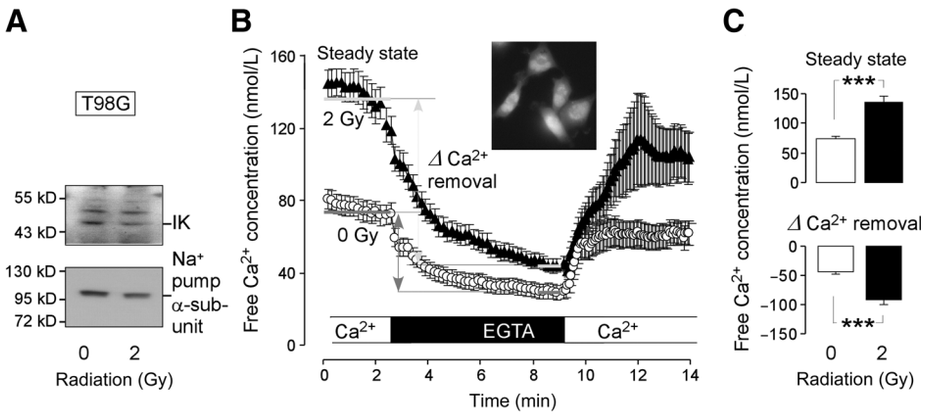

Figure 3.

IR modulates the cytosolic free Ca^{2+} concentration ($i[Ca^{2+}]_{free}$) but not the surface expression of IK channels in T98G cells. A, immunoblots of surface proteins from control (0 Gy) and irradiated T98G cells (2 Gy) probed against IK (top) and for loading control against the α_1 subunit of the Na^+ pump (bottom). B, time course of the mean (±SE) cytosolic free Ca^{2+} concentration ($i[Ca^{2+}]_{free}$) as measured by ratiometrical fura-2 Ca^{2+} imaging 3 to 5 hours after irradiation with 0 Gy (open circles; $n = 32$) or 2 Gy (closed triangles $n = 24$) during removal and re-addition of external Ca^{2+}. C, mean (±SE) steady-state $i[Ca^{2+}]_{free}$ (top, as indicated by gray lines at the beginning of the records in B) and mean (±SE) decrease in $i[Ca^{2+}]_{free}$ (bottom) upon removal of extracellular Ca^{2+} (as indicated by the gray arrows in B) in control (open bars) and irradiated cells (data from B; ***, $P \leq 0.001$, two-tailed t test).

(SHCLNV-NM_002250 and SHC002V, Sigma-Aldrich) according to the provided experimental protocol. Downregulation of IK was controlled by quantitative RT-PCR and immunoblotting (Fig. 7A and B).

Quantitative RT-PCR

mRNAs of stably transfected T98G cells were isolated (Qiagen RNA extraction kit) and reversely transcribed in cDNA (Transcriptor First Strand cDNA Synthesis Kit, Roche). IK K^+ channel and GAPDH-specific fragments were amplified by the use of SYBR Green–based quantitative real-time PCR (QT00003780 and QT01192646 QuantiTect Primer Assay and QuantiFast SYBR Green PCR Kit, Qiagen) in a Roche LightCycler Instrument.

Colony formation assay

To test for clonogenic survival, U87MG, parental T98G, and stably transfected T98G cells (clones #2 and #3) were irradiated (0, 2, 4, or 6 Gy) in RPMI-1640/10% FCS medium additionally containing TRAM-34 (10 μmol/L) or vehicle alone (0.1% DMSO). After 24 hours of incubation with the inhibitor/vehicle, cells were detached, 200 to 800 cells were reseeded in inhibitor-free medium on 3-cm wells and grown for further 2 to 3 weeks. The plating efficiency was defined by dividing the number of colonies by the number of plated cells. Survival fractions as calculated by dividing the plating efficiency of the irradiated cells by those of the unirradiated controls were fitted by the use of the linear quadratic equation.

Ectopic mouse model of human glioblastoma

All experiments were performed according to the German Animal Protection Law and approved by the local authorities (RP Tübingen, reference number PZ3/13). Human U87MG cells (500,000 cells in 100 μL PBS) were injected subcutaneously in the upper outer right hind limb of 8-week-old female $NMRI^{Nu/Nu}$ mice. Tumor growth was monitored at least 3 times per week by measuring tumor size in 3 dimensions using calipers. Upon reaching a tumor volume of around 150 μL, mice were randomly assigned to 4 treatment arms (control, fractionated radiation, TRAM-34, and TRAM-34 combined with fractionated radiation). Beginning with day 0, tumors were locally irradiated under isoflurane anesthesia at room temperature with 5 consecutive daily fractions of 0 (control) or 4 Gy 6 MV photons as described (23). Six hours before each radiation fraction, mice received intraperitoneal injections of the IK channel inhibitor TRAM-34 (0 or 120 mg/kg body weight in Mygliol). The drug TRAM-34 at the applied dose and local fractionated irradiation of the ectopic glioblastoma was well tolerated by the mice.

Querying TGCA datasets

Via the cBIOportal Web resource (24, 25), the provisional Glioblastoma-Multiforme and Lower-Grade-Glioma TCGA databases (http://cancergenome.nih.gov/) were queried for IK mRNA abundance of the tumor specimens and PFS of the patients with glioma. In lower grade glioma and glioblastoma, 14 to 22 of 116 to 346 tumor specimens with RNA Seq V2 mRNA data exhibited an IK mRNA abundance greater than a certain threshold. A threshold of the mean expression value + 2/3 z-score was used for both low-grade glioma and glioblastoma to define middle-rate and high IK mRNA abundance. The z-score of the IK mRNA abundance in an individual glioma specimen is calculated by the number of SDs the individual mRNA abundance differing from the mean value of all gliomas tumors that are diploid for the IK gene. In Fig. 9, PFS and OS of a low number of patients (n = 14–21) with tumors that exhibit an elevated IK mRNA abundance (i.e., above the mean value + 2/3 z-score) was compared with the majority of patients (n = 102–325) with gliomas that exhibit "middle-rate" IK mRNA abundance (i.e., varying within mean value ± 2/3 z-score). Statistical analysis was performed with the log-rank test.

Results

To assess IK protein expression in the embryonic astrocyte cell line SVGA and the glioblastoma cell lines T98G, exponential growing cells were fixed, immunostained with an IK-specific antibody or an IgG isotype control antibody, and analyzed by fluorescence microscopy. Figure 1A suggests higher IK protein abundance in T98G than in SVGA cells. To estimate the

Published OnlineFirst June 3, 2015; DOI: 10.1158/1541-7786.MCR-15-0075

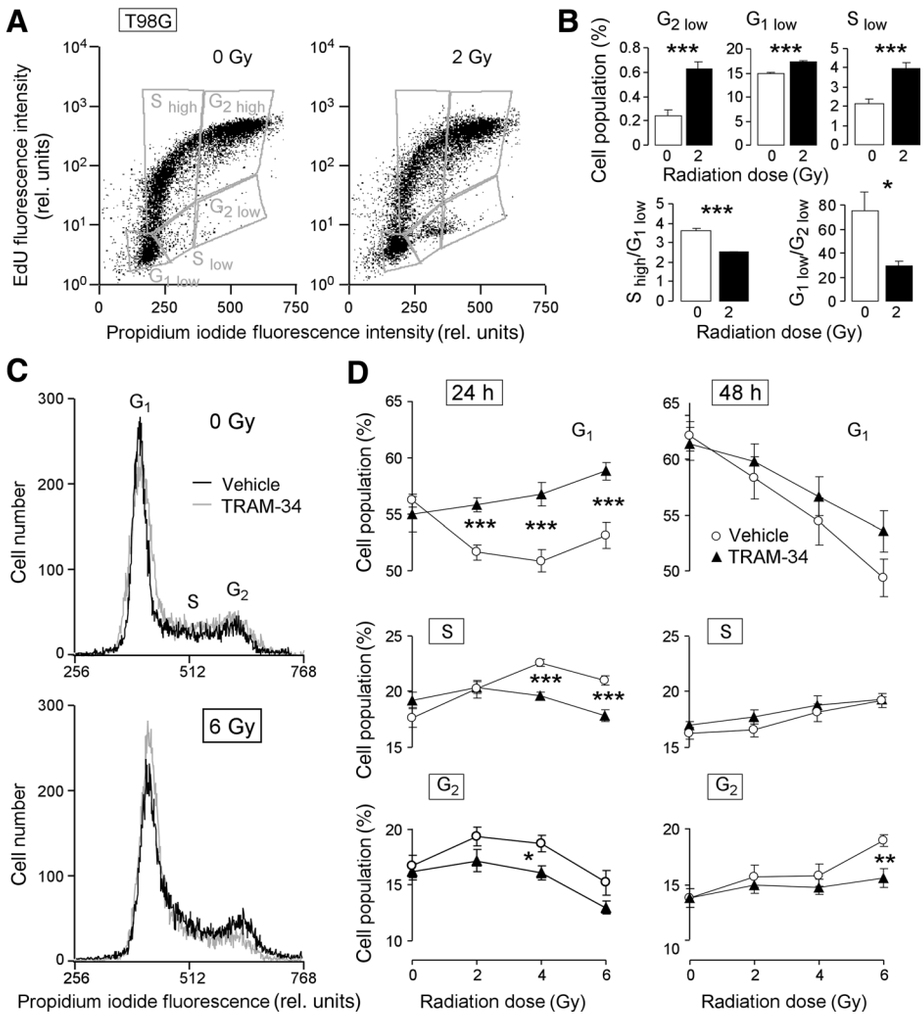

Figure 4.
The IK channel inhibitor TRAM-34 modifies cell-cycle control in irradiated T98G cells. A, dot blots showing EdU incorporation by irradiated (0 or 2 Gy as indicated) T98G cells. Immediately after irradiation cells were incubated for 6 hours with EdU (5 μmol/L) before co-staining with PI and analysis by flow cytometry. Gray gates show the different cell populations. B, mean percentage (±SE, $n = 6$) of irradiated (0 or 2 Gy) EdU-negative T98G cells arrested in G_2, G_1, or S phase of cell cycle (top line). Mean ratios (±SE, $n = 6$) of EdU-positive S-phase and EdU-negative G_1 phase populations (S_{high}/G_{1low}) as well as of EdU-negative G_1 and G_2 populations ($G_{1low}/G_{2\ low}$) in irradiated (0 or 2 Gy) cells as a measure of G_1–S transition and mitosis, respectively (bottom line). C, histograms of PI-stained T98G cells (Nicoletti protocol) recorded by flow cytometry 48 hours after IR with 0 Gy (top) or 6 Gy (bottom). Cells were preincubated (0.5 hours), irradiated, and postincubated in the absence (control, black line) or presence of TRAM-34 (10 μmol/L, gray line). D, mean percentage (±SE, $n = 9$) of irradiated (0, 2, 4, or 6 Gy) T98G cells residing 24 hours (left) or 48 hours (right) after IR in G_1 (top line), S (middle line), or G_2 phase of cell cycle (bottom line). Cells were pre- and postincubated as in A with vehicle alone (open circles) or with 10 μmol/L TRAM-34 (closed triangles; ***, **, and * indicate $P \leq 0.001$, $P \leq 0.01$, and $P \leq 0.05$, respectively, two -tailed (Welch-corrected) t test).

functionality of IK K^+ channels in SVGA, T98G, and a further glioblastoma cell line (U87MG), currents through the plasma membrane were recorded with the patch-clamp technique in whole-cell mode with physiologic bath and pipette solutions. Records were obtained before and after Ca^{2+} permeabilizing the plasma membrane with the Ca^{2+} ionophore ionomycin (2.5 μmol/L). To characterize the Ca^{2+}-stimulated current fraction, the BK K^+ channel inhibitor paxilline (5 μmol/L) and/or the IK K^+ channel inhibitor TRAM-34 (1 μmol/L) were added sequentially to the ionomycin-containing bathing solution. In SVGA astrocytes, ionomycin failed to induce outwardly rectifying whole-cell currents at voltages more negative than −20 mV in 6 of 6 tested cells suggestive of the absence of functional IK channel in the plasma membrane. Accordingly, bath application of TRAM-34 did not inhibit a fraction of the whole-cell currents. A representative experiment is depicted in Fig. 1B and C.

In sharp contrast, ionomycin activated a whole-cell outward current in T98G cells at all voltages more positive than K^+ equilibrium potential ($E_K \approx -90$ mV; Fig. 1D and E, open triangles). Paxilline inhibited about 80% of the outward current in Ca^{2+}-permeabilized T98G cells (Fig. 1D and E, gray filled triangles). Additional application of TRAM-34 blocked almost all of the remaining paxilline-insensitive current fraction (Fig. 1D and E, black filled triangles). This TRAM-34-sensitive current fraction (Fig. 1F) exhibited inward rectification with a conductance density of about 100 pS/pF at negative voltages and had a reversal potential close to E_K. Together, these data indicate functional expression of a Ca^{2+}-activated, inwardly rectifying K^+-selective and TRAM-34–sensitive current fraction, which is characteristic for an IK current (26) in T98G glioblastoma cells but not in the astrocyte cell line. Ca^{2+}-permeabilized U87MG cells showed similarly high IK channel activity albeit having lower paxilline-sensitive currents (data not shown).

To test whether IR induces changes in IK channel activity, T98G cells were irradiated with 2-Gy 6-MV photons by the use of a linear accelerator, postincubated for 2 to 6 hours, and recorded in cell-attached mode using a KCl solution in the pipette (Fig. 2A). IR stimulated an increase in the inward and outward fraction of the macroscopic cell–attached currents (Fig. 2B, top, and C, left). Importantly, when in unpaired experiments the IK channel inhibitor TRAM-34 (10 μmol/L) was added to the pipette solution (Fig. 2B, bottom, and C, right), an IR-stimulated inward current was no more detectable (Fig. 2C and D) indicative of an IR-stimulated IK current.

Reportedly, IR may modulate the Ca^{2+} signaling (for review, see ref. 15). To define signaling events upstream of IK channel

Published OnlineFirst June 3, 2015; DOI: 10.1158/1541-7786.MCR-15-0075

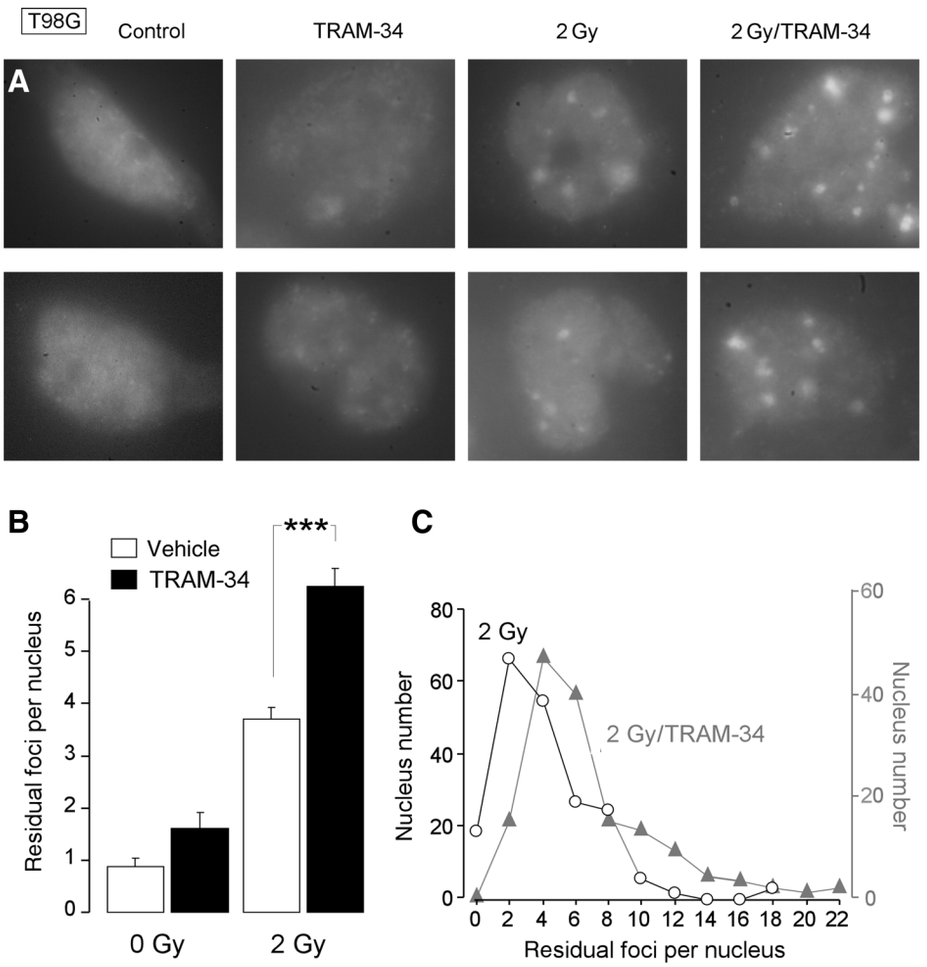

Figure 5.
IK channel inhibition increases the number of residual γH_2AX foci in T98G cells. A, immunofluorescent micrographs of T98G nuclei double-stained against γH_2AX and DNA (DAPI). Cells were fixed 24 hours after irradiation (0 or 2 Gy) and preincubation with TRAM-34 (0 or 10 μmol/L) as indicated. B, mean (±SE, $n = 30$–60 for 0 Gy and 150–200 for 2 Gy) numbers of residual γH_2AX foci per nucleus 24 hours after irradiation (0 or 2 Gy) and incubation with TRAM-34 (10 μmol/L) or vehicle. C, histograms of irradiated (black) and irradiated and TRAM-34–treated cells (gray, data from B) showing the distribution of residual γH_2AX foci counts (***, $P \leq 0.001$, Kruskal–Wallis nonparametric ANOVA test).

activation, cytosolic free Ca^{2+} concentration ($i[Ca^{2+}]_{free}$) was assessed by fura-2 Ca^{2+} imaging experiments in control and irradiated (2 Gy) T98G cells 3 to 5 h after IR. In addition, IK surface expression was analyzed in control and irradiated T98G cells by immunoblots of biotinylated and avidin-separated surface proteins probed against IK and—for loading control—against the α_1 subunit of the Na^+ pump. As shown in Fig. 3, the IR-induced increase in IK activity in T98G was probably due to IR-induced increase in $i[Ca^{2+}]_{free}$ (Fig. 3B and C) rather than to an elevated surface expression of IK channels (Fig. 3A). IR (2 Gy) induced a significant increase in steady-state $i[Ca^{2+}]_{free}$ (Fig. 3B and C, top). Upon removal and re-addition of extracellular Ca^{2+}, irradiated cells showed a larger drop-down and larger re-increase of $i[Ca^{2+}]_{free}$, respectively, as compared with unirradiated cells (Fig. 3B and C, bottom). This suggests that a shift in the Ca^{2+} leak/pump equilibrium of the plasma membrane accounted for the observed IR-induced $i[Ca^{2+}]_{free}$ increase.

K^+ channels have been shown to regulate the cell cycle in irradiated tumor cells (27). Therefore, we analyzed by flow cytometry, the incorporation of the base analogue EdU by irradiated (0 or 2 Gy) T98G cells within the first 6 hours after IR. Figure 4A shows the incorporated EdU in dependence on the DNA amount as defined by co-staining of the cells with PI as DNA-specific fluorescence dye. IR increased the cell populations residing in G_1, S, and G_2 phase in cell cycle with low EdU-specific fluorescence intensity (i.e., cells that did not incorporate EdU, Fig. 4B, top line). This points to an IR-induced G_1, S, and G_2–M arrest in T98G cells. In particular, IR decreased the ratios between cells in the S-phase that incorporated EdU (S_{high}) and the $G_{1\ low}$ population on the one hand and between the $G_{1\ low}$ and the $G_{2\ low}$ populations on the other (Fig. 4B, bottom line) indicative of a profound inhibition of G_1–S transition and mitosis in irradiated T98G cells.

To test for a function of IK channels in cell-cycle control, the effect of IR (0, 2, 4, or 6 Gy) in combination with IK inhibition by TRAM-34 on cell-cycle distribution of T98G cells was analyzed 24 and 48 hours after IR by PI staining in flow cytometry (Fig. 4C). Twenty-four hours after IR with 2 and 4 Gy, the G_1 population was decreased and the S and G_2 increased as compared to 0-hour values (open circles in Fig. 4D, left). This suggests that the G_1 arrest observed in the EdU incorporation experiments was short-living. In contrast, 24 hours after IR with 6 Gy, the accumulation in S and G_2 phase of cell cycle was blunted as compared with 2 or 4 Gy–irradiated cells suggestive of a sustained G_1 arrest induced in a fraction of cells at higher dose (open circles in Fig. 4D, left). However, 48 hours after IR, number of G_1 and G_2 residing cells decreased and increased, respectively, more or less linearly with increasing IR dose (open circles in Fig. 4B and D, right),

Published OnlineFirst June 3, 2015; DOI: 10.1158/1541-7786.MCR-15-0075

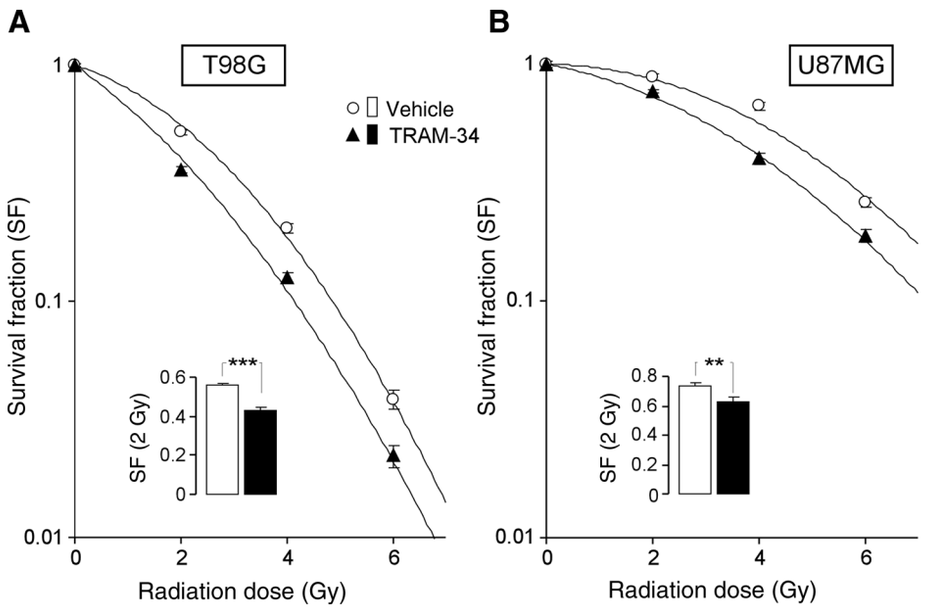

Figure 6.
IK inhibition radiosensitizes T98G and U87MG glioblastoma cells. A and B, mean survival fraction (±SE, $n = 8$) of irradiated (0, 2, 4, or 6 Gy) T98G (A) and U87MG cells (B). Cells were irradiated and postincubated (24 hours) in the presence of vehicle alone (open circles) or TRAM-34 (10 μL, closed triangles) before plating in inhibitor-free medium. The insets show the mean survival fractions (±SE, $n = 24$) upon irradiation with 2 Gy (SF_{2Gy}) in vehicle alone (open bars) and TRAM-34 (10 μmol/L, closed bars)-containing medium from a higher number of experiments (** and *** indicate $P \leq 0.01$ and $P \leq 0.001$, respectively, two-tailed t test).

confirming the transitory nature of the G_1 arrest. Importantly, the IK channel blocker TRAM-34 (10 μmol/L) delayed or even prevented the radiation-induced decrease of cell population in G_1 and accumulation in G_2 (Fig. 4D, closed triangles). Together, the data indicate functional significance of IK channels in cell-cycle control. Because only little effect of TRAM-34 on cell-cycle distribution was apparent in unirradiated cells (0 Gy in Fig. 4D), IK channels seem to regulate cell-cycle predominantly in cells undergoing genotoxic stress.

Next, we estimated the number of residual DNA double-strand breaks in T98G cells 24 hours after IR with 0 or 2 Gy by counting the γH_2AX foci in immunofluorescent micrographs (Fig. 5A). As shown in Fig. B (right), TRAM-34 (10 μmol/L) significantly increased the mean number of residual γH_2AX foci per nucleus from about 4 (vehicle control) to 6 (TRAM-34) 24 hours after IR with 2 Gy. Thereby, foci numbers seemed to be similarly elevated in nuclei with low, intermediate, and high foci counts as compared with the respective vehicle controls giving rise to a TRAM-34–induced right shift of the foci count/nucleus number histogram depicted in Fig. 5C. This right shift might be explained by a delay in DNA double-strand break repair in TRAM-34–treated cells.

Unirradiated cells showed a tendency of increased foci formation when incubated for 24 hours with TRAM-34 (Fig. 5B, left) that might hint to a genotoxic effect of TRAM-34. However, TRAM-34 (10 μmol/L) did not decrease the plating efficacy (0.25 ± 0.001, $n = 36$) when compared with the vehicle control (0.23 ± 0.001, $n = 36$) in delayed plating colony formation assays. Similarly, TRAM-34 did not decrease the plating efficacy of U87MG cells (0.56 ± 0.01 vs. 0.51 ± 0.01, $n = 36$), indicating that IK channel blockade does not impair the clonogenic survival of unirradiated glioblastoma cells. In irradiated T98G (Fig. 6A) and U87MG cells (Fig. 6B), in sharp contrast, TRAM-34 significantly decreased clonogenic survival with a radiosensitizer enhancement factor of about 1.4 (T98G) and 1.3 (U87MG) as determined for the survival fraction of 0.5. This suggests similar radiosensitizing effects of TRAM-34 in 2 human glioblastoma cell lines that differ in radiosensitivity (survival fractions at 2 Gy, SF_{2Gy}, of T98G and U87MG cells were $SF_{2Gy} = 0.56 \pm 0.01$ and $SF_{2Gy} = 0.74 \pm 0.02$, respectively; compare open bars in the insets of Fig. 6A and B).

To proof the IK specificity of the observed TRAM-34 effect on clonogenic survival, we knocked down IK channels in T98G cells by a lentiviral transduction with IK-specific and control shRNAs containing particles (Fig. 7A and B). The IK-depleted T98G clone #3 showed a higher percentage of cells residing in G_1 phase of cell cycle in flow cytometry than in the T98G control clone #2 suggestive of differing doubling times of the 2 clones. Within 24 hours, IR dose dependently and similarly decreased the fraction of cells residing in G_1 in both clones (Fig. 7C, left) and increased the population of cells accumulating in G_2 (Fig. 7C, right). Remarkably, TRAM-34 virtually abolished the IR-induced changes in cell-cycle distribution in the control clone #2 but had no apparent effect on IK-depleted clone #3.

To estimate whether the observed IK-mediated cell-cycle control in irradiated T98G cells might be required for DNA repair, we determined the number of residual γH_2AX foci in both T98G clones 24 hours after IR with 0 or 2 Gy. As shown in Fig. 7D and E, the IK-depleted clone #3 exhibited higher number of basal (0 Gy) and residual γH_2AX foci as compared with the control clone #2 suggestive of an impairment of DNA repair by IK knockdown. To test this assumption, the radioresistance of both clones was determined by delayed plating colony formation assay.

As a result, both T98G clones were more radioresistant than the parental T98G cell line (compare open circles in Fig. 7F and Fig. 6A). Notably, the IK-depleted clone #3 was significantly more radiosensitive ($SF_{2Gy} = 0.74 \pm 0.03$, $n = 12$) than the control clone #2 ($SF_{2Gy} = 0.83 \pm 0.02$, $n = 12$; $P = 0.02$, Welch-corrected two-tailed t test). Most importantly, TRAM-34 radiosensitized only the control clone #2 (Fig. 7F, left) but, again, had no effect on the IK-depleted clone #3 (Fig. 7F, right). Combined, these data indicate both IK-mediated radioresistance in human glioblastoma cell lines and target specificity of the IK channel blocker TRAM-34.

To test whether IK channel targeting may increase the efficacy of fractionated radiation in an *in vivo* ectopic glioblastoma mouse model, immunocompromised nude mice were challenged with

Published OnlineFirst June 3, 2015; DOI: 10.1158/1541-7786.MCR-15-0075

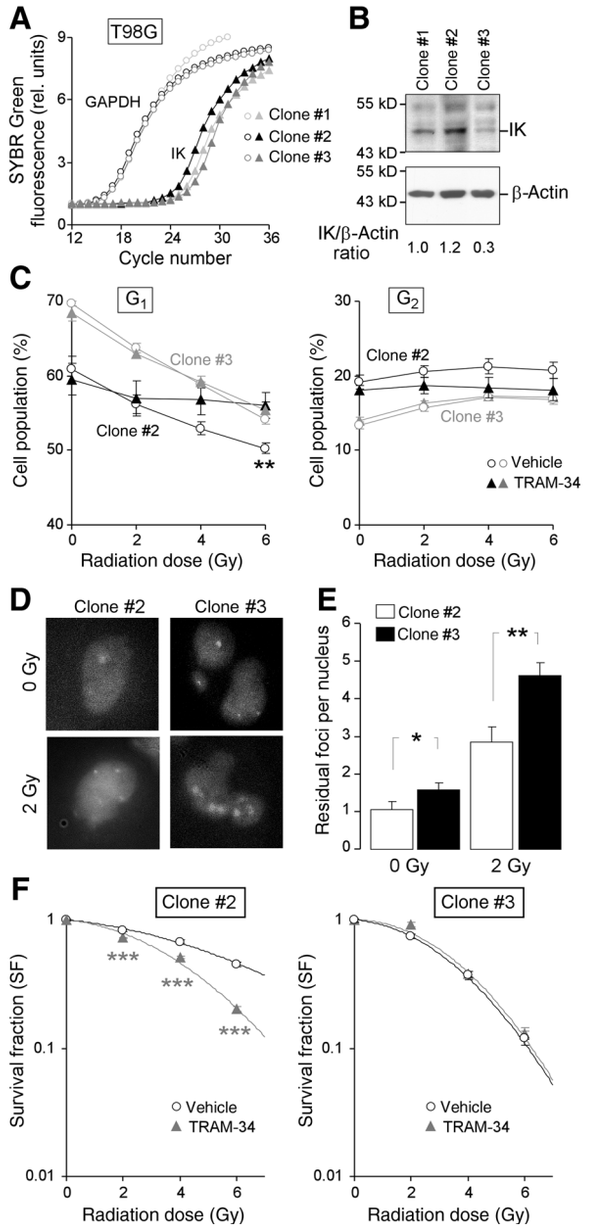

Figure 7.

TRAM-34 has no effect in IK-silenced T98G cells. A and B, abundances of IK mRNA and protein in T98G clones expressing control shRNAs (clones #1 and #2) and IK-specific shRNA (clone #3) as analyzed by quantitative RT-PCR (A) and immunoblotting (B). GAPDH served as housekeeper mRNA (A) and β-actin as loading control (B). C, mean percentage (±SE, $n = 9$) of irradiated (0, 2, 4, or 6 Gy) clone #2 (black) and clone #3 (gray) cells residing 48 hours after IR in G_1 (left) or G_2 phase of cell cycle (right). Cells were pre- and postincubated with vehicle alone (open circles) or with 10 μmol/L TRAM-34 (closed triangles). D, immunofluorescent micrographs of nuclei from T89G clone #2 (left) and clone #3 (right) double-stained against γH2AX and DNA (DAPI). Cells were fixed 24 hours after irradiation with 0 Gy (top) or 2 Gy (bottom) as indicated. E, mean (±SE, $n = 86$–199) numbers of residual γH2AX foci per nucleus of clone #2 (open bars) and clone #3 T98G cells (closed bars) 24 hours after irradiation with 0 (left) or 2 Gy (right). * and **, $P \leq 0.05$ and $P \leq 0.01$, respectively, Kruskal–Wallis nonparametric ANOVA test. F, mean survival fractions (±SE, $n = 12$) of clone #2 (left) and clone #3 (right) after irradiation with 0, 2, 4, or 6 Gy and combined treatment with TRAM-34 (10 μmol/L, filled triangles) or vehicle alone (open circles) as determined by delayed plating colony formation assay: plating efficacies were 0.31, 0.29, 0.18, and 0.14 for vehicle-treated clone #2, TRAM-34–treated clones #2, vehicle-treated clone #3, and TRAM-34–treated clones #3, respectively (*** and **, $P \leq 0.001$ and $P \leq 0.02$, respectively, two-tailed Welch-corrected t test).

human U87MG glioblastoma cells. When the ectopic glioblastoma has reached a volume of around 150 μL (Fig. 8A), mice were allocated to 4 treatment arms [control, $n = 5$; TRAM-34, $n = 4$; fractionated IR (fIR), $n = 9$; and TRAM-34/fIR, $n = 6$]. Figure 8B and C shows the tumor volume (V_t), normalized to the respective tumor volume at the start of treatment on day 0 (V_0), before, during (arrows), and after treatment with fIR (5×0 or 5×4 Gy) and TRAM-34 injections (5×0 or 5×120 mg/kg body weight) 6 hours prior to each IR fraction. One of 6 mice treated with combined fIR/TRAM-34 and 2 of 9 mice treated with fIR alone showed complete tumor remission. One of the latter did even not progress during treatment and could not be included in the calculation of the time to progression (i.e., the period between treatment start on day 0 and the time when the treated glioblastomas exceeded the initial volume, V_0). This time to progression is given for all treatment groups in Fig. 8 demonstrating that only the IR/TRAM-34 group exhibited significant longer time-to-progression periods than the control group.

The exponential growth of the ectopic glioblastoma can be illustrated by the linear relationship between the mean (±SE) logarithmized tumor volume [$\ln(V_t/V_0)$] and the time as depicted for the 4 treatment groups in Fig. 8E and F. The slope of these relationships [$\delta_{(\ln(Vt/V0)}/\delta_t$] as a measure of the exponential growth kinetics before and during the treatment as well as the treatment induced slope decline [$\Delta\delta_{(\ln(Vt/V0)}/\delta_t$] are given for the individual tumors in all 4 treatment groups in Fig. 8G–I. Only the fIR/TRAM-34 group showed a significant treatment-induced decrease in exponential growth as compared with the control group (Fig. 8I). Together, these *in vivo* experiments suggest both that TRAM-34 can be applied at pharmacologically relevant doses and that concomitant TRAM-34 chemotherapy may increase the efficacy of fractionated radiation therapy *in vivo*.

To explore the potential function of IK channels for the glioblastoma therapy resistance observed in the clinic, TCGA was queried using the provisional open access Glioblastoma-Multiforme and Lower-Grade-Glioma databases. As shown in Fig. 9, high IK mRNA abundance is associated with a shorter PFS (Fig. 9A) and OS (Fig. 9B) of patients with lower grade glioma and shorter OS (but not PFS, Fig. 9C) of patients with glioblastoma (Fig. 9D).

Discussion

The present study demonstrates IR-induced Ca^{2+} signaling and activation of Ca^{2+}-activated intermediate conductance IK K^+ channels in glioblastoma cells. The IR-stimulated IK channels, in turn, contribute to the stress response of the glioblastoma cells probably by adjusting the cell cycle. This IK channel-mediated stress response is required for the survival of the irradiated glioblastoma cells as evident from the fact that pharmacologic blockade of the IK channels radiosensitized the glioblastoma cells. In an astrocyte cell line, in contrast, functional IK channels were not apparent.

Published OnlineFirst June 3, 2015; DOI: 10.1158/1541-7786.MCR-15-0075

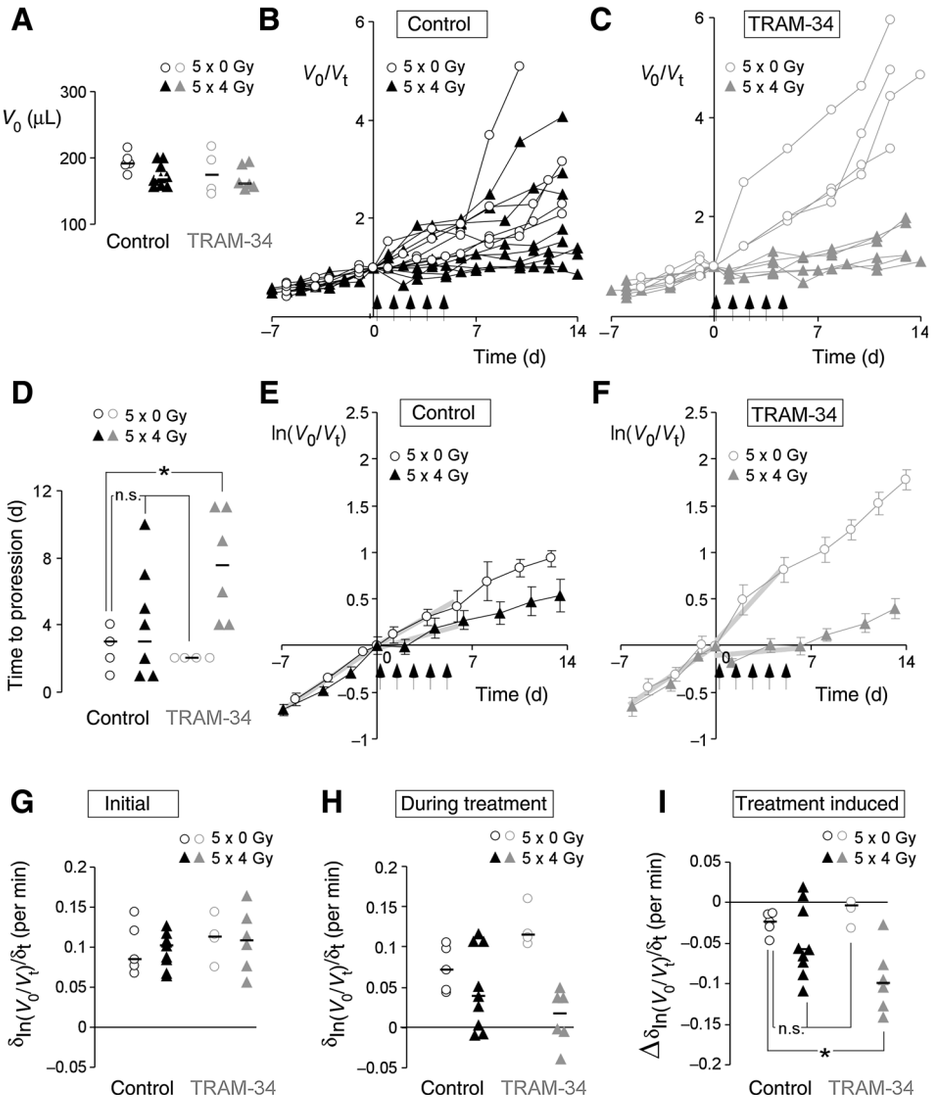

Figure 8.
TRAM-34 application concomitant to fractionated radiation delays ectopic tumor growth in the upper right hind limb of mice. A, volumes of ectopic human U87MG glioblastoma in immunocompromised nude mice at treatment start (day 0). B and C, time-dependent increase in normalized tumor volume (V_t/V_0). Tumors were irradiated with 5 fractions of 0 (open circles) or 4 Gy (closed triangles) on days 0 to 4. On these days, 0 (black symbols) or 120 mg/kg body weight TRAM-34 (gray symbols) were injected intraperitoneally 6 hours prior to radiation (arrows). D, time-to-tumor progression in the 4 treatment groups (one mouse in the radiation group with complete tumor remission did not show tumor progression and was excluded). E and F, time-dependent increase in mean (±SE, $n = 4$–9) logarithmized normalized tumor volume [$\ln(V_t/V_0)$, data from B and C] in the 4 treatment groups. G and H, slope [$\delta_{(\ln(Vt/V0)}/\delta_t$] of the time-dependent increase in logarithmized normalized tumor volume as a measure of exponential tumor growth kinetics before (days −7 to 0, G) and during treatment (days 0 to 8, H). Slopes are indicated by the thick gray lines in E and F. I, treatment-induced changes of $\delta_{(\ln(Vt/V0)}/\delta_t$ (the black line in A, D, and G–I and * in D and I indicate the median and $P \leq 0.05$, ANOVA, respectively).

IR-induced modifications of Ca^{2+} signaling and/or K^+ channel activity have been reported by our group in different tumor entities such as lung adenocarcinoma (28), leukemia cells (27, 29), or glioblastoma (21). In lung adenocarcinoma, K^+ channels contribute to an elevated glucose uptake by the irradiated cells. Increased amounts of glucose are probably needed to counteract energy crisis caused by DNA damage and to provide the carbohydrates required for histone acetylation during DNA decondensation (30). In leukemia, IR-induced co-activation of both Ca^{2+}-permeable channels and K^+ channels gives rise to Ca^{2+} signals that induce cell-cycle arrest via CaMKII-mediated inhibition of the mitosis-promoting factor cdc2. Notably, pharmacologic K^+ channel blockade overrides cell-cycle arrest of irradiated leukemia cells resulting in radiosensitization (27).

In the present study, irradiated cells exhibited an elevated steady state $i[Ca^{2+}]_{free}$ that was almost as double as high as the resting $i[Ca^{2+}]_{free}$ of unirradiated cells (see Fig. 3B and C). Glioblastoma cells functionally express STIM1/Orai1 store-operated Ca^{2+} channels (31) as well as TRPC1 and TRPM8 Ca^{2+}-permeable nonselective cation channels (32, 33), which might be candidates for augmented Ca^{2+} entry pathways in irradiated cells. A contribution of TRPM8 to the IR-induced Ca^{2+} signaling is suggested by the fact that TRPM8 knockdown impairs radioresistance and migration of glioblastoma cell lines (own unpublished observations).

In glioblastoma, IR-induced activation of BK K^+ channels is associated with radiogenic hypermigration of the tumor cells (for review, see refs. 15, 16). Like BK, IK channels have been demonstrated to essentially contribute to the mechanics of serum-induced (34), bradykinin-induced (6), and CXCL12 (SDF-1)-induced glioblastoma cell migration (35). In accordance with these *in vitro* data is the observation that the IK inhibitor TRAM-34 blocks the brain infiltration by xenografted human glioblastoma cells in orthotopic mouse models (36).

High IK channel expression has been associated with upregulation of "stemness" markers (8), and the glioblastoma "stem" cells have been suggested to express a highly migratory phenotype and to be primarily responsible for brain invasion (37, 38). As a matter of fact, IK channels have been demonstrated to mediate the migration of neuronal precursor cells, so-called neuroblasts,

Published OnlineFirst June 3, 2015; DOI: 10.1158/1541-7786.MCR-15-0075

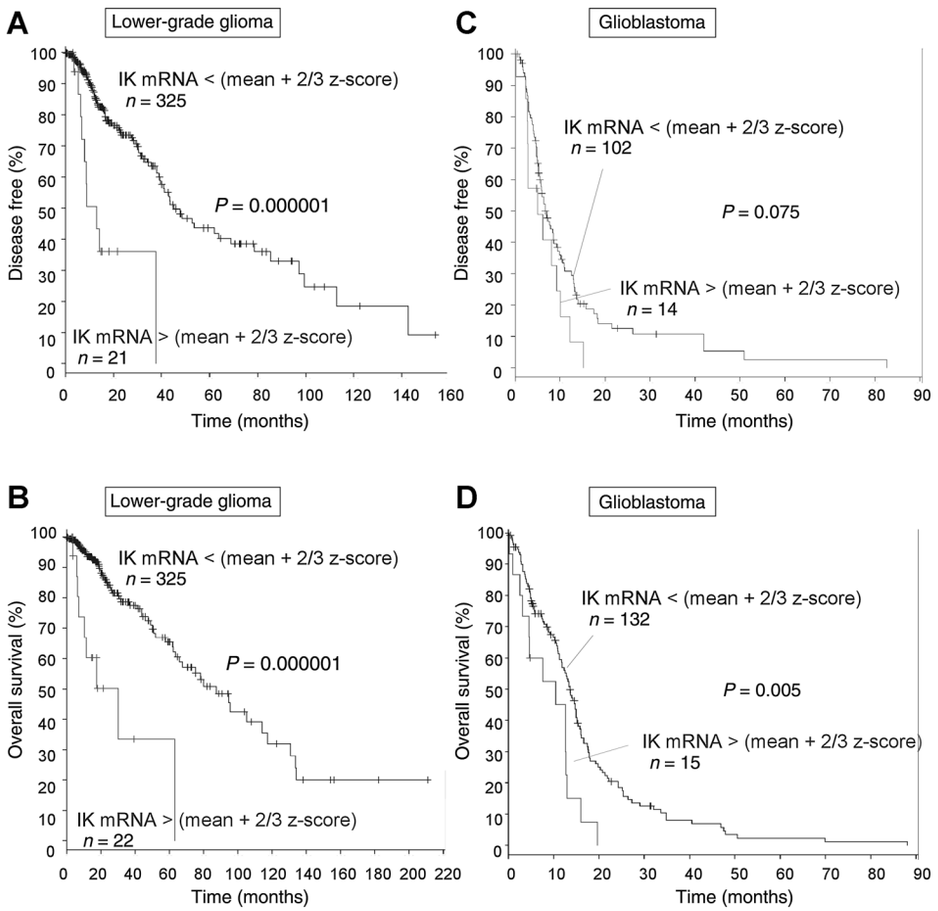

Figure 9.
IK mRNA abundance–dependent PFS (A, C) and OS (B, D) of patients with lower grade glioma (A, B) and glioblastoma (C, D). Data from TCGA. *P* values were calculated by the log-rank test.

along the rostral migratory stream to become interneurons in the olfactory bulb of normal adult mouse brain (39).

Glioblastoma "stem" cells are also thought to be more therapy-resistant than the bulk tumor mass of "differentiated" glioblastoma cells (for review, see ref. 15–17). The data of the present study on glioblastoma cell lines and on an ectopic mouse model suggest that IK channels may confer radioresistance besides promoting brain infiltration. Evidence for such an IK channel function in glioblastoma cells obtained *in vitro* has already been reported (20).

The potential dual function of IK channels for brain invasion and radioresistance of glioblastoma as suggested by the above-mentioned *in vitro* and animal studies might be reflected by recently reported retrospective clinical data. Querying the REMBRANDT patient gene data base of the National Cancer Institute has indicated an upregulation (1.5-fold greater than nontumor samples) of IK channel in more than 30% of the patients (10). Importantly, IK upregulation by the glioma correlates with a decreased survival of the patients (10). Likewise, querying the TCGA databases in the present study suggested that higher IK mRNA abundance in the glioma associates with shorter PFS (low-grade glioma) and OS (low-grade glioma and GBM) of patients with glioma. Subgroup analysis of the patients concerning, for example, tumor size, degree of surgical glioma resection, radiation therapy regimes, etc., could not be performed in the TCGA query and has not been reported in the REMBRANDT query (10), which limits the interpretation of the data. Nevertheless, provided that many patients of the databases received therapy regimes that comprise radiation therapy, the found associations might hint to a radioprotective function of IK channels in glioma.

IK channels might, therefore, become a highly attractive new target for anti-glioma therapy. IK channel targeting has been proposed for therapy of different diseases such as anemia (40, 41), in particular sickle cell anemia (42–45), Alzheimer disease (46), and various further inflammatory diseases (47). The TRAM-34 concentration (1–10 μmol/L) used in the present study is probably far above the plasma concentrations that might be reached in clinical trials. Senicapoc (ICA-17043), a further IK channel inhibitor, which is more potent than TRAM-34 ($IC_{50\text{-Senicapoc}}$, 11 nmol/L vs. $IC_{50\text{-TRAM-34}}$, 20 nmol/L), can be taken orally and has been shown to be safe in clinical trials (46). Moreover, a daily oral dose of 10-mg senicapoc resulted in mean plasma concentrations of 100 ng/mL (~0.3 μmol/L). Most importantly, senicapoc-containing plasma samples of the patients inhibited IK channels by up to 70% as assessed in tracer flux experiments (43). What is also important in this respect is the fact that GBM reportedly impairs the blood–brain barrier (BBB) by, for example, altering/replacing endothelial cells (48) and pericytes (49), suggesting that drugs like senicapoc or TRAM-34 may pass the BBB. In a mouse brain, a BBB passage of TRAM-34 could be directly demonstrated (36). Taken together, these data indicate that IK channel targeting is most probably feasible in a clinical setting. Higher drug levels at lower side effects might even be achieved in patients with glioblastoma by intracranial drug administration.

Published OnlineFirst June 3, 2015; DOI: 10.1158/1541-7786.MCR-15-0075

In conclusion, IK channels may promote beside a migratory and infiltrative phenotype also cellular radioresistance of glioblastoma cells. By doing so, IK channels contribute to those properties of GBM that most probably account for therapy failure associated with the very poor prognosis of patients. Importantly, pharmacologic IK channel targeting seems to be feasible in the clinic in combination with surgery and radiation therapy.

Disclosure of Potential Conflicts of Interest

No potential conflicts of interest were disclosed.

Authors' Contributions

Conception and design: D. Zips, K. Dittmann, P. Ruth, S.M. Huber
Development of methodology: B. Stegen, L. Butz, L. Klumpp, K. Dittmann, S.M. Huber
Acquisition of data (provided animals, acquired and managed patients, provided facilities, etc.): B. Stegen, L. Butz, L. Klumpp, S.M. Huber
Analysis and interpretation of data (e.g., statistical analysis, biostatistics, computational analysis): B. Stegen, L. Butz, D. Zips, P. Ruth, S.M. Huber
Writing, review, and/or revision of the manuscript: B. Stegen, L. Klumpp, D. Zips, S.M. Huber
Administrative, technical, or material support (i.e., reporting or organizing data, constructing databases): B. Stegen, L. Butz, S.M. Huber
Study supervision: P. Ruth, S.M. Huber

Acknowledgments

The authors thank Heidrun Faltin and Ilka Müller for excellent technical assistance.

Grant Support

This work was supported by a grant from the Wilhelm-Sander-Stiftung awarded to P. Ruth and S.M. Huber (2011.083.1). B. Stegen was supported by the DFG International Graduate School 1302 (TP T9 SH) and L. Klumpp by the Robert-Bosch-Stiftung as well as the ICEPHA program of the University of Tübingen.

Received February 11, 2015; revised April 28, 2015; accepted May 22, 2015; published OnlineFirst June 3, 2015.

References

1. Stupp R, van den Bent MJ, Hegi ME. Optimal role of temozolomide in the treatment of malignant gliomas. Curr Neurol Neurosci Rep 2005;5:198–206.
2. Evers P, Lee PP, DeMarco J, Agazaryan N, Sayre JW, Selch M, et al. Irradiation of the potential cancer stem cell niches in the adult brain improves progression-free survival of patients with malignant glioma. BMC Cancer 2010;10:384.
3. Fioretti B, Castigli E, Calzuola I, Harper AA, Franciolini F, Catacuzzeno L. NPPB block of the intermediate-conductance Ca2+-activated K+ channel. Eur J Pharmacol 2004;497:1–6.
4. Fioretti B, Castigli E, Micheli MR, Bova R, Sciaccaluga M, Harper A, et al. Expression and modulation of the intermediate- conductance Ca2+-activated K+channel in glioblastoma GL-15 cells. Cell Physiol Biochem 2006;18:47–56.
5. Fioretti B, Catacuzzeno L, Sforna L, Aiello F, Pagani F, Ragozzino D, et al. Histamine hyperpolarizes human glioblastoma cells by activating the intermediate-conductance Ca2+-activated K+ channel. Am J Physiol Cell Physiol 2009;297:C102–10.
6. Cuddapah VA, Turner KL, Seifert S, Sontheimer H. Bradykinin-induced chemotaxis of human gliomas requires the activation of KCa3.1 and ClC-3. J Neurosci 2013;33:1427–40.
7. Ishii TM, Silvia C, Hirschberg B, Bond CT, Adelman JP, Maylie J. A human intermediate conductance calcium-activated potassium channel. Proc Natl Acad Sci U S A 1997;94:11651–6.
8. Ruggieri P, Mangino G, Fioretti B, Catacuzzeno L, Puca R, Ponti D, et al. The inhibition of KCa3.1 channels activity reduces cell motility in glioblastoma derived cancer stem cells. PLoS One 2012;7:e47825.
9. Catacuzzeno L, Fioretti B, Franciolini F. Expression and Role of the Intermediate-Conductance Calcium-Activated Potassium Channel KCa3.1 in Glioblastoma. J Signal Transduct 2012;2012:421564.
10. Turner KL, Honasoge A, Robert SM, McFerrin MM, Sontheimer H. A proinvasive role for the Ca2+-activated K+ channel KCa3.1 in malignant glioma. Glia 2014;62:971–81.
11. Lallet-Daher H, Roudbaraki M, Bavencoffe A, Mariot P, Gackiere F, Bidaux G, et al. Intermediate-conductance Ca2+-activated K+ channels (IKCa1) regulate human prostate cancer cell proliferation through a close control of calcium entry. Oncogene 2009;28:1792–806.
12. Ouadid-Ahidouch H, Roudbaraki M, Delcourt P, Ahidouch A, Joury N, Prevarskaya N. Functional and molecular identification of intermediate-conductance Ca2+-activated K+ channels in breast cancer cells: association with cell cycle progression. Am J Physiol Cell Physiol 2004;287:C125–34.
13. Jager H, Dreker T, Buck A, Giehl K, Gress T, Grissmer S. Blockage of intermediate-conductance Ca2+-activated K+ channels inhibit human pancreatic cancer cell growth in vitro. Mol Pharmacol 2004;65:630–8.
14. Wang J, Xu YQ, Liang YY, Gongora R, Warnock DG, Ma HP. An intermediate-conductance Ca2+-activated K+ channel mediates B lymphoma cell cycle progression induced by serum. Pflugers Arch 2007;454:945–56.
15. Huber SM. Oncochannels. Cell Calcium 2013;53:241–55.
16. Huber SM, Butz L, Stegen B, Klumpp D, Braun N, Ruth P, et al. Ionizing radiation, ion transports, and radioresistance of cancer cells. Front Physiol 2013;4:212.
17. Huber SM, Butz L, Stegen B, Klumpp L, Klumpp D, Eckert F. Role of ion channels in ionizing radiation-induced cell death. Biochim Biophys Acta. 2014 Nov 15. pii: S0005-2736(14)00390-3.
18. Khalid MH, Shibata S, Hiura T. Effects of clotrimazole on the growth, morphological characteristics, and cisplatin sensitivity of human glioblastoma cells in vitro. J Neurosurg 1999;90:918–27.
19. Khalid MH, Tokunaga Y, Caputy AJ, Walters E. Inhibition of tumor growth and prolonged survival of rats with intracranial gliomas following administration of clotrimazole. J Neurosurg 2005;103:79–86.
20. Liu H, Li Y, Raisch KP. Clotrimazole induces a late G1 cell cycle arrest and sensitizes glioblastoma cells to radiation in vitro. Anticancer Drugs 2010;21:841–9.
21. Steinle M, Palme D, Misovic M, Rudner J, Dittmann K, Lukowski R, et al. Ionizing radiation induces migration of glioblastoma cells by activating BK K+ channels. Radiother Oncol 2011;101:122–6.
22. Barry PH, Lynch JW. Liquid junction potentials and small cell effects in patch-clamp analysis. J Membr Biol 1991;121:101–17.
23. Fotin-Mleczek M, Zanzinger K, Heidenreich R, Lorenz C, Kowalczyk A, Kallen KJ, et al. mRNA-based vaccines synergize with radiation therapy to eradicate established tumors. Radiat Oncol 2014;9:180.
24. Cerami E, Gao J, Dogrusoz U, Gross BE, Sumer SO, Aksoy BA, et al. The cBio cancer genomics portal: an open platform for exploring multidimensional cancer genomics data. Cancer Discov 2012;2:401–4.
25. Gao J, Aksoy BA, Dogrusoz U, Dresdner G, Gross B, Sumer SO, et al. Integrative analysis of complex cancer genomics and clinical profiles using the cBioPortal. Sci Signal 2013;6:pl1.
26. Huber SM, Tschop J, Braun GS, Nagel W, Horster MF. Bradykinin-stimulated Cl- secretion in T84 cells. Role of Ca2+-activated hSK4-like K+ channels. Pflugers Arch 1999;438:53–60.
27. Palme D, Misovic M, Schmid E, Klumpp D, Salih HR, Rudner J, et al. Kv3.4 potassium channel-mediated electrosignaling controls cell cycle and survival of irradiated leukemia cells. Pflugers Arch 2013;465:1209–21.
28. Huber SM, Misovic M, Mayer C, Rodemann HP, Dittmann K. EGFR-mediated stimulation of sodium/glucose cotransport promotes survival of irradiated human A549 lung adenocarcinoma cells. Radiother Oncol 2012;103:373–9.
29. Heise N, Palme D, Misovic M, Koka S, Rudner J, Lang F, et al. Non-selective cation channel-mediated Ca2+-entry and activation of Ca2+/calmodulin-dependent kinase II contribute to G2/M cell cycle arrest and survival of irradiated leukemia cells. Cell Physiol Biochem 2010;26:597–608.
30. Dittmann K, Mayer C, Rodemann HP, Huber SM. EGFR cooperates with glucose transporter SGLT1 to enable chromatin remodeling in response to ionizing radiation. Radiother Oncol 2013;107:247–51.

31. Motiani RK, Hyzinski-Garcia MC, Zhang X, Henkel MM, Abdullaev IF, Kuo YH, et al. STIM1 and Orai1 mediate CRAC channel activity and are essential for human glioblastoma invasion. Pflugers Arch 2013;465:1249–60.
32. Wondergem R, Ecay TW, Mahieu F, Owsianik G, Nilius B. HGF/SF and menthol increase human glioblastoma cell calcium and migration. Biochem Biophys Res Commun 2008;372:210–5.
33. Bomben VC, Sontheimer H. Disruption of transient receptor potential canonical channel 1 causes incomplete cytokinesis and slows the growth of human malignant gliomas. Glia 2010;58:1145–56.
34. Catacuzzeno L, Aiello F, Fioretti B, Sforna L, Castigli E, Ruggieri P, et al. Serum-activated K and Cl currents underlay U87-MG glioblastoma cell migration. J Cell Physiol 2011;226:1926–33.
35. Sciaccaluga M, Fioretti B, Catacuzzeno L, Pagani F, Bertollini C, Rosito M, et al. CXCL12-induced glioblastoma cell migration requires intermediate conductance Ca2+-activated K+ channel activity. Am J Physiol Cell Physiol 2010;299:C175–84.
36. D'Alessandro G, Catalano M, Sciaccaluga M, Chece G, Cipriani R, Rosito M, et al. KCa3.1 channels are involved in the infiltrative behavior of glioblastoma in vivo. Cell Death Dis 2013;4:e773.
37. Liu G, Yuan X, Zeng Z, Tunici P, Ng H, Abdulkadir IR, et al. Analysis of gene expression and chemoresistance of CD133+ cancer stem cells in glioblastoma. Mol Cancer 2006;5:67.
38. Nakada M, Nambu E, Furuyama N, Yoshida Y, Takino T, Hayashi Y, et al. Integrin alpha3 is overexpressed in glioma stem-like cells and promotes invasion. Br J Cancer 2013;108:2516–24.
39. Turner KL, Sontheimer H. KCa3.1 modulates neuroblast migration along the rostral migratory stream (RMS) in vivo. Cereb Cortex 2014;24:2388–400.
40. Foller M, Bobbala D, Koka S, Boini KM, Mahmud H, Kasinathan RS, et al. Functional significance of the intermediate conductance Ca2+-activated K +channel for the short-term survival of injured erythrocytes. Pflugers Arch 2010;460:1029–44.
41. Lang PA, Kaiser S, Myssina S, Wieder T, Lang F, Huber SM. Role of Ca2+-activated K+ channels in human erythrocyte apoptosis. Am J Physiol Cell Physiol 2003;285:C1553–60.
42. Ataga KI, Orringer EP, Styles L, Vichinsky EP, Swerdlow P, Davis GA, et al. Dose-escalation study of ICA-17043 in patients with sickle cell disease. Pharmacotherapy 2006;26:1557–64.
43. Ataga KI, Smith WR, De Castro LM, Swerdlow P, Saunthararajah Y, Castro O, et al. Efficacy and safety of the Gardos channel blocker, senicapoc (ICA-17043), in patients with sickle cell anemia. Blood 2008;111:3991–7.
44. Ataga KI, Stocker J. Senicapoc (ICA-17043): a potential therapy for the prevention and treatment of hemolysis-associated complications in sickle cell anemia. Expert Opin Investig Drugs 2009;18:231–9.
45. Ataga KI, Reid M, Ballas SK, Yasin Z, Bigelow C, James LS, et al. Improvements in haemolysis and indicators of erythrocyte survival do not correlate with acute vaso-occlusive crises in patients with sickle cell disease: a phase III randomized, placebo-controlled, double-blind study of the Gardos channel blocker senicapoc (ICA-17043). Br J Haematol 2011;153:92–104.
46. Maezawa I, Jenkins DP, Jin BE, Wulff H. Microglial KCa3.1 channels as a potential therapeutic target for Alzheimer's disease. Int J Alzheimers Dis 2012;2012:868972.
47. Lam J, Wulff H. The lymphocyte potassium channels Kv1.3 and KCa3.1 as targets for immunosuppression. Drug Dev Res 2011;72:573–84.
48. Wang R, Chadalavada K, Wilshire J, Kowalik U, Hovinga KE, Geber A, et al. Glioblastoma stem-like cells give rise to tumour endothelium. Nature 2010;468:829–33.
49. Cheng L, Huang Z, Zhou W, Wu Q, Donnola S, Liu JK, et al. Glioblastoma stem cells generate vascular pericytes to support vessel function and tumor growth. Cell 2013;153:139–52.

Published OnlineFirst June 3, 2015; DOI: 10.1158/1541-7786.MCR-15-0075

Molecular Cancer Research

Ca^{2+}-Activated IK K^{+} Channel Blockade Radiosensitizes Glioblastoma Cells

Benjamin Stegen, Lena Butz, Lukas Klumpp, et al.

Mol Cancer Res 2015;13:1283-1295. Published OnlineFirst June 3, 2015.

frontiers in
PHYSIOLOGY

REVIEW ARTICLE
published: 14 August 2013
doi: 10.3389/fphys.2013.00212

Ionizing radiation, ion transports, and radioresistance of cancer cells

Stephan M. Huber[1]*, Lena Butz[2], Benjamin Stegen[1], Dominik Klumpp[1], Norbert Braun[1], Peter Ruth[2] and Franziska Eckert[1]

[1] Department of Radiation Oncology, University of Tübingen, Tübingen, Germany
[2] Department of Pharmacology, Toxicology and Clinical Pharmacy, Institute of Pharmacy, University of Tübingen, Tübingen, Germany

Edited by:
Andrea Becchetti, University of Milano-Bicocca, Italy

Reviewed by:
Ildikò Szabò, University of Padova, Italy
Yinsheng Wan, Providence College, USA

***Correspondence:**
Stephan M. Huber, Department of Radiation Oncology, University of Tübingen, Hoppe-Seyler-Str. 3, 72076 Tübingen, Germany
e-mail: stephan.huber@uni-tuebingen.de

The standard treatment of many tumor entities comprises fractionated radiation therapy which applies ionizing radiation to the tumor-bearing target volume. Ionizing radiation causes double-strand breaks in the DNA backbone that result in cell death if the number of DNA double-strand breaks exceeds the DNA repair capacity of the tumor cell. Ionizing radiation reportedly does not only act on the DNA in the nucleus but also on the plasma membrane. In particular, ionizing radiation-induced modifications of ion channels and transporters have been reported. Importantly, these altered transports seem to contribute to the survival of the irradiated tumor cells. The present review article summarizes our current knowledge on the underlying mechanisms and introduces strategies to radiosensitize tumor cells by targeting plasma membrane ion transports.

Keywords: radiation therapy, cell cycle, DNA repair, ion channels

INTRODUCTION

Increasing pieces of evidence strongly indicate that ion transports across biological membranes fulfill functions beyond those described by classical physiology such as epithelial transports and neuronal or muscle excitability. More and more, it turns out that ion transports are involved in virtually all cell-biological processes. By modifying the chemistry, electricity and mechanics of cells, ion transports directly interact with cellular biochemistry and constitute signaling modules that are capable of altering protein function, gene expression (Tolon et al., 1996) and epigenetics (Lobikin et al., 2012). Moreover, ion transport-generating proteins such as ion channels have been identified to directly signal in macromolecular complexes with, e.g., surface receptors and downstream kinases (Arcangeli, 2011), or to directly bind to DNA as transcription factors (Gomez-Ospina et al., 2006).

Over the past two decades, ion transports came more and more in the focus of oncological research. Increasingly, data accumulate indicating tumor-suppressing as well as oncogenic functions of ion transport processes. In particular, ion transports have been identified as key regulators of neoplastic transformation, malignant progression, tissue invasion and metastasis (for review see Huber, 2013). Most recent data suggest that ion transports may also contribute to therapy resistance especially to radioresistance of tumor cells. The second chapter of this review article aims at giving an overview of those data. Since worldwide, only a handful of laboratories including ours are working in this research field only few data on ion transports in radioresistance are available and in most cases, the underlying molecular mechanisms of the observed phenomena remain ill-defined. Because tumor hypoxia is a major obstacle in radiotherapy, the second chapter also includes ion transports in the mitochondria that confer hypoxia resistance to normal tissue and probably also to tumor cells. At the end, this article provides some ideas how the acquired knowledge might be harnessed in the future for new strategies of anti-cancer therapy that combine ion transport-targeting and radiotherapy. To begin with, a brief introduction into radiotherapy and its radiobiological principles is given in the next paragraphs.

RADIOTHERAPY

According to the German Cancer Aid, 490,000 people in Germany are diagnosed with cancer every year (German-Cancer-Aid, 2013a) (data originating from February 2012), 218,000 die from their disease. About half of all cancer patients receive radiation treatment, half of all cures from cancer include radiotherapy (German-Cancer-Aid, 2013b). Radiotherapy is one of the main pillars of cancer treatment together with surgery and systemic therapy, mainly chemotherapy. Examples for curative radiotherapy without surgery are prostate (Eckert et al., 2013; Kotecha et al., 2013) and head and neck cancer (Glenny et al., 2010). Preoperative radiotherapy is applied in rectal cancer (Sauer et al., 2012), postoperative treatment in breast cancer (Darby et al.). Yet, also rare tumor entities like sarcoma and small cell carcinoma are treated with radiotherapy (Eckert et al., 2010a,b; Muller et al., 2012). Despite modern radiation techniques and advanced multimodal treatments local failures and distant metastases often limit the prognosis, especially due to limited salvage treatments (Muller et al., 2011; Zhao et al., 2012).

INTRINSIC AND HYPOXIC RADIORESISTANCE

Radiation therapy impairs the clonogenic survival of tumor cells mainly by causing double strand breaks in the DNA backbone. The number of double strand breaks increases linearly with the absorbed radiation dose (unit Gray, Gy). The intrinsic capacity

to repair these DNA damages by non-homologous end joining or homologous recombination determines how radio resistant a given tumor cell is. Irradiated tumor cells which leave residual DNA double strand breaks unrepaired lose their clonogenicity meaning that these cells cannot restore tumor mass. Ion transports may directly be involved in the cellular stress response to DNA damage by controlling cell cycle, metabolic adaptations or DNA repair and, thus, contribute to intrinsic radioresistance and the survival of the tumor cell.

Besides intrinsic factors, the microenvironment influences the radiosensitivity of a tumor. Hypoxic areas frequently occur in solid tumors. Hypoxic tumor cells, however, are somehow "protected" from radiotherapy [reviewed in Harada (2011)]. This is because ionizing radiation generates directly or indirectly radicals in the deoxyribose moiety of the DNA backbone. In a hypoxic atmosphere, thiols can react with those DNA radicals by hydrogen atom donation which results in chemical DNA repair. In the presence of oxygen, in contrast, oxygen fixes radicals of the deoxyribose moiety to strand break precursors (Cullis et al., 1987). This so called oxygen effect radiosensitizes tumor cells by a factor of two to three (oxygen enhancement ratio) as compared to the hypoxic situation (Langenbacher et al., 2013). Accordingly, patients with hypoxic tumors who undergo radiotherapy have a worse prognosis than those with normoxic tumors [e.g., cervical cancer (Fyles et al., 2002, 2006)]. Notably, ion transport processes have been identified as important players in the adaptation of tumor cells to a hypoxic microenvironment. Hence, ion transports via adaptation to hypoxia also indirectly contribute to the radioresistance of tumors.

In radiotherapy, fractionated treatment regimens have been established which may reoxygenate and thereby radiosensitize the irradiated tumor during therapy time. In addition, fractionated radiotherapy spaces out the single fractions in a way that allows DNA repair of normal tissue, that re-distribute cell cycle of the tumor cells in more sensitive phases and that minimize repopulation of the tumor during therapy. The next paragraphs will give an introduction to the underlying radiobiology.

FRACTIONATED RADIATION THERAPY. REPAIR, REOXYGENATION, REDISTRIBUTION, AND REPOPULATION

Early in historic development of radiotherapy fractionation was introduced as a means to limit side effects when giving therapeutic radiation doses (Bernier et al., 2004). Standard fractionation is defined as single doses of 1.8–2 Gy, once daily, 5 days per week.

The principal rationale for fractionation is based on the fact that recovery after radiation is better in normal tissue than in tumors, especially concerning late reacting tissues responsible for late side effects of radiotherapy (Jones et al., 2006) such as fibrosis, damage of spinal cord and brain, as well as most inner organs. Radiation with high single doses is only possible without increased side effects if the radiation field can be confined to the tumor (e.g., stereotactic radiotherapy of brain metastases [Rodrigues et al., 2013) and SBRT, stereotactic body radiation therapy (Grills et al., 2012)]. Yet, many situations in radiation oncology such as adjuvant treatment or irradiation of nodal regions require irradiation of significant volumes of normal tissue.

Alpha-beta ratios

Acute effects of ionizing irradiation on clonogenic cell survival *in vitro* as well as on late toxicity of the normal tissue in patients which underwent radiotherapy are described by the linear-quadratic model (Barendsen, 1982; Dale, 1985). The mathematical fit of the clonogenic survival (late toxicity) is calculated as follows: $N = N_0 \times E^{-(\alpha D - \beta D\hat{}2)}$ with N being the number of surviving cells (patients without late toxicity), N_0 being the initial number of cells (number of patients receiving radiotherapy), α [1/Gy] and β [1/Gy^2] being cell (tissue)-specific constants and D the delivered radiation dose. Low alpha-beta ratios (α/β) [Gy] as determined for many normal tissues indicate that dose fractionation in daily fractions of usually 2 Gy increases survival and decreases late toxicity as compared to a single equivalent dose. Tumors with high alpha-beta ratios, in contrast do not benefit from fractionation. For some tumors such as squamous cell carcinoma of the head and neck there is even a rationale for hyperfractionated radiotherapy with twice daily irradiation of 1.2–1.4 Gy per fraction [reviewed in Nguyen and Ang (2002)]. The theoretical advantage has been confirmed in clinical trials [e.g., EORTC trial 22791 in advanced head and neck cancer Horiot et al. (1992)]. Different fractionation schedules for distinct clinical situations are applied for example in whole-brain radiotherapy. In prophylactic radiation 2–2.5 Gy fractions are applied to limit neurocognitive deficits (Auperin et al., 1999; Le Pechoux et al., 2011; Eckert et al., 2012). For therapeutic radiation 3 Gy fractions or even 4 Gy fractions are preferred in a palliative setting and limited life expectancy to shorten the treatment time to 5 or 10 days (Lutz, 2007; Rades et al., 2007a,b).

Reoxygenation

As mentioned above, fractionated radiation may also lead to reoxygenation of the tumor during therapy (Withers, 1975; Pajonk et al., 2010). Blood vessels of tumors lack normal architecture and are prone to collapse whenever tissue pressure of the expanding tumor mass increases. This aggravates tumor malperfusion and accelerates intermittent or chronic tumor hypoxia. Being sublethal as related to the whole tumor, single radiation fractions in the range of 2 Gy kill a significant percentage of the tumor cells which give rise to tumor shrinkage. Shrinkage, in turn, is thought to increase blood and oxygen supply of the tumor by improving vessel perfusion and by increasing the ratio of vascularization and the residual tumor mass (Maftei et al., 2011; Narita et al., 2012). Increased oxygenation then reverses hypoxic radioresistance of the tumor and improves the therapeutic outcome of radiotherapy.

Redistribution and repopulation

The sensitivity to radiotherapy during cell cycle differs, being highest in M and lowest in late S phase of cell cycle (Pawlik and Keyomarsi, 2004). Often depending on p53 function, irradiated tumor cells accumulate in G_1 or G_2 phase of cell cycle to repair their DNA damages. In a radiation dose-dependent manner, irradiated cells are released from cell cycle arrest and re-enter cell

cycling and tumor repopulation. Importantly, repopulation after irradiation is often accelerated probably due to selection of more aggressive tumor cells (Marks and Dewhirst, 1991). Fractionated radiation regimes aim to re-distribute tumor cells in a more vulnerable phase of the cell cycle in the time intervals between two fractions and to impair repopulation (Pawlik and Keyomarsi, 2004).

CANCER STEM CELLS (CSCs)

Cancer stem cells (CSCs) may resist radiation therapy [for review see Pajonk et al. (2010)]. Mechanisms that might contribute to the relative resistance of CSCs as compared to the non-CSC cells of a given tumor include (i) higher oxidative defense and, therefore, lower radiation-induced insults, (ii) activated DNA checkpoints resulting in faster DNA repair, and (iii) an attenuated radiation-induced cell cycle redistribution. Fractionation regimes are designed that way that the macroscopically visible bulk of tumor cells (i.e., the non CSCs) and not the rare CSCs become redistributed into a more vulnerable phase of cell cycle between two consecutive fractions of radiotherapy. Finally, radiation therapy is thought to switch CSCs from an asymmetrical into a symmetrical mode of cell division; i.e., a CSC which normally divides into a daughter CSC and a lineage-committed progenitor cell is induced by the radiotherapy to divide symmetrically into two proliferative stem daughter cells. This is thought to accelerate repopulation of the tumor after end of radiotherapy (Pajonk et al., 2010).

In summary, fractionated radiotherapy may radio sensitize tumor cells by reoxygenation of the tumor and redistribution of the tumor cells in more vulnerable phases of cell cycle while protecting at the same time normal tissue if the alpha-beta ratio of the tumor exceeds that of the normal tissue. On the other hand, the applied fractionation protocols might spare CSCs due to their radiobiology that differs from that of the bulk of non-CSCs. Furthermore, single radiation fractions apply sublethal doses of ionizing radiation. Data from *in vitro* and animal studies suggest that sublethal doses of ionizing radiation may stimulate migration and tissue invasion of the tumor cells. Translated into the *in vivo* situation, this might imply that cells at the edge of solid tumors might be stimulated by the first radiation fractions to migrate out of the target volume of radiation resulting in survival of the evaded cells and tumor relapse. Moreover, if radiation fractions further induce tumor cell invasion into blood or lymph vessels, fractionated radiotherapy regimes might also boost metastases. As described in the next paragraphs, ion transports fulfill pivotal functions in cell migration especially in radiation-induced migration.

ION TRANSPORTS AND RADIORESISTANCE

Ion transports can be assessed by tracer-flux measurements, fluorescence microscopy/photometry using ion species-specific fluorescence dyes such as the Ca^{2+}-specific fluorochrome fura-2, as well as by electrophysiological means. The latter can be applied if ion transports are electrogenic. Measurements of ion transports during treatment with ionizing radiation are hardly feasible. Reported electrophysiological *in vitro* data on irradiated tumor cells indicate that radiation-induced transport modifications may occur instantaneously and may last up to 24 h post irradiation (Kuo et al., 1993). They further suggest that these modifications may be induced by doses used for single fractions in the clinic (Steinle et al., 2011). The following paragraphs summarize radiation-induced transport modifications as observed in *in vitro* studies on tumor cell lines and their putative contribution to the radioresistance of tumor cells. Whether these processes may indeed underlie therapy failure in tumor patients can only be answered if more data from tumor mouse models and clinical trials become available.

Tumor cells have been proposed to adapt either a "Grow" or a "Go" phenotype in dependence on changes in their microenvironment. When developing a certain mass, growing solid tumors are prone to become malperfused because of the insufficient tumor vasculature. As a consequence of malperfusion, microenvironmental stress by hypoxia, interstitial nutrient depletion, and low pH increases (Stock and Schwab, 2009; Hatzikirou et al., 2012) which is thought to trigger at a certain point the induction of the "Go" phenotype. By migration and tissue invasion "Go" tumor cells may evade the locally reined stress burden and resettle in distant and less hostile regions. Once re-settled, tumor cells may readapt the "Grow" phenotype by reentering cell cycling and may establish tumor satellites in more or less close vicinity of the primary focus. Moreover, this stress evasion may lead to metastases if the "Go" cells invade into blood or lymph vessels.

Migration and tissue invasion are directed by extracellular hapto- and chemotactic signals which trigger preset "Go" programs (Schwab et al., 2007, 2012). The latter comprise intracellular signaling, cellular motor functions including cell volume changes and cytoskeletal dynamics, as well as extracellular matrix digestion and reorganization. Ion transports have been suggested to contribute to all of these processes (Schwab et al., 2007, 2012). As a matter of fact, highly invasive and metastatic phenotypes of tumor cells often show aberrant activity of certain ion transports. The following paragraphs describe the role of these ion transports in particular of those across the plasma membrane using the example of glioblastoma cells.

MOTOR FUNCTION

Glioblastoma cells exhibit a highly migrative phenotype and "travel" long distances throughout the brain (Johnson et al., 2009). Primary foci of glioblastoma show, therefore, even at early stages of diagnosis a characteristic diffuse and net-like brain infiltration (Niyazi et al., 2011). Tumor margins are often not definable and complete surgical tumor resection as well as capture of all residual tumor cells by the radiation target volume is hardly possible (Weber et al., 2009). This results in therapy failure accompanied by very bad prognosis for the survival of the patient in almost all cases of glioblastoma (Niyazi et al., 2011). Glioblastoma cells typically migrate into the surrounding brain parenchyma primarily by using nerve bundles and the vasculature as tracks. The close vicinity to the vasculature has the advantage for the migrating glioblastoma cell of a continuous and sufficient supply of oxygen, nutrients, growth factors, chemokines, and cytokines (Montana and Sontheimer, 2011). Glioblastoma cells have to squeeze through very narrow interstitial spaces during their brain invasion along those tracks. This

requires highly effective local cell volume decrease and re-increase procedures. Notably, glioblastoma cells are capable to lose all unbound cell water leading to maximal cell shrinkage (Watkins and Sontheimer, 2011). Unusually high cytosolic Cl^- concentrations (100 mM) provide the electrochemical driving force for this tremendous cell volume decrease. The cytosolic Cl^- concentration is built up highly above its electrochemical equilibrium concentration by the Na/K/2Cl cotransporter NKCC1 (Haas and Sontheimer, 2010; Haas et al., 2011) allowing glioblastoma cells to utilize Cl^- as an osmolyte.

Local regulatory volume increase and decrease have been proposed to drive migration mechanics. The latter is generated by the loss of Cl^- and K^+ ions along their electrochemical gradients followed by osmotically obliged water fluxes. Involved transporters probably are ClC-3 Cl^- channels (Olsen et al., 2003; Cuddapah and Sontheimer, 2010; Lui et al., 2010), Ca^{2+}-activated high conductance BK (Ransom and Sontheimer, 2001; Ransom et al., 2002; Sontheimer, 2008) as well as intermediate conductance IK K^+ channels (Catacuzzeno et al., 2010; Sciaccaluga et al., 2010; Ruggieri et al., 2012) and AQP-1 water channels (Mccoy and Sontheimer, 2007; Mccoy et al., 2010). To a lower extent, K^+ and Cl^- efflux is probably also mediated by KCC1-generated cotransport (Ernest et al., 2005). These transports are crucial for glioblastoma migration since either transport blockade inhibits glioblastoma cell migration and invasion (Ernest et al., 2005; Mcferrin and Sontheimer, 2006; Catacuzzeno et al., 2010; Haas and Sontheimer, 2010; Lui et al., 2010; Sciaccaluga et al., 2010).

Notably, Ca^{2+}-activated BK (Ransom and Sontheimer, 2001; Liu et al., 2002; Ransom et al., 2002; Weaver et al., 2006) and IK K^+ channels (Ruggieri et al., 2012) are ontogenetically down-regulated or absent in mature glial cells but up-regulated with neoplastic transformation and malignant tumor progression as shown in expression studies in human glioma tissue. Moreover, glioblastoma cells up-regulate a unique splice variant of the BK channel (Liu et al., 2002) which exhibits a higher Ca^{2+} sensitivity than the other isoforms (Ransom et al., 2002) and is indispensable for glioblastoma proliferation *in vitro*. Similarly, ClC-3 Cl^- channels are mal-expressed in glioblastoma tissue where they traffic, in contrast to normal tissue, to the plasma membrane (Olsen et al., 2003). The predominant (surface) expression of ClC-3 and the BK splice variant by glioblastoma cells renders both channel types putative glioblastoma-specific therapeutic targets.

EVASION FROM RADIATION STRESS

External beam radiation may induce the "Go" phenotype in tumor cells similarly to the situation described for stress arising from an adverse tumor microenvironment (**Figure 1**). Ionizing radiation at doses used in single fractions during fractionated radiotherapy has been demonstrated *in vitro* and by a mouse study (Wild-Bode et al., 2001) to induce migration, invasion and spreading of head and neck squamous carcinoma (Pickhard et al., 2011), lung adenocarinoma (Jung et al., 2007; Zhou et al., 2011), meningioma (Kargiotis et al., 2008), medulloblastoma (Asuthkar et al., 2011), and glioblastoma cells (Wild-Bode et al., 2001; Wick et al., 2002; Badiga et al., 2011; Canazza et al., 2011; Rieken et al., 2011; Steinle et al., 2011; Kil et al., 2012; Vanan et al., 2012). The phenomenon of radiation-stimulated migration might be particularly relevant for highly migrating and brain-infiltrating glioblastoma cells.

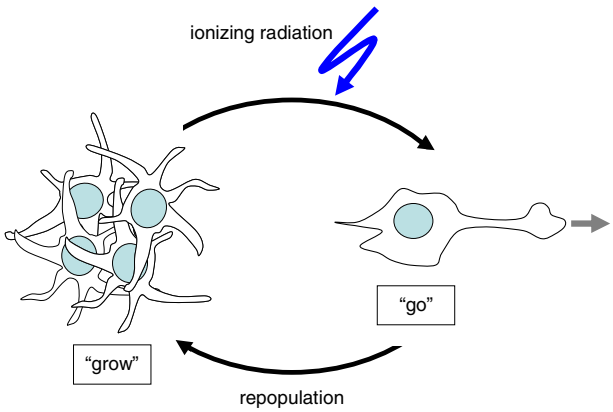

FIGURE 1 | Cellular stress such as ionizing radiation induces the switch from "Grow" to "Go" phenotype.

After macroscopic complete resection glioblastoma is usually treated by adjuvant radiotherapy of the tumor bed applying 54–60 Gy in daily fractions of 1.8–2 Gy combined with temozolomide (Stupp et al., 2005). The median progression-free survival after therapy ranges between 5 and 7 months (Stupp et al., 2005). The recurrence of glioblastoma is typically observed within the former target volume of the adjuvant fractionated radiotherapy. This might be due either to a high intrinsic radioresistance of the glioblastoma cells or to re-invasion of tumor cells into the area of the irradiated primary. One might speculate that this necrotic area, meanwhile cleared by phagocytes, offers optimal growth conditions for such re-invading tumor cells. In this latter scenario, re-invading cells might be recruited from glioblastoma (stem) cells pre-spreaded prior to radiotherapy onset in areas outside the target volume, or from cells that successfully evaded during radiation therapy.

Radiation-induced up-regulation of integrin- (Wild-Bode et al., 2001; Nalla et al., 2010; Canazza et al., 2011; Rieken et al., 2011), VEGF- (Sofia Vala et al., 2010; Badiga et al., 2011; Kil et al., 2012), EGF- (Kargiotis et al., 2008; Pickhard et al., 2011) or/and TGFbeta signaling (Canazza et al., 2011; Zhou et al., 2011) has been proposed to promote tumor cell migration. Downstream ion transport processes have been reported for glioblastoma cells (Steinle et al., 2011). In this study, BK K^+ channel activation and subsequent BK-dependent activation of the CaMKII kinase were identified as key triggers of radiation-induced migration (Steinle et al., 2011). Additionally, ClC-3 anion channels were identified as downstream targets of radiation-induced CaMKII activity (Huber, 2013). This suggests on the one hand motor function (i.e., volume decrease) of radiation-induced BK and ClC-3 currents, on the other hand, it points to a signaling function of BK channels in the programming of radiation-stimulated glioblastoma migration (**Figure 2**). Similar to the situation in migrating glioblastoma cells, radiation-induced plasma membrane K^+ currents and downstream CaMKII activation have been defined as key signaling events in cell cycle control of irradiated leukemia cells as introduced in the following paragraphs.

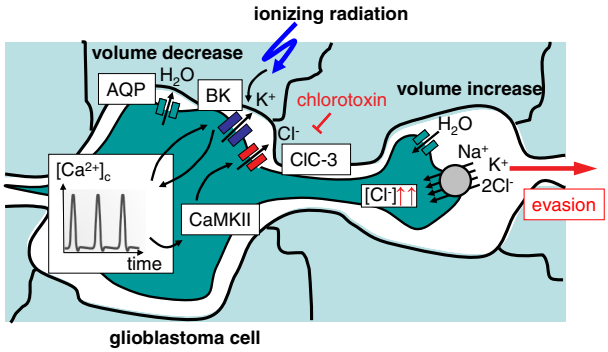

FIGURE 2 | Ionizing radiation (IR)-induced activation of BK K^+ channels results in evasion of glioblastoma cells from radiation stress. Activation of BK channels occurs upstream of CaMKII and ClC-3 Cl^- channels. The $Na^+/K^+/2Cl^-$ cotransporter accumulates Cl^- above its electrochemical equilibrium. Cl^- is used as osmolyte for volume decrease.

DNA REPAIR

Survival of irradiated tumor cells critically depends on DNA repair. This involves cell cycle arrest, elevated energy consumption, chromatin relaxation, and formation of repair complexes at the site of DNA damage. Recent *in vitro* observations suggest that radiation-induced ion transports may contribute to these processes in an indirect manner.

Cell cycle control

Survival of irradiated human leukemia cells depends on Ca^{2+} signaling. Radiation reportedly stimulates Ca^{2+} entry through TRPV5/6-like channels and subsequently activates CaMKII, which in turn fosters G_1/S transition, S progression and accumulation in G_2 phase of the cell cycle (Heise et al., 2010). Moreover, Ca^{2+} signaling in human leukemia cells has been demonstrated to be tightly regulated by voltage-gated $K_v3.4$ K^+ channels and translates into G_2/M cell cycle arrest by CaMKII-mediated inhibitory phosphorylation of the phosphatase cdc25B resulting in inactivation of the mitosis promoting factor and G_2/M arrest. Radiation activates Kv3.4 currents without changing the surface expression of the channel protein. Most importantly, inhibition of $K_v3.4$ by tetraethylammonium and blood-depressing substance-1 and substance-2 or silencing of the $K_v3.4$ channels by RNA interference prevents TRPV5/6-mediated Ca^{2+} entry, CaMKII activation, as well as cdc25B inactivation which results in release from radiation-induced G_2/M arrest, increased apoptosis, and decreased clonogenic survival. Thus, targeting of $K_v3.4$ radiosensitizes the leukemia cells demonstrating the pivotal role of this channel in cell cycle arrest required for DNA repair (Palme et al., 2013). Similar results have been obtained in prostate cancer cells, where TRPV6 inhibition by capsaicin resulted in radiosensitization (Klotz et al., 2011).

Glucose fueling and chromatin relaxation

In addition to cell cycle control, radiation-induced ion transports are proposed to improve glucose fueling of irradiated tumor cells. Fast proliferating tumor cells have a high metabolism at low external glucose and oxygen concentration in the usually chronically under-perfused growing tumor tissue. At the same time, many tumor cells cover their high energy requirements by anaerobic glycolysis with low ATP yield per metabolized glucose even under normoxic conditions. To sustain sufficient glucose fueling, tumor cells may up-regulate the Na^+/glucose cotransporter (SGLT). SGLTs are capable to take up glucose into the tumor cell even against a high chemical gradient (Ganapathy et al., 2009). Several tumor entities such as colorectal, pancreatic, lung, head and neck, prostate, kidney, cervical, mammary, and bladder cancer as well as chondrosarcomas and leukemia have indeed been shown to up-regulate SGLTs (Nelson and Falk, 1993; Ishikawa et al., 2001; Helmke et al., 2004; Casneuf et al., 2008; Weihua et al., 2008; Yu et al., 2008; Leiprecht et al., 2011; Wright et al., 2011). The inwardly directed Na^+ gradient and the voltage across the plasma membrane drive the electrogenic SGLT-generated glucose transport into the cell. The membrane voltage is tightly regulated by the activity of voltage gated K^+ channels which counteract SGLT-mediated depolarization.

Ionizing radiation has been demonstrated to activate EGF receptors (Dittmann et al., 2009). In addition, SGLT1 reportedly is in complex with and under the direct control of the EGF receptor (Weihua et al., 2008) suggesting radiation-induced SGLT1 modifications. As a matter of fact, ionizing radiation stimulates a long lasting EGFR-dependent and SGLT-mediated glucose uptake in A549 lung adenocarcinoma and head and neck squamous carcinoma cell lines (but not in non-transformed fibroblasts) as shown by ^{3}H-glucose uptake and patch-clamp, current clamp recordings (Huber et al., 2012). In the latter experiments, radiation-induced and SGLT-mediated depolarization of membrane potential was preceded by a transient hyperpolarization of the plasma membrane indicative of radiation-induced K^+ channel activation (Huber et al., 2012). Such radiation-induced increase in K^+ channel activity has been reported for several tumor cell lines including A549 lung adenocarcinoma cells (Kuo et al., 1993). In this cell line, radiation at doses between 0.1 and 6 Gy stimulates the activity of voltage gated K^+ channels within 5 min, which gradually declines thereafter. It is tempting to speculate that this radiation-stimulated K^+ channel activity counteracts the depolarization of the membrane potential caused by the SGLT activity shortly after radiation and sustains the driving force for Na^+-coupled glucose uptake (Huber et al., 2012).

Ionizing radiation may lead to necrotic as well as apoptotic cell death depending on cell type, dose, and fractionation (Verheij, 2008). In particular, necrotic cell death may be associated with ATP depletion (Dorn, 2013). Increased SGLT activity in irradiated tumor cells might contribute to ATP replenishment counteracting necrotic cell death. Such function has been suggested in irradiated A549 cells by experiments analyzing cellular ATP concentrations, chromatin remodeling, residual DNA damage, and clonogenic survival of irradiated tumor cells (Dittmann et al., 2013). The data demonstrate that radiation of A549 lung adenocarcinoma cells leads to a transient intracellular ATP depletion and to histone H3 modifications crucial

for both chromatin remodeling and DNA repair in response to irradiation.

Importantly, recovery from radiation-induced ATP crisis was EGFR/SGLT-dependent and associated with improved DNA-repair and increased clonogenic cell survival. The blockade of either EGFR or SGLT inhibited ATP level recovery and histone H3 modifications. *Vice versa*, inhibition of the acetyltransferase TIP60, which is essential for histone H3 modification, prevented chromatin remodeling as well as ATP crisis (Dittmann et al., 2013). Together, these data suggest that radiation-associated interactions between SGLT1 and EGFR result in increased glucose uptake, which counteracts the ATP crisis in tumor cells caused by chromatin remodeling. Importantly, the blockade of recovery from ATP crisis by SGLT1 inhibition may radio-sensitize tumor cells as demonstrated in lung adenocarcinoma and head and neck squamous carcinoma cell lines (Huber et al., 2012; Dittmann et al., 2013).

Formation of repair complexes

In addition to SGLT-generated glucose uptake, radiation-induced electrosignaling via transient receptor potential melastatin 2 (TRPM2) and vanilloid 1 (TRPV1) cation channels, has been shown to stimulate Ataxia telangiectasia mutated (ATM) kinase activation, histone 2AX (H2AX) phosphorylation, and γH2AX focus formation in A549 lung adenocarcinoma cells, processes required to recruit further repair proteins to the DNA double strand break (Masumoto et al., 2013). Furthermore, radiation-induced TRPM2 induces ATP release and P2Y signaling in A549 cells (Masumoto et al., 2013). Radiation-stimulated and $P2X_7$ receptor- and gap junction hemichannel connexin43-mediated ATP release has been suggested to signal in a paracrine manner to unirradiated bystander cells in the B16 melanoma model (Ohshima et al., 2012).

Combined, these recent data indicate that ion transports may regulate processes that mediate intrinsic radioresistance. The investigation of ion transports in radiobiology is at its very beginning and the few data available are mostly phenomenological in nature. The molecular mechanisms that underlie, e.g., regulation of DNA repair by ion transports are ill-defined. Nevertheless, the data prove functional significance of ion transports and electrosignaling for the survival of irradiated tumor cells and might have translational implications for radiotherapy in the future.

Similar to intrinsic radioresistance, the function of ion transports in hypoxia resistance and associated hypoxic radioresistance of tumor cells is not well-defined. The following paragraphs give a summary of what is known about mitochondrial transports and hypoxia resistance of normal tissue and how these findings might also apply for tumor cells.

MITOCHONDRIAL UNCOUPLING AND RESISTANCE TO HYPOXIA, CHEMO-, AND RADIOTHERAPY

Intermittent hypoxia is a common feature of vascularized solid tumors. The pathophysiologial aspects of hypoxia and reoxygenation are well-known from ischemia-reperfusion injuries observed in normal tissue. Reoxygenation-associated production of reactive oxygen species (ROS) is a major cause of the hypoxia/reoxygenation injury after myocardial, hepatic, intestinal, cerebral, renal and other ischemia and mitochondria have been identified as one of the main sources of ROS formation herein (Li and Jackson, 2002). Mitochondrial ROS formation mutually interacts with hypoxia/reoxygenation-associated cellular Ca^{2+} overload. Brief hypoxic periods induce an adaptation to hypoxia in several tissues which lowers ischemia-reperfusion injuries of subsequent ischemic insults (so-called ischemic preconditioning). Similar adaptations which involve alterations in mitochondrial ion transport have been proposed to confer hypoxia resistance of tumor cells.

Mitochondrial ROS formation

Activity and efficacy of the mitochondrial respiration chain are fine-tuned by the dependence of the ATP synthase (complex V) on the membrane potential $\Delta\Psi_m$, by the ATP/ADP ratio, as well as by reversible phosphorylation of the complexes I and IV (**Figure 3**) (Kadenbach, 2003). It is suggested that under physiological conditions (high ATP/ADP ratios), the membrane potential $\Delta\Psi_m$ is kept low [around −100 to −150 mV (Kadenbach, 2003)]. The efficacy of the respiratory chain at low $\Delta\Psi_m$ is high. At higher ATP demand or decreasing cellular ATP levels, cytochrome c oxidase (complex IV) is relieved from ATP blockade and $\Delta\Psi_m$ increases. High $\Delta\Psi_m$ values (up to −180 mV), however, lower the efficacy of cytochrome c oxidase (Kadenbach, 2003) and increase the probability of single electron leakage at complex I and III to molecular oxygen resulting in an increased $O_2{\cdot}^-$ production (**Figure 3**) (Korshunov et al., 1997; Skulachev, 1998; Kadenbach, 2003).

The respiratory chain is also regulated by the cytosolic ($[Ca^{2+}]_i$) and mitochondrial matrix free Ca^{2+} concentration ($[Ca^{2+}]_m$) in a complex manner (for review see Pizzo et al., 2012). The phosphatases that dephosphorylate (and thereby switch-off) the NADH oxidase and that relieve the ATP blockade of complex IV are inhibited by $[Ca^{2+}]_m$ and activated by $[Ca^{2+}]_i$, respectively (**Figure 3**). As a consequence, increase in $[Ca^{2+}]_m$ and $[Ca^{2+}]_i$ results in a higher $\Delta\Psi_m$ and a concurrently increased production of reactive oxygen species (Kadenbach, 2003).

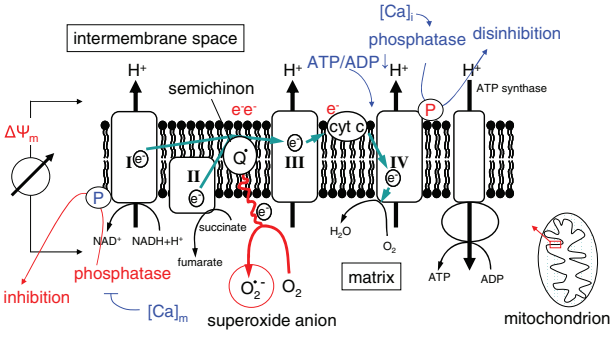

FIGURE 3 | Mitochondrial ROS formation in dependence on $\Delta\Psi_m$ (I, II, III, and IV, electron transport complexes I, II, III, and IV; Q: semiquinone radical; cyt C: cytochrome C). Ca^{2+} and the ATP/ADP ratio regulate the electron chain at complexes I and IV.

Hypoxia decreases the activity of the mitochondrial manganese superoxide dismutase (Mn-SOD) and of the cytochrome c oxidase. Depletion of the final electron acceptor, however, increases the formation of $O_2{\cdot}^-$ during reoxygenation by the enhanced leakage of single electrons from more proximal complexes of the respiration chain (for review see Li and Jackson, 2002; Sack, 2006). Lowered $O_2{\cdot}^-$-detoxifying capability combined with simultaneous elevated $O_2{\cdot}^-$ production results in a highly elevated $O_2{\cdot}^-$ concentration which, e.g., in hepatocytes increases 15-fold within 15 min of reoxygenation (Caraceni et al., 1995).

Hypoxia/reoxygenation-associated Ca^{2+} overload

Hypoxia-associated energy depletion and the concomitant impairment of plasma membrane Na^+ and Ca^{2+} pump activity lead to a decline of the chemical Na^+, Ca^{2+} and K^+ gradients across the plasma membrane and to the depolarization of the plasma membrane potential. In parallel, increased lactic acid fermentation during hypoxia increases the cytosolic proton concentration and lowers the intracellular pH. The proton extrusion machinery that is already active during hypoxia becomes massively activated during reoxygenation and restores a physiological pH by wash-out of lactic acid and activation of the sodium/hydrogen exchanger and sodium/bicarbonate symporter. The latter, Na^+-coupled transports, in turn, further increase the cytosolic Na^+ concentration to a level, where the low affinity high capacity sodium/calcium exchanger in the plasma membrane starts to operate in the reverse mode (i.e., to extrude Na^+ at the expense of Ca^{2+} uptake). At that time, reoxygenation-mediated oxidative stress (see above) stimulates further Ca^{2+} entry through Ca^{2+}-permeable channels in the plasma membrane and the release of Ca^{2+} from the endoplasmic reticulum resulting in an abrupt rise in $[Ca^{2+}]_i$ during the first minutes of reoxygenation. Cytosolic Ca^{2+} is buffered by $\Delta\Psi_m$-driven and uniporter-mediated Ca^{2+} uptake into the mitochondrial matrix which increases $[Ca^{2+}]_m$. Elevated $[Ca^{2+}]_m$ and $[Ca^{2+}]_i$ values, in turn, signal back to the respiratory chain by further increasing $\Delta\Psi_m$ (see above). Exceeding the Ca^{2+} threshold concentration in the matrix, $[Ca^{2+}]_m$ activates the permeability transition pore which leads to breakdown of $\Delta\Psi_m$, swelling of the mitochondrial matrix and eventually release of cytochrome c from the intermembrane space into the cytosol (Crompton, 1999; Rasola and Bernardi, 2011). By reversing the ATP synthase activity, into the ATPase proton pump mode, the F_0/F_1 complex in the inner mitochondrial delays the break-down of $\Delta\Psi_m$ at the expense of ATP hydrolysis. In addition to this ATP depletion, the loss of cytochrome c and the concurrent decline of the final electron acceptor (cytochrome c oxidase of complex IV) further increases the formation of $O_2{\cdot}^-$ by more proximal complexes. The pivotal role of membrane transports in this process is illustrated by the fact that inhibition of the sodium/hydrogen antiporter in the plasma membrane, the Ca^{2+} uniporter in the inner mitochondrial membrane, or Ca^{2+} channels in the endoplasmic reticulum (ER) decreases the hypoxia/reoxygenation injury *in vitro* (for review see Crompton, 1999; Li and Jackson, 2002; Sack, 2006; Yellon and Hausenloy, 2007).

Ischemic pre-conditioning

Cells can also adapt to repetitive periods of hypoxia. This so-called ischemic preconditioning has been demonstrated in the myocardium where it reduces ischemia-caused infarct size, myocardial stunning, and incidence of cardiac arrhythmias (Gross and Peart, 2003). Since mitochondrial ROS formation increases with increasing $\Delta\Psi_m$ (Korshunov et al., 1997; Skulachev, 1998; Kadenbach, 2003) lowering of the mitochondrial $\Delta\Psi_m$ is proposed to be a key adaptation event in ischemic preconditioning (Sack, 2006). Lowering of $\Delta\Psi_m$ reduces not only mitochondrial $O_2{\cdot}^-$ production but also the mitochondrial Ca^{2+} overload during reoxygenation (Gross and Peart, 2003; Prasad et al., 2009). The hypoxic preconditioning-associated reduction of $\Delta\Psi_m$ is in part achieved by up-regulation of ATP-sensitive (mitoKATP) and Ca^{2+}-activated (mitoKCa) K^+ channels in the inner mitochondrial membrane which short-circuit $\Delta\Psi_m$ (Murata et al., 2001; Gross and Peart, 2003; Prasad et al., 2009; Singh et al., 2012; Szabo et al., 2012). The uncoupling proteins-2 and -3 (UCP-2, -3) constitute two further proteins that have been suggested to play a role in counteracting cardiac hypoxia/reoxygenation injury and in hypoxic preconditioning in heart and brain (Mcleod et al., 2005; Sack, 2006; Ozcan et al., 2013). Activation of these proteins results in a modest depolarization of $\Delta\Psi_m$ by maximally 15 mV (Fink et al., 2002). High expression of UCP-3 has also been demonstrated in skeletal muscle where it suppresses mitochondrial oxidant emission during fatty acid-supported respiration (Anderson et al., 2007). Accordingly, overexpression of UCP-3 in cultured human muscle cells lowers $\Delta\Psi_m$, raises the ATP/ADP ratio, and favors fatty acid vs. glucose oxidation (Garcia-Martinez et al., 2001). Conversely, knockdown of UCP-3 increased the coupling between electron and proton transfer across the inner mitochondrial membrane and ROS production (Vidal-Puig et al., 2000; Talbot and Brand, 2005). UCP-3 protein is robustly up-regulated in chondrocytes (Watanabe et al., 2008) and skeletal muscle during hypoxia and the absence of UCP-3 exacerbates hypoxia-induced ROS (Lu and Sack, 2008). UCP-3 is not constitutively active. $O_2{\cdot}^-$ has been demonstrated to stimulate the activity of UCP-3 in skeletal muscle suggesting that UCP-3 is the effector of a feed back loop which restricts overshooting ROS production (Echtay et al., 2002).

Mitochondrial uncoupling in tumor cells

Recent studies suggest that UCPs are upregulated in a number of aggressive human cancers. In particular, over-expression of UCP2 has been reported in leukemia as well as in breast, colorectal, ovarian, bladder, esophagus, testicular, kidney, pancreatic, lung, and prostate cancer (Ayyasamy et al., 2011; Su et al., 2012). In human colon cancer, UCP2 mRNA and protein expression reportedly is increased by factor of 3–4 as compared to peritumoral normal epithelium. In addition, UCP2 expression gradually increases during the colon adenoma-carcinoma sequence (Horimoto et al., 2004) and is higher in clinical stages III and IV colon cancer than in stage I and II (Kuai et al., 2010). Similarly, UCP4 expression has been shown to correlate with lymph node metastases in breast cancer (Gonidi et al., 2011) and UCP1 expression in prostate cancer with disease progression from primary to bone metastatic cancers (Zhau et al., 2011). Moreover, postmenopausal breast

tumors with low estrogen receptor (ER) alpha to ER beta ratios that associate with higher UCP5 expression and higher oxidative defense have a poor prognosis (Sastre-Serra et al., 2013). Finally, ectopic expression of UCP2 in MCF7 breast cancer cells has been demonstrated to enhance proliferation, migration and matrigel invasion *in vitro* and to promote tumor growth *in viv*o (Ayyasamy et al., 2011). Together, these observations suggest that UCPs may contribute to the malignant progression of tumor cells.

In addition to malignant progression, UCPs may alter the therapy sensitivity of tumor cells. In specimens of human ovarian cancers carboplatin/paclitaxel-resistant cancers showed decreased UCP2 protein abundances as compared to the sensitive ones (Pons et al., 2012). Likewise, progression-free and overall survival of patients with inoperable lung cancer who received cisplatin-based chemotherapy was higher when tumors expressed high levels of UCP2 as compared to tumors with low UCP2 levels (Su et al., 2012). A possible explanation of the latter observation is that especially in lung tumors with mutated p53, cisplatin elicits oxidative stress that induces pro-survival signaling. High UCP2 expression, however, diminishes cisplatin-evoked oxidative stress and, in turn, decreases the pro-survival signals (Su et al., 2012).

In lung cancer cell lines with wildtype p53, in contrast, down-regulation of UCP2 results in significantly increased paclitaxel-induced cell death (Su et al., 2012). Similarly, overexpression of UCP2 in a human colon cancer cell line has been shown to blunt topoisomerase I inhibitor CPT-11-induced accumulation of reactive oxygen species and apoptosis *in vitro* and to confer CPT-11 resistance of tumor *xeno*grafts (Derdak et al., 2008). In addition, in pancreatic adenocarcinoma, non-small cell lung adenocarcinoma, and bladder carcinoma cell lines IC_{50} values of the anticancer drug gemcitabine increase with intrinsic UCP2 mRNA abundance. Furthermore, UCP2 overexpression strongly decreases gemcitabine-induced mitochondrial superoxide formation and protects cancer cells from apoptosis (Dalla Pozza et al., 2012). Finally, metabolic changes including UCP2 up-regulation and UCP2-mediated uncoupling of oxidative phosphorylation have been demonstrated in multidrug-resistant subclones of various tumor cell lines (Harper et al., 2002). Similarly, in acute myeloid leukemia cells, UCP2 up-regulation has been shown to foster the Warburg effect (i.e., anaerobic glycolysis in the absence of respiratory impairment) (Samudio et al., 2008).

UCP2 expression is stimulated by co-culturing of these leukemia cells with bone marrow-derived mesenchymal stromal cells (Samudio et al., 2008). Other stimuli of UCP expression/activity are hydrogen peroxide as shown for UCP5 in colon cancer cells (Santandreu et al., 2009) and gemcitabine chemotherapy as reported for UCP2 in pancreatic, lung and bladder cancer cell lines (Dalla Pozza et al., 2012). Collectively, these data suggest that tumor cells may acquire resistance to chemotherapy by up-regulation of UCPs and lowering of the therapy-evoked mitochondrial formation of reactive oxygen species (Robbins and Zhao, 2011).

Accordingly, experimental targeting of UCPs has been demonstrated to sensitize tumor cells to chemotherapy *in vitro*. For instance, genipin-induced inhibition or glutathionylation of UCP2 sensitizes drug-resistant leukemia subclones to chemotherapy with menadione, doxorubicin, or epirubicin (Mailloux et al., 2010; Pfefferle et al., 2012). Likewise, UCP2 inhibition by genipin or UCP2 mRNA silencing strongly enhances gemcitabine-induced mitochondrial superoxide generation and apoptotic cell death of pancreatic, lung and bladder cancer cell lines (Dalla Pozza et al., 2012). Moreover, UCP2 inhibition has been reported to trigger reactive oxygen species-dependent nuclear translocation of GAPDH and autophagic cell death in pancreatic adenocarcinoma cells (Dando et al., 2013) Together, this suggests that targeting UCPs might be a promising strategy to overcome resistance to anti-cancer therapies in the clinic. Notably, in an acute myeloid leukemia cell line, the cytotoxicity of cisplatin has been proposed to be in part mediated by cisplatin-dependent down-regulation of UCPs (Samudio et al., 2008) suggesting that established chemotherapy regimes already may co-target UCPs.

It is tempting to speculate that UCPs may also confer resistance to radiotherapy. One could hypothesize that UCPs adapt the tumor cells to a "relatively radioprotected" hypoxic microenvironment by decreasing hypoxia-associated mitochondrial formation of reactive oxygen species. Such UCP function in hypoxia resistance has been demonstrated for a lung adenocarcinoma cell line (Deng et al., 2012). Notably, radiation induces up-regulation of UCP2 expression as shown in colon carcinoma cells (Sreekumar et al., 2001) and in a radiosensitive subclone of B cell lymphoma (Voehringer et al., 2000). On the one hand, this UCP2 up-regulation might facilitate radiation-induced apoptosis induction by accelerating the break-down of $\Delta\Psi_m$ as proposed by the authors of these studies. On the other hand, radiation-induced UCP2 upregulation might be radioprotective by lowering the radiation-induced burden of reactive oxygen species. As a matter of fact, multi-resistant subclones of leukemia cells show higher UCP2 protein expression, lower $\Delta\Psi_m$, lower radiation induced formation of reactive oxygen species and decreased DNA damage as compared to their parental sensitive cells (Harper et al., 2002).

In summary, UCPs suppress the formation of $O_2{\cdot}^-$, a byproduct of the mitochondrial respiration chain and a major source of oxidative stress. In some cancers UCPs in particular UCP2 are highly upregulated and may contribute to the reprogramming of the cell metabolism that results in chemoresistance (for review see Baffy, 2010; Baffy et al., 2011) or even radioresistance. Moreover, recent studies imply that UCP2 may repress p53-mediated apoptosis providing a potential new mechanism of how UCP2 contributes to cancer development (Robbins and Zhao, 2011).

Together, these observations suggest that ion transport processes are critically involved in evasion from radiation stress, and intrinsic or hypoxic radioresistance. Since ion transport-mediated radioresistance might underlie failure of radiotherapy, concepts which combine ion transport targeting with radiotherapy hold promise for new therapy strategies in the future. A summary of how ion transport can be harnessed for anticancer therapy and how these therapy strategies might be combined with radiotherapy is given in the next paragraphs.

TARGETING ION TRANSPORTS IN RADIOTHERAPY

An important reason for the study of ion transports in the context of radiotherapy is the possible translation of the acquired knowledge into anti-cancer therapy. Many pharmacological modulators

of ion transports are already in clinical use or currently tested in clinical trials (Wulff and Castle, 2010). Moreover, tumors often over-express certain types of transport proteins.

These proteins such as the transient receptor melastatin 8 (TRPM8) non-selective cation channel in prostate cancer have been used in clinical trials as tumor-associated antigen for anti-tumor vaccination (Fuessel et al., 2006). Tumor promoting inflammation and anti-tumor immune effects are evolving fields of preclinical and clinical research (Hanahan and Weinberg, 2011). Preclinical evidence supports the thesis that tumors have to develop immune-evading capacities in order to grow into macroscopic, clinically detectable lesions (Koebel et al., 2007; Teng et al., 2008). Possible mechanisms are the secretion of cytokines and chemokines by cancer and tumor stroma cells (Vianello et al., 2006; Shields et al., 2010), the priming of infiltrating T-lymphocytes toward immunosuppressive regulatory T-cells and the recruitment of myeloid-derived suppressor cells and tumor-associated macrophages (Tanchot et al., 2013; Oleinika et al., 2013). Irradiation of tumors has been shown to impair on the one hand the immunosuppressive action of the tumor and on the other to induce so-called "immunogenic" cell death within the tumor with translocation of calreticulin to the plasma membrane, release of HMGB1 or ATP (Formenti and Demaria, 2013). Preclinical studies showed a synergistic effect of irradiation and several immunotherapeutic approaches such as dendritic cell injection (Finkelstein et al., 2012), anti-CTLA-4-antibody (Grosso and Jure-Kunkel, 2013), and vaccines (Chakraborty et al., 2004). Interestingly, for combination with anti-CTLA-4 antibody a synergistic effect could only be demonstrated for fractionated but not for single-dose irradiation (Demaria and Formenti, 2012).

In addition, over-expressed transport proteins in tumors can be harnessed to target drugs, cytokines, or radioactivity to the tumor cells (Hartung et al., 2011). One example is the specific surface expression of ClC-3 Cl^- channels by glioblastoma (and other tumor entities) which suggests ClC-3 as an excellent and highly specific target for anti-glioblastoma therapy. Chlorotoxin which is a 36 amino acid-long peptide from the venom of the scorpion *Leiurus quinquestriatus* has been found to inhibit ClC-3 and to preferentially bind to the cell surface of a variety of human malignancies. This specificity probably comes from the highly affine binding of chlorotoxin to a lipid raft-anchored complex of matrix metalloproteinase-2, membrane type-I MMP, and transmembrane inhibitor of metalloproteinase-2, as well as ClC-3 (Veiseh et al., 2007). Ongoing clinical trials successfully used ^{131}I-labeled chlorotoxin as glioblastoma-specific PET-tracer (Hockaday et al., 2005) and for targeted radiation of glioblastoma cells (Mamelak and Jacoby, 2007). Due to the low surface expression of ClC-3 in normal tissue, chlorotoxin exhibits little or no affinity to normal cells (Lyons et al., 2002). If the *in vitro* and mouse data on radiation-stimulated glioblastoma migration reflect indeed the *in vivo* situation in glioblastoma patients, a clinical setting might be envisaged in which radiation-induced glioblastoma spreading is prevented by combining radiotherapy with chlorotoxin blockade of ClC-3 channels.

CONCLUDING REMARKS

Interdisciplinary approaches linking radiobiology with physiology brought about the first peaces of evidence suggesting a functional significance of ion transport processes for the survival of irradiated tumor cells. The few reports published up to now on this topic are confined to phenomena occurring in the plasma membrane due to the methodological restrictions of studying these processes in the membranes of mitochondria, endoplasmic reticulum, or nuclear envelope. Intracellular membrane transports, however, might similarly impact tumor cell radiosensitivity. This is suggested by the notion that intracellular Cl^- channel CLIC1 protein expression regulates radiosensitivity in laryngeal cancer cells (Kim et al., 2010). However, the molecular mechanisms underlying, e.g., radiation-induced transport modifications, or downstream signaling events are far from being understood. Despite all these limitations, our current knowledge already clearly indicates that the observed transport processes may be crucial for the survival of the tumor and, thus, are worthwhile to spend further and more effort in this field which might lead to new strategies for cancer treatment in the future.

ACKNOWLEDGMENTS

This work has been supported by the Wilhelm-Sander-Stiftung (2011.083.1). Dominik Klumpp and Benjamin Stegen were supported by the DFG International Graduate School 1302 (TP T9).

REFERENCES

Anderson, E. J., Yamazaki, H., and Neufer, P. D. (2007). Induction of endogenous uncoupling protein 3 suppresses mitochondrial oxidant emission during fatty acid-supported respiration. *J. Biol. Chem.* 282, 31257–31266. doi: 10.1074/jbc.M706129200

Arcangeli, A. (2011). Ion channels and transporters in cancer. 3. Ion channels in the tumor cell-microenvironment cross talk. *Am. J. Physiol. Cell Physiol.* 301, C762–C771.

Asuthkar, S., Nalla, A. K., Gondi, C. S., Dinh, D. H., Gujrati, M., Mohanam, S., et al. (2011). Gadd45a sensitizes medulloblastoma cells to irradiation and suppresses MMP-9-mediated EMT. *Neuro Oncol.* 13, 1059–1073. doi: 10.1093/neuonc/nor109

Auperin, A., Arriagada, R., Pignon, J. P., Le Pechoux, C., Gregor, A., Stephens, R. J., et al. (1999). Prophylactic cranial irradiation for patients with small-cell lung cancer in complete remission. prophylactic cranial irradiation overview collaborative group. *N. Engl. J. Med.* 341, 476–484. doi: 10.1056/NEJM199908123410703

Ayyasamy, V., Owens, K. M., Desouki, M. M., Liang, P., Bakin, A., Thangaraj, K., et al. (2011). Cellular model of Warburg effect identifies tumor promoting function of UCP2 in breast cancer and its suppression by genipin. *PLoS ONE* 6:e24792. doi: 10.1371/journal.pone.0024792

Badiga, A. V., Chetty, C., Kesanakurti, D., Are, D., Gujrati, M., Klopfenstein, J. D., et al. (2011). MMP-2 siRNA inhibits radiation-enhanced invasiveness in glioma cells. *PLoS ONE* 6:e20614. doi: 10.1371/journal.pone.0020614

Baffy, G. (2010). Uncoupling protein-2 and cancer. *Mitochondrion* 10, 243–252. doi: 10.1016/j.mito.2009.12.143

Baffy, G., Derdak, Z., and Robson, S. C. (2011). Mitochondrial recoupling: a novel therapeutic strategy for cancer. *Br. J. Cancer* 105, 469–474.

Barendsen, G. W. (1982). Dose fractionation, dose rate and iso-effect relationships for normal tissue responses. *Int. J. Radiat. Oncol. Biol. Phys.* 8, 1981–1997. doi: 10.1016/0360-301690459-X

Bernier, J., Hall, E. J., and Giaccia, A. (2004). Radiation oncology: a century of achievements. *Nat. Rev. Cancer* 4, 737–747. doi: 10.1038/nrc1451

Canazza, A., Calatozzolo, C., Fumagalli, L., Bergantin, A., Ghielmetti,

F., Fariselli, L., et al. (2011). Increased migration of a human glioma cell line after *in vitro* CyberKnife irradiation. *Cancer Biol. Ther.* 12, 629–633. doi: 10.4161/cbt.12.7.16862

Caraceni, P., Ryu, H. S., Van Thiel, D. H., and Borle, A. B. (1995). Source of oxygen free radicals produced by rat hepatocytes during postanoxic reoxygenation. *Biochim. Biophys. Acta* 1268, 249–254. doi: 10.1016/0167-488900077-6

Casneuf, V. F., Fonteyne, P., Van Damme, N., Demetter, P., Pauwels, P., De Hemptinne, B., et al. (2008). Expression of SGLT1, Bcl-2 and p53 in primary pancreatic cancer related to survival. *Cancer Invest.* 26, 852–859. doi: 10.1080/07357900801956363

Catacuzzeno, L., Aiello, F., Fioretti, B., Sforna, L., Castigli, E., Ruggieri, P., et al. (2010). Serum-activated K and Cl currents underlay U87-MG glioblastoma cell migration. *J. Cell Physiol.* 226, 1926–1933. doi: 10.1002/jcp.22523

Chakraborty, M., Abrams, S. I., Coleman, C. N., Camphausen, K., Schlom, J., and Hodge, J. W. (2004). External beam radiation of tumors alters phenotype of tumor cells to render them susceptible to vaccine-mediated T-cell killing. *Cancer Res.* 64, 4328–4337. doi: 10.1158/0008-5472.CAN-04-0073

Crompton, M. (1999). The mitochondrial permeability transition pore and its role in cell death. *Biochem. J.* 341, 233–249.

Cuddapah, V. A., and Sontheimer, H. (2010). Molecular interaction and functional regulation of ClC-3 by Ca2+/calmodulin-dependent protein kinase II (CaMKII) in human malignant glioma. *J. Biol. Chem.* 285, 11188–11196. doi: 10.1074/jbc.M109.097675

Cullis, P. M., Jones, G. D. D., Lea, J., Symons, M. C. R., and Sweeney, M. (1987). The effects of ionizing radiation on deoxyribonucleic acid. Part 5. The role of thiols in chemical repair. *J. Chem. Soc., Perkin Trans. 2,* 1907–1914. doi: 10.1039/p29870001907

Dale, R. G. (1985). The application of the linear-quadratic dose-effect equation to fractionated and protracted radiotherapy. *Br. J. Radiol.* 58, 515–528. doi: 10.1259/0007-1285-58-690-515

Dalla Pozza, E., Fiorini, C., Dando, I., Menegazzi, M., Sgarbossa, A., Costanzo, C., et al. (2012). Role of mitochondrial uncoupling protein 2 in cancer cell resistance to gemcitabine. *Biochim. Biophys. Acta* 1823, 1856–1863. doi: 10.1016/j.bbamcr.2012.06.007

Dando, I., Fiorini, C., Pozza, E. D., Padroni, C., Costanzo, C., Palmieri, M., et al. (2013). UCP2 inhibition triggers ROS-dependent nuclear translocation of GAPDH and autophagic cell death in pancreatic adenocarcinoma cells. *Biochim. Biophys. Acta* 1833, 672–679. doi: 10.1016/j.bbamcr.2012.10.028

Darby, S., Mcgale, P., Correa, C., Taylor, C., Arriagada, R., Clarke, M., et al. (2011). Effect of radiotherapy after breast-conserving surgery on 10-year recurrence and 15-year breast cancer death: meta-analysis of individual patient data for 10, 801 women in 17 randomised trials. *Lancet* 378, 1707–1716. doi: 10.1016/S0140-673661629-2

Demaria, S., and Formenti, S. C. (2012). Radiation as an immunological adjuvant: current evidence on dose and fractionation. *Front. Oncol.* 2:153. doi: 10.3389/fonc.2012.00153

Deng, S., Yang, Y., Han, Y., Li, X., Wang, X., Li, X., et al. (2012). UCP2 inhibits ROS-mediated apoptosis in A549 under hypoxic conditions. *PLoS ONE* 7:e30714. doi: 10.1371/journal.pone.0030714

Derdak, Z., Mark, N. M., Beldi, G., Robson, S. C., Wands, J. R., and Baffy, G. (2008). The mitochondrial uncoupling protein-2 promotes chemoresistance in cancer cells. *Cancer Res.* 68, 2813–2819. doi: 10.1158/0008-5472.CAN-08-0053

Dittmann, K., Mayer, C., Kehlbach, R., Rothmund, M. C., and Peter Rodemann, H. (2009). Radiation-induced lipid peroxidation activates src kinase and triggers nuclear EGFR transport. *Radiother. Oncol.* 92, 379–382. doi: 10.1016/j.radonc.2009.06.003

Dittmann, K., Mayer, C., Rodemann, H. P., and Huber, S. M. (2013). EGFR cooperates with glucose transporter SGLT1 to enable chromatin remodeling in response to ionizing radiation. *Radiother. Oncol.* 107, 247–251. doi: 10.1016/j.radonc.2013.03.016

Dorn, G. W. 2nd. (2013). Molecular mechanisms that differentiate apoptosis from programmed necrosis. *Toxicol. Pathol.* 41, 227–234. doi: 10.1177/0192623312466961

Echtay, K. S., Roussel, D., St-Pierre, J., Jekabsons, M. B., Cadenas, S., Stuart, J. A., et al. (2002). Superoxide activates mitochondrial uncoupling proteins. *Nature* 415, 96–99. doi: 10.1038/415096a

Eckert, F., Alloussi, S., Paulsen, F., Bamberg, M., Zips, D., Spillner, P. et al. (2013). Prospective evaluation of a hydrogel spacer for rectal separation in dose-escalated intensity-modulated radiotherapy for clinically localized prostate cancer. *BMC Cancer* 13:27. doi: 10.1186/1471-2407-13-27

Eckert, F., Fehm, T., Bamberg, M., and Muller, A. C. (2010a). Small cell carcinoma of vulva: curative multimodal treatment in face of resistance to initial standard chemotherapy. *Strahlenther. Onkol.* 186, 521–524.

Eckert, F., Matuschek, C., Mueller, A. C., Weinmann, M., Hartmann, J. T., Belka, C., et al. (2010b). Definitive radiotherapy and single-agent radiosensitizing ifosfamide in patients with localized, irresectable soft tissue sarcoma: a retrospective analysis. *Radiat. Oncol.* 5, 55.

Eckert, F., Gani, C., Bamberg, M., and Muller, A. C. (2012). Cerebral metastases in extrapulmonary cell carcinoma: implications for the use of prophylactic cranial irradiation. *Strahlenther. Onkol.* 188, 478–483. doi: 10.1007/s00066-012-0084-5

Ernest, N. J., Weaver, A. K., Van Duyn, L. B., and Sontheimer, H. W. (2005). Relative contribution of chloride channels and transporters to regulatory volume decrease in human glioma cells. *Am. J. Physiol. Cell Physiol.* 288, C1451–1460. doi: 10.1152/ajpcell.00503.2004

Fink, B. D., Hong, Y. S., Mathahs, M. M., Scholz, T. D., Dillon, J. S., and Sivitz, W. I. (2002). UCP2-dependent proton leak in isolated mammalian mitochondria. *J. Biol. Chem.* 277, 3918–3925. doi: 10.1074/jbc.M107955200

Finkelstein, S. E., Iclozan, C., Bui, M. M., Cotter, M. J., Ramakrishnan, R., Ahmed, J., et al. (2012). Combination of external beam radiotherapy (EBRT) with intratumoral injection of dendritic cells as neo-adjuvant treatment of high-risk soft tissue sarcoma patients. *Int. J. Radiat. Oncol. Biol. Phys.* 82, 924–932. doi: 10.1016/j.ijrobp.2010.12.068

Formenti, S. C., and Demaria, S. (2013). Combining radiotherapy and cancer immunotherapy: a paradigm shift. *J. Natl. Cancer Inst.* 105, 256–265. doi: 10.1093/jnci/djs629

Fuessel, S., Meye, A., Schmitz, M., Zastrow, S., Linne, C., Richter, K., et al. (2006). Vaccination of hormone-refractory prostate cancer patients with peptide cocktail-loaded dendritic cells: results of a phase I clinical trial. *Prostate* 66, 811–821. doi: 10.1002/pros.20404

Fyles, A., Milosevic, M., Hedley, D., Pintilie, M., Levin, W., Manchul, L., et al. (2002). Tumor hypoxia has independent predictor impact only in patients with node-negative cervix cancer. *J. Clin. Oncol.* 20, 680–687. doi: 10.1200/JCO.20.3.680

Fyles, A., Milosevic, M., Pintilie, M., Syed, A., Levin, W., Manchul, L., et al. (2006). Long-term performance of interstial fluid pressure and hypoxia as prognostic factors in cervix cancer. *Radiother. Oncol.* 80, 132–137. doi: 10.1016/j.radonc.2006.07.014

Ganapathy, V., Thangaraju, M., and Prasad, P. D. (2009). Nutrient transporters in cancer: relevance to Warburg hypothesis and beyond. *Pharmacol. Ther.* 121, 29–40. doi: 10.1016/j.pharmthera.2008.09.005

Garcia-Martinez, C., Sibille, B., Solanes, G., Darimont, C., Mace, K., Villarroya, F., et al. (2001). Overexpression of UCP3 in cultured human muscle lowers mitochondrial membrane potential, raises ATP/ADP ratio, and favors fatty acid vs. glucose oxidation. *FASEB J.* 15, 2033–2035.

German-Cancer-Aid. (2013a). *Homepage*. Available online at: http://www.krebshilfe.de/krebszahlen.html

German-Cancer-Aid. (2013b). *Information Booklet*. Available online at: http://www.krebshilfe.de/fileadmin/Inhalte/Downloads/PDFs/Blaue_Ratgeber/053_strahlen.pdf.

Glenny, A. M., Furness, S., Worthington, H. V., Conway, D. I., Oliver, R., Clarkson, J. E., et al. (2010). Interventions for the treatment of oral cavity and oropharyngeal cancer: radiotherapy. *Cochrane Database Syst. Rev.* CD006387. doi: 10.1002/14651858.CD006387.pub2

Gomez-Ospina, N., Tsuruta, F., Barreto-Chang, O., Hu, L., and Dolmetsch, R. (2006). The C terminus of the L-type voltage-gated calcium channel Ca(V)1.2 encodes a transcription factor. *Cell* 127, 591–606. doi: 10.1016/j.cell.2006.10.017

Gonidi, M., Athanassiadou, A. M., Patsouris, E., Tsipis, A., Dimopoulos, S., Kyriakidou, V., et al. (2011). Mitochondrial UCP4 and bcl-2 expression in imprints of breast carcinomas: relationship with DNA ploidy and classical prognostic factors.

Pathol. Res. Pract. 207, 377–382. doi: 10.1016/j.prp.2011.03.007

Grills, I. S., Hope, A. J., Guckenberger, M., Kestin, L. L., Werner-Wasik, M., Yan, D., et al. (2012). A collaborative analysis of stereotactic lung radiotherapy outcomes for early-stage non-small-cell lung cancer using daily online cone-beam computed tomography image-guided radiotherapy. *J. Thorac. Oncol.* 7, 1382–1393. doi: 10.1097/JTO.0b013e318260e00d

Gross, G. J., and Peart, J. N. (2003). KATP channels and myocardial preconditioning: an update. *Am. J. Physiol. Heart Circ. Physiol.* 285, H921–H930.

Grosso, J. F., and Jure-Kunkel, M. N. (2013). CTLA-4 blockade in tumor models: an overview of preclinical and translational research. *Cancer Immun.* 13, 5.

Haas, B. R., Cuddapah, V. A., Watkins, S., Rohn, K. J., Dy, T. E., and Sontheimer, H. (2011). With-No-Lysine Kinase 3 (WNK3) stimulates glioma invasion by regulating cell volume. *Am. J. Physiol. Cell Physiol.* 301, C1150–C1160. doi: 10.1152/ajpcell.00203.2011

Haas, B. R., and Sontheimer, H. (2010). Inhibition of the sodium-potassium-chloride cotransporter isoform-1 reduces glioma invasion. *Cancer Res.* 70, 5597–5606. doi: 10.1158/0008-5472.CAN-09-4666

Hanahan, D., and Weinberg, R. A. (2011). Hallmarks of cancer: the next generation. *Cell* 144, 646–674. doi: 10.1016/j.cell.2011.02.013

Harada, H. (2011). How can we overcome tumor hypoxia in radiation therapy. *J. Radiat. Res.* 52, 545–556.

Harper, M. E., Antoniou, A., Villalobos-Menuey, E., Russo, A., Trauger, R., Vendemelio, M., et al. (2002). Characterization of a novel metabolic strategy used by drug-resistant tumor cells. *FASEB J.* 16, 1550–1557. doi: 10.1096/fj.02-0541com

Hartung, F., Stuhmer, W., and Pardo, L. A. (2011). Tumor cell-selective apoptosis induction through targeting of K(V)10.1 via bifunctional TRAIL antibody. *Mol. Cancer* 10, 109.

Hatzikirou, H., Basanta, D., Simon, M., Schaller, K., and Deutsch, A. (2012). 'Go or Grow': the key to the emergence of invasion in tumour progression. *Math. Med. Biol.* 29, 49–65. doi: 10.1093/imammb/dqq011

Heise, N., Palme, D., Misovic, M., Koka, S., Rudner, J., Lang, F., et al. (2010). Non-selective cation channel-mediated Ca2+-entry and activation of Ca2+/calmodulin-dependent kinase II contribute to G2/M cell cycle arrest and survival of irradiated leukemia cells. *Cell Physiol. Biochem.* 26, 597–608. doi: 10.1159/000322327

Helmke, B. M., Reisser, C., Idzko, M., Dyckhoff, G., and Herold-Mende, C. (2004). Expression of SGLT-1 in preneoplastic and neoplastic lesions of the head and neck. *Oral Oncol.* 40, 28–35. doi: 10.1016/S1368-837500129-5

Hockaday, D. C., Shen, S., Fiveash, J., Raubitschek, A., Colcher, D., Liu, A., et al. (2005). Imaging glioma extent with 131I-TM-601. *J. Nucl. Med.* 46, 580–586.

Horimoto, M., Resnick, M. B., Konkin, T. A., Routhier, J., Wands, J. R., and Baffy, G. (2004). Expression of uncoupling protein-2 in human colon cancer. *Clin. Cancer Res.* 10, 6203–6207. doi: 10.1158/1078-0432.CCR-04-0419

Horiot, J. C., Le Fur, R., N'guyen, T., Chenal, C., Schraub, S., Alfonsi, S., et al. (1992). Hyperfractionation versus conventional fractionation in oropharyngeal carcinoma: final analysis of a randomized trial of the EORTC cooperative group of radiotherapy. *Radiother. Oncol.* 25, 231–241. doi: 10.1016/0167-814090242-M

Huber, S. M. (2013). Oncochannels. *Cell Calcium*. 53, 241–255. doi: 10.1016/j.ceca.2013.01.001

Huber, S. M., Misovic, M., Mayer, C., Rodemann, H. P., and Dittmann, K. (2012). EGFR-mediated stimulation of sodium/glucose cotransport promotes survival of irradiated human A549 lung adenocarcinoma cells. *Radiother. Oncol.* 103, 373–379. doi: 10.1016/j.radonc.2012.03.008

Ishikawa, N., Oguri, T., Isobe, T., Fujitaka, K., and Kohno, N. (2001). SGLT gene expression in primary lung cancers and their metastatic lesions. *Jpn. J. Cancer Res.* 92, 874–879. doi: 10.1111/j.1349-7006.2001.tb01175.x

Johnson, J., Nowicki, M. O., Lee, C. H., Chiocca, E. A., Viapiano, M. S., Lawler, S. E., et al. (2009). Quantitative analysis of complex glioma cell migration on electrospun polycaprolactone using time-lapse microscopy. *Tissue Eng. Part C Methods* 15, 531–540. doi: 10.1089/ten.tec.2008.0486

Jones, B., Dale, R. G., and Gaya, A. M. (2006). Linear quadratic modeling of increased late normal-tissue effects in special clinical situations. *Int. J. Radiat. Oncol. Biol. Phys.* 64, 948–953. doi: 10.1016/j.ijrobp.2005.10.016

Jung, J. W., Hwang, S. Y., Hwang, J. S., Oh, E. S., Park, S., and Han, I. O. (2007). Ionising radiation induces changes associated with epithelial-mesenchymal transdifferentiation and increased cell motility of A549 lung epithelial cells. *Eur. J. Cancer* 43, 1214–1224. doi: 10.1016/j.ejca.2007.01.034

Kadenbach, B. (2003). Intrinsic and extrinsic uncoupling of oxidative phosphorylation. *Biochim. Biophys. Acta* 1604, 77–94. doi: 10.1016/S0005-272800027-6

Kargiotis, O., Chetty, C., Gogineni, V., Gondi, C. S., Pulukuri, S. M., Kyritsis, A. P., et al. (2008). uPA/uPAR downregulation inhibits radiation-induced migration, invasion and angiogenesis in IOMM-Lee meningioma cells and decreases tumor growth *in vivo*. *Int. J. Oncol.* 33, 937–947.

Kil, W. J., Tofilon, P. J., and Camphausen, K. (2012). Post-radiation increase in VEGF enhances glioma cell motility *in vitro*. *Radiat. Oncol.* 7, 25. doi: 10.1186/1748-717X-7-25

Kim, J. S., Chang, J. W., Yun, H. S., Yang, K. M., Hong, E. H., Kim, D. H., et al. (2010). Chloride intracellular channel 1 identified using proteomic analysis plays an important role in the radiosensitivity of HEp-2 cells via reactive oxygen species production. *Proteomics* 10, 2589–2604. doi: 10.1002/pmic.200900523

Klotz, L., Venier, N., Colquhoun, A. J., Sasaki, H., Loblaw, D. A., Fleshner, N., et al. (2011). Capsaicin, a novel radiosensitizer, acts via a TRPV6 mediated phenomenon. *J. Clin. Oncol.* 29(Suppl. 7; Abstr. 23).

Koebel, C. M., Vermi, W., Swann, J. B., Zerafa, N., Rodig, S. J., Old, L. J., et al. (2007). Adaptive immunity maintains occult cancer in an equilibrium state. *Nature* 450, 903–907. doi: 10.1038/nature06309

Korshunov, S. S., Skulachev, V. P., and Starkov, A. A. (1997). High protonic potential actuates a mechanism of production of reactive oxygen species in mitochondria. *FEBS Lett.* 416, 15–18. doi: 10.1016/S0014-579301159-9

Kotecha, R., Yamada, Y., Pei, X., Kollmeier, M. A., Cox, B., Cohen, G. N., et al. (2013). Clinical outcomes of high-dose-rate brachytherapy and external beam radiotherapy in the management of clinically localized prostate cancer. *Brachytherapy* 12, 44–49. doi: 10.1016/j.brachy.2012.05.003

Kuai, X. Y., Ji, Z. Y., and Zhang, H. J. (2010). Mitochondrial uncoupling protein 2 expression in colon cancer and its clinical significance. *World J. Gastroenterol.* 16, 5773–5778. doi: 10.3748/wjg.v16.i45.5773

Kuo, S. S., Saad, A. H., Koong, A. C., Hahn, G. M., and Giaccia, A. J. (1993). Potassium-channel activation in response to low doses of gamma-irradiation involves reactive oxygen intermediates in nonexcitatory cells. *Proc. Natl. Acad. Sci. U.S.A.* 90, 908–912. doi: 10.1073/pnas.90.3.908

Langenbacher, M., Abdel-Jalil, R. J., Voelter, W., Weinmann, M., and Huber, S. M. (2013). *In vitro* hypoxic cytotoxicity and hypoxic radiosensitization. Efficacy of the novel 2-nitroimidazole N, N, N-tris[2-(2-nitro-1H-imidazol-1-yl)ethyl]amine. *Strahlenther. Onkol.* 189, 246–254. doi: 10.1007/s00066-012-0273-2

Le Pechoux, C., Laplanche, A., Faivre-Finn, C., Ciuleanu, T., Wanders, R., Lerouge, D., et al. (2011). Clinical neurological outcome and quality of life among patients with limited small-cell cancer treated with two different doses of prophylactic cranial irradiation in the intergroup phase III trial (PCI99-01, EORTC 22003-08004, RTOG (0212). and IFCT 99-01). *Ann. Oncol.* 22, 1154–1163. doi: 10.1093/annonc/mdq576

Leiprecht, N., Munoz, C., Alesutan, I., Siraskar, G., Sopjani, M., Foller, M., et al. (2011). Regulation of Na(+)-coupled glucose carrier SGLT1 by human papillomavirus 18 E6 protein. *Biochem. Biophys. Res. Commun.* 404, 695–700. doi: 10.1016/j.bbrc.2010.12.044

Li, C., and Jackson, R. M. (2002). Reactive species mechanisms of cellular hypoxia-reoxygenation injury. *Am. J. Physiol. Cell Physiol.* 282, C227–241. doi: 10.1152/ajpcell.00112.2001

Liu, X., Chang, Y., Reinhart, P. H., Sontheimer, H., and Chang, Y. (2002). Cloning and characterization of glioma BK, a novel BK channel isoform highly expressed in human glioma cells. *J. Neurosci.* 22, 1840–1849.

Lobikin, M., Chernet, B., Lobo, D., and Levin, M. (2012). Resting potential, oncogene-induced tumorigenesis, and metastasis: the bioelectric basis of cancer *in vivo*. *Phys. Biol.* 9, 065002. doi: 10.1088/1478-3975/9/6/065002

Lu, Z., and Sack, M. N. (2008). ATF-1 is a hypoxia-responsive transcriptional activator of skeletal muscle mitochondrial-uncoupling protein 3. *J. Biol. Chem.* 283, 23410–23418. doi: 10.1074/jbc.M801236200

Lui, V. C., Lung, S. S., Pu, J. K., Hung, K. N., and Leung, G. K. (2010). Invasion of human glioma cells is regulated by multiple chloride channels including ClC-3. *Anticancer Res.* 30, 4515–4524.

Lutz, S. (2007). Palliative whole-brain radiotherapy fractionation: convenience versus cognition. *Cancer* 110, 2363–2365.

Lyons, S. A., O'neal, J., and Sontheimer, H. (2002). Chlorotoxin, a scorpion-derived peptide, specifically binds to gliomas and tumors of neuroectodermal origin. *Glia* 39, 162–173. doi: 10.1002/glia.10083

Maftei, C. A., Bayer, C., Shi, K., Astner, S. T., and Vaupel, P. (2011). Changes in the fraction of total hypoxia and hypoxia subtypes in human squamous cell carcinomas upon fractionated irradiation: evaluation using pattern recognition in microcirculatory supply units. *Radiother. Oncol.* 101, 209–216. doi: 10.1016/j.radonc.2011.05.023

Mailloux, R. J., Adjeitey, C. N., and Harper, M. E. (2010). Genipin-induced inhibition of uncoupling protein-2 sensitizes drug-resistant cancer cells to cytotoxic agents. *PLoS ONE* 5:e13289. doi: 10.1371/journal.pone.0013289

Mamelak, A. N., and Jacoby, D. B. (2007). Targeted delivery of antitumoral therapy to glioma and other malignancies with synthetic chlorotoxin (TM-601). *Expert Opin. Drug Deliv.* 4, 175–186. doi: 10.1517/17425247.4.2.175

Marks, L. B., and Dewhirst, M. (1991). Accelerated repopulation: friend or foe. Exploiting changes in tumor growth characteristics to improve the "efficiency" of radiotherapy. *Int. J. Radiat. Oncol. Biol. Phys.* 21, 1377–1383. doi: 10.1016/0360-301690301-J

Masumoto, K., Tsukimoto, M., and Kojima, S. (2013). Role of TRPM2 and TRPV1 cation channels in cellular responses to radiation-induced DNA damage. *Biochim. Biophys. Acta* 1830, 3382–3390. doi: 10.1016/j.bbagen.2013.02.020

Mccoy, E. S., Haas, B. R., and Sontheimer, H. (2010). Water permeability through aquaporin-4 is regulated by protein kinase C and becomes rate-limiting for glioma invasion. *Neuroscience* 168, 971–981. doi: 10.1016/j.neuroscience.2009.09.020

Mccoy, E., and Sontheimer, H. (2007). Expression and function of water channels (aquaporins) in migrating malignant astrocytes. *Glia* 55, 1034–1043. doi: 10.1002/glia.20524

Mcferrin, M. B., and Sontheimer, H. (2006). A role for ion channels in glioma cell invasion. *Neuron Glia Biol.* 2, 39–49. doi: 10.1017/S1740925X06000044

Mcleod, C. J., Aziz, A., Hoyt, R. F. Jr., Mccoy, J. P. Jr., and Sack, M. N. (2005). Uncoupling proteins 2 and 3 function in concert to augment tolerance to cardiac ischemia. *J. Biol. Chem.* 280, 33470–33476. doi: 10.1074/jbc.M505258200

Montana, V., and Sontheimer, H. (2011). Bradykinin promotes the chemotactic invasion of primary brain tumors. *J. Neurosci.* 31, 4858–4867. doi: 10.1523/JNEUROSCI.3825-10.2011

Muller, A. C., Eckert, F., Heinrich, V., Bamberg, M., Brucker, S., and Hehr, T. (2011). Re-surgery and chest wall re-irradiation for recurrent breast cancer: a second curative approach. *BMC Cancer* 11:197. doi: 10.1186/1471-2407-11-197

Muller, A. C., Gani, C., Weinmann, M., Mayer, F., Sipos, B., Bamberg, M., et al. (2012). Limited disease of extra-pulmonary small cell carcinoma. Impact of local treatment and nodal status, role of cranial irradiation. *Strahlenther. Onkol.* 188, 269–273. doi: 10.1007/s00066-011-0045-4

Murata, M., Akao, M., O'rourke, B., and Marban, E. (2001). Mitochondrial ATP-sensitive potassium channels attenuate matrix Ca(2+) overload during simulated ischemia and reperfusion: possible mechanism of cardioprotection. *Circ. Res.* 89, 891–898. doi: 10.1161/hh2201.100205

Nalla, A. K., Asuthkar, S., Bhoopathi, P., Gujrati, M., Dinh, D. H., and Rao, J. S. (2010). Suppression of uPAR retards radiation-induced invasion and migration mediated by integrin beta1/FAK signaling in medulloblastoma. *PLoS ONE* 5:e13006. doi: 10.1371/journal.pone.0013006

Narita, T., Aoyama, H., Hirata, K., Onodera, S., Shiga, T., Kobayashi, H., et al. (2012). Reoxygenation of glioblastoma multiforme treated with fractionated radiotherapy concomitant with temozolomide: changes defined by 18F-fluoromisonidazole positron emission tomography: two case reports. *Jpn. J. Clin. Oncol.* 42, 120–123. doi: 10.1093/jjco/hyr181

Nelson, J. A., and Falk, R. E. (1993). The efficacy of phloridzin and phloretin on tumor cell growth. *Anticancer Res.* 13, 2287–2292.

Nguyen, L. N., and Ang, K. K. (2002). Radiotherapy for cancer of the head and neck: altered fractionation regimens. *Lancet Oncol.* 3, 693–701. doi: 10.1016/S1470-204500906-3

Niyazi, M., Siefert, A., Schwarz, S. B., Ganswindt, U., Kreth, F. W., Tonn, J. C., et al. (2011). Therapeutic options for recurrent malignant glioma. *Radiother. Oncol.* 98, 1–14. doi: 10.1016/j.radonc.2010.11.006

Ohshima, Y., Tsukimoto, M., Harada, H., and Kojima, S. (2012). Involvement of connexin43 hemichannel in ATP release after gamma-irradiation. *J. Radiat. Res.* 53, 551–557. doi: 10.1093/jrr/rrs014

Oleinika, K., Nibbs, R. J., Graham, G. J., and Fraser, A. R. (2013). Suppression, subversion and escape: the role of regulatory T cells in cancer progression. *Clin. Exp. Immunol.* 171, 36–45. doi: 10.1111/j.1365-2249.2012.04657.x

Olsen, M. L., Schade, S., Lyons, S. A., Amaral, M. D., and Sontheimer, H. (2003). Expression of voltage-gated chloride channels in human glioma cells. *J. Neurosci.* 23, 5572–5582.

Ozcan, C., Palmeri, M., Horvath, T. L., Russell, K. S., and Russell, R. R. (2013). Role of uncoupling protein 3 in ischemia-reperfusion injury, arrhythmias and preconditioning. *Am. J. Physiol. Heart Circ. Physiol.* 304, H1192–H1200. doi: 10.1152/ajpheart.00592.2012

Pajonk, F., Vlashi, E., and Mcbride, W. H. (2010). Radiation resistance of cancer stem cells: the 4 R's of radiobiology revisited. *Stem Cells* 28, 639–648. doi: 10.1002/stem.318

Palme, D., Misovic, M., Schmid, E., Klumpp, D., Salih, H. R., Rudner, J., et al. (2013). Kv3.4 potassium channel-mediated electrosignaling controls cell cycle and survival of irradiated leukemia cells. *Pflugers Archiv* 465, 1209–1221. doi 10.1007/s00424-013-1249-5

Pawlik, T. M., and Keyomarsi, K. (2004). Role of cell cycle in mediating sensitivity to radiotherapy. *Int. J. Radiat. Oncol. Biol. Phys.* 59, 928–942. doi: 10.1016/j.ijrobp.2004.03.005

Pfefferle, A., Mailloux, R. J., Adjeitey, C. N., and Harper, M. E. (2012). Glutathionylation of UCP2 sensitizes drug resistant leukemia cells to chemotherapeutics. *Biochim. Biophys. Acta* 1833, 80–89. doi: 10.1016/j.bbamcr.2012.10.006

Pickhard, A. C., Margraf, J., Knopf, A., Stark, T., Piontek, G., Beck, C., et al. (2011). Inhibition of radiation induced migration of human head and neck squamous cell carcinoma cells by blocking of EGF receptor pathways. *BMC Cancer* 11:388. doi: 10.1186/1471-2407-11-388

Pizzo, P., Drago, I., Filadi, R., and Pozzan, T. (2012). Mitochondrial Ca(2)(+) homeostasis: mechanism, role, and tissue specificities. *Pflugers Arch.* 464, 3–17. doi: 10.1007/s00424-012-1122-y

Pons, D. G., Sastre-Serra, J., Nadal-Serrano, M., Oliver, A., Garcia-Bonafe, M., Bover, I., et al. (2012). Initial activation status of the antioxidant response determines sensitivity to carboplatin/paclitaxel treatment of ovarian cancer. *Anticancer Res.* 32, 4723–4728.

Prasad, A., Stone, G. W., Holmes, D. R., and Gersh, B. (2009). Reperfusion injury, microvascular dysfunction, and cardioprotection: the "dark side" of reperfusion. *Circulation* 120, 2105–2112. doi: 10.1161/CIRCULATIONAHA.108.814640

Rades, D., Kieckebusch, S., Lohynska, R., Veninga, T., Stalpers, L. J., Dunst, J., et al. (2007a). Reduction of overall treatment time in patients irradiated for more than three brain metastases. *Int. J. Radiat. Oncol. Biol. Phys.* 69, 1509–1513.

Rades, D., Lohynska, R., Veninga, T., Stalpers, L. J., and Schild, S. E. (2007b). Evaluation of 2 whole-brain radiotherapy schedules and prognostic factors for brain metastases in breast cancer patients. *Cancer* 110, 2587–2592.

Ransom, C. B., Liu, X., and Sontheimer, H. (2002). BK channels in human glioma cells have enhanced calcium sensitivity. *Glia* 38, 281–291. doi: 10.1002/glia.10064

Ransom, C. B., and Sontheimer, H. (2001). BK channels in human glioma cells. *J. Neurophysiol.* 85, 790–803.

Rasola, A., and Bernardi, P. (2011). Mitochondrial permeability transition in Ca(2+)-dependent apoptosis and necrosis. *Cell Calcium* 50, 222–233. doi: 10.1016/j.ceca.2011.04.007

Rieken, S., Habermehl, D., Mohr, A., Wuerth, L., Lindel, K., Weber, K., et al. (2011). Targeting alphanubeta3 and alphanubeta5 inhibits photon-induced hypermigration of malignant glioma cells. *Radiat. Oncol.* 6, 132. doi: 10.1186/1748-717X-6-132

Robbins, D., and Zhao, Y. (2011). New aspects of mitochondrial uncoupling proteins (UCPs) and their roles in tumorigenesis. *Int. J. Mol. Sci.* 12, 5285–5293. doi: 10.3390/ijms12085285

Rodrigues, G., Zindler, J., Warner, A., and Lagerwaard, F. (2013). Recursive partitioning analysis for the prediction of stereotactic radiosurgery brain metastases lesion

control. *Oncologist* 18, 330–335. doi: 10.1634/theoncologist.2012-0316

Ruggieri, P., Mangino, G., Fioretti, B., Catacuzzeno, L., Puca, R., Ponti, D., et al. (2012). The inhibition of KCa3.1 channels activity reduces cell motility in glioblastoma derived cancer stem cells. *PLoS ONE* 7:e47825. doi: 10.1371/journal.pone.0047825

Sack, M. N. (2006). Mitochondrial depolarization and the role of uncoupling proteins in ischemia tolerance. *Cardiovasc. Res.* 72, 210–219. doi: 10.1016/j.cardiores.2006.07.010

Samudio, I., Fiegl, M., Mcqueen, T., Clise-Dwyer, K., and Andreeff, M. (2008). The warburg effect in leukemia-stroma cocultures is mediated by mitochondrial uncoupling associated with uncoupling protein 2 activation. *Cancer Res.* 68, 5198–5205. doi: 10.1158/0008-5472.CAN-08-0555

Santandreu, F. M., Valle, A., Fernandez De Mattos, S., Roca, P., and Oliver, J. (2009). Hydrogen peroxide regulates the mitochondrial content of uncoupling protein 5 in colon cancer cells. *Cell Physiol. Biochem.* 24, 379–390. doi: 10.1159/000257430

Sastre-Serra, J., Nadal-Serrano, M., Pons, D. G., Valle, A., Garau, I., Garcia-Bonafe, M., et al. (2013). The oxidative stress in breast tumors of postmenopausal women is ERalpha/ERbeta ratio dependent. *Free Radic. Biol. Med.* 61C, 11–17. doi: 10.1016/j.freeradbiomed.2013.03.005

Sauer, R., Liersch, T., Merkel, S., Fietkau, R., Hohenberger, W., Hess, C., et al. (2012). Preoperative versus postoperative chemoradiotherapy for locally advanced rectal cancer: results of the German CAO/ARO/AIO-94 randomized phase III trial after a median follow-up of 11 years. *J. Clin. Oncol.* 30, 1926–1933. doi: 10.1200/JCO.2011.40.1836

Schwab, A., Fabian, A., Hanley, P. J., and Stock, C. (2012). Role of ion channels and transporters in cell migration. *Physiol. Rev.* 92, 1865–1913. doi: 10.1152/physrev.00018.2011.

Schwab, A., Nechyporuk-Zloy, V., Fabian, A., and Stock, C. (2007). Cells move when ions and water flow. *Pflugers Arch.* 453, 421–432. doi: 10.1007/s00424-006-0138-6

Sciaccaluga, M., Fioretti, B., Catacuzzeno, L., Pagani, F., Bertollini, C., Rosito, M., et al. (2010). CXCL12-induced glioblastoma cell migration requires intermediate conductance Ca2+-activated K+ channel activity. *Am. J. Physiol. Cell Physiol.* 299, C175–C184. doi: 10.1152/ajpcell.00344.2009

Shields, J. D., Kourtis, I. C., Tomei, A. A., Roberts, J. M., and Swartz, M. A. (2010). Induction of lymphoidlike stroma and immune escape by tumors that express the chemokine CCL21. *Science* 328, 749–752. doi: 10.1126/science.1185837

Singh, H., Stefani, E., and Toro, L. (2012). Intracellular BK(Ca) (iBK(Ca)) channels. *J. Physiol.* 590, 5937–5947. doi: 10.1113/jphysiol.2011.215533

Skulachev, V. P. (1998). Uncoupling: new approaches to an old problem of bioenergetics. *Biochim. Biophys. Acta* 1363, 100–124. doi: 10.1016/S0005-272800091-1

Sofia Vala, I., Martins, L. R., Imaizumi, N., Nunes, R. J., Rino, J., Kuonen, F., et al. (2010). Low doses of ionizing radiation promote tumor growth and metastasis by enhancing angiogenesis. *PLoS ONE* 5:e11222. doi: 10.1371/journal.pone.0011222

Sontheimer, H. (2008). An unexpected role for ion channels in brain tumor metastasis. *Exp. Biol. Med. (Maywood)* 233, 779–791. doi: 10.3181/0711-MR-308

Sreekumar, A., Nyati, M. K., Varambally, S., Barrette, T. R., Ghosh, D., Lawrence, T. S., et al. (2001). Profiling of cancer cells using protein microarrays: discovery of novel radiation-regulated proteins. *Cancer Res.* 61, 7585–7593.

Steinle, M., Palme, D., Misovic, M., Rudner, J., Dittmann, K., Lukowski, R., et al. (2011). Ionizing radiation induces migration of glioblastoma cells by activating BK K(+) channels. *Radiother. Oncol.* 101, 122–126. doi: 10.1016/j.radonc.2011.05.069

Stock, C., and Schwab, A. (2009). Protons make tumor cells move like clockwork. *Pflugers Arch.* 458, 981–992. doi: 10.1007/s00424-009-0677-8

Stupp, R., Van Den Bent, M. J., and Hegi, M. E. (2005). Optimal role of temozolomide in the treatment of malignant gliomas. *Curr. Neurol. Neurosci. Rep.* 5, 198–206. doi: 10.1007/s11910-005-0047-7

Su, W. P., Lo, Y. C., Yan, J. J., Liao, I. C., Tsai, P. J., Wang, H. C., et al. (2012). Mitochondrial uncoupling protein 2 regulates the effects of paclitaxel on Stat3 activation and cellular survival in lung cancer cells. *Carcinogenesis* 33, 2065–2075. doi: 10.1093/carcin/bgs253

Szabo, I., Leanza, L., Gulbins, E., and Zoratti, M. (2012). Physiology of potassium channels in the inner membrane of mitochondria. *Pflugers Arch.* 463, 231–246. doi: 10.1007/s00424-011-1058-7

Talbot, D. A., and Brand, M. D. (2005). Uncoupling protein 3 protects aconitase against inactivation in isolated skeletal muscle mitochondria. *Biochim. Biophys. Acta* 1709, 150–156.

Tanchot, C., Terme, M., Pere, H., Tran, T., Benhamouda, N., Strioga, M., et al. (2013). Tumor-infiltrating regulatory T cells: phenotype, role, mechanism of expansion in situ and clinical significance. *Cancer Microenviron.* 6, 147–157. doi: 10.1007/s12307-012-0122-y

Teng, M. W., Swann, J. B., Koebel, C. M., Schreiber, R. D., and Smyth, M. J. (2008). Immune-mediated dormancy: an equilibrium with cancer. *J. Leukoc. Biol.* 84, 988–993. doi: 10.1189/jlb.1107774

Tolon, R. M., Sanchez-Franco, F., Lopez Fernandez, J., Lorenzo, M. J., Vazquez, G. F., and Cacicedo, L. (1996). Regulation of somatostatin gene expression by veratridine-induced depolarization in cultured fetal cerebrocortical cells. *Brain Res. Mol. Brain Res.* 35, 103–110. doi: 10.1016/0169-328X(95)00188-X

Vanan, I., Dong, Z., Tosti, E., Warshaw, G., Symons, M., and Ruggieri, R. (2012). Role of a DNA damage checkpoint pathway in ionizing radiation-induced glioblastoma cell migration and invasion. *Cell Mol. Neurobiol.* doi: 10.1007/s10571–012-9846-y

Veiseh, M., Gabikian, P., Bahrami, S. B., Veiseh, O., Zhang, M., Hackman, R. C., et al. (2007). Tumor paint: a chlorotoxin:Cy5.5 bioconjugate for intraoperative visualization of cancer foci. *Cancer Res.* 67, 6882–6888. doi: 10.1158/0008-5472.CAN-06-3948

Verheij, M. (2008). Clinical biomarkers and imaging for radiotherapy-induced cell death. *Cancer Metastasis Rev.* 27, 471–480. doi: 10.1007/s10555-008-9131-1

Vianello, F., Papeta, N., Chen, T., Kraft, P., White, N., Hart, W. K., et al. (2006). Murine B16 melanomas expressing high levels of the chemokine stromal-derived factor-1/CXCL12 induce tumor-specific T cell chemorepulsion and escape from immune control. *J. Immunol.* 176, 2902–2914.

Vidal-Puig, A. J., Grujic, D., Zhang, C. Y., Hagen, T., Boss, O., Ido, Y., et al. (2000). Energy metabolism in uncoupling protein 3 gene knockout mice. *J. Biol. Chem.* 275, 16258–16266. doi: 10.1074/jbc.M910179199

Voehringer, D. W., Hirschberg, D. L., Xiao, J., Lu, Q., Roederer, M., Lock, C. B., et al. (2000). Gene microarray identification of redox and mitochondrial elements that control resistance or sensitivity to apoptosis. *Proc. Natl. Acad. Sci. U.S.A.* 97, 2680–2685. doi: 10.1073/pnas.97.6.2680

Watanabe, H., Bohensky, J., Freeman, T., Srinivas, V., and Shapiro, I. M. (2008). Hypoxic induction of UCP3 in the growth plate: UCP3 suppresses chondrocyte autophagy. *J. Cell Physiol.* 216, 419–425. doi: 10.1002/jcp.21408

Watkins, S., and Sontheimer, H. (2011). Hydrodynamic cellular volume changes enable glioma cell invasion. *J. Neurosci.* 31, 17250–17259. doi: 10.1523/JNEUROSCI.3938-11.2011

Weaver, A. K., Bomben, V. C., and Sontheimer, H. (2006). Expression and function of calcium-activated potassium channels in human glioma cells. *Glia* 54, 223–233. doi: 10.1002/glia.20364

Weber, D. C., Casanova, N., Zilli, T., Buchegger, F., Rouzaud, M., Nouet, P., et al. (2009). Recurrence pattern after [(18)F]fluoroethyltyrosine-positron emission tomography-guided radiotherapy for high-grade glioma: a prospective study. *Radiother. Oncol.* 93, 586–592. doi: 10.1016/j.radonc.2009.08.043

Weihua, Z., Tsan, R., Huang, W. C., Wu, Q., Chiu, C. H., Fidler, I. J., et al. (2008). Survival of cancer cells is maintained by EGFR independent of its kinase activity. *Cancer Cell* 13, 385–393. doi: 10.1016/j.ccr.2008.03.015

Wick, W., Wick, A., Schulz, J. B., Dichgans, J., Rodemann, H. P., and Weller, M. (2002). Prevention of irradiation-induced glioma cell invasion by temozolomide involves caspase 3 activity and cleavage of focal adhesion kinase. *Cancer Res.* 62, 1915–1919.

Wild-Bode, C., Weller, M., Rimner, A., Dichgans, J., and Wick, W. (2001). Sublethal irradiation promotes migration and invasiveness of glioma cells: implications for radiotherapy of human glioblastoma. *Cancer Res.* 61, 2744–2750.

Withers, H. R. (Ed). (1975). "The four R's of radiotherapy," in *Advances in Radiation Biology,* Vol. 5, ed J. T. A. H. Lett (New York, NY: Academic Press).

Wright, E. M., Loo, D. D., and Hirayama, B. A. (2011). Biology of human sodium glucose transporters. *Physiol. Rev.* 91, 733–794. doi: 10.1152/physrev.00055.2009

Wulff, H., and Castle, N. A. (2010). Therapeutic potential of KCa3.1 blockers: recent advances and promising trends. *Expert Rev. Clin. Pharmacol.* 3, 385–396. doi: 10.1586/ecp.10.11

Yellon, D. M., and Hausenloy, D. J. (2007). Myocardial reperfusion injury. *N. Engl. J. Med.* 357, 1121–1135. doi: 10.1056/NEJMra071667

Yu, L. C., Huang, C. Y., Kuo, W. T., Sayer, H., Turner, J. R., and Buret, A. G. (2008). SGLT-1-mediated glucose uptake protects human intestinal epithelial cells against Giardia duodenalis-induced apoptosis. *Int. J. Parasitol.* 38, 923–934. doi: 10.1016/j.ijpara.2007.12.004

Zhao, J., Du, C. Z., Sun, Y. S., and Gu, J. (2012). Patterns and prognosis of locally recurrent rectal cancer following multidisciplinary treatment. *World J. Gastroenterol.* 18, 7015–7020. doi: 10.3748/wjg.v18.i47.7015

Zhau, H. E., He, H., Wang, C. Y., Zayzafoon, M., Morrissey, C., Vessella, R. L., et al. (2011). Human prostate cancer harbors the stem cell properties of bone marrow mesenchymal stem cells. *Clin. Cancer Res.* 17, 2159–2169. doi: 10.1158/1078-0432.CCR-10-2523

Zhou, Y. C., Liu, J. Y., Li, J., Zhang, J., Xu, Y. Q., Zhang, H. W., et al. (2011). Ionizing radiation promotes migration and invasion of cancer cells through transforming growth factor-beta-mediated epithelial-mesenchymal transition. *Int. J. Radiat. Oncol. Biol. Phys.* 81, 1530–1537. doi: 10.1016/j.ijrobp.2011.06.1956

Conflict of Interest Statement: The authors declare that the research was conducted in the absence of any commercial or financial relationships that could be construed as a potential conflict of interest.

Received: 30 April 2013; paper pending published: 28 May 2013; accepted: 24 July 2013; published online: 14 August 2013.

*Citation: Huber SM, Butz L, Stegen B, Klumpp D, Braun N, Ruth P and Eckert F (2013) Ionizing radiation, ion transports, and radioresistance of cancer cells. Front. Physiol. **4**:212. doi: 10.3389/fphys.2013.00212*

This article was submitted to Frontiers in Membrane Physiology and Membrane Biophysics, a specialty of Frontiers in Physiology.

Biochimica et Biophysica Acta xxx (2014) xxx–xxx

Contents lists available at ScienceDirect

Biochimica et Biophysica Acta

journal homepage: www.elsevier.com/locate/bbamem

Review

Role of ion channels in ionizing radiation-induced cell death☆

Stephan M. Huber [a,*], Lena Butz [a,b], Benjamin Stegen [a], Lukas Klumpp [a], Dominik Klumpp [a], Franziska Eckert [a]

[a] Department of Radiation Oncology, University of Tübingen, Germany
[b] Department of Pharmacology, Toxicology and Clinical Pharmacy, Institute of Pharmacy, University of Tübingen, Germany

ARTICLE INFO

Article history:
Received 31 July 2014
Received in revised form 30 October 2014
Accepted 5 November 2014
Available online xxxx

Keywords:
Ion transport
Radiation
Cancer
Cell death
Therapy resistance
Ca^{2+}-activated K^+ channels

ABSTRACT

Neoadjuvant, adjuvant or definitive fractionated radiation therapy are implemented in first line anti-cancer treatment regimens of many tumor entities. Ionizing radiation kills the tumor cells mainly by causing double strand breaks of their DNA through formation of intermediate radicals. Survival of the tumor cells depends on both, their capacity of oxidative defense and their efficacy of DNA repair. By damaging the targeted cells, ionizing radiation triggers a plethora of stress responses. Among those is the modulation of ion channels such as Ca^{2+}-activated K^+ channels or Ca^{2+}-permeable nonselective cation channels belonging to the super-family of transient receptor potential channels. Radiogenic activation of these channels may contribute to radiogenic cell death as well as to DNA repair, glucose fueling, radiogenic hypermigration or lowering of the oxidative stress burden. The present review article introduces these channels and summarizes our current knowledge on the mechanisms underlying radiogenic ion channel modulation. This article is part of a Special Issue entitled: Membrane channels and transporters in cancers.

Contents

1. Introduction

Ionizing radiation kills or inactivates cells mostly by damaging the nuclear DNA and cell survival critically depends on successful repair of the DNA damage [1]. Ionizing radiation may lead to necrotic as well as apoptotic cell death depending on cell type, dose and fractionation protocols [2]. The major death pathway in this scenario in normal tissue cells is apoptosis. However, cancer cells which often have developed strategies to evade apoptosis [3] may either undergo (regulated) necrosis or reenter the cell cycle with accumulated DNA damages. During the subsequent cell divisions those cells will not be able to segregate the chromosomes and end up as multinucleated giant cells in mitotic catastrophe. Mitotic catastrophe again leads either to apoptotic or necrotic cell death. Another possible mechanism of radiation-induced death in cells with disturbed apoptosis machinery is excess autophagy. While autophagy is a survival strategy [4] excess autophagy overdigests the cytoplasm and cell organelles forcing the cell into apoptosis or necrosis [5].

Meanwhile, the evidence is overwhelming that ion channels fulfill pivotal functions in cell death mechanisms such as apoptosis (for review see the article by Annarosa Arcangeli in this special issue on "Membrane channels and transporters in cancers") as well as in stress response and survival strategies. Notably, tumor cells have been demonstrated to express a set of ion channels which is different to that of the parental normal cells. These channels may fulfill specific oncogenic functions in neoplastic transformation, malignant progression or tissue

☆ This article is part of a Special Issue entitled: Membrane channels and transporters in cancers.

* Corresponding author at: Department of Radiation Oncology, University of Tübingen, Hoppe-Seyler-Str. 3, 72076 Tübingen, Germany. Tel.: +49 7071 29 82183.
E-mail address: stephan.huber@uni-tuebingen.de (S.M. Huber).

http://dx.doi.org/10.1016/j.bbamem.2014.11.004
0005-2736/

invasion and metastasis (for review see [1]). In addition, they may contribute to the cellular stress response for instance during fractionated radiation therapy and may confer radioresistance.

The present review intends to sum up data on ion channel function in the stress response to ionizing radiation. In particular, ion channels that may induce cell death in tumor cells and facilitate radiogenic cell killing are introduced. In addition, data on ion channels which, in contrast to the before mentioned, confer radioresistance are reviewed. Finally, ion channels of tumor cells that might contribute to acquired radioresistance, e.g. by promoting radiogenic hypermigration or transition into relatively radioresistant ***c***ancer ***s***tem (cell)-like ***c***ells (CSCs) are described. Prior to that, a brief introduction into radiotherapy and its radiobiological principles is given in the next paragraphs.

2. Radiotherapy

Radiation therapy together with surgery and systemic chemotherapy is the main pillar of anti-cancer treatment. About half of all cancer patients receive radiation therapy, half of all cures from cancer include radiotherapy [6]. Despite modern radiation techniques and advanced multimodal treatments, local failures and distant metastases often limit the prognosis of the patients, especially due to limited salvage treatments [7].

Ionizing radiation impairs the clonogenic survival of tumor cells mainly by causing double strand breaks in the DNA backbone. The number of double strand breaks increases linearly with the absorbed radiation dose. The intrinsic capacity to detoxify radicals formed during transfer of radiation energy to cellular molecules such as H_2O (giving rise to hydroxyl radicals, $^{\bullet}OH$) and the ability to efficiently repair DNA double strand breaks by non-homologous end joining or homologous recombination determines the radiosensitivity of a given tumor cell. Irradiated tumor cells which leave residual DNA double strand breaks un-repaired lose their clonogenicity meaning that these cells can not restore tumor mass (for review see [8]).

In addition to these intrinsic resistance factors, the microenvironment may lower the radiosensitivity of tumor cells. Hypoxic areas are frequent in solid tumors reaching a certain mass. Tumor hypoxia, however, decreases the efficacy of radiation therapy [9]. Ionizing radiation directly or indirectly generates radicals in the deoxyribose moiety of the DNA backbone. In a hypoxic atmosphere, cellular thiols can react with those DNA radicals resulting in chemical DNA repair. At higher oxygen partial pressure, in sharp contrast, radicals of the deoxyribose moiety are chemically transformed to strand break precursors [10]. By this mechanism, hypoxia increases radioresistance by a factor of two to three (oxygen enhancement ratio) [11].

Fractionated treatment regimens which improve recovery of the normal tissue after irradiation but not of the tumor have been established in radiotherapy [12]. In addition to limit normal tissue toxicity, killing of tumor mass by initial radiation fractions has been demonstrated to reoxygenate and thereby radiosensitize solid tumors during further fractionated radiotherapy. Beyond that, fractionated radiation regimens aim to redistribute tumor cells in a more vulnerable phase of the cell cycle in the time intervals between two fractions [13]. Accelerated repopulation of the tumor after irradiation is a frequently reported phenomenon. Possible mechanisms of accelerated repopulation include induction of CSCs: It has been proposed that radiation therapy induces CSCs to switch from an asymmetrical into a symmetrical mode of cell division; i.e., a CSC which is thought to normally divide into a daughter CSC and a lineage-committed progenitor cells is induced by the radiotherapy to divide symmetrically into two proliferative CSC daughter cells. This is thought to accelerate repopulation of the tumor after end of radiotherapy. Importantly, CSCs are thought be relatively radioresistant possibly due to i) high oxidative defense and, therefore, low radiation-induced insults, ii) activated DNA checkpoints resulting in fast DNA repair, and iii) an attenuated radiation-induced cell cycle redistribution [14].

Finally, fractionated radiation therapy, which applies fractions of sublethal radiation doses (usually 2 Gy per fraction), has been demonstrated in a variety of tumor entities *in vitro* and in animal models to stimulate hypermigration and hypermetastasis of tumor cells as well as infiltration of the tumor by CD11b-positive myeloid cells and subsequent vasculogenesis. It is tempting to speculate that radiogenic hypermigration boosts cellular interaction of tumor cells with non-tumor cells, e.g. endothelial cells. It has been proposed that CSCs lodge within perivascular niches where a complex regulatory network supports CSC survival [15]. As a matter of fact, CSCs but not non-CSCs gain radioresistance when transplanted orthotopically in mice [16] supporting the idea of a tumor microenvironment-dependent acquired radioresistance. Ion channels contribute to both, intrinsic and acquired radioresistance of tumor cells as discussed in the next paragraphs

3. Radiosensitizing ion channels

Member 2 of the melastatin family of transient receptor potential channel (TRPM2) is a Ca^{2+}-permeable nonselective cation channel. Heterologous expression of TRPM2 in human embryonic kidney cells [17] or A172 human glioblastoma cells [18] facilitates oxidative stress-induced cell death. Reactive oxygen species (ROS) have been demonstrated to trigger TRPM2 activation [19,20]. The principal activator, however, of TRPM2 is ADP-ribose (ADPR) that binds to a special domain located at the C-terminus of the channel [21,22]. Sources of ADPR are the mitochondria [23] or ADPR polymers. The latter are formed, e.g., during DNA repair by poly (ADP-ribose) polymerases (PARPs). ADPR is released from the ADPR polymers by glycohydrolases [21,24].

Expression of TRPM2 has been demonstrated in several tumor entities such as insulinoma [25], hepatocellular carcinoma [25], prostate cancer [26], lymphoma [27], leukemia [28] and lung cancer cell lines [29]. TRPM2 activity increases the susceptibility to cell death [30] probably by overloading cells with Ca^{2+} (Fig. 1A).

Remarkably, cancer cells may evade TRPM2-mediated cell death. In lung cancer cells, de-methylation of a GpC island within the TRPM2 gene gives rise to new promoters that regulate transcription of a non-functional truncated TRPM2 channel [29] and to a TRPM2 specific antisense RNA. This antisense RNA inhibits TRPM2 translation. Moreover, the truncated channel is non-functional and acts dominant negative, thus switching off the tumor-suppressing function of the full-length TRPM2 protein [29] (Fig. 1B).

The initially described member of the vanilloid family of TRP channels, the nociceptive and heat receptor TRPV1, is reportedly expressed in several tumor entities such as uveal melanoma [31], pancreatic [32] and prostatic neuroendocrine tumors [33], glioblastoma [34] and urothelial cancer of human bladder [35]. At least in the latter two tumor entities, TRPV1 exerts anti-oncogenic effects [35,36]. TRPV1 expression inversely correlates with glioma grading [34]. Remarkably, neural precursor cells have been demonstrated to induce ER stress-mediated cell death of glioblastoma cells by activating glioblastoma TRPV1 channels through secretion of endogenous vanilloids [37]. Along those lines is the observation that a TRPV1 antagonist promotes tumorigenesis in mouse skin [38].

Notably, targeting of TRPM2 and TRPV1 by RNA interference has been demonstrated to decrease gamma irradiation-induced formation of nuclear γH2AX foci and further DNA damage response in A549 lung adenocarcinoma cells [39]. Since γH2AX foci are used as a surrogate for DNA double strand breaks, one might speculate that TRPM2 or TRPV1 may amplify ionizing radiation-induced insults (Fig. 1). Another interpretation which has been favored by the author of the study [39] would be that activity of TRPM2 and TRPV1 is required for the formation of DNA repair complexes. In combination, the data hint to the possibility of radiosensitizing cancer cells by pharmacologically activating TRPM2 or TRPV1 channels. Whether this might become a promising new strategy of tumor radiosensitization has to await animal studies.

Please cite this article as: S.M. Huber, et al., Role of ion channels in ionizing radiation-induced cell death, Biochim. Biophys. Acta (2014), http://dx.doi.org/10.1016/j.bbamem.2014.11.004

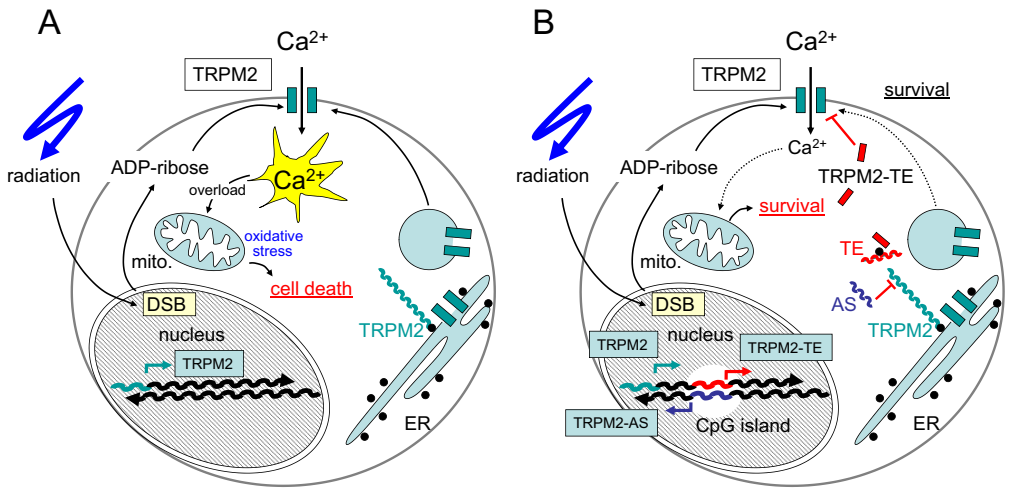

Fig. 1. Speculative mechanism of a putative TRPM2-mediated radiosensitization (A) and reported strategy [29] of lung cancer cells to avoid TRPM2-mediated susceptibility to cell death (B), for details see text. TRPM2-TE (TE): truncated TRPM2, TRPM2-AS (AS): TRPM2 antisense RNA, mito.: mitochondrion).

4. Ion channels conferring intrinsic radioresistance

DNA repair involves cell cycle arrest, chromatin relaxation and formation of repair complexes at the site of DNA damage. Moreover, radiation-induced formation of radicals requires activated radical detoxification pathways and increased oxidative defense to constrain the radiation-induced insults. All these processes of stress response lead to elevated ATP consumption which requires intensified energy supply. Recent *in vitro* observations suggest that these processes depend at least partially on radiation-induced ion channel activation.

Studies of our laboratory indicate that survival of irradiated human leukemia cells critically depends on Ca^{2+} signaling involving radiogenic activation of TRPV5/6-like nonselective cation and $K_v3.4$ voltage-gated K^+ channels [40,41]. The nonselective cation channels in concert with $K_v3.4$ generate radiogenic Ca^{2+} signals that contribute to G_2/M cell cycle arrest by CaMKII-mediated inhibition of the phosphatase cdc25B. Activity of the latter is required in these cells for release from radiation-induced G_2/M arrest via dephosphorylation and thereby activation of cdc2, a component of the mitosis promoting factor. Experimental interference with the radiogenic Ca^{2+} signals, e.g. by pharmacological inhibition or knock-down of $K_v3.4$ overrides cell cycle arrest resulting in increased apoptosis and decreased clonogenic survival of irradiated leukemia cells [40,41]. This radiosensitization by $K_v3.4$ targeting demonstrates the pivotal role of radiogenic $K_v3.4$ channel activation for cell cycle arrest and DNA repair.

Similar to leukemia cells, A549 lung adenocarcinoma cells reportedly respond to ionizing radiation with activation of K_v K^+ channels [42] and transient hyperpolarization of the plasma membrane. Later on, the membrane potential of the irradiated A549 cells strongly depolarizes. This depolarization is dependent on external glucose and inhibited by phlorizin, a sodium glucose cotransporter (SGLT) blocker. In parallel, irradiation induces phlorizin-sensitive ^{3}H-glucose uptake within few minutes after irradiation [43]. Combined, these data suggest that radiogenic activation of SGLT transporters and K_v K^+ channels cooperate in glucose fuelling of the irradiated A549 cells, the former by generating the glucose entry routes, the latter by increasing and maintaining the driving force for Na^+-coupled glucose entry. Glucose uptake by SGLTs is mainly driven by the inwardly directed electrochemical driving force for Na^+ which in turn is highly dependent on the K^+ channel-regulated membrane potential. SGLTs allow efficient glucose uptake even from a glucose-depleted microenvironment which is typical for malperfused solid tumors [44]. It is therefore not surprising that several tumor entities such as colorectal, pancreatic, lung, head and neck, prostate, kidney, cervical, breast, bladder and prostate cancer as well as chondrosarcomas and leukemia upregulate SGLTs [45–53].

SGLT has been shown to be in complex with the EGFR [50,53] and radiogenic SGLT activation depends on EGFR tyrosine kinase activity [43]. Importantly, radiogenic increase in glucose fuelling seems to be required for cell survival since the SGLT inhibitor phlorizin radiosensitizes A549 lung adenocarcinoma and FaDu head and neck squamous carcinoma cells [43].

Intracellular ATP concentration has been reported to drop in irradiated A549 cells indicative of an irradiation-caused energy crisis. Notably, recovery from radiation-induced ATP decline is EGFR/SGLT-dependent and associated with improved DNA-repair leading to increased clonogenic cell survival. This is evident from the fact that EGFR or SGLT blockade delays recovery of intracellular ATP concentration and histone modifications necessary for chromatin remodeling during DNA repair. *Vice versa*, inhibition of the histone H3 modification prevents chromatin remodeling as well as energy crisis [8]. Together, these data suggest that irradiation-associated interactions between SGLT1 and EGFR result in increased glucose uptake, which counteracts the energy crisis in tumor cells caused by chromatin remodeling required for DNA repair (Fig. 2) [8,43].

Besides plasma membrane ion channels, mitochondrial transport pathways have been shown to contribute to cellular stress response. Stress-induced upregulation of uncoupling proteins (UCPs) conveys hyperpolarization of the membrane potential across the inner mitochondrial membrane ($\Delta\Psi_m$,) and thereby formation of reactive oxygen species [54]. UCPs are reportedly upregulated in a number of aggressive human tumors (leukemia, breast, colorectal, ovarian, bladder, esophagus, testicular, kidney, pancreatic, lung, and prostate cancer) in which they are proposed to contribute to malignant progression (for review see [54]).

In addition to malignant progression, UCPs may alter the therapy sensitivity of tumor cells. UCP-2 expression has been associated with paclitaxel resistance of p53 wildtype lung cancer, CPT-11 resistance of colon cancer and gemcitabine resistance of pancreatic adenocarcinoma, lung adenocarcinoma, or bladder carcinoma. Accordingly, experimental targeting of UCPs has been demonstrated to sensitize tumor cells to chemotherapy *in vitro* (for review see [54]).

Notably, ionizing radiation induces up-regulation of UCP-2 expression in colon carcinoma cells [55] and in a radiosensitive subclone of B cell lymphoma [56], as well as UCP-3 expression in rat retina [57]. Radioprotection might result from lowering the radiation-induced burden of reactive oxygen species. As a matter of fact, multi-resistant subclones of leukemia cells reportedly show higher UCP-2 protein expression, lower $\Delta\Psi_m$, lower radiation induced formation of reactive oxygen species, and decreased DNA damage as compared to their parental sensitive cells [58].

Please cite this article as: S.M. Huber, et al., Role of ion channels in ionizing radiation-induced cell death, Biochim. Biophys. Acta (2014), http://dx.doi.org/10.1016/j.bbamem.2014.11.004

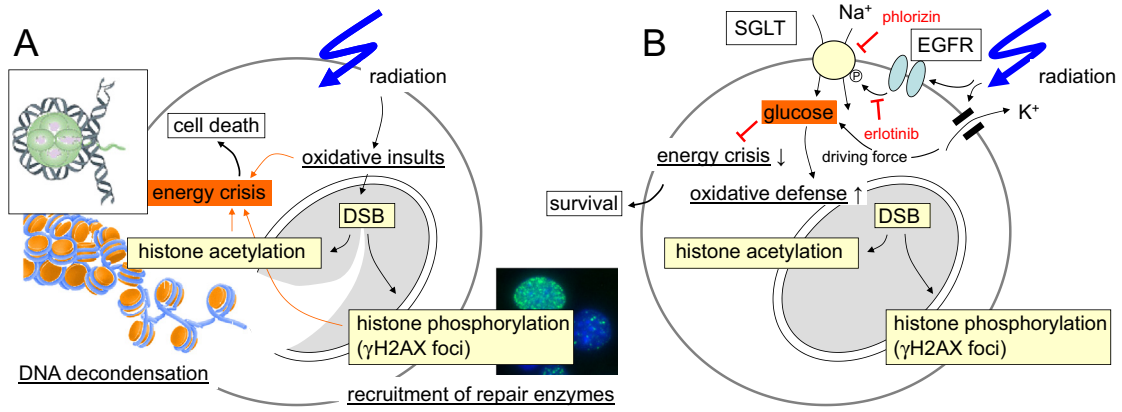

Fig. 2. Radiation-caused energy crisis (A) and functional significance of SGLT1-mediated glucose fueling for DNA repair and cell survival (B) of irradiated A549 lung adenocarcinoma cells (DSB: double strand breaks).

In summary, these data indicate that ion transports through channels may regulate processes that mediate intrinsic radioresistance. Only few laboratories worldwide including ours are working on the radiophysiology of tumor cells. The investigation of ion transports in irradiated cells therefore is at its very beginning and the few data available are mostly phenomenological in nature. The molecular mechanisms that underlie e.g. radiogenic channel activation are still ill-defined. Nevertheless, the data prove functional significance of ion transports and electrosignaling for the survival of irradiated tumor cells and might have translational implications for radiotherapy in the future.

5. Ion channels in acquired radioresistance

Microenvironmental stress such as hypoxia, interstitial nutrient depletion or low pH has been proposed to switch tumor cells from a "Grow" into a "Go" phenotype. By migration and tissue invasion "Go" tumor cells may evade the locally confined stress burden and resettle in distant and less hostile regions. Once resettled, tumor cells may readapt the "Grow" phenotype by reentering cell cycling and may establish tumor satellites in more or less close vicinity of the primary focus (for review see [54]).

In accordance with this hypothesis, sublethal ionizing irradiation as applied in single fractions of fractionated radiotherapy has been demonstrated *in vitro* and/or in rodent tumor models to induce migration, invasion and metastasis or spreading of cervix carcinoma [59], head and neck squamous cell carcinoma [60], lung adenocarinoma [61,62], colorectal carcinoma [62], breast cancer [62–64], meningioma [65], medulloblastoma [66] and glioblastoma. In particular, in glioblastoma the experimental evidence for such radiogenic hypermigration is meanwhile overwhelming [67–80]. Glioblastoma cells show a highly migrative phenotype that may "travel" large distances through the brain [81]. At least in theory, radiogenic hypermigration might, therefore, contribute to locoregional treatment failure by promoting emigration of tumor cells from the target volume during fractionated radiation therapy.

Migration and radiogenic hypermigration are well documented in glioma cells. They invade the surrounding brain parenchyma primarily by moving along axon bundles and the vasculature. During brain invasion along those tracks cells have to squeeze between very narrow interstitial spaces which requires effective local cell volume decrease and reincrease. Glioblastoma cells are capable of losing all unbound cell water [82]. The electrochemical driving force for this tremendous cell volume decrease is provided by an unusually high cytosolic Cl^- concentration (100 mM) [83,84] which is utilized as an osmolyte. During local regulatory volume decrease, extrusion of Cl^- and K^+ along their electrochemical gradients involves ClC-3 Cl^-- channels [85,86], Ca^{2+}-activated high conductance BK- [74,87,88] and intermediate

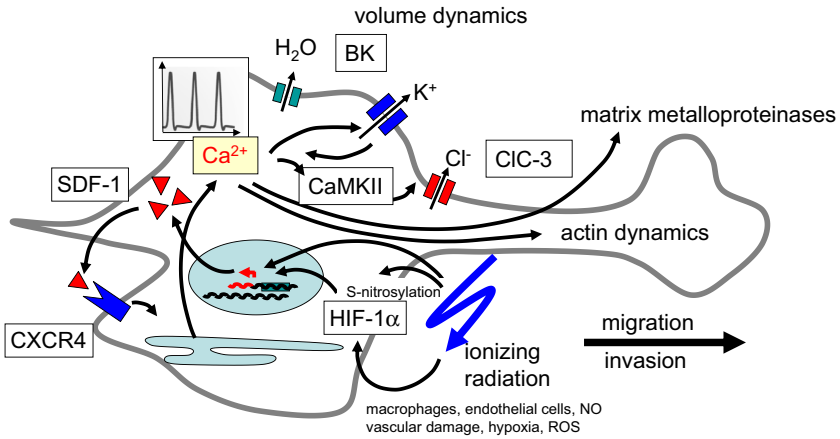

Fig. 3. Hypothetical signaling underlying radiogenic hypermigration of glioblastoma cells. SDF-1 is a HIF-1α target gene and hypoxia is a strong inductor of SDF-1 expression. IR-caused damage of the tumor vasculature and resultant tumor hypoxia has been proposed to induce SDF-1 expression [111]. Beyond that, ionizing radiation reportedly stimulates the generation of NO in tumor-associated macrophages leading to HIF-1α stabilization by S-nitrosylation [100]. Finally, radiation may directly stabilize HIF-1α as deduced from *in vitro* experiments (own unpublished results). SDF-1 induces Ca^{2+} signals through CXCR4 chemokine receptor that in turn contribute to the programming and mechanics of migration (for details see text) and possibly invasion, e.g., via calpain-dependent [112] activation of matrix metalloproteinases [113,114].

Please cite this article as: S.M. Huber, et al., Role of ion channels in ionizing radiation-induced cell death, Biochim. Biophys. Acta (2014), http://dx.doi.org/10.1016/j.bbamem.2014.11.004

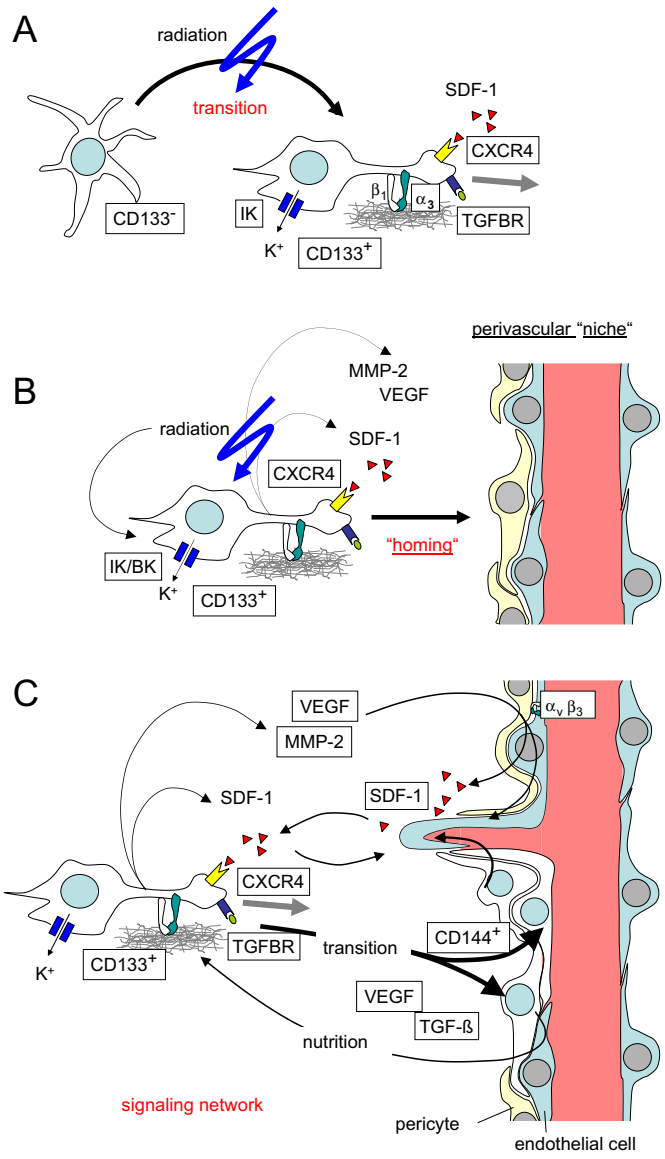

Fig. 4. Synopsis of the signaling network in glioblastoma conferring radioresistance and speculative role of ionizing radiation herein. A. Irradiation induces secretion of SDF-1 [80,95–97] and transition of $CD133^-$ "differentiated" glioblastoma cells to $CD133^+$ GSCs with up-regulated CXCR4 [106], β1/α3 integrins [108], TGFB2 receptor [115], TGF-β responsiveness [115], and IK Ca^{2+}-activated K^+ channel-dependent highly migratory and invasive phenotype [109] B. Irradiation promotes "homing" of GSCs to perivascular niches by stimulating cell migration. C. The reciprocal interaction between glioblastoma and endothelial cells strongly depends on matrix metalloproteinase-2 (MMP-2) expression by glioblastoma [114] and SDF-1 signaling of endothelial cells [110]. Importantly, irradiation induces upregulation of MMP-2 in glioblastoma cells (B) which is required for tissue invasion [67,71,72,79,114] and VEGF secretion (B) [71,75] which reportedly may promote angiogenesis [116]. In addition, transition of glioblastoma cells into endothelial cells [117] and pericytes [15] reconstruct the glioblastoma vasculature which supports both, vessel function and tumor growth.

conductance IK K^+ channels [86,89]. Inhibition of either of these channels attenuates glioblastoma cell migration or invasion [83,90–94] confirming their pivotal function in these processes.

Ionizing radiation has been demonstrated in our laboratory to activate BK K^+ channels in glioblastoma cells *in vitro* [74]. Radiogenic BK channel activity, in turn, is required for Ca^{2+}/calmodulin kinase II (CaMKII)- [74] and consecutive CaMKII-dependent ClC-3 channel activation (own unpublished observation and [85]). Inhibition of BK or CaMKII abolishes radiogenic hypermigration [74] indicating BK channel activation as key event of radiogenic hypermigration of glioblastoma cells. Radiogenic hypermigration is paralleled by radiogenic expression of the chemokine SDF-1 (stromal cell-derived factor-1, CXCL12) in different tumor entities including glioblastoma [80,95–97]. Glioblastoma cells reportedly express CXCR4 chemokine receptors and SDF-1 stimulates glioblastoma cell migration via CXCR4-mediated Ca^{2+} signaling [93]. CXCR4 receptors reportedly signal through phospholipase C and BK channels have been shown to be functionally coupled with IP_3 receptors in the ER [98] suggesting (and confirmed by own unpublished observations) that radiogenic SDF1/CXCR4 signaling is upstream of BK channel activation. SDF-1, in turn, is a target gene of the transcription factor HIF-1α which reportedly becomes stabilized, e.g. by S-nitrosylation, upon irradiation [95,99–101] (Fig. 3). Together, this gives a good example of radiogenic signaling which integrates biochemical signaling, electrosignaling (i.e., BK-dependent regulation of membrane potential) and Ca^{2+} signaling modules (more details are given in the legend to Fig. 3).

Ionizing radiation has been demonstrated to select stem (cell)-like glioblastoma cells (GSCs) or even induce transition of "differentiated" cancer cells to GSCs/CSCs in glioblastoma [102–104] and other tumor entities [14]. Notably, "stemness" is associated with SDF-1 secretion [105] and markedly increased CXCR4 chemokine expression [106]. Importantly, CXCR4 upregulation is required to maintain "stemness" of non-small cell lung cancer [107] and glioblastoma cells [105]. In accordance to CXCR4 upregulation, GSCs show a highly migratory/invasive phenotype [108,109]. Most importantly, this phenotype is highly dependent on the Ca^{2+}-activated IK K^+ channel [89,109]. Furthermore, IK channels have been demonstrated to be overexpressed in about one third of the glioma patients with IK protein expression correlating with poor patient survival [89].

Unexpectedly, a previous report demonstrated that *xeno*grafted $CD133^+$ stem-like subpopulations of glioblastoma exhibit a higher radioresistance than *xeno*grafted $CD133^-$ cells while radiosensitivity of both subpopulations does not differ *in vitro* [16]. This clearly indicates a function of the brain microenvironment for radioresistance. In particular, endothelial cells have been postulated to promote glioblastoma therapy resistance [110]. Part of the reported reciprocal interaction between glioblastoma cells and endothelial cells as well as of the complex signaling network in perivascular "niches" is schematically summarized in Fig. 4.

Albeit merely speculative, the idea that radiogenic hypermigration might promote "homing" of (CXCR4-highly-expressing stem-like) glioblastoma cells to perivascular niches is highly attractive. The subsequent reciprocal modifications of glioblastoma and endothelial cells might eventually induce radioresistance of glioblastoma cells. Together, these data suggest that radiogenic hypermigration might contribute to the apparently high radioresistance of glioblastoma cells either by promoting evasion from the radiation target volume or by stimulating the chemotaxis of glioblastoma cells to "radioprotective" perivascular niches.

6. Concluding remarks

The radiation physiology of cancer cells is yet a neglected research field. While the number of reports on ion channel function in neoplastic transformation, malignant progression or metastasis of cancer cells increases constantly only little is known about the role of ion channels in radiotherapy. The few data available strongly suggest that ionizing radiation-induced ion channel modifications are a common phenomenon. Importantly, these modifications impact on the stress response and survival of irradiated tumor cells. By modulating intracellular Ca^{2+} signals radiosensitive ion channels may directly crosstalk with the biochemical signaling of the DNA damage response. By driving local cell volume changes radiogenic ion channel modifications may promote cell migration and stress evasion of irradiated tumor cells. By stabilizing the membrane potential ionizing radiation-induced K^+ channel activity might facilitate Na^+-coupled glucose uptake providing the energy for DNA-repair. Finally, mitochondrial channels upregulated

Please cite this article as: S.M. Huber, et al., Role of ion channels in ionizing radiation-induced cell death, Biochim. Biophys. Acta (2014), http://dx.doi.org/10.1016/j.bbamem.2014.11.004

by ionizing radiation might lower the oxidative insults associated with ionizing radiation. Given the aberrant and partly specific ion channel expression of tumor cells, a more profound understanding of the mechanisms underlying radiogenic ion channel modifications might be harnessed in the future to develop new strategies for the radiosensitization of tumors.

Acknowledgment

This work was supported by a grant from the Wilhelm-Sander-Stiftung awarded to SH (2011.083.1). BS and DK were supported by the DFG International Graduate School 1302 (TP T9 SH).

References

[1] S.M. Huber, Oncochannels, Cell Calcium 53 (2013) 241–255.
[2] M. Verheij, Clinical biomarkers and imaging for radiotherapy-induced cell death, Cancer Metastasis Rev. 27 (2008) 471–480.
[3] D. Hanahan, R.A. Weinberg, The hallmarks of cancer, Cell 100 (2000) 57–70.
[4] A. Apel, I. Herr, H. Schwarz, H.P. Rodemann, A. Mayer, Blocked autophagy sensitizes resistant carcinoma cells to radiation therapy, Cancer Res. 68 (2008) 1485–1494.
[5] S. Palumbo, S. Comincini, Autophagy and ionizing radiation in tumors: the "survive or not survive" dilemma, J. Cell. Physiol. 228 (2013) 1–8.
[6] German-Cancer-Aid, Information Booklet, http://www.krebshilfe.de/fileadmin/Inhalte/Downloads/PDFs/Blaue_Ratgeber/053_strahlen.pdf 2013.
[7] A.C. Muller, F. Eckert, V. Heinrich, M. Bamberg, S. Brucker, T. Hehr, Re-surgery and chest wall re-irradiation for recurrent breast cancer: a second curative approach, BMC Cancer 11 (2011) 197.
[8] K. Dittmann, C. Mayer, H.P. Rodemann, S.M. Huber, EGFR cooperates with glucose transporter SGLT1 to enable chromatin remodeling in response to ionizing radiation, Radiother. Oncol. (2013), http://dx.doi.org/10.1016/j.radonc.2013.03.016 (pii: S0167-8140(13)00145-X).
[9] H. Harada, How can we overcome tumor hypoxia in radiation therapy? J. Radiat. Res. 52 (2011) 545–556.
[10] P.M. Cullis, G.D.D. Jones, J. Lea, M.C.R. Symons, M. Sweeney, The effects of ionizing radiation on deoxyribonucleic acid. Part 5. The role of thiols in chemical repair, J. Chem. Soc. Perkin Trans. 2 (1987) 1907–1914.
[11] M. Langenbacher, R.J. Abdel-Jalil, W. Voelter, M. Weinmann, S.M. Huber, *In vitro* hypoxic cytotoxicity and hypoxic radiosensitization. Efficacy of the novel 2-nitroimidazole N, N, N-tris[2-(2-nitro-1H-imidazol-1-yl)ethyl]amine, Strahlenther. Onkol. 189 (2013) 246–254.
[12] B. Jones, R.G. Dale, A.M. Gaya, Linear quadratic modeling of increased late normal-tissue effects in special clinical situations, Int. J. Radiat. Oncol. Biol. Phys. 64 (2006) 948–953.
[13] T.M. Pawlik, K. Keyomarsi, Role of cell cycle in mediating sensitivity to radiotherapy, Int. J. Radiat. Oncol. Biol. Phys. 59 (2004) 928–942.
[14] F. Pajonk, E. Vlashi, W.H. McBride, Radiation resistance of cancer stem cells: the 4 R's of radiobiology revisited, Stem Cells 28 (2010) 639–648.
[15] L. Cheng, Z. Huang, W. Zhou, Q. Wu, S. Donnola, J.K. Liu, X. Fang, A.E. Sloan, Y. Mao, J.D. Lathia, W. Min, R.E. McLendon, J.N. Rich, S. Bao, Glioblastoma stem cells generate vascular pericytes to support vessel function and tumor growth, Cell 153 (2013) 139–152.
[16] M. Jamal, B.H. Rath, P.S. Tsang, K. Camphausen, P.J. Tofilon, The brain microenvironment preferentially enhances the radioresistance of $CD133^{+}$ glioblastoma stem-like cells, Neoplasia 14 (2012) 150–158.
[17] Y. Hara, M. Wakamori, M. Ishii, E. Maeno, M. Nishida, T. Yoshida, H. Yamada, S. Shimizu, E. Mori, J. Kudoh, N. Shimizu, H. Kurose, Y. Okada, K. Imoto, Y. Mori, LTRPC2 Ca^{2+}-permeable channel activated by changes in redox status confers susceptibility to cell death, Mol. Cell 9 (2002) 163–173.
[18] M. Ishii, A. Oyama, T. Hagiwara, A. Miyazaki, Y. Mori, Y. Kiuchi, S. Shimizu, Facilitation of H2O2-induced A172 human glioblastoma cell death by insertion of oxidative stress-sensitive TRPM2 channels, Anticancer Res. 27 (2007) 3987–3992.
[19] M. Naziroglu, A. Luckhoff, A calcium influx pathway regulated separately by oxidative stress and ADP-Ribose in TRPM2 channels: single channel events, Neurochem. Res. 33 (2008) 1256–1262.
[20] M. Naziroglu, A. Luckhoff, Effects of antioxidants on calcium influx through TRPM2 channels in transfected cells activated by hydrogen peroxide, J. Neurol. Sci. 270 (2008) 152–158.
[21] E. Fonfria, I.C. Marshall, C.D. Benham, I. Boyfield, J.D. Brown, K. Hill, J.P. Hughes, S.D. Skaper, S. McNulty, TRPM2 channel opening in response to oxidative stress is dependent on activation of poly(ADP-ribose) polymerase, Br. J. Pharmacol. 143 (2004) 186–192.
[22] F.J. Kuhn, I. Heiner, A. Luckhoff, TRPM2: a calcium influx pathway regulated by oxidative stress and the novel second messenger ADP-ribose, Pflugers Arch. 451 (2005) 212–219.
[23] A.L. Perraud, C.L. Takanishi, B. Shen, S. Kang, M.K. Smith, C. Schmitz, H.M. Knowles, D. Ferraris, W. Li, J. Zhang, B.L. Stoddard, A.M. Scharenberg, Accumulation of free ADP-ribose from mitochondria mediates oxidative stress-induced gating of TRPM2 cation channels, J. Biol. Chem. 280 (2005) 6138–6148.
[24] J. Eisfeld, A. Luckhoff, Trpm2, Handb. Exp. Pharmacol. (2007) 237–252.
[25] K. Inamura, Y. Sano, S. Mochizuki, H. Yokoi, A. Miyake, K. Nozawa, C. Kitada, H. Matsushime, K. Furuichi, Response to ADP-ribose by activation of TRPM2 in the CRI-G1 insulinoma cell line, J. Membr. Biol. 191 (2003) 201–207.
[26] X. Zeng, S.C. Sikka, L. Huang, C. Sun, C. Xu, D. Jia, A.B. Abdel-Mageed, J.E. Pottle, J.T. Taylor, M. Li, Novel role for the transient receptor potential channel TRPM2 in prostate cancer cell proliferation, Prostate Cancer Prostatic Dis. 13 (2010) 195–201.
[27] W. Zhang, I. Hirschler-Laszkiewicz, Q. Tong, K. Conrad, S.C. Sun, L. Penn, D.L. Barber, R. Stahl, D.J. Carey, J.Y. Cheung, B.A. Miller, TRPM2 is an ion channel that modulates hematopoietic cell death through activation of caspases and PARP cleavage, Am. J. Physiol. Cell Physiol. 290 (2006) C1146–C1159.
[28] W. Zhang, X. Chu, Q. Tong, J.Y. Cheung, K. Conrad, K. Masker, B.A. Miller, A novel TRPM2 isoform inhibits calcium influx and susceptibility to cell death, J. Biol. Chem. 278 (2003) 16222–16229.
[29] U. Orfanelli, A.K. Wenke, C. Doglioni, V. Russo, A.K. Bosserhoff, G. Lavorgna, Identification of novel sense and antisense transcription at the TRPM2 locus in cancer, Cell Res. 18 (2008) 1128–1140.
[30] S. McNulty, E. Fonfria, The role of TRPM channels in cell death, Pflugers Arch. 451 (2005) 235–242.
[31] S. Mergler, R. Derckx, P.S. Reinach, F. Garreis, A. Bohm, L. Schmelzer, S. Skosyrski, N. Ramesh, S. Abdelmessih, O.K. Polat, N. Khajavi, A.I. Riechardt, Calcium regulation by temperature-sensitive transient receptor potential channels in human uveal melanoma cells, Cell. Signal. 26 (2014) 56–69.
[32] S. Mergler, M. Skrzypski, M. Sassek, P. Pietrzak, C. Pucci, B. Wiedenmann, M.Z. Strowski, Thermo-sensitive transient receptor potential vanilloid channel-1 regulates intracellular calcium and triggers chromogranin A secretion in pancreatic neuroendocrine BON-1 tumor cells, Cell. Signal. 24 (2012) 233–246.
[33] S. Malagarie-Cazenave, N. Olea-Herrero, D. Vara, C. Morell, I. Diaz-Laviada, The vanilloid capsaicin induces IL-6 secretion in prostate PC-3 cancer cells, Cytokine 54 (2011) 330–337.
[34] C. Amantini, M. Mosca, M. Nabissi, R. Lucciarini, S. Caprodossi, A. Arcella, F. Giangaspero, G. Santoni, Capsaicin-induced apoptosis of glioma cells is mediated by TRPV1 vanilloid receptor and requires p38 MAPK activation, J. Neurochem. 102 (2007) 977–990.
[35] G. Santoni, S. Caprodossi, V. Farfariello, S. Liberati, A. Gismondi, C. Amantini, Antioncogenic effects of transient receptor potential vanilloid 1 in the progression of transitional urothelial cancer of human bladder, ISRN Urol. 2012 (2012) 458238.
[36] C. Amantini, P. Ballarini, S. Caprodossi, M. Nabissi, M.B. Morelli, R. Lucciarini, M.A. Cardarelli, G. Mammana, G. Santoni, Triggering of transient receptor potential vanilloid type 1 (TRPV1) by capsaicin induces Fas/CD95-mediated apoptosis of urothelial cancer cells in an ATM-dependent manner, Carcinogenesis 30 (2009) 1320–1329.
[37] K. Stock, J. Kumar, M. Synowitz, S. Petrosino, R. Imperatore, E.S. Smith, P. Wend, B. Purfurst, U.A. Nuber, U. Gurok, V. Matyash, J.H. Walzlein, S.R. Chirasani, G. Dittmar, B.F. Cravatt, S. Momma, G.R. Lewin, A. Ligresti, L. De Petrocellis, L. Cristino, V. Di Marzo, H. Kettenmann, R. Glass, Neural precursor cells induce cell death of high-grade astrocytomas through stimulation of TRPV1, Nat. Med. 18 (2012) 1232–1238.
[38] S. Li, A.M. Bode, F. Zhu, K. Liu, J. Zhang, M.O. Kim, K. Reddy, T. Zykova, W.Y. Ma, A.L. Carper, A.K. Langfald, Z. Dong, TRPV1-antagonist AMG9810 promotes mouse skin tumorigenesis through EGFR/Akt signaling, Carcinogenesis 32 (2011) 779–785.
[39] K. Masumoto, M. Tsukimoto, S. Kojima, Role of TRPM2 and TRPV1 cation channels in cellular responses to radiation-induced DNA damage, Biochim. Biophys. Acta 1830 (2013) 3382–3390.
[40] N. Heise, D. Palme, M. Misovic, S. Koka, J. Rudner, F. Lang, H.R. Salih, S.M. Huber, G. Henke, Non-selective cation channel-mediated Ca^{2+}-entry and activation of Ca^{2+}/calmodulin-dependent kinase II contribute to G2/M cell cycle arrest and survival of irradiated leukemia cells, Cell. Physiol. Biochem. 26 (2010) 597–608.
[41] D. Palme, M. Misovic, E. Schmid, D. Klumpp, H.R. Salih, J. Rudner, S. Huber, Kv3.4 potassium channel-mediated electrosignaling controls cell cycle and survival of irradiated leukemia cells, Pflugers Arch. (2013), http://dx.doi.org/10.1007/s00424-013-1249-5.
[42] S.S. Kuo, A.H. Saad, A.C. Koong, G.M. Hahn, A.J. Giaccia, Potassium-channel activation in response to low doses of gamma-irradiation involves reactive oxygen intermediates in nonexcitatory cells, Proc. Natl. Acad. Sci. U. S. A. 90 (1993) 908–912.
[43] S.M. Huber, M. Misovic, C. Mayer, H.P. Rodemann, K. Dittmann, EGFR-mediated stimulation of sodium/glucose cotransport promotes survival of irradiated human A549 lung adenocarcinoma cells, Radiother. Oncol. 103 (2012) 373–379.
[44] V. Ganapathy, M. Thangaraju, P.D. Prasad, Nutrient transporters in cancer: relevance to Warburg hypothesis and beyond, Pharmacol. Ther. 121 (2009) 29–40.
[45] J.A. Nelson, R.E. Falk, The efficacy of phloridzin and phloretin on tumor cell growth, Anticancer Res. 13 (1993) 2287–2292.
[46] N. Ishikawa, T. Oguri, T. Isobe, K. Fujitaka, N. Kohno, SGLT gene expression in primary lung cancers and their metastatic lesions, Jpn. J. Cancer Res. 92 (2001) 874–879.
[47] B.M. Helmke, C. Reisser, M. Idzko, G. Dyckhoff, C. Herold-Mende, Expression of SGLT-1 in preneoplastic and neoplastic lesions of the head and neck, Oral Oncol. 40 (2004) 28–35.
[48] L.C. Yu, C.Y. Huang, W.T. Kuo, H. Sayer, J.R. Turner, A.G. Buret, SGLT-1-mediated glucose uptake protects human intestinal epithelial cells against Giardia duodenalis-induced apoptosis, Int. J. Parasitol. 38 (2008) 923–934.
[49] V.F. Casneuf, P. Fonteyne, N. Van Damme, P. Demetter, P. Pauwels, B. de Hemptinne, M. De Vos, C. Van de Wiele, M. Peeters, Expression of SGLT1, Bcl-2 and p53 in primary pancreatic cancer related to survival, Cancer Invest. 26 (2008) 852–859.

Please cite this article as: S.M. Huber, et al., Role of ion channels in ionizing radiation-induced cell death, Biochim. Biophys. Acta (2014), http://dx.doi.org/10.1016/j.bbamem.2014.11.004

[50] Z. Weihua, R. Tsan, W.C. Huang, Q. Wu, C.H. Chiu, I.J. Fidler, M.C. Hung, Survival of cancer cells is maintained by EGFR independent of its kinase activity, Cancer Cell 13 (2008) 385–393.
[51] N. Leiprecht, C. Munoz, I. Alesutan, G. Siraskar, M. Sopjani, M. Foller, F. Stubenrauch, T. Iftner, F. Lang, Regulation of Na^+-coupled glucose carrier SGLT1 by human papillomavirus 18 E6 protein, Biochem. Biophys. Res. Commun. 404 (2011) 695–700.
[52] E.M. Wright, D.D. Loo, B.A. Hirayama, Biology of human sodium glucose transporters, Physiol. Rev. 91 (2011) 733–794.
[53] J. Ren, L.R. Bollu, F. Su, G. Gao, L. Xu, W.C. Huang, M.C. Hung, Z. Weihua, EGFR-SGLT1 interaction does not respond to EGFR modulators, but inhibition of SGLT1 sensitizes prostate cancer cells to EGFR tyrosine kinase inhibitors, Prostate 73 (2013) 1453–1461.
[54] S.M. Huber, L. Butz, B. Stegen, D. Klumpp, N. Braun, P. Ruth, F. Eckert, Ionizing radiation, ion transports, and radioresistance of cancer cells, Frontiers in Physiology | Membrane Physiology and Membrane Biophysics 4 (2013) 212.
[55] A. Sreekumar, M.K. Nyati, S. Varambally, T.R. Barrette, D. Ghosh, T.S. Lawrence, A.M. Chinnaiyan, Profiling of cancer cells using protein microarrays: discovery of novel radiation-regulated proteins, Cancer Res. 61 (2001) 7585–7593.
[56] D.W. Voehringer, D.L. Hirschberg, J. Xiao, Q. Lu, M. Roederer, C.B. Lock, L.A. Herzenberg, L. Steinman, L.A. Herzenberg, Gene microarray identification of redox and mitochondrial elements that control resistance or sensitivity to apoptosis, Proc. Natl. Acad. Sci. U. S. A. 97 (2000) 2680–2685.
[57] X.W. Mao, J.D. Crapo, D.S. Gridley, Mitochondrial oxidative stress-induced apoptosis and radioprotection in proton-irradiated rat retina, Radiat. Res. 178 (2012) 118–125.
[58] M.E. Harper, A. Antoniou, E. Villalobos-Menuey, A. Russo, R. Trauger, M. Vendemelio, A. George, R. Bartholomew, D. Carlo, A. Shaikh, J. Kupperman, E.W. Newell, I.A. Bespalov, S.S. Wallace, Y. Liu, J.R. Rogers, G.L. Gibbs, J.L. Leahy, R.E. Camley, R. Melamede, M.K. Newell, Characterization of a novel metabolic strategy used by drug-resistant tumor cells, FASEB J. 16 (2002) 1550–1557.
[59] W.H. Su, P.C. Chuang, E.Y. Huang, K.D. Yang, Radiation-induced increase in cell migration and metastatic potential of cervical cancer cells operates via the K-Ras pathway, Am. J. Pathol. 180 (2012) 862–871.
[60] A.C. Pickhard, J. Margraf, A. Knopf, T. Stark, G. Piontek, C. Beck, A.L. Boulesteix, E.Q. Scherer, S. Pigorsch, J. Schlegel, W. Arnold, R. Reiter, Inhibition of radiation induced migration of human head and neck squamous cell carcinoma cells by blocking of EGF receptor pathways, BMC Cancer 11 (2011) 388.
[61] J.W. Jung, S.Y. Hwang, J.S. Hwang, E.S. Oh, S. Park, I.O. Han, Ionising radiation induces changes associated with epithelial–mesenchymal transdifferentiation and increased cell motility of A549 lung epithelial cells, Eur. J. Cancer 43 (2007) 1214–1224.
[62] Y.C. Zhou, J.Y. Liu, J. Li, J. Zhang, Y.Q. Xu, H.W. Zhang, L.B. Qiu, G.R. Ding, X.M. Su, S. Mei, G.Z. Guo, Ionizing radiation promotes migration and invasion of cancer cells through transforming growth factor-beta-mediated epithelial–mesenchymal transition, Int. J. Radiat. Oncol. Biol. Phys. 81 (2011) 1530–1537.
[63] S. Biswas, M. Guix, C. Rinehart, T.C. Dugger, A. Chytil, H.L. Moses, M.L. Freeman, C.L. Arteaga, Inhibition of TGF-beta with neutralizing antibodies prevents radiation-induced acceleration of metastatic cancer progression, J. Clin. Invest. 117 (2007) 1305–1313.
[64] D.M. Kambach, V.L. Sodi, P.I. Lelkes, J. Azizkhan-Clifford, M.J. Reginato, ErbB2, FoxM1 and 14-3-3zeta prime breast cancer cells for invasion in response to ionizing radiation, Oncogene 33 (2014) 589–598.
[65] O. Kargiotis, C. Chetty, V. Gogineni, C.S. Gondi, S.M. Pulukuri, A.P. Kyritsis, M. Gujrati, J.D. Klopfenstein, D.H. Dinh, J.S. Rao, uPA/uPAR downregulation inhibits radiation-induced migration, invasion and angiogenesis in IOMM-Lee meningioma cells and decreases tumor growth *in vivo*, Int. J. Oncol. 33 (2008) 937–947.
[66] S. Asuthkar, A.K. Nalla, C.S. Gondi, D.H. Dinh, M. Gujrati, S. Mohanam, J.S. Rao, Gadd45a sensitizes medulloblastoma cells to irradiation and suppresses MMP-9-mediated EMT, Neuro Oncol. 13 (2011) 1059–1073.
[67] C. Wild-Bode, M. Weller, A. Rimner, J. Dichgans, W. Wick, Sublethal irradiation promotes migration and invasiveness of glioma cells: implications for radiotherapy of human glioblastoma, Cancer Res. 61 (2001) 2744–2750.
[68] W. Wick, A. Wick, J.B. Schulz, J. Dichgans, H.P. Rodemann, M. Weller, Prevention of irradiation-induced glioma cell invasion by temozolomide involves caspase 3 activity and cleavage of focal adhesion kinase, Cancer Res. 62 (2002) 1915–1919.
[69] B. Hegedus, J. Zach, A. Czirok, J. Lovey, T. Vicsek, Irradiation and Taxol treatment result in non-monotonous, dose-dependent changes in the motility of glioblastoma cells, J. Neuro Oncol. 67 (2004) 147–157.
[70] S. Rieken, D. Habermehl, A. Mohr, L. Wuerth, K. Lindel, K. Weber, J. Debus, S.E. Combs, Targeting alphanubeta3 and alphanubeta5 inhibits photon-induced hypermigration of malignant glioma cells, Radiat. Oncol. 6 (2011) 132.
[71] A.V. Badiga, C. Chetty, D. Kesanakurti, D. Are, M. Gujrati, J.D. Klopfenstein, D.H. Dinh, J.S. Rao, MMP-2 siRNA inhibits radiation-enhanced invasiveness in glioma cells, PLoS One 6 (2011) e20614.
[72] S.Y. Kwak, J.S. Yang, B.Y. Kim, I.H. Bae, Y.H. Han, Ionizing radiation-inducible miR-494 promotes glioma cell invasion through EGFR stabilization by targeting p190B rhoGAP, Biochim. Biophys. Acta 1843 (2014) 508–516.
[73] A. Canazza, C. Calatozzolo, L. Fumagalli, A. Bergantin, F. Ghielmetti, L. Fariselli, D. Croci, A. Salmaggi, E. Ciusani, Increased migration of a human glioma cell line after *in vitro* CyberKnife irradiation, Cancer Biol. Ther. 12 (2011) 629–633.
[74] M. Steinle, D. Palme, M. Misovic, J. Rudner, K. Dittmann, R. Lukowski, P. Ruth, S.M. Huber, Ionizing radiation induces migration of glioblastoma cells by activating BK K^+ channels, Radiother. Oncol. 101 (2011) 122–126.
[75] W.J. Kil, P.J. Tofilon, K. Camphausen, Post-radiation increase in VEGF enhances glioma cell motility *in vitro*, Radiat. Oncol. 7 (2012) 25.
[76] I. Vanan, Z. Dong, E. Tosti, G. Warshaw, M. Symons, R. Ruggieri, Role of a DNA damage checkpoint pathway in ionizing radiation-induced glioblastoma cell migration and invasion, Cell. Mol. Neurobiol. 32 (2012) 1199–1208.
[77] W.T. Arscott, A.T. Tandle, S. Zhao, J.E. Shabason, I.K. Gordon, C.D. Schlaff, G. Zhang, P.J. Tofilon, K.A. Camphausen, Ionizing radiation and glioblastoma exosomes: implications in tumor biology and cell migration, Transl. Oncol. 6 (2013) 638–648.
[78] W. Zhou, Y. Xu, G. Gao, Z. Jiang, X. Li, Irradiated normal brain promotes invasion of glioblastoma through vascular endothelial growth and stromal cell-derived factor 1alpha, Neuroreport 24 (2013) 730–734.
[79] A. Shankar, S. Kumar, A. Iskander, N.R. Varma, B. Janic, A. Decarvalho, T. Mikkelsen, J.A. Frank, M.M. Ali, R.A. Knight, S. Brown, A.S. Arbab, Subcurative radiation significantly increases proliferation, invasion, and migration of primary GBM *in vivo*, Chin. J. Cancer 33 (2013) 148–158.
[80] S.C. Wang, C.F. Yu, J.H. Hong, C.S. Tsai, C.S. Chiang, Radiation therapy-induced tumor invasiveness is associated with SDF-1-regulated macrophage mobilization and vasculogenesis, PLoS One 8 (2013) e69182.
[81] J. Johnson, M.O. Nowicki, C.H. Lee, E.A. Chiocca, M.S. Viapiano, S.E. Lawler, J.J. Lannutti, Quantitative analysis of complex glioma cell migration on electrospun polycaprolactone using time-lapse microscopy, Tissue Eng. C Methods 15 (2009) 531–540.
[82] S. Watkins, H. Sontheimer, Hydrodynamic cellular volume changes enable glioma cell invasion, J. Neurosci. 31 (2011) 17250–17259.
[83] B.R. Haas, H. Sontheimer, Inhibition of the sodium-potassium-chloride cotransporter isoform-1 reduces glioma invasion, Cancer Res. 70 (2010) 5597–5606.
[84] C.W. Habela, N.J. Ernest, A.F. Swindall, H. Sontheimer, Chloride accumulation drives volume dynamics underlying cell proliferation and migration, J. Neurophysiol. 101 (2009) 750–757.
[85] V.A. Cuddapah, H. Sontheimer, Molecular interaction and functional regulation of ClC-3 by Ca^{2+}/calmodulin-dependent protein kinase II (CaMKII) in human malignant glioma, J. Biol. Chem. 285 (2010) 11188–11196.
[86] V.A. Cuddapah, K.L. Turner, S. Seifert, H. Sontheimer, Bradykinin-induced chemotaxis of human gliomas requires the activation of KCa3.1 and ClC-3, J. Neurosci. 33 (2013) 1427–1440.
[87] C.B. Ransom, H. Sontheimer, BK channels in human glioma cells, J. Neurophysiol. 85 (2001) 790–803.
[88] H. Sontheimer, An unexpected role for ion channels in brain tumor metastasis, Exp. Biol. Med. (Maywood) 233 (2008) 779–791.
[89] K.L. Turner, A. Honasoge, S.M. Robert, M.M. McFerrin, H. Sontheimer, A proinvasive role for the Ca^{2+}-activated K^+ channel KCa3.1 in malignant glioma, Glia 62 (2014) 971–981.
[90] N.J. Ernest, A.K. Weaver, L.B. Van Duyn, H.W. Sontheimer, Relative contribution of chloride channels and transporters to regulatory volume decrease in human glioma cells, Am. J. Physiol. Cell Physiol. 288 (2005) C1451–C1460.
[91] M.B. McFerrin, H. Sontheimer, A role for ion channels in glioma cell invasion, Neuron Glia Biol. 2 (2006) 39–49.
[92] L. Catacuzzeno, F. Aiello, B. Fioretti, L. Sforna, E. Castigli, P. Ruggieri, A.M. Tata, A. Calogero, F. Franciolini, Serum-activated K and Cl currents underlay U87-MG glioblastoma cell migration, J. Cell. Physiol. 226 (2010) 1926–1933.
[93] M. Sciaccaluga, B. Fioretti, L. Catacuzzeno, F. Pagani, C. Bertollini, M. Rosito, M. Catalano, G. D'Alessandro, A. Santoro, G. Cantore, D. Ragozzino, E. Castigli, F. Franciolini, C. Limatola, CXCL12-induced glioblastoma cell migration requires intermediate conductance Ca^{2+}-activated K^+ channel activity, Am. J. Physiol. Cell Physiol. 299 (2010) C175–C184.
[94] V.C. Lui, S.S. Lung, J.K. Pu, K.N. Hung, G.K. Leung, Invasion of human glioma cells is regulated by multiple chloride channels including ClC-3, Anticancer Res. 30 (2010) 4515–4524.
[95] G. Tabatabai, B. Frank, R. Mohle, M. Weller, W. Wick, Irradiation and hypoxia promote homing of haematopoietic progenitor cells towards gliomas by TGF-beta-dependent HIF-1alpha-mediated induction of CXCL12, Brain 129 (2006) 2426–2435.
[96] M. Kioi, H. Vogel, G. Schultz, R.M. Hoffman, G.R. Harsh, J.M. Brown, Inhibition of vasculogenesis, but not angiogenesis, prevents the recurrence of glioblastoma after irradiation in mice, J. Clin. Invest. 120 (2010) 694–705.
[97] S.V. Kozin, W.S. Kamoun, Y. Huang, M.R. Dawson, R.K. Jain, D.G. Duda, Recruitment of myeloid but not endothelial precursor cells facilitates tumor regrowth after local irradiation, Cancer Res. 70 (2010) 5679–5685.
[98] A.K. Weaver, M.L. Olsen, M.B. McFerrin, H. Sontheimer, BK channels are linked to inositol 1,4,5-triphosphate receptors via lipid rafts: a novel mechanism for coupling $[Ca^{2+}]_i$ to ion channel activation, J. Biol. Chem. 282 (2007) 31558–31568.
[99] C. Garcia-Moruja, J.M. Alonso-Lobo, P. Rueda, C. Torres, N. Gonzalez, M. Bermejo, F. Luque, F. Arenzana-Seisdedos, J. Alcami, A. Caruz, Functional characterization of SDF-1 proximal promoter, J. Mol. Biol. 348 (2005) 43–62.
[100] F. Li, P. Sonveaux, Z.N. Rabbani, S. Liu, B. Yan, Q. Huang, Z. Vujaskovic, M.W. Dewhirst, C.Y. Li, Regulation of HIF-1alpha stability through S-nitrosylation, Mol. Cell 26 (2007) 63–74.
[101] B.J. Moeller, Y. Cao, C.Y. Li, M.W. Dewhirst, Radiation activates HIF-1 to regulate vascular radiosensitivity in tumors: role of reoxygenation, free radicals, and stress granules, Cancer Cell 5 (2004) 429–441.
[102] M.J. Kim, R.K. Kim, C.H. Yoon, S. An, S.G. Hwang, Y. Suh, M.J. Park, H.Y. Chung, I.G. Kim, S.J. Lee, Importance of PKCdelta signaling in fractionated-radiation-induced expansion of glioma-initiating cells and resistance to cancer treatment, J. Cell Sci. 124 (2011) 3084–3094.

Please cite this article as: S.M. Huber, et al., Role of ion channels in ionizing radiation-induced cell death, Biochim. Biophys. Acta (2014), http://dx.doi.org/10.1016/j.bbamem.2014.11.004

[103] C. Lagadec, E. Vlashi, L. Della Donna, C. Dekmezian, F. Pajonk, Radiation-induced reprogramming of breast cancer cells, Stem Cells 30 (2012) 833–844.
[104] K. Tamura, M. Aoyagi, N. Ando, T. Ogishima, H. Wakimoto, M. Yamamoto, K. Ohno, Expansion of CD133-positive glioma cells in recurrent de novo glioblastomas after radiotherapy and chemotherapy, J. Neurosurg. 119 (2013) 1145–1155.
[105] M. Gatti, A. Pattarozzi, A. Bajetto, R. Wurth, A. Daga, P. Fiaschi, G. Zona, T. Florio, F. Barbieri, Inhibition of CXCL12/CXCR4 autocrine/paracrine loop reduces viability of human glioblastoma stem-like cells affecting self-renewal activity, Toxicology 314 (2013) 209–220.
[106] G. Liu, X. Yuan, Z. Zeng, P. Tunici, H. Ng, I.R. Abdulkadir, L. Lu, D. Irvin, K.L. Black, J.S. Yu, Analysis of gene expression and chemoresistance of CD133^{+} cancer stem cells in glioblastoma, Mol. Cancer 5 (2006) 67.
[107] M.J. Jung, J.K. Rho, Y.M. Kim, J.E. Jung, Y.B. Jin, Y.G. Ko, J.S. Lee, S.J. Lee, J.C. Lee, M.J. Park, Upregulation of CXCR4 is functionally crucial for maintenance of stemness in drug-resistant non-small cell lung cancer cells, Oncogene 32 (2013) 209–221.
[108] M. Nakada, E. Nambu, N. Furuyama, Y. Yoshida, T. Takino, Y. Hayashi, H. Sato, Y. Sai, T. Tsuji, K.I. Miyamoto, A. Hirao, J.I. Hamada, Integrin alpha3 is overexpressed in glioma stem-like cells and promotes invasion, Br. J. Cancer 108 (2013) 2516–2524.
[109] P. Ruggieri, G. Mangino, B. Fioretti, L. Catacuzzeno, R. Puca, D. Ponti, M. Miscusi, F. Franciolini, G. Ragona, A. Calogero, The inhibition of KCa3.1 channels activity reduces cell motility in glioblastoma derived cancer stem cells, PLoS One 7 (2012) e47825.
[110] S. Rao, R. Sengupta, E.J. Choe, B.M. Woerner, E. Jackson, T. Sun, J. Leonard, D. Piwnica-Worms, J.B. Rubin, CXCL12 mediates trophic interactions between endothelial and tumor cells in glioblastoma, PLoS One 7 (2012) e33005.
[111] J.P. Greenfield, W.S. Cobb, D. Lyden, Resisting arrest: a switch from angiogenesis to vasculogenesis in recurrent malignant gliomas, J. Clin. Invest. 120 (2010) 663–667.
[112] H.S. Jang, S. Lal, J.A. Greenwood, Calpain 2 is required for glioblastoma cell invasion: regulation of matrix metalloproteinase 2, Neurochem. Res. 35 (2010) 1796–1804.
[113] C.M. Park, M.J. Park, H.J. Kwak, H.C. Lee, M.S. Kim, S.H. Lee, I.C. Park, C.H. Rhee, S.I. Hong, Ionizing radiation enhances matrix metalloproteinase-2 secretion and invasion of glioma cells through Src/epidermal growth factor receptor-mediated p38/Akt and phosphatidylinositol 3-kinase/Akt signaling pathways, Cancer Res. 66 (2006) 8511–8519.
[114] D.R. Maddirela, D. Kesanakurti, M. Gujrati, J.S. Rao, MMP-2 suppression abrogates irradiation-induced microtubule formation in endothelial cells by inhibiting alphavbeta3-mediated SDF-1/CXCR4 signaling, Int. J. Oncol. 42 (2011) 1279–1288.
[115] X.Z. Ye, S.L. Xu, Y.H. Xin, S.C. Yu, Y.F. Ping, L. Chen, H.L. Xiao, B. Wang, L. Yi, Q.L. Wang, X.F. Jiang, L. Yang, P. Zhang, C. Qian, Y.H. Cui, X. Zhang, X.W. Bian, Tumor-associated microglia/macrophages enhance the invasion of glioma stem-like cells via TGF-beta1 signaling pathway, J. Immunol. 189 (2012) 444–453.
[116] S. Bao, Q. Wu, S. Sathornsumetee, Y. Hao, Z. Li, A.B. Hjelmeland, Q. Shi, R.E. McLendon, D.D. Bigner, J.N. Rich, Stem cell-like glioma cells promote tumor angiogenesis through vascular endothelial growth factor, Cancer Res. 66 (2006) 7843–7848.
[117] R. Wang, K. Chadalavada, J. Wilshire, U. Kowalik, K.E. Hovinga, A. Geber, B. Fligelman, M. Leversha, C. Brennan, V. Tabar, Glioblastoma stem-like cells give rise to tumour endothelium, Nature 468 (2010) 829–833.

Please cite this article as: S.M. Huber, et al., Role of ion channels in ionizing radiation-induced cell death, Biochim. Biophys. Acta (2014), http://dx.doi.org/10.1016/j.bbamem.2014.11.004

BK K^+ channel blockade inhibits radiation-induced migration/brain infiltration of glioblastoma cells

Lena Butz[1,2*], Benjamin Stegen[2*], Lukas Klumpp[2,5], Erik Haehl[2], Karin Schilbach[3], Robert Lukowski[1], Matthias Kühnle[4], Günther Bernhardt[4], Armin Buschauer[4], Daniel Zips[2], Peter Ruth[1§] and Stephan Huber[2§]

Departments of [1]Pharmacology, Toxicology and Clinical Pharmacy, [2]Radiation Oncology, and [3]General Pediatrics, Oncology/Hematology, University of Tübingen, Germany, [4]Department of Pharmaceutical/Medicinal Chemistry II, University of Regensburg, Germany, [5]Dr. Margarete Fischer-Bosch-Institute of Clinical Pharmacology, Stuttgart, Germany

* LB and BS contributed equally to this study and, thus, share first-authorship

§ Correspondence to: Peter Ruth
Department of Pharmacology, Toxicology and Clinical Pharmacy
University of Tübingen
Auf der Morgenstelle 8
72076 Tübingen
Germany
Tel. +49-(0)7071-29-78795
E-mail peter.ruth@uni-tuebingen.de

Stephan Huber
Department of Radiation Oncology
University of Tübingen
Hoppe-Seyler-Str. 3
72076 Tübingen
Germany
Tel. +49-(0)7071-29-82183
E-mail stephan.huber@uni-tuebingen.de

Conflict of interest: The authors declare no conflict of interest.

Translational Relevance: Ionizing radiation has been proposed to promote migration, invasion and metastasis of cancer cells. Here, we show in an orthotopic mouse model that fractionated radiation at doses used in standard radiotherapy stimulates an adaptive stress response in glioblastoma cells. This response involves up-regulation of the chemokine SDF-1 (CXCL12), subsequent-CXCR4 chemokine receptor-mediated Ca^{2+} signaling and activation of BK Ca^{2+}-activated K^+ channels. The latter drives migration and brain infiltration of glioblastoma cells. Radiation-induced migration/infiltration may contribute to therapy resistance by disseminating glioblastoma cells during fractionated radiotherapy out-side the target volume of the radiation beam. Importantly, BK K^+ channel targeting suppresses radiation-induced migration and might be applied concomitant to radiation therapy since BK-inhibiting drugs are already in clinical use.

Abstract

Infiltration of the brain by glioblastoma cells reportedly requires Ca^{2+} signals and BK K^+ channels that program and drive glioblastoma cell migration, respectively. Ionizing radiation (IR) has been shown to induce expression of the chemokine SDF-1, to alter the Ca^{2+} signaling, and to stimulate cell migration of glioblastoma cells. Here, we quantified fractionated IR-induced migration/brain infiltration of human glioblastoma cells *in vitro* and in an orthotopic mouse model and analyzed the role of SDF-1/CXCR4 signaling and BK channels. To this end, the radiation-induced migratory phenotypes of human T98G and far-red fluorescent U87MG-Katushka glioblastoma cells were characterized by mRNA and protein expression, fura-2 Ca^{2+} signaling, BK patch-clamp recording and transfilter migration assay. In addition U87MG-Katushka cells were grown to solid glioblastomas in the right hemispheres of immunocompromised mice, fractionated irradiated (6 MV photons) with 5 x 0 or 5 x 2 Gy, and SDF-1, CXCR4, and BK protein expression by the tumor as well as glioblastoma brain infiltration was analyzed in dependence on BK channel targeting by systemic paxilline application concomitant to IR. As a result, IR stimulated SDF-1 signaling and induced migration of glioblastoma cells *in vitro and in vivo*. Importantly, paxilline blocked IR-induced migration *in vivo*.

Conclusions. Collectively, our data demonstrate that fractionated IR of glioblastoma stimulates and BK K^+ channel targeting mitigates migration and brain infiltration of glioblastoma cells *in vivo*. This suggests that BK channel targeting might represent a novel approach to overcome acquired treatment resistance in malignant brain tumors.

Key words. glioma, radiation therapy, radioresistance, fura-2 Ca^{2+} imaging, transfilter migration, tumor invasion, NSG mice, CXCL12 chemokine, chemotaxis, KCNMA1, radiogenic hypermigration

Introduction

Glioblastoma multiforme consists of cells with a highly migratory phenotype that may "travel" long distances throughout the brain (1). Primary foci of glioblastoma usually show a characteristic diffuse and net-like brain infiltration which represents a major challenge for surgical tumor resection as well as for adequate coverage by radiotherapy (2). This migratory phenotype in concert with a pronounced resistance to radiotherapy and chemotherapy probably contributes to frequent therapy failure and bad prognosis observed in the vast majority of patients with glioblastoma.

Microenvironmental stress such as hypoxia, interstitial nutrient depletion or low pH has been proposed to switch tumor cells from a "Grow" into a "Go" phenotype. By migration and tissue invasion "Go" tumor cells may evade the locally refined stress burden and resettle in distant and less hostile regions. Once resettled, tumor cells may readapt the "Grow" phenotype by reentering cell cycling and may establish tumor satellites in more or less close vicinity of the primary focus (3). External beam radiation may induce the "Go" phenotype similar to microenvironmental stress. Sublethal IR has been demonstrated *in vitro* and/or in rodent tumor models to induce migration, metastasis, invasion and spreading of a variety of tumor entitites. In particular, a plethora of *in vitro* and *in vivo* studies suggest that IR induces migration of glioblastoma cells (for review see (4)). Three-dimensional-glioblastoma *in vitro* models, however, could not confirm this phenomenon (5) and whether or not IR induces migration of glioblastoma cells *in vivo* is still under debate.

If IR-induced migration, however, reaches relevant levels during fractionated radiotherapy of glioblastoma patients it might boost glioblastoma brain infiltration and - in the worst case - evasion of glioblastoma cells from the target volume of the radiotherapy. Moreover, IR-induced migration might foster homing of glioblastoma cells to perivascular niches. The subsequent reciprocal interaction between endothelial and glioblastoma cells within these niches has been demonstrated to induce/maintain "stemness" in glioblastoma cells. Stemness, in turn is associated with radioresistance (6,7). Along those lines, the chemokine SDF-1 (stromal cell-derived factor-1, CXCL12) via its receptor CXCR4 (8-10) stimulates migration of glioblastoma cells (11). IR reportedly induces the expression of SDF-1 in different tumor entities including glioblastoma (12-15) as well as in normal brain tissue (9). Notably,

maintenance of glioblastoma stemness and formation of the perivascular glioblastoma stem cell niches highly depend on CXCR4 signaling (16,17).

Combined, these data suggest that IR-induced migration directly or indirectly may contribute to therapy resistance of glioblastoma. The present study, therefore, aimed to to provide a quantitative analysis of IR-induced migration/brain infiltration in an orthotopic *xeno*graft model of human glioblastoma. Importantly, a previous *in vitro* study of our group disclosed IR-induced BK K^+ channel activation as a key event in IR-induced migration. Since BK channel blockade by paxilline, a toxin of the fungus *Penicillium paxilli*, suppresses IR-induced migration *in vitro* (18) the present study further tested whether BK channel targeting with paxilline might be a powerful strategy to suppress IR-induced migration of glioblastoma cells *in vivo*. To this end, a subclone of human U87MG glioblastoma cells transfected with the far-red fluorescent Katushka protein was transplanted into the right striatum of immunocompromised mice. Upon tumor formation, glioblastoma were fractionated irradiated with clinical relevant single fractions combined with concomitant systemic administration of the BK channel inhibitor paxilline. Thereafter, number and migration distances of individual brain-infiltrating glioblastoma cells were analyzed. In addition, the functional significance of SDF-1 signaling in IR-induced migration of glioblastoma cells was defined by immunofluorescence microscopy and by further *in vitro* experiments. Our data strongly suggest that fractionated IR stimulates migration/infiltration *in vivo* via auto-/paracrine SDF-1 signaling and subsequent BK channel activation.

Material and Methods

Cell Culture. Human T98G and U87MG glioblastoma cells were from ATCC (Bethesda, Maryland, USA) and were grown in 10% fetal calf serum (FCS)-supplemented RPMI-1640 medium as described (18). The human U87MG glioblastoma cells were transfected with the far-red Katushka fluorescent protein expression vector pTurboFP635-N (BioCat, Heidelberg, Germany) using the transfection reagent FUGENE HD (Roche Diagnostics GmbH, Mannheim, Germany) according to the manufacturer's instruction. Stably transfected cells were grown in 10% FCS-supplemented RPMI-1640 selection medium containing G418 (750 µg/ml). Exponential growing T98G and U87MG-Katushka cells were irradiated with 6 MV photons (IR, single dose of 0, 2, 4 and 6 Gy) or five daily fractions of 0 or 2 Gy (fractionated IR) by using a linear accelerator (LINAC SL25 Philips) at a dose rate of 4 Gy/min at room temperature. Following IR, cells were post-incubated in RPMI-1640/10% FCS medium for 2-4.5 h (immunoblot, patch-clamp, fura-2 Ca^{2+}-imaging, transfilter migration, immunofluorescence microscopy), 24 h (RT-PCR, transfilter migration), or 2-3 weeks (colony formation assay). In some experiments, cells were pre-incubated (0.5 h) and post-incubated after IR with the BK channel inhibitor paxilline (5 µM, Sigma-Aldrich, Taufkirchen, Germany) or the CXCR4 chemokine receptor antagonist AMD3100 (1 µM, Sigma-Aldrich) or vehicle alone (0.1% DMSO). shRNA-transfected T98G cells were grown in RPMI-1640/10% FCS selection medium containing puromycin (2 µg/ml).

Patch-clamp recording. Whole-cell and on-cell currents were evoked by 41 (whole-cell) or 33 (on-cell) voltage square pulses (700 ms each) from -66 mV (whole-cell) or 4 mV holding potential (on-cell) to voltages between -116 (whole-cell) or -56 mV (on-cell) and 84 (whole-cell) or +104 mV (on-cell) delivered in 5 mV increments. The liquid junction potentials between the pipette and the bath solutions were estimated as described (19), and data were corrected for the estimated liquid junction potentials. Cells were superfused at 37°C temperature with NaCl solution (in mM: 125 NaCl, 32 N-2-hydroxyethylpiperazine-N-2-ethanesulfonic acid (HEPES), 5 KCl, 5 D-glucose, 1 $MgCl_2$, 1 $CaCl_2$, titrated with NaOH to pH 7.4). In the whole-cell experiments shown in Fig. 1, a K-D-gluconate pipette solution was used containing (in mM): 140 K-D-gluconate, 5 HEPES, 5 $MgCl_2$, 1 K_2-EGTA, 1 K_2-ATP, titrated with KOH to pH 7.4. Paxilline (5 µM) was added to the bath solution.

For the on-cell experiments (Figs. 2-4, 8, 10) the pipette solution contained (in mM) 0 or 0.05 paxilline in DMSO, 130 KCl, 32 HEPES, 5 D-glucose, 1 $MgCl_2$, 1 $CaCl_2$, titrated with KOH to pH 7.4. In some experiments, the chemokine stromal cell-derived factor-1 (SDF-1, CXCL12, 50 nM, Immuno Tools, Friesoythe, Germany) and paxilline (5 µM) was added to the bath solution. Whole-cell and macroscopic on-cell currents were analyzed by averaging the currents between 100 and 700 ms of each square pulse. Applied voltages refer to the cytoplasmic face of the membrane with respect to the extracellular space. In the current tracings (whole-cell and macroscopic on-cell currents), the individual current sweeps recorded at the different clamp-voltages are superimposed. Outward currents, defined as flow of positive charge (here: K^+) from the cytoplasmic to the extracellular membrane face, are positive currents and depicted as upward deflections of the original current tracings.

Colony formation assay. To test for clonogenic survival, U87MG-Katushka and T98G cells were preincubated (0.5 h), irradiated (0, 2, 4 or 6 Gy) and post-incubated (24 h) in RPMI-1640/10% FCS medium additionally containing paxilline (0 or 5 µM in 0.1% DMSO). 24 h after IR, cells were detached, 300 and 600 cells were re-seeded in inhibitor-free medium on 3 cm wells and grown for further 2 weeks. The plating efficiency was defined by dividing the number of colonies by the number of plated cells. Plating efficiencies of control and paxilline-treated cells were 0.23 ± 0.001 and 0.22 ± 0.001 for T98G (n = 36) and 0.10 ± 0.003 and 0.06 ± 0.006 (n = 12) for U87MG-Katushka cells, respectively. Survival fractions as calculated by dividing the plating efficiency of the irradiated cells by those of the unirradiated controls were fitted by the use of the linear quadratic equation.

Transfilter migration. The lower and upper chamber of a CIM-Plate 16 (Roche, Mannheim, Germany) were filled with 160 µl (lower chamber) and 100 µl (upper chamber) of RPMI-1640 medium containing 5% and 1% FCS, respectively, equilibrated at 37°C and 5% CO_2 for 30-60 min. The upper and lower chamber additionally contained SDF-1 (0 or 50 nM) and paxilline (0 or 5 µM in 0.1% DMSO). After CO_2 equilibration and resetting the impedance to zero, 100 µl of cell suspension containing 40.000 of unirradiated (SDF-1 experiments) or irradiated cells (0 or 2 Gy, 1-2 h after IR) in RPMI-1640/1% FCS were added to the upper chamber. After sedimentation and adherence of the cells (2-3 h after IR), migration was analyzed in real-time by measuring the impedance increase between electrodes which cover the lower surface of the filter membrane and the reference electrode in the lower chamber. Upon trans-filter migration, cells adhere to the filter electrode surface and increase the

impedance. To compare between individual experiments the impedances were normalized to the 0.5 h values of the respective controls.

Quantitative RT-PCR. Messenger RNAs of fractionated irradiated (5 x 0 Gy or 5 x 2 Gy) U87MG-Katushka and stably transfected T98G cells (see below) were isolated (Qiagen RNA extraction kit, Hilden, Germany) 24 h after the last IR fraction and reversely transcribed in cDNA (Transcriptor First Strand cDNA Synthesis Kit, Roche, Mannheim, Germany). BK K^+ channel-, CXCR4 chemokine receptor-, SDF-1 (CXCL12)-, matrix metalloproteinases MMP-2- and MMP-9-, and housekeeper β-actin (ACTB)-, pyruvate dehydrogenase beta (PDHB)-, and glyceraldehyde-3-phosphate dehydrogenase (GAPDH)-specific fragments were amplified by the use of SYBR Green-based quantitative real-time PCR (QT00024157, QT00223188, QT00087591, QT00088396, QT00040040, QT01192646, QT00095431, and QT00031227 QuantiTect Primer Assay and QuantiFast SYBR® Green PCR Kit, Qiagen) in a Roche LightCycler Instrument. Abundances of the individual mRNAs were normalized to the geometrical mean of the three housekeeper mRNAs.

Western Blotting. Whole protein lysates were prepared from semiconfluent irradiated (0 or 2 Gy, 2 h after IR) U87MG-Katushka and stably transfected T98G cells (see below) using a buffer containing (in mM) 50 HEPES pH 7.5, 150 NaCl, 1 EDTA, 10 sodium pyrophosphate, 10 NaF, 2 Na_3VO_4, 1 phenylmethylsulfonylfluorid (PMSF) additionally containing 1% Triton X-100, 5 µg/ml aprotinin, 5 µg/ml leupeptin, and 3 µg/ml pepstatin (all Sigma-Aldrich), and separated by SDS-PAGE under reducing conditions. Segregated proteins were electro-transferred onto PVDF membranes (Roth, Karlsruhe, Germany). Blots were blocked in tris(hydroxymethyl)aminomethane-buffered saline (TBS) buffer containing 0.05% Tween 20 and 5% non-fat dry milk for 1 h at room temperature. The membranes were incubated overnight at 4°C with the following primary antibodies in TBS -Tween/5% milk against human CXCR4 (rabbit polyclonal antibody, #ab2074, 1:500 dilution, Abcam, Cambridge, UK), human HIF-1α (rabbit monoclonal, #61275, 1:1000 dilution, Active Motif, La Hulpe, Belgium) and human BK (rabbit polyclonal, #APC-107, 1:500 dilution, Alamone Labs, Jerusalem, Israel). Equal gel loading was verified by an antibody against β-actin (mouse anti-β-actin antibody, clone AC-74, Sigma #A2228 1:30,000). Antibody binding was detected with a horseradish peroxidase-linked goat anti-rabbit or horse anti-mouse IgG antibody (# 7074 and #7076, respectively; 1:2000 dilution in TBS-Tween/5% milk, Cell Signaling, Merck-Millipore, Darmstadt, Germany) incubated for 1 h at room temperature and enhanced

chemoluminescence (ECL Western blotting analysis system, GE Healthcare/Amersham-Biosciences, Freiburg, Germany).

Immunofluorescence microscopy of cultured cells. U87MG-Katushka and T98G cells (0 or 2 Gy, 2 h after IR) were grown on object slides and irradiated with 0 or 2 Gy. Two hours after IR, cells were fixed for 15 min at room temperature with phosphate buffered saline (PBS)-containing 4% formaldehyde, 3 times rinsed with PBS for 5 min and blocked for 1 h at 21°C with PBS additionally containing 1% bovine serum albumin (BSA), 5 % goat serum and 0.3% Triton X-100. Cells were then incubated with polyclonal rabbit anti-SDF-1 antibody (NBP1-19778, Novus Biologicals, R&D Systems Europe, Abingdon, UK) or rabbit IgG isotype control antibody (#12-370, Merck-Millipore, both 1 mg/ml) diluted (both 1:1000) in PBS containing 1% BSA and 0.3% Triton X-100. Thereafter, cells were rinsed 3 times for 5 min with PBS, incubated for 2 h at room temperature in the dark with goat FITC-conjugated anti-rabbit IgG antibody (1:1000, NB730-F, Novus Biologicals) diluted in PBS/1% BSA/0.3% Triton X-100, rinsed 3 times for 5 min with PBS, and coverslipped with 4',6-diamidino-2-phenylindole (DAPI) Vectashield Antifade Mounting Medium (Vector Laboratories, Loerrach, Germany).

Fura-2 Ca^{2+} imaging. Fluorescence measurements were performed using an inverted phase-contrast microscope (Axiovert 100; Zeiss, Oberkochen, Germany). Fluorescence was evoked by a filter wheel (Visitron Systems, Puchheim, Germany)-mediated alternative excitation at 340/26 or 387/11 nm (AHF, Analysentechnik, Tübingen, Germany). Excitation and emission light was deflected by a dichroic mirror (409/LP nm beam splitter, AHF) into the objective (Fluar x40/1.30 oil; Zeiss) and transmitted to the camera (Visitron Systems), respectively. Emitted fluorescence intensity was recorded at 587/35 nm (AHF). Excitation was controlled and data acquired by Metafluor computer software (Universal Imaging, Downingtown, PA, USA). The 340/380-nm fluorescence ratio was used as a measure of cytosolic free Ca^{2+} concentration ($_{free}[Ca^{2+}]_i$). U87MG-Katushka and T98G cells were incubated with fura-2/AM (2 μM for 30 min at 37°C; Molecular Probes, Goettingen, Germany) in RPMI-1640/10% FCS medium. $_{free}[Ca^{2+}]_i$ was determined 2-3 h post-IR at 37°C during superfusion with NaCl solution (in mM: 125 NaCl, 32 HEPES, 5 KCl, 5 D-glucose, 1 $MgCl_2$, 2 $CaCl_2$, titrated with NaOH to pH 7.4) before and during stimulation with SDF-1 (50 nM) or conditioned NaCl solution harvested from irradiated cells. For conditioning, 250.000 cells were grown for 24 h in RPMI 1640/10% FCS. After further 24 h of serum depletion, cells were washed once with

NaCl solution, overlayed with 1 ml of NaCl solution, irradiated (0 or 2 Gy) and further incubated for 2 h before harvesting the NaCl solution.

Orthotopic mouse model of human glioblastoma. Animal experiments were carried out according to the German animal protection law and approved by the local authorities. U87MG-Katushka cells were inoculated stereotactically into the right striatum of 12 week old immunocompromised male and female NOD/SCID/IL2Rγ^{null} (NSG) mice. The skullcap was trepanated 2.5 mm laterally and 0.5 mm caudally of the bregma (as indicated in the drawing of Fig. 5B) by the use of a dental driller and 30.000 U87MG-Katushka cells (in 10 µl of FCS-free EMEM medium) were injected in 3 mm depth from the dura surface into the right striatum. Starting at day 8, Isofluran-anaesthesized mice were immobilized under a 6 MV linear accelerator (LINAC SL25 Philips) and the right hemispheres were irradiated with daily fractions of 0 or 2 Gy 6 MV photons using mouse holders and shieldings as described in Fig. 5E and F. On the days of radiation, paxilline (0 or 8 mg/kg BW i.p. in 70 µl 90% DMSO) was administered 6 h prior to and 6 h after each radiation fraction to some of the mice. In particular, 6 mice of the 5 x 0 Gy and 5 x 2 Gy control groups received vehicle alone while 14 mice were not i.p. injected. The data did not differ between the respective groups and were pooled. For dosimetry, Gafchromic 3 films (Ashland Inc., Covington, KY) placed in a mouse phantom (in 5 mm depth form the phantom surface) were exposed. By comparison with unshielded calibration films, dose distribution was defined by the film blackening inside and outside the target volume. For the dosimetry film shown in Fig. 5G, background blackening (as defined by unexposed films) was subtracted.

Immunofluorescence microscopy and immunohistochemistry of brain sections. One, two, or three weeks after tumor challenge, mice were sacrificed and brains were fixed (2% paraformaldehyd in phosphate buffered solution, PBS for 24 h), cryo-protected (30% sucrose in PBS for 24 h), frozen at -80° C in Richard-Allan Scientific™ Neg-50™ Frozen Section Medium (Thermo Scientific, Germany), and cryosectioned (20 µm). For glioblastoma cell migration, cryosections were directly coverslipped in Vectashield Antifade Mounting Medium with DAPI and Katushka and DAPI fluorescence was evaluated by conventional fluorescence microscopy. For SDF-1 protein immunostaining, sections were post-fixed 15 min (4 % paraformaldehyde in PBS) and processed identically to the protocol described above for the cultured cells. After mounting, SDF-1-specific FITC was analyzed by confocal fluorescence microscopy. Antibody specificity was confirmed by the isotype which didn't

produce any considerable fluorescence staining (data not shown). For CXCR-4 staining, the brain sections were fixed and permeabilized with 100% icecold methanol for 10 min instead of PFA fixation. As primary antibody, an anti-CXCR4 antibody (rabbit polyclonal antibody, Abcam #ab2074) was used in a 1:100 dilution.

For BK channel staining, sections were washed three times for 5 min with PBS, fixed and permeabilized for 10 min with 100% icecold methanol, again washed with PBS for 5 min and blocked for one hour in blocking solution (PBS containing 1% BSA, 0,2% Glycin, 0,2% Lysin, 5% goat serum and 0,3% Triton X-100). Sections were incubated overnight (4°C) with rabbit anti $BKa_{(674-1115)}$ antibody (20), 1:500 in blocking solution and after washing three times 5 min with PBS incubated for 1 h with the biotinylated secondary antibody, 1:200 (anti rabbit IgG, Vector Laboratories) in blocking solution. The staining was visualized with the alkaline phosphatase method and the sections were covered with Aquatex (Merck-Millipore). For positive and negative control hippocampus sections from a NSG mouse (Fig. 5I) and a $BK^{-/-}$ mouse (20) (Fig. 5K) were used, respectively.

BK knockdown. BK channels were down-regulated in T98G cells by transduction with a pool of five BK-specific MISSION® shRNA Lentiviral Transduction Particles and as a control with MISSION® pLKO.1-puro Empty Vector Control Transduction Particles (SHCLNV-NM_002247 and SHC001V, Sigma-Aldrich). Cells were transduced according to the provided experimental protocol positively transduced clones were selected by the use of 2 µg/ml puromycin in the culture medium. Down-regulation of BK was controlled by quantitative RT-PCR and immunoblotting (Suppl. Fig. IG, insert).

SDF-1 ELISA. T98G cells (250.000) were seeded in 75 cm^2 cell culture flasks in RPMI-1640 medium containing 10% FCS and grown over night. Cells were washed with PBS and serum depleted for 24 h. Thereafter, cells were washed with PBS and overlaid with NaCl solution (see patch-clamp section) containing protease inhibitors (Roche, cOmplete Mini, EDTA-free, #04693159001). After 30 min incubation, cells were irradiated with 0 or 2 Gy. After further 2 h the medium was harvested and the SDF-1 concentration determined using an ELISA assay kit (R&D Systems, Human CXCL12/SDF-1 DuoSet ELISA, #DY350).

Results

Studies using human U87MG glioblastoma cells to generate orthotopic mouse models report encapsulated and low brain infiltrative tumor growth (21). Therefore, U87MG glioblastoma seemed excellently suited for quantitative analysis of number and migration distances of individual glioblastoma cells. We used the U87MG-Katushka clone stably transfected with the far-red fluorescent protein Katushka for histological glioblastoma cell tracking.

First, we studied *in vitro* both BK channel expression in U87MG-Katushka cells and putative radiosensitizing effects of the BK channel inhibitor paxilline. Issuing the latter was plausible since pharmacological blockade of the BK-related Ca^{2+}-activated IK channels reportedly radiosensitizes T98G and U87MG glioblastoma cells (19). Similar radiosensitizing action of paxilline would complicate the interpretation of any paxilline *in vivo* effect on tumor cell migration and brain infiltration.

As described for T98G and the parental U87MG cells (18), the U87MG-Katushka clone functionally expressed BK channels. This was evident from whole-cell patch-clamp recordings with K-gluconate in the pipette and NaCl in the bath. U87MG-Katuska cells exhibited large outward currents in the range of several nano-amperes (Fig. 1A, left). These currents were outwardly rectifying and blocked by the BK channel inhibitor paxilline (Fig. 1A right and 1 B) indicative of functional expression of BK channels. To test for a radiosensitizing action of BK channel targeting, the influence of paxilline on clonogenic survival of irradiated U87MG-Katushka and T98G cells was determined by delayed plating colony formation assays. In contrast to IK channel targeting (19), BK channel blockade by paxilline did not radiosensitize both glioblastoma cell models (Fig. 1C and D).

Reportedly, IR stimulates *in vivo* the expression of the chemokine SDF-1 by the glioma invasion front (15). Therefore, U87MG-Katushka and T98G were tested *in vitro* for IR-induced BK channel activity, transfilter migration and the role of SDF-1 signaling herein in order to define radiation-induced signaling events upstream of BK channel activation. In on-cell patch-clamp recordings (KCl pipette- and NaCl bath solution) from U87MG-Katushka cells (Fig. 2A), large conductance ion channels (unitary conductance, $g \approx 200$ pS, Fig. 2B) became increasingly active with increasing positive voltage. In irradiated cells (2 Gy, 2-4.5 h after IR), channel activity was observed at much lower clamp-voltage than in non-irradiated

cells (Fig. 2 A, right and Fig 2 C, closed triangles). In on-cell mode, a clamp-voltage between pipette and bath solution of 0 mV is recording the transmembrane currents at physiological membrane potential. Therefore, the current transitions at 0 mV observed in irradiated cells indicated the activity of the large conductance ion channel at physiological membrane potential. In unirradiated control cells, in contrast, channel activity was triggered not until increasing the clamp-voltage above +50 mV (Fig. 2C, open circles). Accordingly, mean macroscopic on-cell outward currents in irradiated cells exceeded that of control cells by twofold (Fig. 2D, black symbols and Fig. 2E, left). Notably, paxilline (5 μM; Fig. 2D, grey symbols and Fig. 2E, right) blocked about half of the outward current in irradiated cells while having no effect in control cells. The paxilline-sensitive current fractions of irradiated cells showed typical outward rectification (Fig. 2F, closed triangles). In combination, voltage-dependence of open probability, high unitary conductance and paxilline-sensitivity defined the large conductance channel as BK K^+ channel. Importantly, BK channels were active in irradiated cells at physiological membrane potential suggesting their functional significance for the irradiated glioblastoma cells.

BK channel activation in irradiated U87MG-Katushka cells was paralleled by faster chemotaxis when compared to unirradiated control cells as determined by FCS gradient-stimulated transfilter migration assays (Fig. 2G and 2H, left). The BK channel inhibitor paxilline (5 μM) abolished IR-induced migration while not interfering with basic migration (Fig. 2H, right). Together, these data indicate radiation-induced migration in U87MG-Katushka cells depending on IR-induced BK channel activity.

To confirm previously published data on paxilline-sensitive IR-induced migration (18), irradiated (0 or 2 Gy, 2-4.5 h after IR) T98G cells were on-cell patch-clamp recorded with KCl in the pipette and NaCl bath solution. Similar to the U87MG-Katushka model, irradiated T98G glioblastoma cells showed voltage-dependent activity of large conductance ($g \approx 200$ pS) channels at more negative clamp-voltages than unirradiated T98G control cells (Suppl. Fig IA-C). Channels were active in irradiated T98 cells at physiological membrane potential (i.e., 0 mV clamp-voltage, Suppl. Fig. IB) and generated an outwardly rectifying paxilline-sensitive macroscopic on-cell current (Suppl. Fig. ID-F) indicative of IR-induced BK channel activation. This activation resulted in IR-induced migration (Suppl. Fig. IG and I H, left) which was dependent on BK channels since BK knockdown (Suppl. Fig. IG, insert) decreased migration velocity of irradiated cells to the control values while not affecting basal

migration of unirradiated control cells (Suppl. Fig. IH, right). These results suggest that the previously reported IR-induced and paxilline-sensitive migration of T98G cells (18) is mediated by IR-induced BK channel activation.

To estimate, whether IR-induced migration might be associated with an hyperinvasive phenotype and to identify radiation-triggered signaling events, abundances of selected mRNAs were compared between fractionated irradiated (5 x 2 Gy) and control (5 x 0 Gy) U87MG-Katushka cells. Specifically, mRNAs encoding for BK, the matrix metalloproteinases MMP-2 and MMP-9, SDF-1 and the SDF-1 receptor CXCR4 were analyzed. As shown in Fig. 3A, fractionated IR did not alter BK or CXCR4 mRNA but significantly increased the abundance of MMP-2, MMP-9, and SDF-1 mRNA hinting to a radiation-induced hyperinvasive phenotype and chemokine signaling.

The transcription factor hypoxia-inducible factor-1α (HIF-1α) has been reported to up-regulate CXCR4 and SDF-1 expression (for review see (8)). In U87MG-Katushka, IR (1 x 2 Gy, 2 h after IR) stabilized HIF-1α protein as shown by immunoblotting (Fig. 3B, upper blot and Fig. 3 C, left). In accordance with the mRNA data (Fig. 3A), HIF-1α stabilization was not associated with an IR-induced increase in CXCR4 chemokine receptor protein abundance (immunoblot in Fig. 3B, middle and Fig. 3C, right) but was paralleled by a significantly elevated SDF-1 immunofluorescence (Fig. 3D, E).

SDF-1 has been shown to induce Ca^{2+} release from the Ca^{2+} stores via CXCR4, phospholipase C, and formation of inositol 1,4,5-trisphosphate (22). Notably, BK channels have been demonstrated to be linked to inositol 1,4,5-triphosphate receptors via lipid rafts (23). To estimate the functional significance of SDF-1 signaling in IR-induced BK activation and migration the effect on Ca^{2+} signaling of conditioned medium harvested from control and irradiated U87MG-Katushka cells (2 h after IR) was determined in dependence of CXCR4 blockade by AMD3100 (1 μM). In fura-2 Ca^{2+} imaging experiments, conditioned medium from irradiated cells evoked a significant faster rise in cytosolic $_{free}[Ca^{2+}]_i$ than that from unirradiated control cells (Fig. 3F and G, open bars). Importantly, AMD3100, when washed-in together with the conditioned medium, completely abolished the IR effect on $_{free}[Ca^{2+}]_i$ (Fig. 3G, closed bars). This suggests that IR induces enrichment of factors stimulating the CXCR4 signaling in the medium. Likewise, AMD3100 blocked the BK channel activation by IR when applied before on-cell patch-clamp recording (Fig. 3H, I). Together, these data

suggest the involvement of SDF-1/CXCR4 signaling in IR-induced BK channel activation of U87MG-Katushka cells.

Similarly to U87MG-Katushka cells, T98G cells expressed CXCR4 and SDF1 mRNA and protein (RT-PCR and immunoblot data not shown). IR (2 Gy, 2 h after IR) induced an increase in SDF-1 protein abundance in T98G cells as determined by immunofluorescence microscopy (Suppl. Fig. IIA-C). Conditioned medium from irradiated (2 Gy, 2 h after IR) T98G cells exhibited higher SDF-1 concentrations than control cells as determined by ELISA (Suppl. Fig. IID). Accordingly, superfusion of conditioned medium from irradiated T98G cells (2 Gy, 2 h after IR) stimulated an increase in $_{free}[Ca^{2+}]_i$ in T98G cells while medium from control cells did not (Suppl. Fig. IIE and F, left). The CXCR4 antagonist AMD3100 (1 μM) prevented the Ca^{2+} signals in T98G cells elicited by conditioned medium from irradiated cells (Suppl. Fig. IIF, right). Together, these data suggest IR-induced SDF-1 signaling also in T98G cells.

To test, whether SDF-1 can mimic IR-induced BK channel activation and migration in U87MG-Katushka cells, $_{free}[Ca^{2+}]_i$ was recorded during wash-in of SDF-1 (Fig. 4A, B). Acute application of SDF-1 (50 nM) stimulated a long-lasting increase in $_{free}[Ca^{2+}]_i$. In addition, acute application of SDF-1 induced paxilline-sensitive outward currents in on-cell patch-clamp recordings (Fig. 4C-F). Remarkably, the SDF-1-stimulated current fraction was outwardly rectifying (Fig. 4E) and closely resembled the radiation-induced currents (compare Fig. 4E with Fig. 2F, closed triangles) in voltage-dependence and absolute values. Finally, SDF-1 (50 nM) stimulated transfilter migration of U87MG-Katushka cells (Fig. 4G and 4H, open bars). The BK channel inhibitor paxilline (5 μM) blocked the SDF-1 induced augmentation of transfilter migration without significantly inhibiting basal migration (Fig. 4H, closed bars). In summary, SDF-1 very similarly to radiation stimulates migration that depends on BK channel activation.

Analogous to U87MG-Katushka, acute application of SDF-1 (50 nM) induced in T98G cells a long-lasting increase in $_{free}[Ca^{2+}]_i$, (Suppl. Fig IIIA, B), an activation of macroscopic outward current in on-cell patch-clamp recordings (Suppl. Fig. IIIC, D). Single channel analysis (Suppl. Fig. IIIE) revealed BK-like large conductance channels ($p \approx 170$ pS; Fig. IIIF) that activated increasingly with increasing voltage (Suppl. Fig. IIIG). SDF-1 (50 nM) shifted the activation voltage towards more negative clamp-voltages (Suppl. Fig. IIIG). In summary, the

in vitro data on the U87MG-Katushka clone demonstrated IR-induced BK K^+ channel-dependent migration similar to that observed in the present study and/or reported previously for T98G and the parental U87MG cells (18). Moreover, these *in vitro* experiments strongly suggest that IR-induced SDF-1 signaling is triggering upstream of BK at least part of the IR-induced migration.

For generation of orthotopic glioblastoma, U87MG-Katushka (Fig. 5A) cells were stereotactically inoculated into the right striatum of NSG mice (Fig. 5B). Inoculation resulted in the formation of solid and most widely encapsulated glioblastoma (Fig. 5C) that grew exponentially during the first 3 weeks after tumor challenge (Fig. 5D). As illustrated in Figs. 5E and F, the glioblastoma-bearing right hemisphere of isofluran-anaesthesized mice was fractionated irradiated (6 MV photons) on days 8 - 12 with daily fractions of 2 Gy by the use of mouse holders mounted in the radiation beam of a linear accelerator. The mouse torso and head outside the radiation field were shielded by multileaf collimator and/or an 8 cm thick on-body lead block. The film dosimetry revealed steep dose decline outside the radiation field restricting the area bounded by the 50% isodose line to about 0.8 cm x 0.5 cm = 0.4 cm^2 (with about 1/3 of this field outside the animal (Fig. 5F, G). Fractionated IR (5 x 2 Gy) was well tolerated by the mice as deduced from the only minute IR-associated decline of body weight (Fig. 5H, black symbols). The mice receiving paxilline developed mild and transient ataxia and showed a body weight loss of some 10-15% as compared to the respective control groups (Fig. 5H, pink symbols). After end of paxilline treatment, mice recovered completely. On day 22, mice of the 4 treatment groups were sacrificed and brains excised for histological analysis. Importantly, U87MG-Katushka cells continued to express BK channels when grown in mouse brain as demonstrated by immunohistochemistry (Fig. 5I-K).

Besides BK, orthotopic U87MG-Katuska cells expressed SDF-1 protein as evident from immunofluorescence microscopy. In particular, fractionated IR (5 x 2 Gy) induced marked up-regulation of SDF-1 protein expression 9 days after end of radiotherapy (Fig. 6A and B). Specifically, brain invading cells at the glioblastoma margin (Fig. 6B) and emigrated tumor cells that infiltrate healthy brain parenchyma were SDF-1 positive (Fig. 6C) while unirradiated glioblastoma showed only weak SDF-1-specific staining (Fig. 6A).

In addition to SDF-1, unirradiated and fractionated irradiated orthotopic U87MG-Katushka cells expressed CXCR4 chemokine receptor protein (Fig. 6D, E). CXCR4 protein abundance

was similar in fractionated irradiated (Fig. 6F) and in unirradiated tumors and localized in the plasma membrane (green fluorescence) and the cytoplasm (merged yellow fluorescence due to colocalization with the far-red Katushka protein, Fig. 6G).

To quantify the emigration activity of untreated and irradiated tumors, the number of evaded glioblastoma cells was counted and the migration distances determined. The margin of untreated tumors was usually clearly delimited with tangentially oriented glioblastoma cells at the tumor surface (Fig. 7A). Irradiated tumors (Fig. 7B), in contrast, exhibited zones where glioblastoma cells invaded in the adjacent brain parenchyma (white arrow heads) giving the tumor margin a fringed appearance. Figs. 7C depict numbers and emigration distances of glioblastoma cells emigrated from unirradiated (5 x 0 Gy, open circles) and fractionated irradiated (5 x 2 Gy, closed triangles) glioblastoma. IR regimes were applied in the absence (Fig. 7C) or presence (Fig. 7D) of systemic paxilline administration (8 mg/kg B.W. i.p., 6 h prior to and 6 h after each IR fraction). IR significantly stimulated emigration from the tumor (Fig. 7E, left) and paxilline administration prevented this IR-induced migration but didn't affect basal emigration (Fig. 7E, right). Importantly, neither IR nor paxilline changed the glioblastoma volume (Fig. 7F).

In summary, our data on IR-induced migration of glioblastoma cells acquired *in vitro* by the use of the 2D-cultures and those obtained *in vivo* in an orthotopic glioblastoma mouse model strikingly coincided. The IR-induced induction of migration possibly occurs via IR-induced stabilization of HIF-1α. The subsequent up-regulation of the HIF-1α target gene SDF-1 was observed *in vitro* and *in vivo,* suggesting that SDF-1 can stimulate Ca^{2+} transients that lead to BK K^+ channel activation. *In vitro* and *in vivo*, BK channel targeting was capable to prevent IR-induced migration indicating its functional significance for IR-induced migration of glioblastoma cells.

Discussion

The present study demonstrates that fractionated IR stimulated migration/infiltration on a cellular and quantitative level in an orthotopic mouse model of human glioblastoma. Migration was associated with upregulation of the chemokine SDF-1 particularly in brain parenchyma-infiltrating glioblastoma cells suggesting an involvement of autocrine/paracrine SDF-1 signaling in IR-induced hypermigation *in vivo*.

The previously reported *in vivo* data on IR-induced migration of glioblastoma were acquired with cells or brains pre-irradiated prior to transplantation (24,25), whole brain irradiation with a single dose of 8 Gy (12), partial brain irradiation with large irradiation fields (1 cm^2) and single doses of 8 and 15 Gy (15), or stereotactical glioblastoma irradiation with a single dose of 50 Gy (26). The present study demonstrated in a setting which resembled more the clinical situation that fractionated radiation doubled the number of glioblastoma cells emigrating from the primary focus suggesting that standard fractionation protocols may substantially promote glioblastoma brain infiltration during radiotherapy of patients.

Glioblastoma migration is programmed by Ca^{2+} signaling involving CaMKII (for review see (4)). Besides glioblastoma, IR-stimulated Ca^{2+} signaling via CaMKII activation has been described in leukemia (27,28) suggesting IR-induced Ca^{2+} signaling as a general phenomenon. Like IR, SDF-1 occupation of the G protein coupled chemokine receptor CXCR4 induces Ca^{2+} signaling and migration/invasion in glioblastoma (11,29) and pancreatic cancer (30).

SDF-1 is a HIF-1α target gene and hypoxia is a strong inductor of SDF-1 expression. IR causes damage of the tumor vasculature and the resultant tumor hypoxia has been proposed to induce SDF-1 expression (for review see (8)). Besides hypoxia-mediated SDF-1 upregulation, IR may directly stimulate SDF-1 expression in glioblastoma deduced from the *in vitro* experiments of the present study and a previous report using SDF-1 promoter reporter assays (12).

Glioblastoma-derived SDF-1 reportedly recruits bone marrow-derived $CD11b^+$ cells to the tumor site and formation of new blood vessels promoting neovascularization of the tumor (12-15,31,32). Importantly, SDF-1 signaling (29) and vasculogenesis has been reported to

predominantly occur at the invasion fronts of glioblastoma and SDF-1 knockdown in the glioblastoma cells decreases both, vasculogenesis and IR-induced migration/infiltration (15) suggesting that IR-induced revascularization might facilitate IR-induced migration.

Moreover, IR has been demonstrated to select cancer stem-like cells or even induce transition of "differentiated" to stem-like tumor cells in glioblastoma (33-35) and other tumor entities (36). Notably, "stemness" is associated with markedly increased CXCR4 expression (37) and a highly migratory/invasive phenotype (38,39). One might, therefore, hypothesize that IR-induced transition of "differentiated" to stem-like glioblastoma cells further contributes to IR-stimulated migration.

Does IR-induced migration/infiltration contribute to the apparent high radioresistance of glioblastoma? After clinical radio(chemo)therapy, most (70-90%) volume of the recurrent glioblastoma reportedly lays within the IR target volume (2, 40, 41). At a first glance, this suggests that the overall contribution of target volume-emigrated tumor cells on tumor recurrence – if existent – is low. On the other hand, one might speculate that recurrent glioblastoma preferentially and much faster re-expand into irradiated and necrotic brain volumes than infiltrating intact brain parenchyma. If so, the extent of recurrences within the IR target volume would be overestimated. Along those lines, detailed imaging analysis has suggested that significant volume of the recurrent glioblastoma lays in the outermost zone of the IR target volume, i.e., outside the initial gross tumor volume or biological target volume as defined by MRI or PET (2) which might fit to the idea of re-settling the IR-target volume by formerly emigrated glioblastoma cells. Along those lines, accumulation of SDF-1 (42) and $CD133^+$ stem-like glioblastoma cells (35) has been reported in necrotic glioblastoma areas.

Moreover, a previous report showed that *xeno*grafted $CD133^+$ stem-like subpopulations of glioblastoma exhibit a higher radioresistance than *xeno*grafted $CD133^-$ cells while radiosensitivity of both subpopulations does not differ *in vitro*. This clearly indicates a function of the brain microenvironment for radioresitance (43). In particular, endothelial cells have been postulated to promote glioblastoma therapy resistance (44). The reciprocal interaction between glioblastoma and endothelial cells strongly depends on MMP matrix metalloproteinase-2 (MMP-2) expression by glioblastoma (45) and SDF-1 signaling of endothelial cells (44). Importantly, irradiation induces upregulation of MMP-2 in glioblastoma cells which is required for tissue invasion (24,26,45,46). This might hint to the

possibility, that IR-induced migration promotes "homing" of (highly CXCR4-expressing stem-like) glioblastoma cells to perivascular niches. The subsequent reciprocal modifications of glioblastoma and endothelial cells eventually might contribute to the high radioresistance of glioblastoma cells. Together, these data suggest that IR-induced migration might contribute to the apparent high radioresistance of glioblastoma cells either by promoting evasion from the IR target volume or by stimulating the chemotaxis of glioblastoma cells to perivascular niches.

The present study identified BK channel targeting as effective *in vivo* strategy to prevent IR-induced migration. BK channels are expressed in neurons of the central nervous system, e.g., in hippocampus, where they can be found in pre- and postsynaptic membranes (20). The BK channel blocker paxilline, applied in the present study, is a neurotoxin produced by the endophytic fungus *Penicillium paxilli* and causes "ryegrass staggers" in sheep which is characterized by ataxia and uncontrollable tremors (47). Paxilline at the applied dose induced besides ataxia no severe side effects and was well tolerated by the mice. This might suggest that BK channel targeting might be applied in glioblastoma patients. As a matter of fact, drugs with BK channel modulating side effects are already in clinical use. Classical neuroleptics such as haloperidol or chlorpromazine inhibit BK channels with an IC_{50} in the low micromolar range (48). Reportedly, haloperidol may accumulate in the human brain up to micromolar (49) and chlorpromazine up to several ten micromolar concentrations (50) suggesting that the therapeutic concentrations of the classical neuroleptics affect BK channel activity.

In conclusion, fractionated radiation stimulates migration of glioblastoma cells *in vivo* which might contribute to the resistant phenotype of glioblastoma. Radiation-induced BK K^+ channel activation triggers and BK channel targeting suppresses migration upon irradiation.. Thus, BK channel targeting during fractionated irradiation might represent a novel concept to overcome acquired radiation resistance.

Acknowledgement: This work has been supported by a grant from the Wilhelm-Sander-Stiftung awarded to SH and PR (2011.083.1). BS was supported by the DFG International Graduate School 1302 (TP T9 SH) and LK by the ICEPHA program of the University of Tübingen and the Robert-Bosch-Gesellschaft für Medizinische Forschung, Stuttgart. We thank Heidrun Faltin and Ilka Müller for excellent technical assistance, Savas Tsitsekidis for the dosimetry, and Andreas Hönes for constructing the mouse holders and lead shieldings.

References

1. Johnson J, Nowicki MO, Lee CH, Chiocca EA, Viapiano MS, Lawler SE, et al. Quantitative analysis of complex glioma cell migration on electrospun polycaprolactone using time-lapse microscopy. Tissue Eng Part C Methods 2009;15:531-40.
2. Weber DC, Casanova N, Zilli T, Buchegger F, Rouzaud M, Nouet P, et al. Recurrence pattern after [(18)F]fluoroethyltyrosine-positron emission tomography-guided radiotherapy for high-grade glioma: a prospective study. Radiother Oncol 2009;93:586-92.
3. Hatzikirou H, Basanta D, Simon M, Schaller K, Deutsch A. 'Go or Grow': the key to the emergence of invasion in tumour progression? Math Med Biol 2012;29:49-65.
4. Huber SM, Butz L, Stegen B, Klumpp L, Klumpp D, Eckert F. Role of ion channels in ionizing radiation-induced cell death. Biochim Biophys Acta 2015; 1848:2657-64.
5. Eke I, Storch K, Kastner I, Vehlow A, Faethe C, Mueller-Klieser W, et al. Three-dimensional Invasion of Human Glioblastoma Cells Remains Unchanged by X-ray and Carbon Ion Irradiation In Vitro. Int J Radiat Oncol Biol Phys 2012; 84:e515-23.
6. Anido J, Saez-Borderias A, Gonzalez-Junca A, Rodon L, Folch G, Carmona MA, et al. TGF-beta Receptor Inhibitors Target the $CD44_{high}/Id1_{high}$ Glioma-Initiating Cell Population in Human Glioblastoma. Cancer Cell 2010;18:655-68.
7. Pietras A, Katz AM, Ekstrom EJ, Wee B, Halliday JJ, Pitter KL, et al. Osteopontin-CD44 signaling in the glioma perivascular niche enhances cancer stem cell phenotypes and promotes aggressive tumor growth. Cell Stem Cell 2014;14:357-69.
8. Greenfield JP, Cobb WS, Lyden D. Resisting arrest: a switch from angiogenesis to vasculogenesis in recurrent malignant gliomas. J Clin Invest 2010;120:663-7.
9. Zhou W, Xu Y, Gao G, Jiang Z, Li X. Irradiated normal brain promotes invasion of glioblastoma through vascular endothelial growth and stromal cell-derived factor 1alpha. Neuroreport 2013;24:730-4.
10. Pham K, Luo D, Siemann DW, Law BK, Reynolds BA, Hothi P, et al. VEGFR inhibitors upregulate CXCR4 in VEGF receptor-expressing glioblastoma in a TGFbetaR signaling-dependent manner. Cancer Lett 2015;360:60-7.
11. Sciaccaluga M, Fioretti B, Catacuzzeno L, Pagani F, Bertollini C, Rosito M, et al. CXCL12-induced glioblastoma cell migration requires intermediate conductance Ca^{2+}-activated K^+ channel activity. Am J Physiol Cell Physiol 2010;299:C175-84.
12. Tabatabai G, Frank B, Mohle R, Weller M, Wick W. Irradiation and hypoxia promote homing of haematopoietic progenitor cells towards gliomas by TGF-beta-dependent HIF-1alpha-mediated induction of CXCL12. Brain 2006;129:2426-35.
13. Kioi M, Vogel H, Schultz G, Hoffman RM, Harsh GR, Brown JM. Inhibition of vasculogenesis, but not angiogenesis, prevents the recurrence of glioblastoma after irradiation in mice. J Clin Invest 2010;120:694-705.
14. Kozin SV, Kamoun WS, Huang Y, Dawson MR, Jain RK, Duda DG. Recruitment of myeloid but not endothelial precursor cells facilitates tumor regrowth after local irradiation. Cancer Res 2010;70:5679-85.
15. Wang SC, Yu CF, Hong JH, Tsai CS, Chiang CS. Radiation therapy-induced tumor invasiveness is associated with SDF-1-regulated macrophage mobilization and vasculogenesis. PLoS One 2013;8:e69182.
16. Barone A, Sengupta R, Warrington NM, Smith E, Wen PY, Brekken RA, et al. Combined VEGF and CXCR4 antagonism targets the GBM stem cell population and synergistically improves survival in an intracranial mouse model of glioblastoma. Oncotarget 2014;5:9811-22.
17. Richardson PJ. CXCR4 and Glioblastoma. Anticancer Agents Med Chem 2015.

18. Steinle M, Palme D, Misovic M, Rudner J, Dittmann K, Lukowski R, et al. Ionizing radiation induces migration of glioblastoma cells by activating BK K^+ channels. Radiother Oncol 2011;101:122-6.
19. Stegen B, Butz L, Klumpp L, Zips D, Dittmann K, Ruth P, et al. Ca^{2+}-activated IK K^+ Channel Blockade Radiosensitizes Glioblastoma Cells. Mol Cancer Res 2015;doi: 10.1158/1541-7786.MCR-15-007.
20. Sausbier U, Sausbier M, Sailer CA, Arntz C, Knaus HG, Neuhuber W, et al. Ca^{2+} - activated K^+ channels of the BK-type in the mouse brain. Histochem Cell Biol 2006;125:725-41.
21. Woo SR, Ham Y, Kang W, Yang H, Kim S, Jin J, et al. KML001, a telomere-targeting drug, sensitizes glioblastoma cells to temozolomide chemotherapy and radiotherapy through DNA damage and apoptosis. BioMed research international 2014;2014:747415.
22. Peng H, Huang Y, Rose J, Erichsen D, Herek S, Fujii N, et al. Stromal cell-derived factor 1-mediated CXCR4 signaling in rat and human cortical neural progenitor cells. J Neurosci Res 2004;76:35-50.
23. Weaver AK, Olsen ML, McFerrin MB, Sontheimer H. BK channels are linked to inositol 1,4,5-triphosphate receptors via lipid rafts: a novel mechanism for coupling $[Ca^{2+}]_i$ to ion channel activation. J Biol Chem 2007;282:31558-68.
24. Wild-Bode C, Weller M, Rimner A, Dichgans J, Wick W. Sublethal irradiation promotes migration and invasiveness of glioma cells: implications for radiotherapy of human glioblastoma. Cancer Res 2001;61:2744-50.
25. Desmarais G, Charest G, Fortin D, Bujold R, Mathieu D, Paquette B. Cyclooxygenase-2 inhibitor prevents radiation-enhanced infiltration of F98 glioma cells in brain of Fischer rat. Int J Radiat Biol 2015;91:624-33.
26. Shankar A, Kumar S, Iskander A, Varma NR, Janic B, Decarvalho A, et al. Subcurative radiation significantly increases proliferation, invasion, and migration of primary GBM in vivo. Chin J Cancer 2014;33:148-58.
27. Heise N, Palme D, Misovic M, Koka S, Rudner J, Lang F, et al. Non-selective cation channel-mediated Ca^{2+}-entry and activation of Ca^{2+}/calmodulin-dependent kinase II contribute to G_2/M cell cycle arrest and survival of irradiated leukemia cells. Cell Physiol Biochem 2010;26:597-608.
28. Palme D, Misovic M, Schmid E, Klumpp D, Salih HR, Rudner J, et al. Kv3.4 potassium channel-mediated electrosignaling controls cell cycle and survival of irradiated leukemia cells. Pflugers Arch 2013;465:1209-21.
29. Zagzag D, Esencay M, Mendez O, Yee H, Smirnova I, Huang Y, et al. Hypoxia- and vascular endothelial growth factor-induced stromal cell-derived factor-1alpha/CXCR4 expression in glioblastomas: one plausible explanation of Scherer's structures. The Am J Pathol 2008;173:545-60.
30. Saur D, Seidler B, Schneider G, Algul H, Beck R, Senekowitsch-Schmidtke R, et al. CXCR4 expression increases liver and lung metastasis in a mouse model of pancreatic cancer. Gastroenterology 2005;129:1237-50.
31. Tseng D, Vasquez-Medrano DA, Brown JM. Targeting SDF-1/CXCR4 to inhibit tumour vasculature for treatment of glioblastomas. Br J Cancer 2011;104:1805-9.
32. Liu SC, Alomran R, Chernikova SB, Lartey F, Stafford J, Jang T, et al. Blockade of SDF-1 after irradiation inhibits tumor recurrences of autochthonous brain tumors in rats. Neuro Oncol 2014;16:21-8.
33. Kim MJ, Kim RK, Yoon CH, An S, Hwang SG, Suh Y, et al. Importance of PKCdelta signaling in fractionated-radiation-induced expansion of glioma-initiating cells and resistance to cancer treatment. J Cell Sci 2011;124:3084-94.
34. Lagadec C, Vlashi E, Della Donna L, Dekmezian C, Pajonk F. Radiation-induced reprogramming of breast cancer cells. Stem Cells 2012;30:833-44.

35. Tamura K, Aoyagi M, Ando N, Ogishima T, Wakimoto H, Yamamoto M, et al. Expansion of CD133-positive glioma cells in recurrent de novo glioblastomas after radiotherapy and chemotherapy. J Neurosurg 2013;119:1145-55.
36. Pajonk F, Vlashi E, McBride WH. Radiation resistance of cancer stem cells: the 4 R's of radiobiology revisited. Stem Cells 2010;28:639-48.
37. Liu G, Yuan X, Zeng Z, Tunici P, Ng H, Abdulkadir IR, et al. Analysis of gene expression and chemoresistance of $CD133^+$ cancer stem cells in glioblastoma. Mol Cancer 2006;5:67.
38. Nakada M, Nambu E, Furuyama N, Yoshida Y, Takino T, Hayashi Y, et al. Integrin alpha3 is overexpressed in glioma stem-like cells and promotes invasion. Br J Cancer 2013;108:2516-24.
39. Ruggieri P, Mangino G, Fioretti B, Catacuzzeno L, Puca R, Ponti D, et al. The inhibition of KCa3.1 channels activity reduces cell motility in glioblastoma derived cancer stem cells. PLoS One 2012;7:e47825.
40. Minniti G, Amelio D, Amichetti M, Salvati M, Muni R, Bozzao A, et al. Patterns of failure and comparison of different target volume delineations in patients with glioblastoma treated with conformal radiotherapy plus concomitant and adjuvant temozolomide. Radiother Oncol 2010;97:377-81.
41. Chen L, Chaichana KL, Kleinberg L, Ye X, Quinones-Hinojosa A, Redmond K. Glioblastoma recurrence patterns near neural stem cell regions. Radiother Oncol 2015.
42. Rempel SA, Dudas S, Ge S, Gutierrez JA. Identification and localization of the cytokine SDF1 and its receptor, CXC chemokine receptor 4, to regions of necrosis and angiogenesis in human glioblastoma. Clin Cancer Res 2000;6:102-11.
43. Jamal M, Rath BH, Tsang PS, Camphausen K, Tofilon PJ. The brain microenvironment preferentially enhances the radioresistance of $CD133^+$ glioblastoma stem-like cells. Neoplasia 2012;14:150-8.
44. Rao S, Sengupta R, Choe EJ, Woerner BM, Jackson E, Sun T, et al. CXCL12 mediates trophic interactions between endothelial and tumor cells in glioblastoma. PLoS One 2012;7:e33005.
45. Maddirela DR, Kesanakurti D, Gujrati M, Rao JS. MMP-2 suppression abrogates irradiation-induced microtubule formation in endothelial cells by inhibiting alphavbeta3-mediated SDF-1/CXCR4 signaling. Int J Oncol 2011;42(4):1279-88.
46. Badiga AV, Chetty C, Kesanakurti D, Are D, Gujrati M, Klopfenstein JD, et al. MMP-2 siRNA inhibits radiation-enhanced invasiveness in glioma cells. PLoS One 2011;6:e20614.
47. Imlach WL, Finch SC, Dunlop J, Meredith AL, Aldrich RW, Dalziel JE. The molecular mechanism of "ryegrass staggers," a neurological disorder of K^+ channels. J Pharmacol Exp Ther 2008;327:657-64.
48. Lee K, McKenna F, Rowe IC, Ashford ML. The effects of neuroleptic and tricyclic compounds on BKCa channel activity in rat isolated cortical neurones. Br J Pharmacol 1997;121:1810-6.
49. Korpi ER, Kleinman JE, Costakos DT, Linnoila M, Wyatt RJ. Reduced haloperidol in the post-mortem brains of haloperidol-treated patients. Psychiatry Res 1984;11:259-69.
50. Huang CL, Ruskin BH. Determination of Serum Chlorpromazine Metabolites in Psychotic Patients. J Nerv Ment Dis 1964;139:381-6.

Figures and Figure Legends

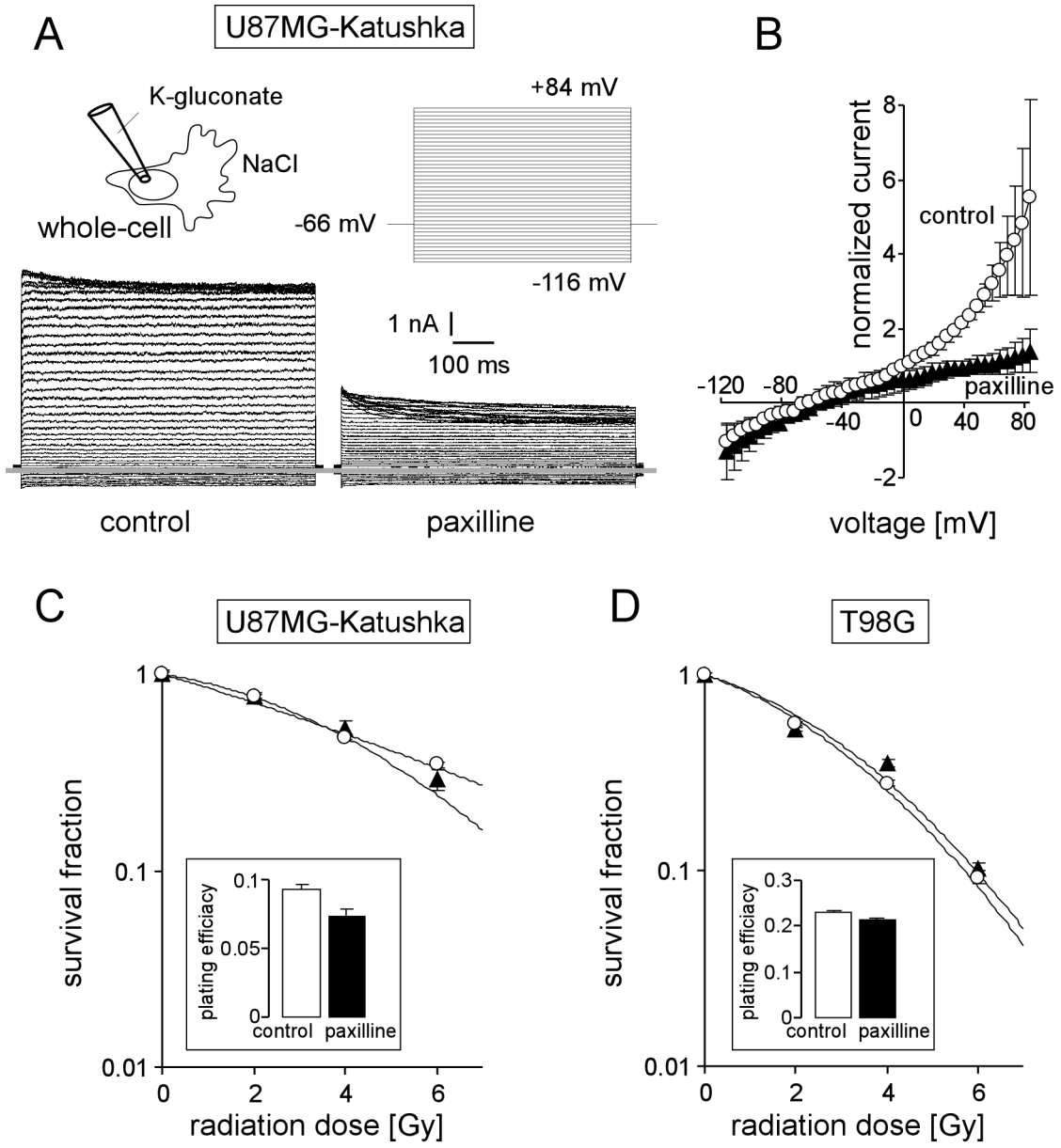

Figure 1

Fig. 1. The glioblastoma cell lines T98G and U87MG-Katushka functionally express BK Ca^{2+}-activated K^+ channels which, in contrast to IK channels, do not modulate radioresistance. **A.** Whole-cell current tracings recorded from the cell rear of a migrating U87MG-Katushka cell before (left) und during (right) bath application of the BK channel inhibitor paxilline. Records were obtained in voltage-clamp mode with K-gluconate pipette- and NaCl bath solution. The applied pulse protocol is shown in the upper right, the grey line indicates zero current level. **B.** Mean (± SE, n = 3) whole-cell current densities of migrating U87MG-Katushka cells recorded as in (A) before (circles) and during paxilline administration (triangles). **C, D.** Mean survival (± SE, n = 12-36) fraction of irradiated (0 - 6 Gy) U87MG-Katushka (C) and T98G cells (D) as determined by delayed plating colony formation assay. Cells were irradiated and post-incubated (24 h) in the absence (open bars) or presence (closed triangles) of paxilline. The inserts show the plating efficacies of both cell lines in the absence (open bars) or presence of paxilline (closed bars).

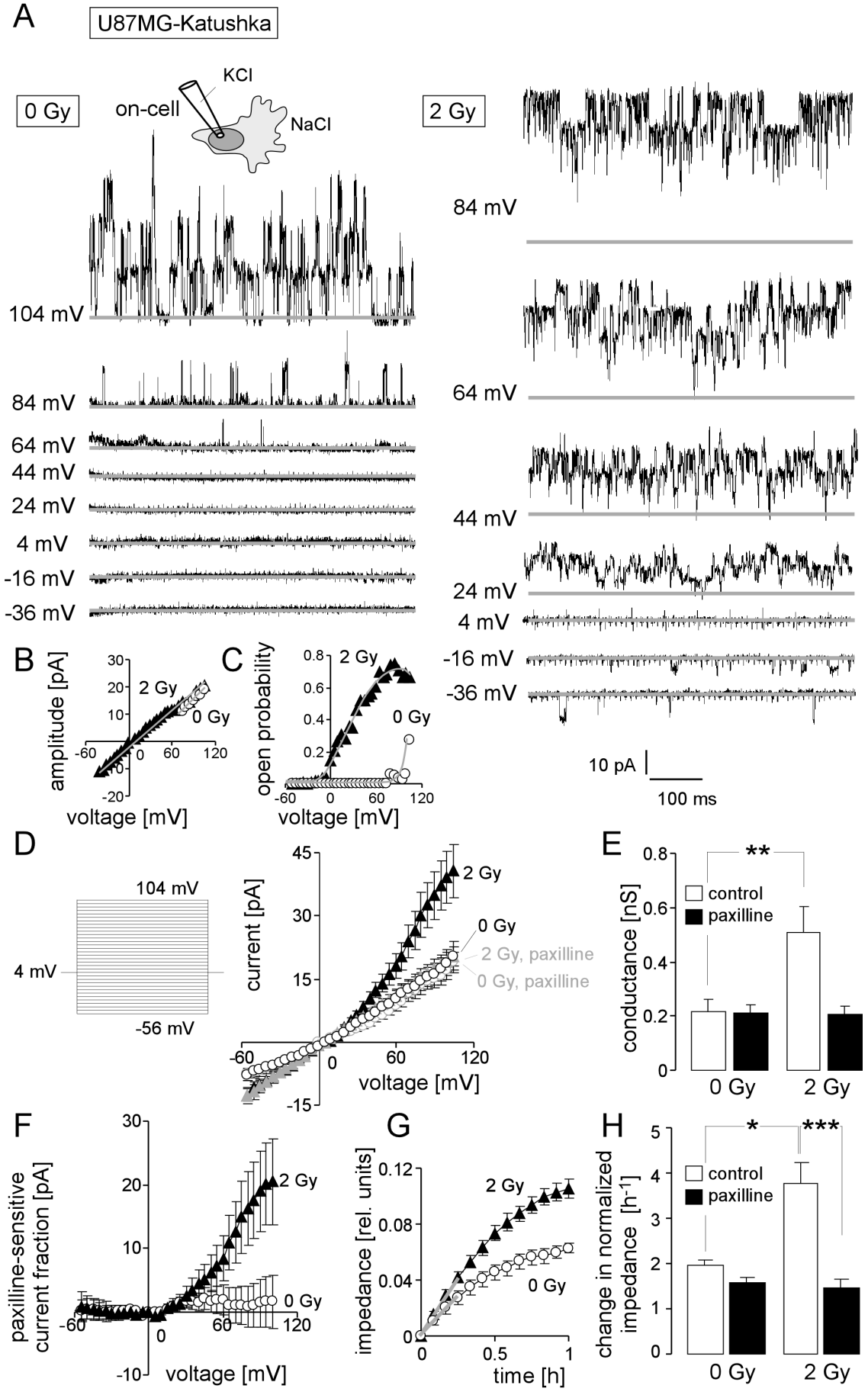
A
U87MG-Katushka
0 Gy
on-cell
KCl
NaCl
104 mV
84 mV
64 mV
44 mV
24 mV
4 mV
-16 mV
-36 mV
2 Gy
84 mV
64 mV
44 mV
24 mV
4 mV
-16 mV
-36 mV
10 pA
100 ms
B
amplitude [pA]
2 Gy
0 Gy
voltage [mV]
C
open probability
2 Gy
0 Gy
voltage [mV]
D
104 mV
4 mV
-56 mV
current [pA]
2 Gy
0 Gy
2 Gy, paxilline
0 Gy, paxilline
voltage [mV]
E
conductance [nS]
control
paxilline
**
0 Gy
2 Gy
F
paxilline-sensitive current fraction [pA]
2 Gy
0 Gy
voltage [mV]
G
impedance [rel. units]
2 Gy
0 Gy
time [h]
H
change in normalized impedance [h-1]
control
paxilline
*
***
0 Gy
2 Gy

Figure 2

Fig. 2. Ionizing radiation (IR) stimulates BK K^+ channel-dependent migration of U87MG-Katushka cells. **A.** Single channel current transitions recorded in on-cell mode at different holding potentials (as indicated) with KCl pipette- and NaCl bath solutions from a control (left) and an irradiated (3 h after 2 Gy) U87MG-Katushka cell. The voltage-dependent increase in open probability is shifted towards more negative potentials in the irradiated as compared to the control cell. **B, C.** Dependence of the mean unitary current transition (B) and open probability (P_o, C) on the voltage of the channels recorded in the control (open circles) and the irradiated cell (closed triangle) shown in (A). The channels exhibiting a unitary conductance of $g \approx 200$ pS and a depolarization-induced increase of P_o typically for BK channels. **D.** Mean (± SE, n = 8-15) macroscopic on-cell currents recorded as in (A) from control (open circles) and irradiated (2 Gy, closed triangles) U87MG-Katushka cells. Records were obtained in the absence (black) or presence of the BK inhibitor paxilline. **E.** Mean (± SE) conductance of the clamped membrane patch as calculated from (D) for the outward currents for control and irradiated cells in the absence (open bars) or presence (closed bars) of paxilline. **F.** Mean (± SE) paxilline-sensitive current fractions of control (open circles) and irradiated cells (closed triangles, data from D). **G.** Mean (± SE, n = 4) impedance as measure of transfilter migration of cells irradiated with 0 Gy (open circles) or 2 Gy (closed triangles). The experiment started at 2 h after IR. **H.** Mean (± SE, n = 9-24) normalized migration velocity as calculated for the first 0.25 h of transfilter migration (slopes in G shown by the grey lines) in control (0 Gy) and irradiated (2 Gy) cells recorded in the absence (open bars) or presence of the BK inhibitor paxilline (closed bars). *, ** and *** indicate $p \leq 0.05$, $p \leq 0.01$, and $p \leq 0.001$, ANOVA, respectively.

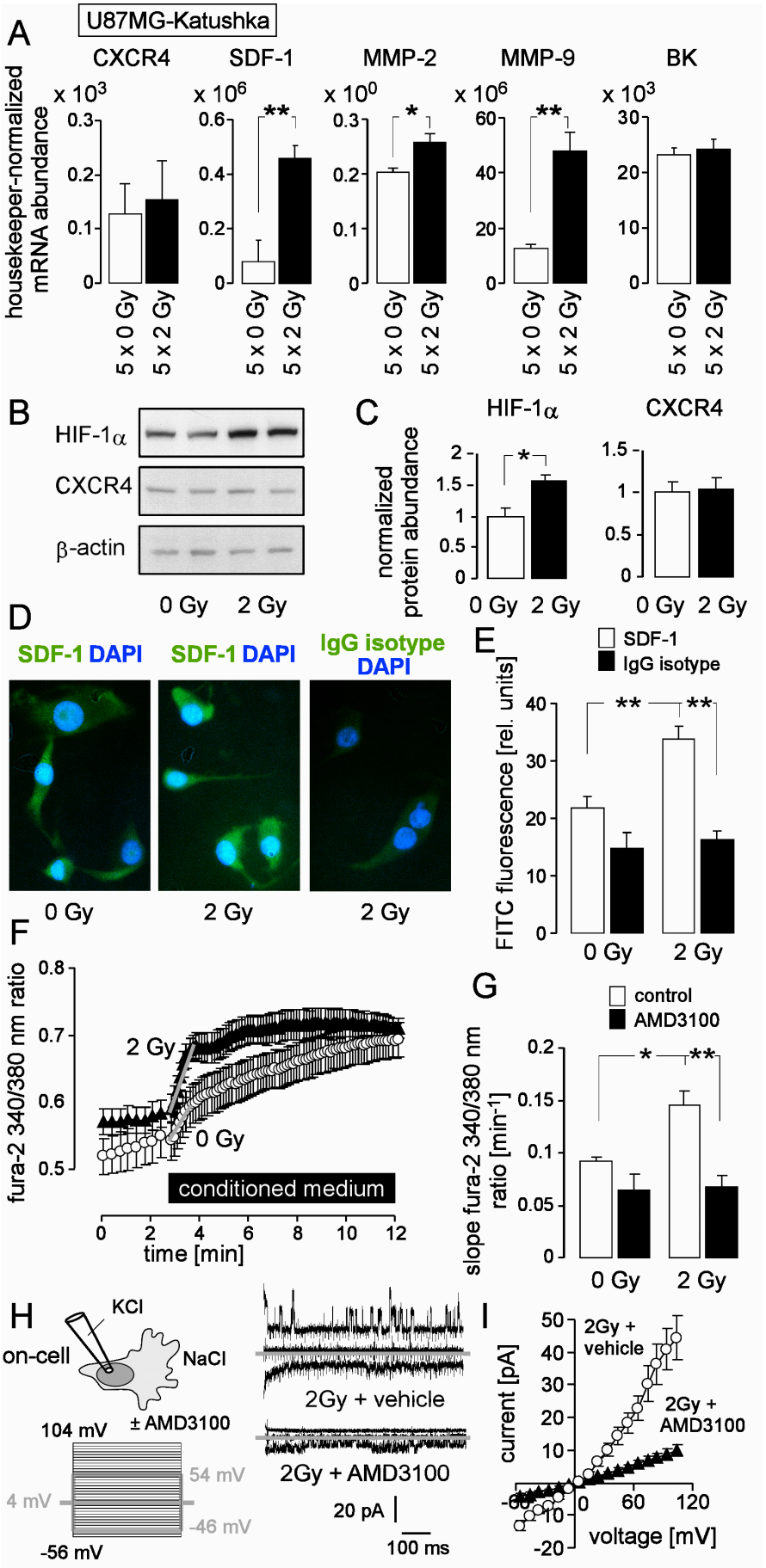
A
U87MG-Katushka
CXCR4
SDF-1
MMP-2
MMP-9
BK
housekeeper-normalized mRNA abundance
5 x 0 Gy
5 x 2 Gy
B
HIF-1α
CXCR4
β-actin
0 Gy
2 Gy
C
HIF-1α
CXCR4
normalized protein abundance
D
SDF-1 DAPI
SDF-1 DAPI
IgG isotype DAPI
E
SDF-1
IgG isotype
FITC fluorescence [rel. units]
F
fura-2 340/380 nm ratio
2 Gy
0 Gy
conditioned medium
time [min]
G
control
AMD3100
slope fura-2 340/380 nm ratio [min-1]
H
KCl
on-cell
NaCl
± AMD3100
104 mV
54 mV
4 mV
-46 mV
-56 mV
2Gy + vehicle
2Gy + AMD3100
20 pA
100 ms
I
2Gy + vehicle
2Gy + AMD3100
current [pA]
voltage [mV]

Figure 3

Fig. 3. IR stimulates a migratory and invasive phenotype in U87MG-Katushka cells probably via stabilization of HIF-1α, upregulation of SDF-1, CXCR4-mediated Ca^{2+} signaling and BK channel activation. **A.** Mean (± SE, n = 5) mRNA abundances of U87MG-Katushka cells fractionated irradiated with 5 x 0 Gy (open bars) or 5 x 2 Gy (closed bar, mRNA was extracted 24 h after the last IR fraction). Shown are the mRNAs encoding for the chemokine receptor CXCR4, the chemokine SDF-1 (CXCL12), the matrix metalloproteinase MMP-2 and MMP-9, as well as for the BK channel. **B.** Immunoblots of two lysates each prepared from U87MG-Katuskha cells irradiated with a single dose of 0 Gy (left) or 2 Gy (2 h after IR, right) probed against HIF-1α, CXCR4 and the loading control β-actin. **C.** Mean (± SE, n = 4) β-actin-normalized HIF-1α (left) and CXCR4 (right) protein abundance in 0 Gy (open bars) or 2 Gy (2 h after IR, closed bars) U87MG-Katushka cells. **D.** Immunofluorescence micrographs of 0 Gy- (left) or 2 Gy (2 h after IR, middle and right) stained with an anti-SDF-1 (left and middle) or the IgG isotype control antibody (right) as detected with a FITC-coupled secondary antibody (green) and co-stained with the DNA-specific dye DAPI (blue). **E.** Mean (± SE, n =) FITC fluorescence intensity of anti-SDF-1 (open bars) or IgG isotype antibody-stained cells from 0 Gy (left) or 2 Gy irradiated U87MG-Katushka cells. **F.** Mean (± SE, n = 36-60) fura-2 340/380 nm fluorescence ratio as measure of cytosolic free Ca^{2+} concentration ($_{free}[Ca^{2+}]_i$) recorded in U87MG-Katushka cells before and during superfusion with conditioned medium harvested from U87MG-Katushka cultures 2 h after IR with 0 Gy (open circles) or 2 Gy (closed triangles). **G.** Mean (± SE, n = 24 - 60) increase in $_{free}[Ca^{2+}]_i$ as determined by the slope (grey lines in F) of the conditioned medium-evoked rise in the 340/380 nm ratio. The conditioned medium harvested from 0 Gy (left) or 2 Gy irradiated U87MG-Katushka cells was administered without (open bars) or together with the CXCR4 antagonist AMD3100 (closed bars). **H.** AMD3100 prevents IR-induced induction of BK channel activity in U87MG-Katushka cells. On-cell current tracings of irradiated cells (2 Gy, 2 h after IR) irradiated and post-incubated in the absence (top) or presence of AMD3100. Macroscopic on-cell currents were obtained with KCl pipette- and NaCl bath solutions in the absence of AMD3100 as described in Fig. 2. Only currents evoked by voltage sweeps to -56, 4, and 54 mV are shown. **I.** Dependence of mean (± SE, n = 16) macroscopic on-cell currents on voltage recorded as in (H) from vehicle- (open circles) or AMD3100-pretreated (closed triangles) irradiated U87MG-Katushka cells. * and ** indicate $p \leq 0.05$ and 0.01, respectively, (Welch)-corrected t-test in (A) and (C) and ANOVA in (G) and (E).

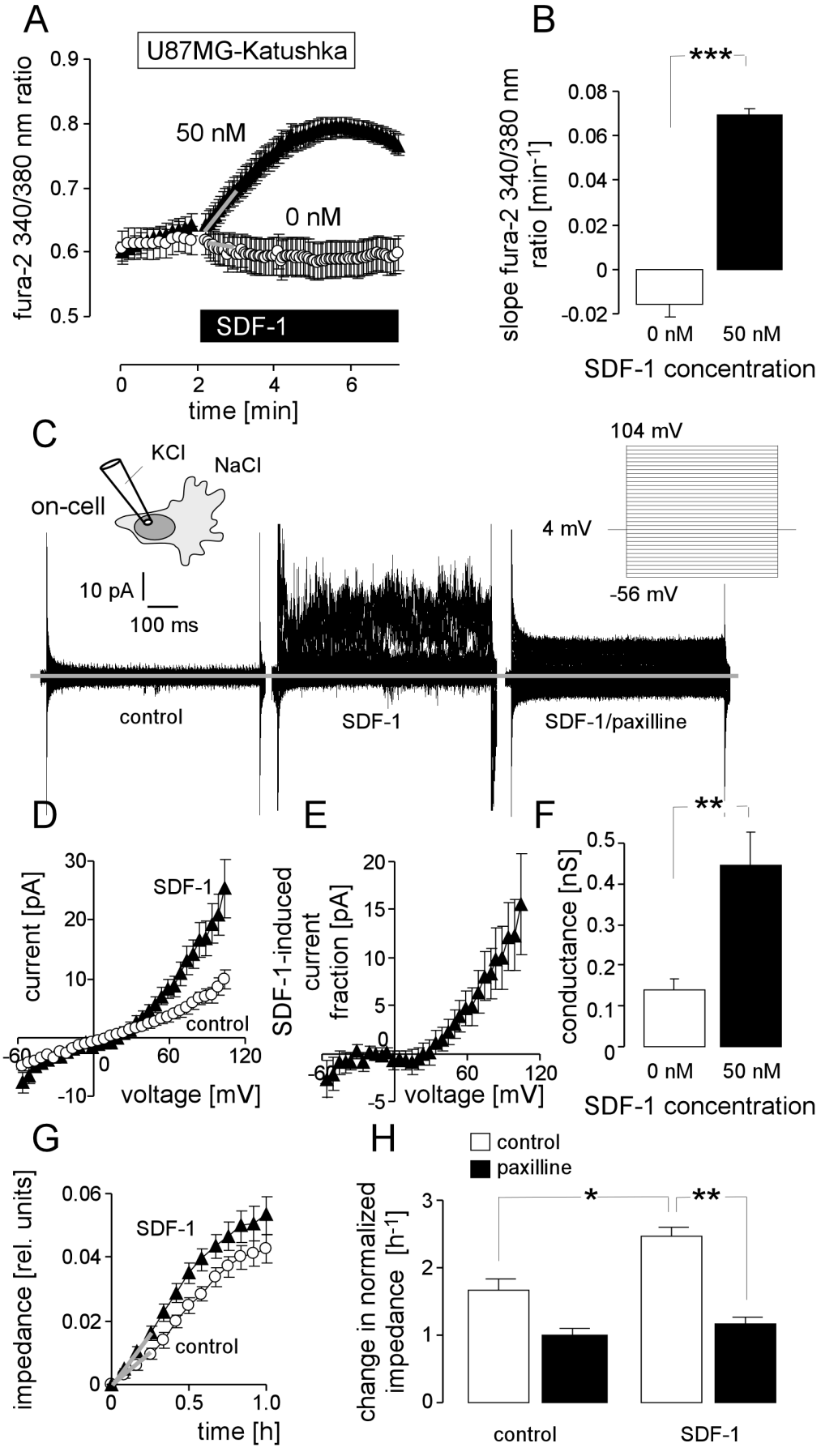
A
U87MG-Katushka
fura-2 340/380 nm ratio
50 nM
0 nM
SDF-1
time [min]
B
***
slope fura-2 340/380 nm ratio [min-1]
0 nM
50 nM
SDF-1 concentration
C
KCl
NaCl
on-cell
10 pA
100 ms
104 mV
4 mV
-56 mV
control
SDF-1
SDF-1/paxilline
D
current [pA]
SDF-1
control
voltage [mV]
E
SDF-1-induced current fraction [pA]
voltage [mV]
F
**
conductance [nS]
0 nM
50 nM
SDF-1 concentration
G
impedance [rel. units]
SDF-1
control
time [h]
H
control
paxilline
change in normalized impedance [h-1]
*
**
control
SDF-1

Figure 4

Fig. 4. Stimulation with the chemokine SDF-1 mimics the effect of IR on BK channel activity and transfilter migration in U87MG-Katushka cells. A. Mean (± SE, n = 19-23) fura-2 340/380 nm fluorescence ratio before and during superfusion with SDF-1 or control solution. **B.** Mean (± SE) change in $_{free}[Ca^{2+}]_i$ as determined by the slope (grey lines in A) of the SDF-1- or control solution-evoked change in the 340/380 nm ratio. **C.** On-cell current tracings recorded with KCl pipette- and NaCl bath solution from a U87MG-Katuska cell before (left) and during bath application of SDF-1 (middle) and the BK inhibitor paxilline (right). **D.** Mean (± SE, n = 10) macroscopic on-cell currents recorded as in (C) before (open circles) and during administration of SDF-1 (closed triangles). **E.** Mean (± SE) SDF-1-stimulated current fraction (data from C). **F.** Mean (± SE) conductance of the clamped membrane patch as calculated from (C) for the outward currents recorded in the absence (open bars) and presence of SDF-1 stimulation (closed bars). **G.** Mean (± SE, n = 4) impedance as measure of transfilter migration of control (open circles) and SDF-1-stimulated (closed triangles) U87MG-Katushka cells. **H.** Mean (± SE, n = 9-24) normalized migration velocity in control and SDF-1-stimulated U87MG-Katushka cells recorded in the absence (open bars) or presence (closed bars) of the BK inhibitor paxilline. *, ** and *** indicate $p \leq 0.05$, $p \leq 0.01$, and $p \leq 0.001$, respectively, Welch-corrected t-test in (B) and (F), ANOVA in (H).

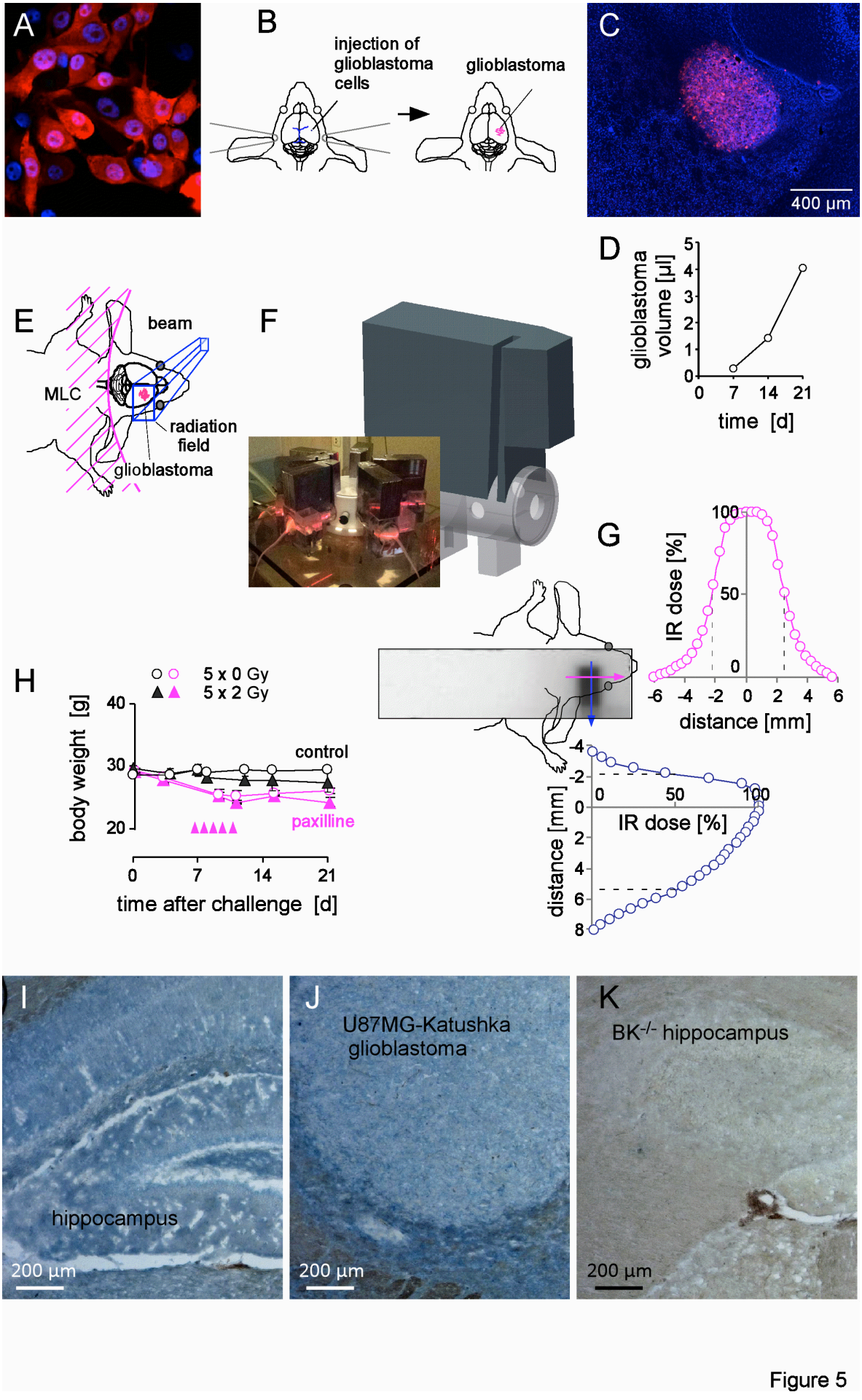
A
B
injection of glioblastoma cells
glioblastoma
C
400 µm
D
glioblastoma volume [µl]
time [d]
E
beam
MLC
radiation field
glioblastoma
F
G
IR dose [%]
distance [mm]
H
5 x 0 Gy
5 x 2 Gy
body weight [g]
control
paxilline
time after challenge [d]
I
hippocampus
200 µm
J
U87MG-Katushka glioblastoma
200 µm
K
BK-/- hippocampus
200 µm

Figure 5

Fig. 5. Fractionated IR of human glioblastoma *xeno*grafted orthotopically in NSG mice. **A.** Fluorescence micrograph of human U87MG-Katushka glioblastoma cells grown *in vitro* (red and blue fluorescence indicate the Katushka protein and the DNA-specific DAPI fluorochrome, respectively). **B.** Scheme illustrating the stereotactic transplantation of U87MG-Katushka cells in mouse right striatum. The blue lines (left drawing) indicate bregma (top) and lambda (bottom). **C.** Fluorescence micrograph of a U87MG-Katushka glioblastoma in mouse brain 7 d after tumor cell challenge into the right striatum (DAPI-stained cryosection). **D.** Time-dependent intracranial growth of U87MG-Katushka glioblastoma. **E.** Cartoon illustrating the radiation field. On-body lead shielding has been left out for better clarity (MLC: multileaf collimator). **F.** Drawing of the mouse holder with mounted on-body leaf shielding. The photography on the lower left shows 6 mice during radiotherapy. **G.** Dosimetry film and densitometrically analyzed dose distribution in y- (blue) and x-axis (pink) across the radiation field and adjacent shielded brain area. The site of dose deposition is indicated by the superimposed drawing of the mouse head. The dashed lines in the dose distribution plots indicate the 50% isodose. **H.** Mean (± SE, n = 3) body weight of control (open circles) and fractionated irradiated NSG mice (closed triangles) during the first 3 weeks after intracranial challenge with U87MG-Katushka cells. Control (black symbols) and mice receiving paxilline (pink symbols) are shown. IR fractions (2 Gy each) are indicated by the pink arrow heads. **I, J.** BK protein expression (blue) in hippocampus and *xeno*grafted U87MG-Katushka tumor of NSG mice. **K.** Hippocampus of $BK^{-/-}$ mice served as negative control.

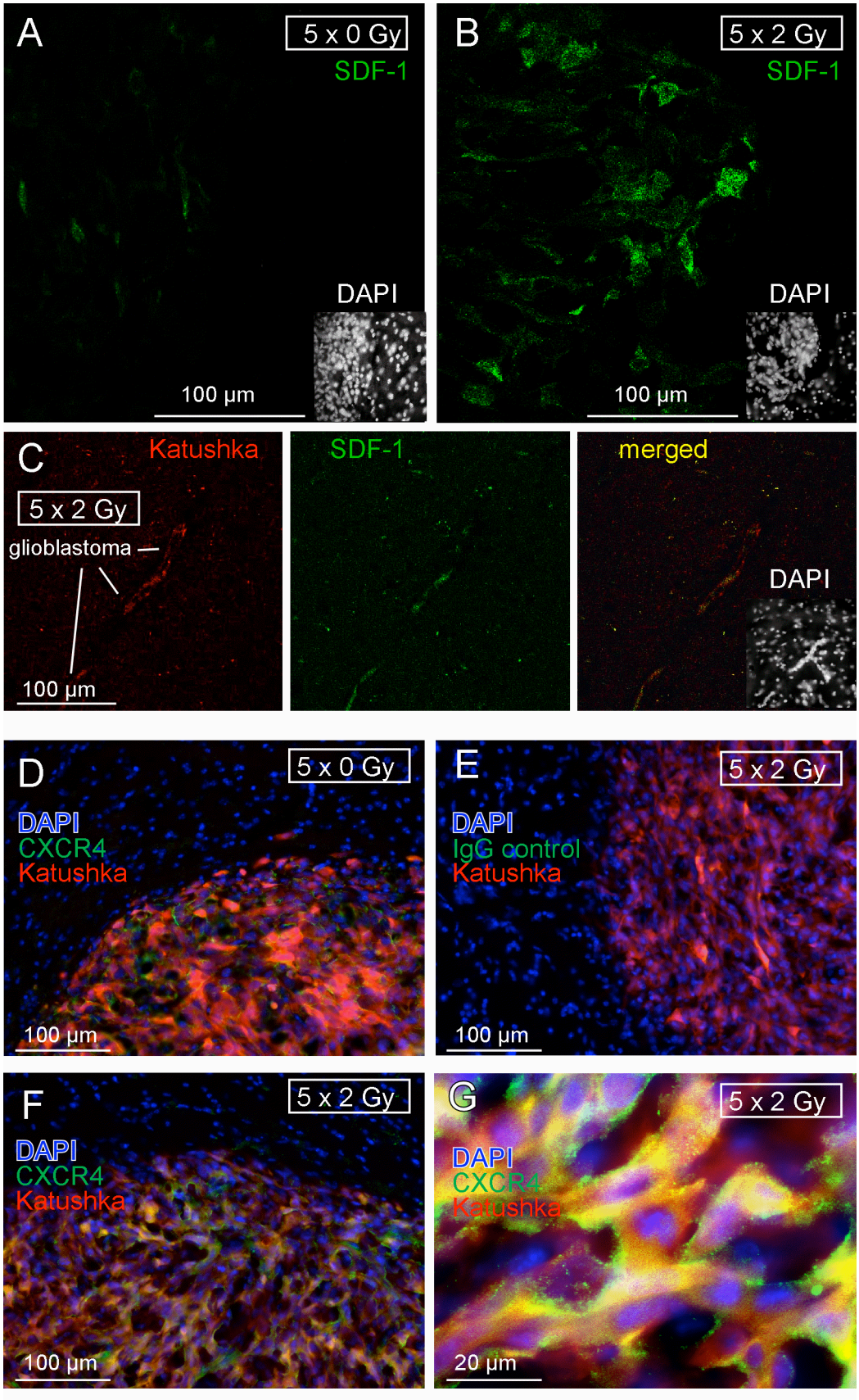
A
5 x 0 Gy
SDF-1
DAPI
100 µm
B
5 x 2 Gy
SDF-1
DAPI
100 µm
C
Katushka
5 x 2 Gy
glioblastoma
100 µm
SDF-1
merged
DAPI
D
5 x 0 Gy
DAPI
CXCR4
Katushka
100 µm
E
5 x 2 Gy
DAPI
IgG control
Katushka
100 µm
F
5 x 2 Gy
DAPI
CXCR4
Katushka
100 µm
G
5 x 2 Gy
DAPI
CXCR4
Katushka
20 µm

Figure 6

Fig. 6. Fractionated IR stimulates *in vivo* SDF-1 protein expression by glioblastoma cells. **A, B.** SDF-1 specific immunofluorescence (green) of (A) control (5 x 0 Gy) and (B) fractionated irradiated (5 x 2 Gy) U87MG-Katushka glioblastoma and surrounding normal brain tissue. **C.** U87MG-Katushka cells (red) migrating through mouse brain and expressing SDF-1 protein (green). The inserts in the lower right show the corresponding DAPI staining (white) of the nuclei in lower power. The glioblastoma in (A) and (B) can be easily identified by the dense array of nuclei. **D-G.** U87MG-Katushka glioblastoma express chemokine receptor CXCR4. CXCR4-specific immunofluorescence (green) in control (5 x 0 Gy, D) and fractionated irradiated (5 x 2 Gy) tumors (F, G; Katushka: red, DAPI: blue). CXCR4 was detectable in plasma membrane and cytoplasma of the glioblastoma cells (merged yellow Katushka and CXCR4-specific fluorescence, G). The IgG isotope control did not show green fluorescence (E).

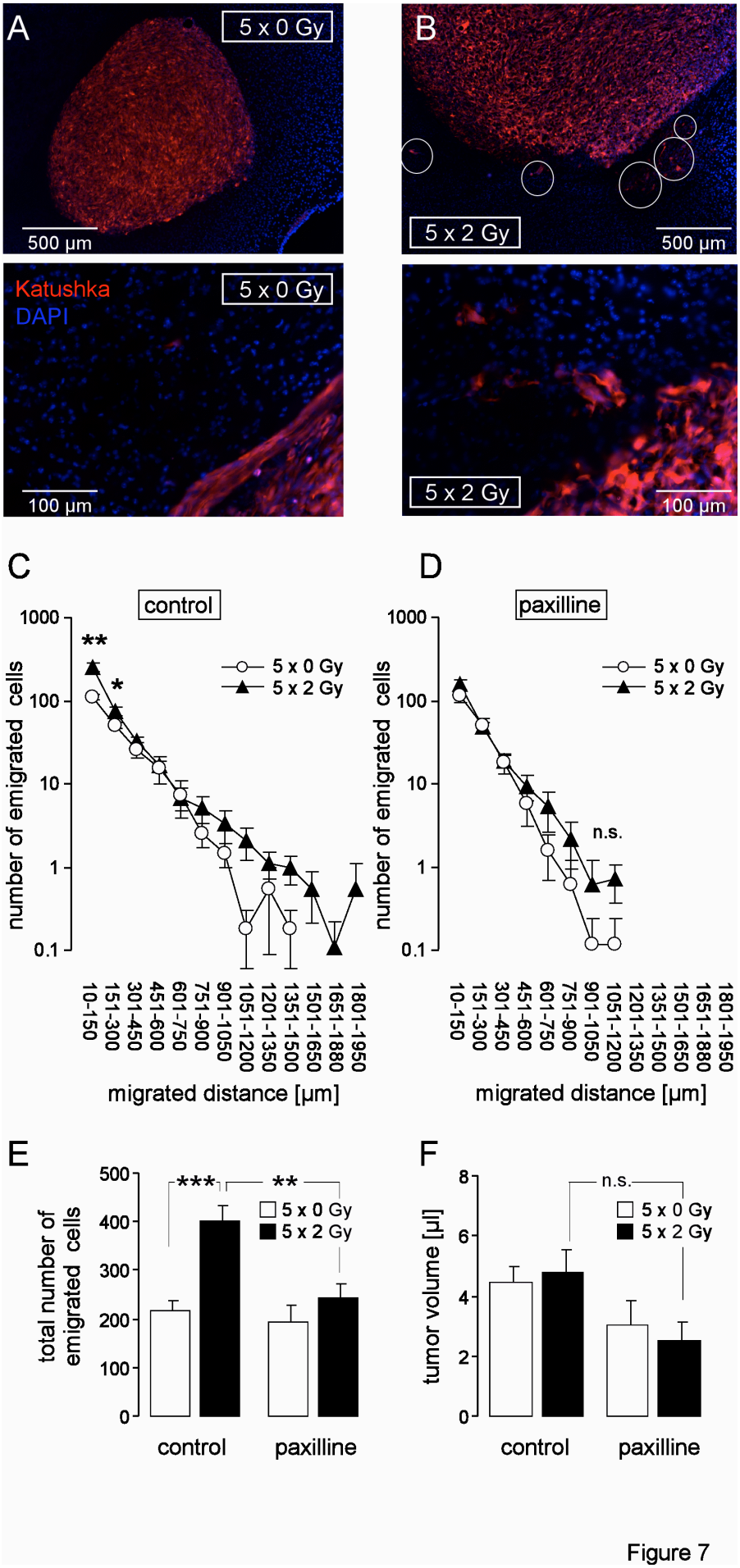
A
5 x 0 Gy
500 µm
B
5 x 2 Gy
500 µm
Katushka
DAPI
5 x 0 Gy
100 µm
5 x 2 Gy
100 µm
C
control
number of emigrated cells
1000
100
10
1
0.1
**
*
5 x 0 Gy
5 x 2 Gy
10-150
151-300
301-450
451-600
601-750
751-900
901-1050
1051-1200
1201-1350
1351-1500
1501-1650
1651-1880
1801-1950
migrated distance [µm]
D
paxilline
n.s.
E
total number of emigrated cells
500
400
300
200
100
0
***
**
control
paxilline
F
tumor volume [µl]
8
6
4
2
0
n.s.

Figure 7

Fig. 7. Fractionated IR stimulates migration of glioblastoma cells *in vivo*. **A, B.** Fluorescence micrographs of control (5 x 0 Gy, A) and fractionated irradiated (5 x 2 Gy, B) U87MG-Katushka glioblastoma () in low (top) and high (bottom) magnification. The nuclei are stained with DAPI (blue), some emigrating U87MG-Katushka cells are highlighted by white circles. **C, D** Number of emigrated cells per tumor (mean ± SE, n = 8-11) as function of the migrated distance of glioblastoma cells fractionated irradiated (5 x 0 Gy, open circles or 5 x 2 Gy, closed triangles) in the absence (C) or presence (D) of concomitant BK channel targeting with paxilline. **E, F.** Mean (± SE, n = 8-11) total number of emigrated glioblastoma cells (E) and mean (± SE) corresponding glioma volume (F) of fractionated irradiated glioma (5 x 0 Gy, open bars or 5 x 2 Gy, closed bars) of control mice or mice receiving concomitant paxilline chemotherapie. *, **, ***, and n.s. indicate $p \leq 0.05$, $p \leq 0.01$, $p \leq 0.001$ and not significantly different, respectively, Welch-corrected t-test in (C, D) and ANOVA in (E, F).

Supplementary Material

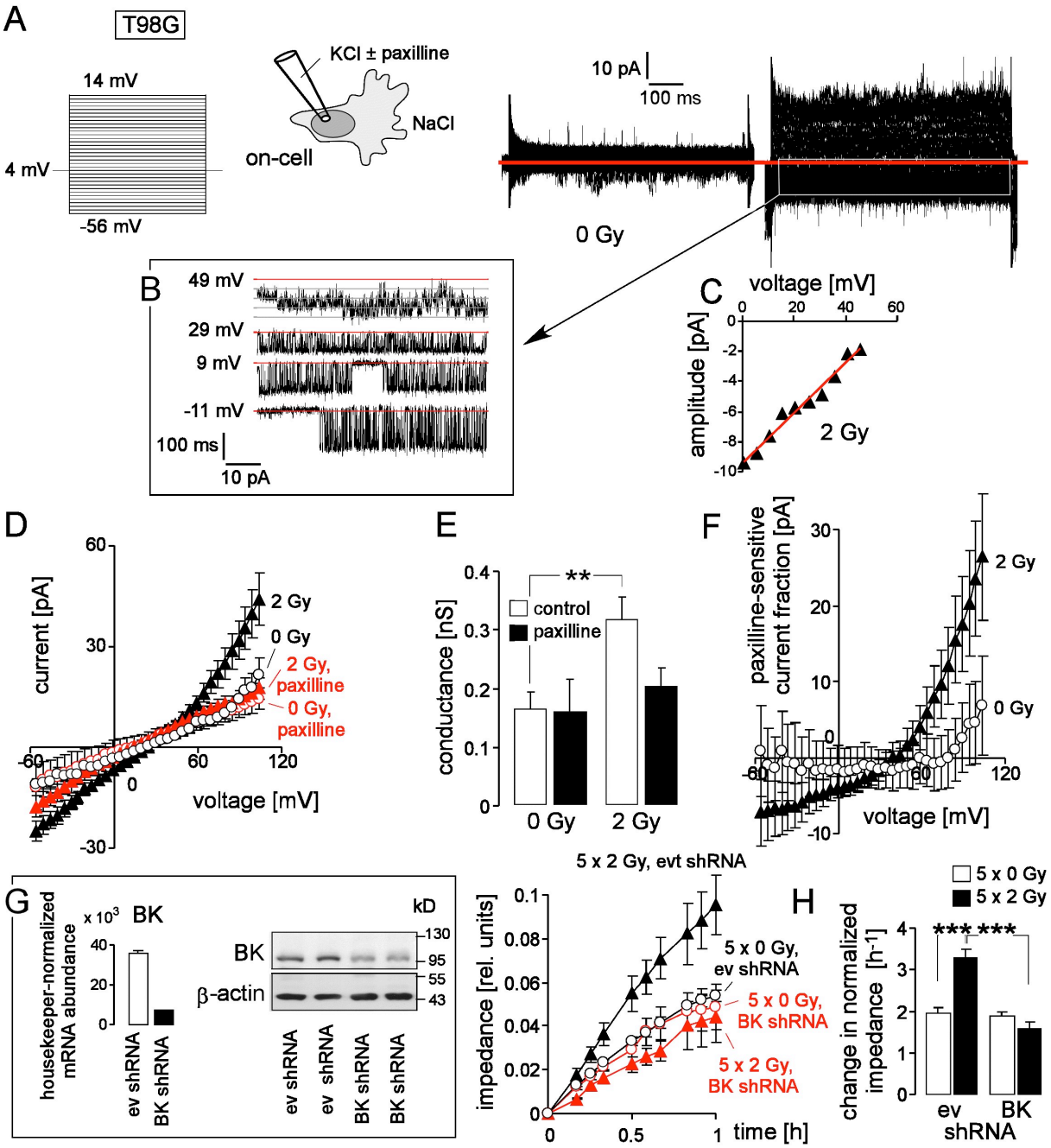

Fig. I. IR stimulates BK channel activity and BK channel-dependent migration of human T98G glioblastoma cells. **A.** Macroscopic on-cell currents recorded at different voltages (as indicated) with KCl pipette- and NaCl bath solutions from a control (left) and an irradiated T98G cell. **B, C.** Single channel current transitions at different holding potentials (B) and dependence of the current amplitude on voltage (C) extracted from the current tracings in (A, right) indicate a voltage-dependent activation and a unitary conductance characteristic for BK channels. **D.** Mean (± SE, n = 8-34) macroscopic on-cell currents recorded as in (A) from control (open circles) and irradiated (2 Gy, closed triangles) T98G cells. Records were obtained in the absence (black) or presence (red) of the BK inhibitor paxilline. **E.** Mean (± SE) conductance of the clamped membrane patch as calculated from (D) for the outward currents for control and irradiated cells in the absence (open bars) or presence (closed bars) of paxilline. **F.** Mean (± SE) paxilline-sensitive current fractions of control (open circles) and irradiated (closed triangles) cells (data from D). **G.** Knockdown of BK channels in T98G cells abrogates radiation-induced migration. Mean (± SE, n = 4) impedance as measure of transfilter migration of empty vector control (ev, black) or BK-specific shRNA-expressing T98G cells (red) irradiated with 5 x 0 Gy (open circles) or 5 x 2 Gy (closed triangles). The experiment started 24 h after the last IR fraction. The insert (left) shows the housekeeper-normalized BK-encoding mRNA abundance (left) as well as BK and β-actin protein abundances of T98G cells stably transduced with empty vector control (ev) or BK-specific shRNA. **H.** Mean (± SE, n = 8) normalized migration velocity as calculated from the data in (G) for the first 0.25 h of transfilter migration in control (0 Gy, open bars) and irradiated (2 Gy, closed bars) cells expressing non or BK-specific shRNA. ** and *** indicate $p \leq 0.01$ and 0.001, ANOVA, respectively.

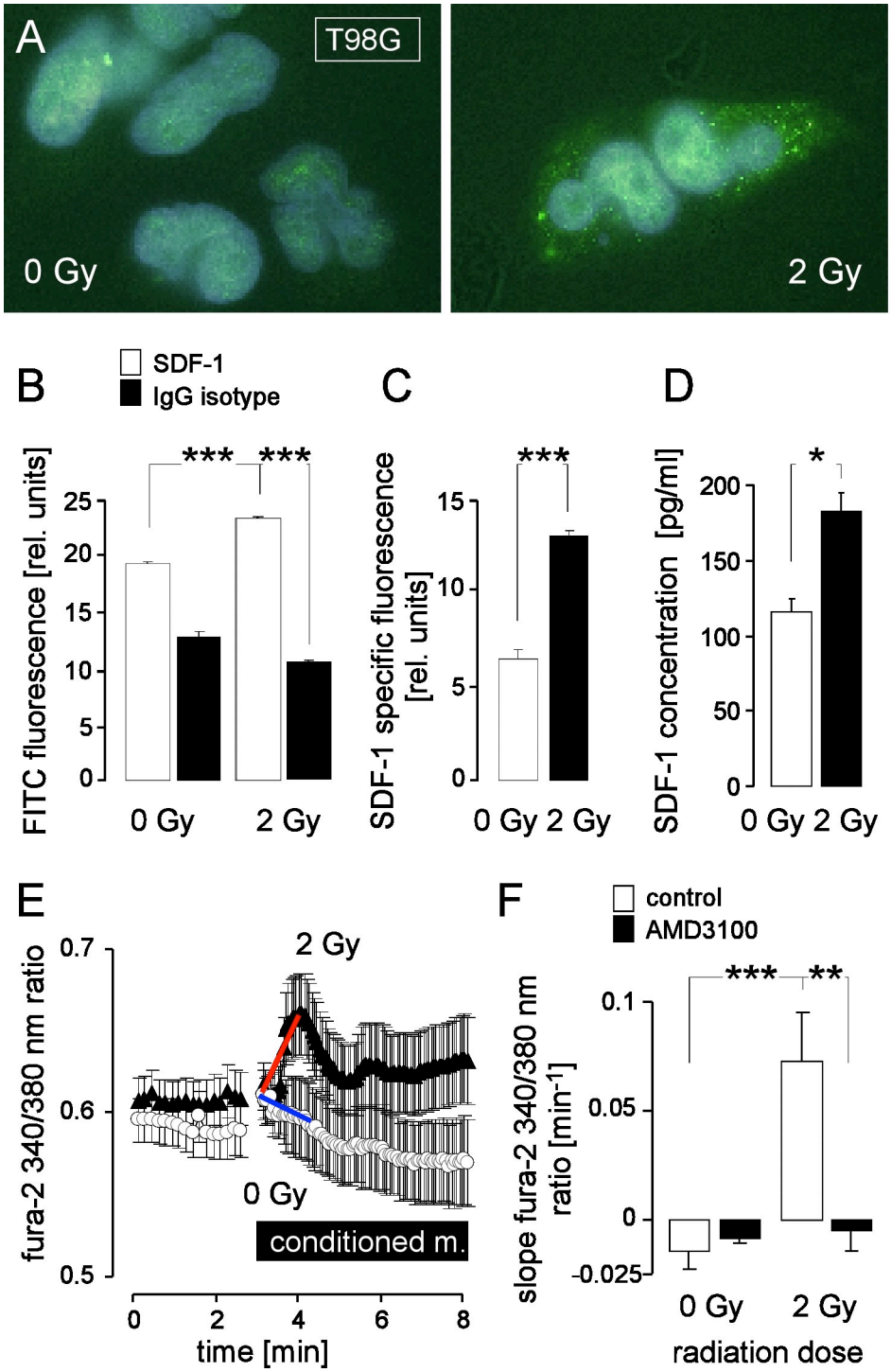
A
T98G
0 Gy
2 Gy
B
SDF-1
IgG isotype
FITC fluorescence [rel. units]
***
***
0 Gy
2 Gy
C
SDF-1 specific fluorescence [rel. units]
***
0 Gy 2 Gy
D
SDF-1 concentration [pg/ml]
*
0 Gy 2 Gy
E
fura-2 340/380 nm ratio
2 Gy
0 Gy
conditioned m.
time [min]
F
control
AMD3100
slope fura-2 340/380 nm ratio [min-1]
***
**
0 Gy
2 Gy
radiation dose

Fig. II. IR induces SDF-1 signaling of T98G cells. **A.** Immunofluorescence micrographs of 0 Gy (left) or 2 Gy (2 h after IR, right) irradiated cells stained with an anti-SDF-1 antibody and a FITC-coupled secondary antibody (green). **B.** Mean (± SE) FITC fluorescence intensity of anti-SDF-1 (open bars, n = 286-364) or IgG isotype antibody-stained (closed bars, n = 42-75) cells (left) and SDF-1-specific fluorescence (right) from 0 Gy (left) or 2 Gy irradiated T98G cells. **C.** Mean (± SE, n = 4) SDF-1 concentration in the medium of T98G cells 2 h after irradiaton with 0 Gy (open bar) or 2 Gy (closed bar). **E-F**. CXCR4 chemokine receptor antagonist AMD3100 prevents IR-induced Ca^{2+} signaling. (E) Mean (± SE, n = 7-27) fura-2 340/380 nm fluorescence ratio as measure of cytosolic $_{free}[Ca^{2+}]_i$ recorded in T89G cells before and during superfusion with conditioned medium harvested from T98G cultures 2 h after IR with 0 Gy (open circles) or 2 Gy (closed circles). (F). Mean (± SE) increase in $_{free}[Ca^{2+}]_i$ as determined by the slope (colored lines in E) of the conditioned medium-evoked rise in the 340/380 nm ratio. The conditioned media were administered without (open bars) or together with the CXCR4 antagonist AMD3100 (closed bars). * **, and *** indicate $p \leq 0.05$, $p \leq 0.01$, and $p \leq 0.001$, respectively, ANOVA in (B) and (F) and Welch-corrected t-test in C and D.

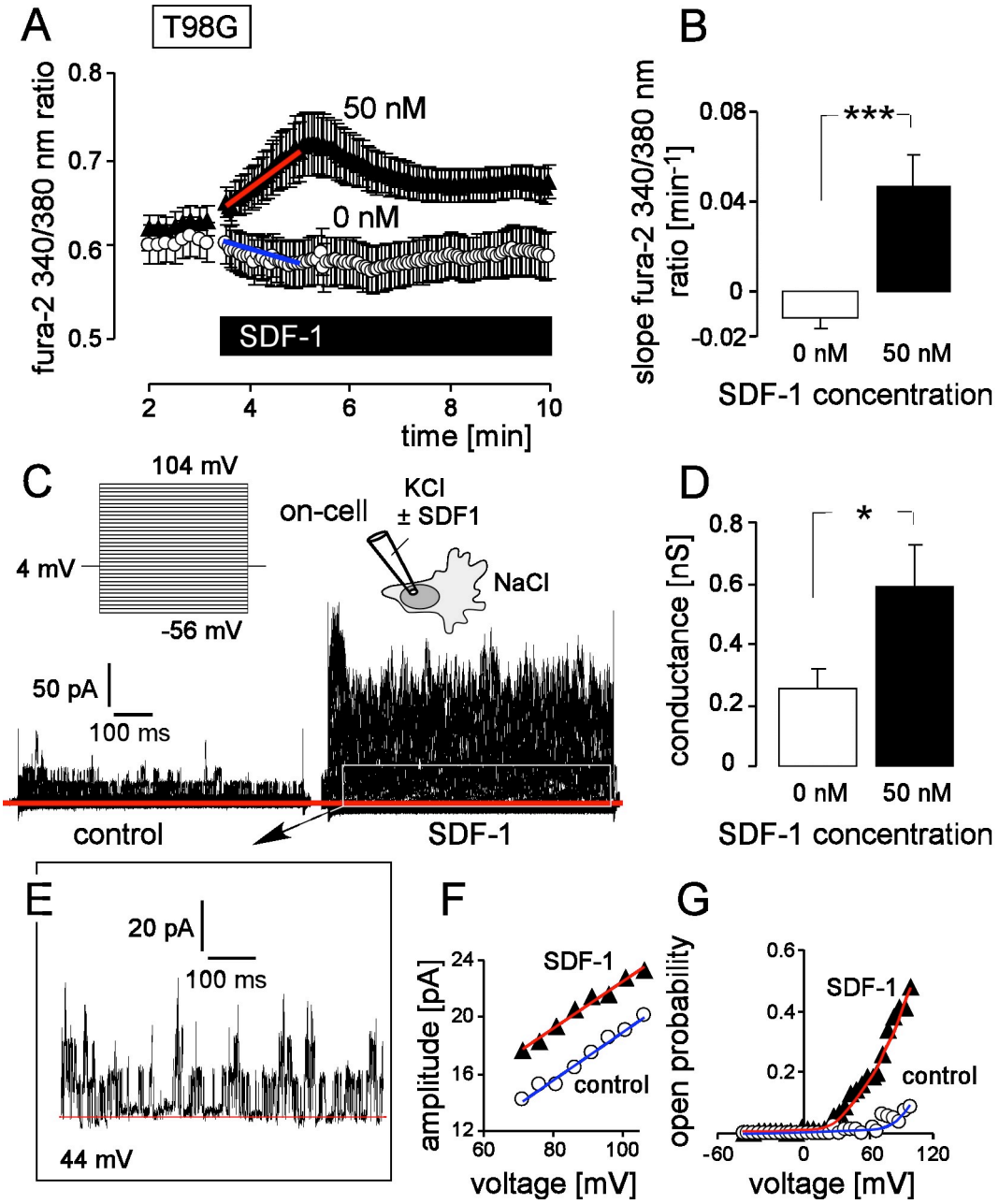

Fig. III. SDF-1 elicits Ca^{2+} signals and mimics the effect of IR on BK channel activity and migration in T98G cells. **A.** Mean (± SE, n = 21-36) fura-2 340/380 nm fluorescence ratio before and during superfusion with SDF-1 or control solution. **B.** Mean (± SE, n = 21-36) change in $_{free}[Ca^{2+}]_i$ as determined by the slope (colored lines in A) of the SDF-1- or control solution-evoked change in the 340/380 nm ratio. **C.** On-cell current tracings recorded with KCl pipette- and NaCl bath solution from a control (left) and SDF-1-stimulated T98G cell (right). **D.** Mean (± SE; n = 11) conductance of the clamped membrane patch as calculated from (C) for the outward currents. **E-G.** Single channel current transitions (E) and dependence of the current amplitude on voltage (F) and open probability (G) of the control (open circles) and SDF-1-stimulated current tracings (closed triangles) shown in (C). * and *** indicate $p \leq 0.05$ and 0.001, Welch-corrected t-test, respectively.